Interactions of charged particles and hydrogen atoms

Thesis for the Degree of Doctor of Philosophy (PhD)

Iman Ziaeian

Supervisor

Dr. Károly Tőkési

UNIVERSITY OF DEBRECEN

Doctoral Council of Natural Sciences and Information Technology

Doctoral School of Physics

Debrecen, 2022

Prepared at
The University of Debrecen
PhD School in Physics
and
the Institute for Nuclear Research,
(ATOMKI)

Keszült
A Debrecen Egyetem
Fizikai Tudományok Doktori Iskolájának
Nukleáris fizika programja keretében
az Atommagkutató Intézetében
(ATOMKI)

Hereby I declare that I prepared this thesis within the Doctoral Council of Natural Sciences and Information Technology, Doctoral School of Physics, University of Debrecen in order to obtain a PhD Degree in Natural Sciences at Debrecen University.
The results published in the thesis are not reported in any other PhD theses.

Debrecen, 2022. March 2.

Iman Ziaeian
Doctoral candidate

Hereby I confirm that Iman Ziaeian candidate conducted his studies with my supervision within the Nuclear Physics Doctoral Program of the Doctoral School of Physics between 2018. and 2022. The independence studies and research work of the candidate significantly contributed to the results published in the thesis.
I also declare that the results published in the thesis are not reported in any other theses.
I support the acceptance of the thesis.

Debrecen, 2022. March 2.

Dr. Károly Tőkési
Supervisor

Interactions of charged particles and hydrogen atoms

Dissertation submitted in partial fulfilment of the requirements for the doctoral (PhD) degree in Physics

Written by: Iman Ziaeian certified Physicist

Prepared in the framework of the Physics Doctoral School of the University of Debrecen

Nuclear Physics programme

Dissertation advisor: Dr. Károly Tőkesi

The official opponents of the dissertation:

Dr. ……. …….
Dr. ……. …….

The evaluation committee:

Chairperson:	Dr.	…….	……
Members:	Dr.	…….	……...
	Dr.	……	……
	Dr.	……	……
	Dr.	……	……

The date of the dissertation defense: ... ……20…

Contents

List of publications

Publications related to the thesis

1. **I. Ziaeian** and Károly Tőkési, *Interaction of Be^{4+} and Ground State Hydrogen Atom—Classical Treatment of the Collision,* Atoms, 8 (2020) 27.

2. **I. Ziaeian** and Károly Tőkési, *State-selective charge exchange cross sections in Be^{4+} - H(2lm) collision based on the classical trajectory Monte Carlo method,* Eur. Phys. J. D. 75 (2021) 1-5.

3. **I. Ziaeian** and Károly Tőkési, *State selective classical electron capture cross sections in Be^{4+} + H(1s) collisions with mimicking quantum effect,* Sci. Rep. 11 (2021) 20164.

4. **I. Ziaeian**, K. Tőkési, *nl-selective classical charge exchange cross sections in Be^{4+} and ground state hydrogen atom collisions,* submitted to Physics Letters A.

5. **I. Ziaeian**, K. Tőkési, *Effects of Heisenberg constraint on the classical cross sections in in proton hydrogen collision,* submitted to Journal of Physics B: Atomic, Molecular and Optical Physics.

6. **I. Ziaeian**, K. Tőkési, *State-selective electron capture cross sections in collision between fully striped ions and ground state hydrogen – classical treatment of the collision,* accepted for publication in Atomic Data and Nuclear Data Tables.

Other scientific publications

1. S. Soheyli and **I. Ziaeian**, *Fission fragment angular distribution in heavy ion induced fission,* Iranian Journal of Physics Research, 6 (2006) 25-36.

2. S. Soheyli, H. Noshad and **I. Ziaeian**, *Calculation of Fission Fragment Angular Anisotropy in Heavy- Ion Induced Fission*, International Journal of Modern Physics E, 17 (2008) 425-433.

3. **I. Ziaeian**, H. Noshad, *Theoretical study of the effect of damping force on higher stability regions in a Paul trap,* International journal of Mass Spectrometry, (2010) 289.

4. **I. Ziaeian** and H. Noshad, *Ion separation in a Paul trap in the presence of damping force,* Iranian Journal of Physics Research, 10 (2010) 25- 31.

5. **I. Ziaeian**, S.M. Sadat Kiai, M. Ellahi, S. Sheibani, A. Safarian, S. Farhangi, *Theoretical study of the effect of ion trap geometry on the dynamic behavior of ions in a Paul trap,* International Journal of Mass Spectrometry, 304 (2011) 25-28.

6. S. Seddighi Chahrborj, S. M. Sadat Kiai, M. R. Abu Bakar, **I. Ziaeian** and Y. Gheisari, *Homotopy analysis method to study a quadrupole mass filter,* Journal of Mass Spectrometry, (2012) 2041.

7. S. Seddighi Chaharborja,b, S.M. Sadat Kiai, M.R. Abu Bakara, **I. Ziaeian**, I. Fudziah, *A new impulsional potential for a Paul ion trap,* International Journal of Mass Spectrometry, 309 (2012) 63-69.

8. **I. Ziaeian**, S.M. Sadat Kiai, M. Zebardast, A.R. Goosheh*, Modification of the stability regions in stretched Paul ion trap by damping force*, Nuclear science and Technology Research Institute, 78 (2017) 12-17.

Selected talk

1. **I. Ziaeian**, K. Tőkési. (July 16, 2019) *Classical Simulation of the Collision Between* Be^{+4} *and H*. The 26th International Symposium on Ion-Atom Collisions-virtual format (ISIAC 2019), Sorbonne University, Paris, France

Seminar talk

1. **I. Ziaeian** and K. Tőkési (October 14, 2021). *Study the cross sections of the* Be^{4+} *and ground state hydrogen collisions in the thermonuclear fusion plasmas using the classical models*. Atomic Energy Research Institute, Centre for Energy Research Eötvös Loránd Research Network Fusion Plasma Physics Department, Budapest, Hungary.

Conference publications and Posters

1. **I. Ziaeian**, K.Tőkési, (August 24, 2020) *State-selective Charge Exchange Cross Section in* Be^{+4} *+ H(1s) Collision, Part I*, The 30th Summer school and International Symposium on the Physics of Ionized Gases (SPIG 2020), Sabac, Serbia

2. **I. Ziaeian** and K. Tőkési. (July 16, 2021). *State selective charge exchange cross section in* Be^{4+} *+ H(1s) collisions.* The 27th International Symposium on Ion-Atom Collisions-virtual format (ISIAC 2021), Faculty of Physics, Babes-Bolyai University. Cluj-Napoca, Romania.

3. **I. Ziaeian** and K. Tőkési. (October 5, 2021). *State selective charge exchange cross section in* Be^{4+} *+ H(1s) collisions.* The 2nd Annual virtual meeting on the Molecular Dynamics in the Gas Phase (MD-GAS 2021) – Cost Action CA18212.

1. Introduction

In recent decades, ITER has been developed to take a significant step in supplying energy cleanly and safely by the implementation of fusion power plants [1-4]. The temperature and pressure inside the thermonuclear reactor are extremely high. Since the reactor wall directly faces the hot plasma, it requires materials with special properties. Due to the unique thermal properties, beryllium is considered as the first wall of the ITER [5, 6]. Chemical and physical erosion of the first wall releases beryllium atoms and several molecular species, which eventually lead to the presence of fully stripped beryllium ions in the plasma core.

Therefore, the accurate knowledge of the interaction between charged particles and hydrogen atoms is the focus of fusion plasma research, including when energetically neutral hydrogen is injected into the plasma for heating and diagnostic purposes [7]. Significant atomic processes whose knowledge is essential in fusion research are ionization, electron capture, state-selective electron capture, and excitation. The target ionization channel is the process when the target loses electron during the collision with a projectile particle. Electron capture channel is a process in which the projectile captures one electron into its bound state from the target. The excitation channel is the process in which the target electron remained bound after the collision but its energy level changes from a lower energy to a higher one.

The cross sections in a collision between charged particles and atomic hydrogen have been studied using various quantum-mechanical models and methods such as applying the quantum-mechanical molecular orbital close-coupling (QMOCC) [8], the atomic orbital close-coupling (AOCC) [9], the hyper spherical close-coupling (HSCC) models [10], using the solution of the time dependent Schrödinger equation (TDSE) [11], the lattice time dependent Schrödinger equation (LTDSE) [12], the classical over barrier model (COBM) [13], one-electron diatomic molecule (OEDM) [14], and the boundary corrected continuum intermediate state (BCCIS) [15]. However, in many cases, quantum-mechanical calculations are very complicated and unfeasible.

Therefore, as an alternative calculation scheme and due to the simplicity of calculations, classical models have been developed. In my research work, I also used classical approaches to calculate the collisional cross sections related to fusion research in various collision channels.

During my PhD studies, I performed my calculations based on the standard three-body classical trajectory Monte Carlo (CTMC) and quasi-classical trajectory Monte Carlo (QCTMC) models. The CTMC method is based on the calculation of a large number of individual particle

orbits when the initial atomic states are chosen randomly. The cross sections for a given final channel can be obtained from the results of the trajectory calculations [16, 17]. The QCTMC model was proposed by Kirschbaum and Wilets in 1980. This model represents one step further towards a better description of the classical atomic collisions. In the QCTMC model, the Heisenberg correction term is added via a model potential to the standard classical Hamiltonian of the collision system to mimic the Heisenberg uncertainty principle. The effective potential enforce the Heisenberg uncertainty principle $rp \geq \xi_H \hbar$, where r and p are the distance and momentum of an electron with respect to a nucleus and ξ_H is a constant.

My dissertation is organized as follows: in the second chapter, I describe the nuclear fusion process and I explain why my thesis topic is related to nuclear fusion research. In the third chapter, I briefly summarize the theoretical background of the classical collision. In the fourth chapter, I describe the Monte Carlo simulation. In the fifth and sixth chapters, I explain the classical trajectory Monte Carlo and quasi-classical trajectory Monte Carlo models, respectively. In the seventh chapter, I present the new results of my PhD research work. The dissertation is finished with a summary, an outlook, acknowledgment, bibliography, and appendix.

2. Nuclear fusion

In a fusion reactor, the energy is produced by the joining of two light atomic nuclei. Regarding the Einstein relation, $E = mc^2$, a small amount of mass is converted into a large amount of energy in a fusion reaction between two nuclei (see Figure 2.1). I note that the mass can be converted to energy also by nuclear fission, the splitting of a heavy nucleus.

The electrical repulsive Coulomb force inhibits the fusion reactions. This force acts between two same-sign charged nuclei. For fusion to occur, the two nuclei must approach each other at high speed to overcome their electrical repulsion so that the short-range strong force dominates. If two nuclei get too close, enough temperature is needed to break down the Coulomb barrier between them to be fussed. To reach this temperature, the fusion nuclei must be under high pressure. In this condition, these nuclei gain energy to bump into each other, but it's still not enough for fusion. Fusion is inherently a quantum mechanical process. The quantum tunneling effect explains how fusion can happen. This effect enhances the fusion process as even nuclei which have not enough kinetic energy to overcome the Coulomb barrier.

A large number of nuclei must undergo fusion to produce large amounts of energy. This condition needs a very energetic fuel which is made by heating an ordinary gas at an extremely high temperature. The result is an ionized gas consisting of free electrons and positive ions. This ionized gas is in a plasma state, the fourth state of matter.

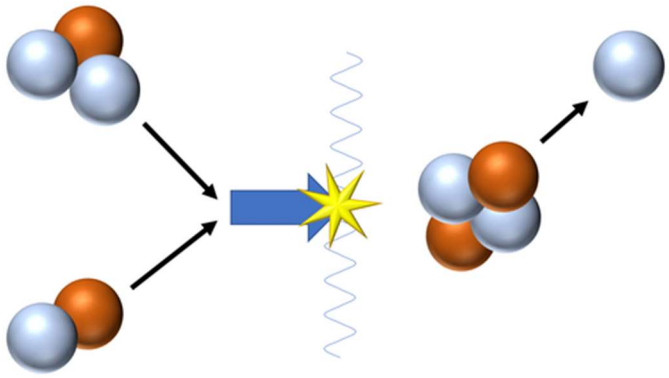

Figure 2.1. Schematic of the nuclear fusion process.

2.1 Nuclear fusion reactors

Nowadays, the human dream is to produce clean energy by developing a fusion reactor. Fusion offers several advantages such as less radioactive of the products of the fusion and its inherent safety. Because there is a very little amount of fusion material in the reactor at any given time, the possibility of a fusion reaction will be very low. Under these conditions, even the small perturbations in the reactor would probably terminate it [18]. There is an extremely hot plasma (about 10^8 kelvins) at the core of experimental fusion reactors. Fusion occurs between the nuclei, with the electrons present only to maintain macroscopic charge neutrality. A plasma loses energy through processes such as conduction, convection, and radiation, so keeping a hot plasma requires that fusion reactions add enough energy to balance the energy losses. In order to achieve this balance, the product of the plasma's density and its energy confinement time (the time it takes the plasma to lose its energy if unreplaced) must exceed a critical value. The most important fusion challenges are summarized as follows:

1. Heating of the reacting mixture to a very high temperature, to overcome the Coulomb repulsive forces of positively charged nuclei. This challenge is that of providing a lot of energy for the reactants. This is why the reaction fusion is called thermonuclear reaction.
2. Compressing the mixture to a high density so that the probability of collision among the nuclei can be high; and
3. Set the energy confinement time to insulate the plasma.

The second and third challenges are collectively referred to as the confinement problem. It is clear that the reacting mixture into the plasma cannot be confined in solid vessels. Because these vessels would carry away the heat necessary to reach the very high ignition temperatures. Instead, magnets (magnetic confinement) and lasers (inertial confinement) are used.

2.2 ITER

ITER is one of the most ambitious energy projects in the world aimed to generate energy by the fusion reaction. "ITER is established at Cadarache (France) to demonstrate the technical and scientific feasibility of controlled fusion. ITER is the first magnetic confinement fusion reactor to require a construction license decree under French nuclear facilities regulations. The decree was passed in 2012 after the institute for radiological protection and nuclear safety conducted an in-depth assessment of the safety and radiation protection measures adopted by the operator. Due to its design and operation, ITER presents unique safety and radiation

protection issue including the risk of dust and hydrogen isotope explosion, plasma malfunction, magnetic system failures, etc" [19]. Figure 2.2 shows the schematic of the ITER.

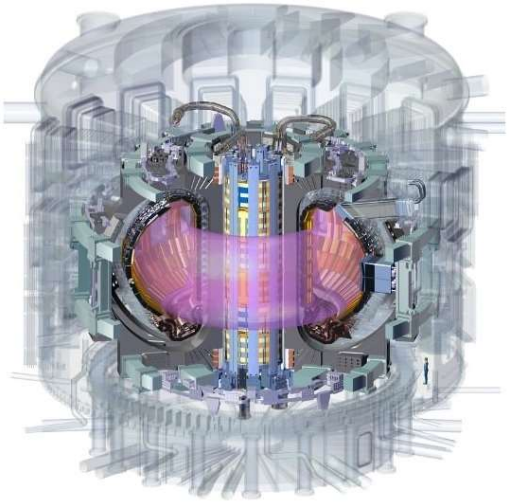

Figure 2.2. Schematic of the ITER.

2.3 Tokamak

A tokamak is a device, which uses a powerful magnetic field to confine plasma in the shape of a torus. The tokamak is one of several types of magnetic confinement devices developed to produce controlled thermonuclear fusion power [20, 21]. Figure 2.3 shows the schematic of the tokamak.

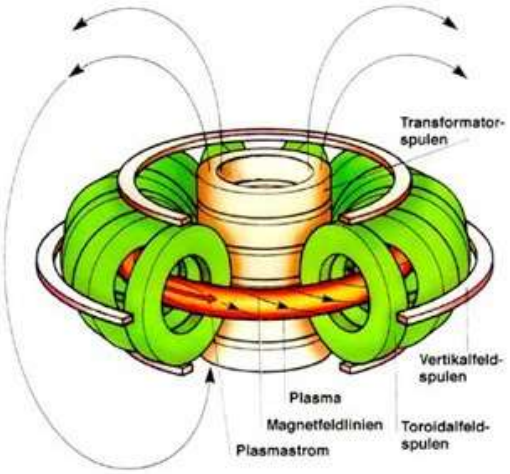

Figure 2.3. Schematic of the tokamak.

In a nuclear fusion facility using the tokamak magnetic confinement concept, fusion reactions take place inside a toroidal plasma. To produce magnetic confinement, two magnetic fields act on plasma such as 1) poloidal magnetic field (B_p) produced by an electric current in the plasma and 2) toroidal magnetic field (B_t) produced by toroidal field coils. Regarding both magnetic fields, helical magnetic field lines are produced around which ions and electrons spiral, thereby containing the plasma within a sealed toroidal vessel is called a vacuum vessel. Figure 2.4 shows the principle of magnetic confinement of a plasma in a tokamak.

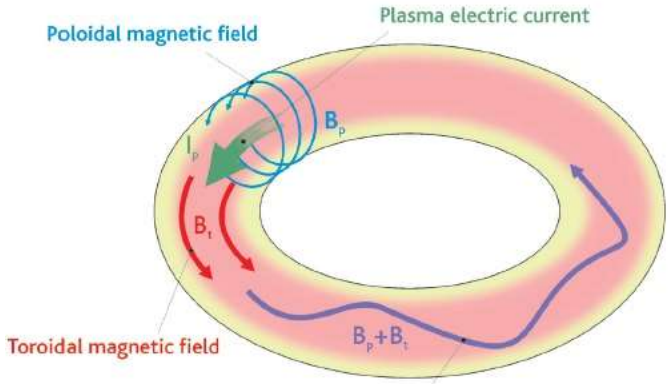

Figure 2.4. Principle of magnetic confinement of a plasma in a tokamak.

2.4 Wall panel in fusion reactor

The inner surface of the ITER fusion reactor is covered with several wall panels consisting of two sections that provide plasma protection and heat transfer, respectively. To increase the plasma operation yield, strong magnetic fields are used to keep the plasma away from the walls; these are produced by superconducting coils surrounding the vessel, and by an electrical current through the plasma.

The blanket covers the inner surfaces of the vacuum vessel, protect the vessel and the superconducting toroidal magnets from the heat and neutron flux produced by the fusion reactions (see Figure 2.5). The neutrons are slowed down in the blanket where their kinetic energy is transformed into heat energy and collected by the water coolant. In a fusion power plant, this energy will be used for electrical power production. For ease of maintenance on the interior of the vacuum vessel, the blanket wall is modular. It consists of several segments. Each segment has a detachable first wall, which directly faces the hot plasma. Because of its unique physical properties, beryllium has been chosen to cover the first wall

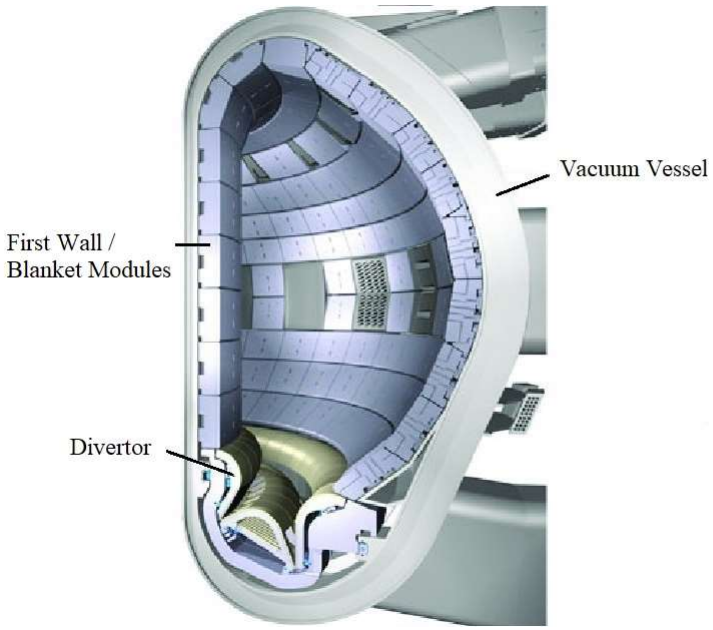

Figure 2.5. ITER vacuum vessel showing the blanket modules.

"Panel fabrication has many challenging steps, including bonding the beryllium armor tiles to the copper alloy heat sink, manufacturing an intricate cooling circuit, integrating mechanical and hydraulic connections, and isolating the coatings. Bonding the beryllium armor tile to the copper alloy heat sink is especially challenging, for two reasons. Beryllium and copper have different coefficients of thermal expansion, so large shear stresses develop in the bond when the temperature changes. The stresses grow very large, due to the singularity at the free edge of the bond. The bonding is subject to temperatures changes of several hundred degrees during manufacturing and operation. The tile bonding joint must withstand stresses close to or beyond the yield strength. What is more, the phase diagram has brittle intermetallic and intermediate metastable phases. Industrial experience of beryllium-to-copper bonding for commercial applications has been developed during the last 20 years using small scale mock-ups" [22].

2.5 Impurities in fusion reactor

Beryllium is considered as the armor material for plasma facing components (PFCs) in the first wall of the ITER (see Figure 2.6) [1]. Chemical and physical erosion of the first wall releases beryllium atoms and several molecular species, which eventually lead to the presence of fully

stripped beryllium ions in the plasma core. These impurities cool the plasma by re-emit ultraviolet radiation or X-radiation and thus reduce the fusion yield [23, 24]. Beryllium is attractive as a plasma facing reactor material because of its low atomic number (i.e., low potential for radiative plasma power losses), excellent gettering properties concerning oxygen (unavoidably present in any fusion plasma), and adequate thermo-mechanical and erosion properties when exposed to plasma energy and particle fluxes. The presence of large amount of beryllium impurity has deleterious effect on the fusion plasma performance for two reasons: 1) dilution of the D-T mixture, 2) energy loss due to enhanced Bremsstrahlung. The inelastic collision processes between Be^{q+} ions and H are particularly important when energetic neutral hydrogen is injected into the plasma for heating and diagnostic purposes [7]. Therefore, the accurate description and knowledge of these interactions are extremely important for fusion research.

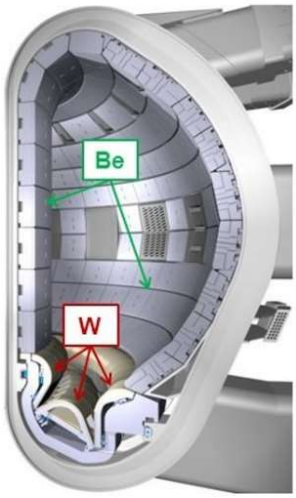

Figure 2.6. Placing beryllium in wall panels in ITER.

2.6 Detection of impurities by charge exchange recombination spectroscopy

In the fusion reactor, beryllium ion as an impurity, captures one electron into its bound state from the hydrogen atom. The radiative decay of excited impurity ions can be the source for the energy loss of the plasma and can cool the plasma. These radiative decays are detected and analyzed by the charge exchange recombination spectroscopy (CXRS).

CXRS is the most successful tool for the measurement of impurity ion temperature, rotation, and density profiles [25, 26]. This device uses optical detectors in the visible range, and it has to view the path of the neutral beam in the plasma. The emission is based on the resonant charge

exchange process between a fast neutral atom injected into the tokamak and the ions inside the hot plasma core. The rotation measurements are obtained via Doppler shift spectroscopy from the spectral position with respect to an un-shifted reference, the temperature measurements are based on the broadening of the spectra, while the impurity density can be calculated based on the intensity.

3. Classical collision theory

In the collision between two bodies, the conservation of momentum is a general law that should be considered. If there are no external forces acting in some direction, the component of the momentum of the system along that direction is constant. In particular, we consider cases in which the objects do not stick together. The momentum along a certain direction may still be constant but the mechanical energy of the system may change. We will begin our analysis by considering two-particle collisions. We use the concept that the relative velocity between two particles is independent of the choice of reference frame. Since the change in kinetic energy only depends on the change of the square of the relative velocity, therefore is independent of the choice of reference frame. In particular, we will characterize the types of collisions by the change in kinetic energy and analyse the possible outcomes of the collisions.

3.1 Relative reference frames and velocities

Imagine $\vec{R}$ is the vector from the origin of frame S to the origin of reference frame S'. Denote the position vector of particle i with respect to the origin of the reference frame S by $\vec{r_i}$ and similarly, denote the position vector of particle i with respect to the origin of reference frame S' by $\vec{r_i}'$ (see Figure 3.1).

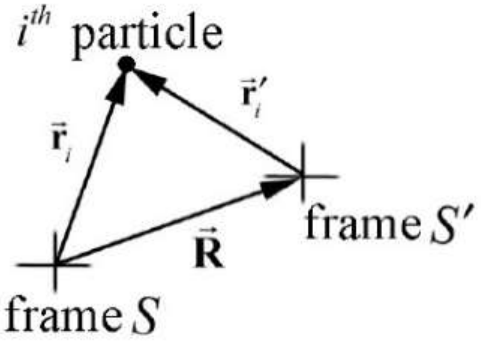

Figure 3.1. Position vector of i^{th} particle in two-reference frame.

The position vectors are related by

$$\vec{r_i} = \vec{r_i}' + \vec{R} \, . \tag{3.1}$$

Assume the boost velocity between the two reference frames is constant. Then, the relative acceleration between the two references is zero.

Suppose the i^{th} particle in Figure 3.1 is moving; then the observers in different reference frames will measure different velocities. Denote the velocity of i^{th} particle in frame S by $\vec{v_i}$, and the velocity of the same particle in frame $\acute{S}$ by $\vec{v_i}'$. Taking derivative, the velocities of the particles in two different reference frames are related to

$$\vec{v_i} = \vec{v_i}' + \vec{V}. \tag{3.2}$$

3.2 Center of mass reference frame

$\vec{R}_{cm}$ shows the vector from the origin of frame S to the center of mass of the system of particles that we call S_{cm}. Denote the position vector of particle i with respect to the origin of reference frame S by $\vec{r_i}$ and the position vector of particle i with respect to the origin of reference frame S_{cm} by $\vec{r}_{cm.i}$ (see Figure 3.2).

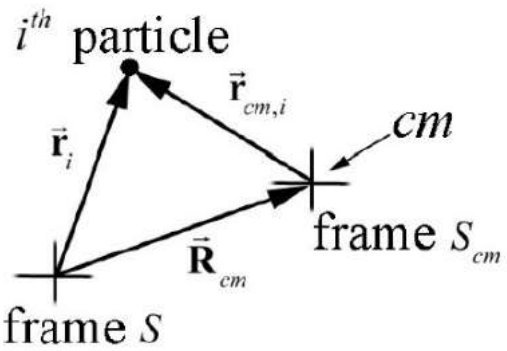

Figure 3.2. Position vector of i^{th} particle in the centre of mass reference frame.

The position vector of particle i in the centre of mass frame is given by

$$\vec{r}_{cm.i} = \vec{r}_i - \vec{R}_{cm}. \tag{3.3}$$

The velocity of particle i in the centre of mass reference frame is defined by

$$\vec{v}_{cm.i} = \vec{v}_i - \vec{V}_{cm}. \tag{3.4}$$

The centre of mass reference frame is the most convenient reference frame to analyse the collision in many collision problems and I also used this frame in the basic of my calculations.

3.3 Relative velocities

We consider two particles of mass m_1 and m_2 interacting via some force (see Figure 3.3)

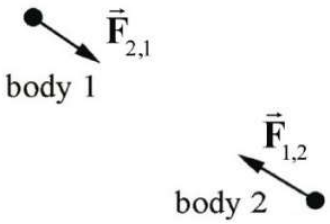

Figure 3.3. Two interacting particles

Choose a coordinate system (see Figure 3.4) in which the position vector of body 1 and body 2 are given by $\vec{r}_1$ and $\vec{r}_2$, respectively. The relative position of body 1 with respect to body 2 is given by $\vec{r}_{1.2} = \vec{r}_1 - \vec{r}_2$.

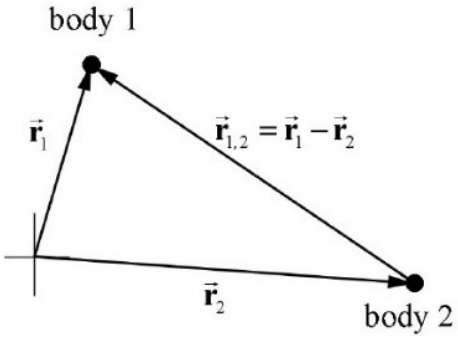

Figure 3.4. Coordinate system for two bodies

During the interaction, body 1 and body 2 are displaced by $d\vec{r}_1$ and $d\vec{r}_2$, respectively. Therefore the relative displacement of the two bodies during the interaction is given by $d\vec{r}_{1.2} = d\vec{r}_1 - d\vec{r}_2$. The relative velocity between the particles is given by $\vec{v}_{1.2} = \vec{v}_1 - \vec{v}_2$.

We show that the relative velocity between the two particles is independent of the choice of reference frame providing that the reference frames are relatively inertial. The relative velocity $\vec{v}'_{1.2}$ in reference frame S' is determined as follows:

$$\vec{v}_{1.2} = \vec{v}_1 - \vec{v}_2 = \left(\vec{v}'_1 + \vec{V}\right) - \left(\vec{v}'_2 + \vec{V}\right) = \vec{v}'_1 - \vec{v}'_2 = \vec{v}'_{1.2}\,. \tag{3.5}$$

and is equal to the relative velocity in frame *S*. Therefore, for a two-particle interaction, the relative velocity between the two vectors is independent of the choice of relatively inertial

reference frames. When two particles of mass m_1 and m_2 interact, the change of kinetic energy between the final state B and the initial state A due to the interaction force is equal to

$$\Delta K = \frac{1}{2}\mu(v_B^2 - v_A^2), \tag{3.6}$$

where $v_B \equiv |(\vec{v}_{1.2})_B| = |(\vec{v}_1)_B - (\vec{v}_2)_B|$ denotes the relative velocity in the state B and $v_A \equiv |(\vec{v}_{1.2})_A| = |(\vec{v}_1)_A - (\vec{v}_2)_A|$ denotes the relative velocity in state A, and $\mu = m_1 m_2/(m_1+m_2)$ is the reduced mass. Although kinetic energy is a dependent quantity, by expressing the change of kinetic energy in terms of the relative velocity, then the change in kinetic energy is independent of the choice of relatively inertial reference frames.

3.4 Characterizing the collisions

In a collision, the ratio of the magnitudes of the initial and final relative velocities is called the coefficient of restitution and denoted by the symbol ε,

$$\varepsilon = \frac{v_f}{v_i}. \tag{3.7}$$

According to the coefficient of restitution, one can define the elastic and inelastic collisions as follows:

1- Collisions in which there is no change in kinetic energy, $\varepsilon = 1$, are called elastic collisions.

2- Collisions in which the kinetic energy decreases, $\varepsilon < 1$, are called inelastic collisions.

3- Collisions in which the relative final velocity is zero, $\varepsilon = 0$, are called totally inelastic collisions. In this case two objects stick together after the collision.

4- Collisions in which the magnitude of the final relative velocity is greater than the magnitude of the initial relative velocity, $\varepsilon > 1$, are called super-elastic collisions.

Due to the importance of elastic and inelastic collisions, I describe them in detail in subsection 3.5.

3.5 Elastic and inelastic collision theory

Momentum is a vector quantity, which means that direction is a necessary part of the data. For a system of more than one particle, the total momentum is the vector sum of the individual momenta:

$$\vec{p} = \overrightarrow{p_1} + \overrightarrow{p_1} + \cdots \tag{3.8}$$

Therefore, to make sure that we consider the direction of motion of each particle, we add the momenta of all the particles together. One of the most fundamental laws of physics is that the total momentum, $\vec{p}$, of any system of particles is conserved, or constant, as long as the net external force on the system is zero.

For a system of many particles, the total kinetic energy is simply the sum of the individual kinetic energies of each particle:

$$KE = KE_1 + KE_2 + \ldots \tag{3.9}$$

Another fundamental law of physics is that the total energy of a system is always conserved. However, within a given system one form of energy may be converted to another. Kinetic energy alone is often not conserved.

There are two basic kinds of collisions, elastic and inelastic. In an elastic collision, two or more bodies collide together and then move apart again with no loss in kinetic energy. In an inelastic collision, the bodies collide and come apart again, but some kinetic energy is lost. That is, some of the kinetic energy is converted to another form of energy.

Consider a one-dimensional elastic collision between two objects moving in the *x*-direction. One object, with mass m_1 and initial *x*-component of the velocity $v_{1x.i}$, collide with an object of mass m_2 and initial *x*-component of the velocity $v_{2x.i}$. The scalar components $v_{1x.i}$ and $v_{2x.i}$ can be positive, negative, or zero. No forces other than the interaction force between the objects act during the collision. After the collision, the final *x*-component of the velocity $v_{1x.f}$ and $v_{2x.f}$. We call this reference frame the 'laboratory reference frame'.

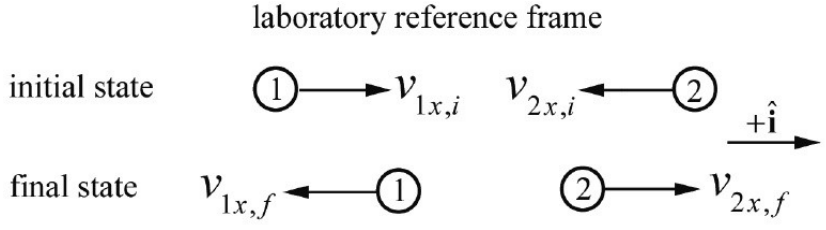

Figure 3.5. One-dimensional elastic collision, laboratory reference frame.

For the collision depicted in Figure 3.5, $v_{1x.i} > 0$, $v_{2x.i} < 0$, $v_{1x.f} < 0$, and $v_{2x.f} > 0$. Because there are no external forces in the *x*-direction, momentum is constant in the *x*-direction. Equating the momentum components before and after the collision gives the relation

$$m_1 v_{1x.i} + m_2 v_{2x.i} = m_1 v_{1x.f} + m_2 v_{2x.f} \ . \tag{3.10}$$

Due to the elastic collision, kinetic energy is constant. Equating the kinetic energy before and after the collision gives the relation

$$\frac{1}{2} m_1 v_{1x.i}^2 + \frac{1}{2} m_2 v_{2x.i}^2 = \frac{1}{2} m_1 v_{1x.f}^2 + \frac{1}{2} m_2 v_{2x.f}^2 \ . \tag{3.11}$$

By solving Equations (3.10) and (3.11), the final *x*-component of the velocity $v_{1x.f}$ and $v_{2x.f}$ are dines as follows:

$$v_{1x.f} = \frac{m_1 - m_2}{m_1 + m_2} v_{1x.i} + \frac{2m_2}{m_1 + m_2} v_{2x.i} \tag{3.12}$$

$$v_{2x.f} = \frac{m_2 - m_1}{m_1 + m_2} v_{2x.i} + \frac{2m_1}{m_1 + m_2} v_{1x.i} \ . \tag{3.13}$$

It is worth noting that these equations were the basis of my calculations in the simulation of elastic and inelastic collisions.

3.6 Direct collision

Collisions between two bodies in which the direction of the motion of each body is along their common normal at the point of contact are called direct collision (see Figure 3.6). When the direction of motion of either or both is not along the common normal, the impact is oblique.

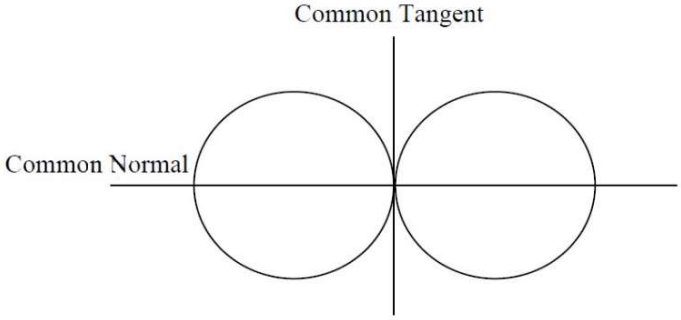

Figure 3.6. Schematic of direct collision between two bodies.

If two bodies of mass m_1 and m_2, moving with initial velocities u_1 and u_2 respectively, collide directly and v_1 and v_2 be their velocities after the collision (see Figure 3.7). Then

$$\frac{v_1-v_2}{u_1-u_2} = -\varepsilon \;\rightarrow v_1 - v_2 = -\varepsilon(u_1 - u_2)\,, \tag{3.14}$$

where ε is called the coefficient of restitution of the bodies.

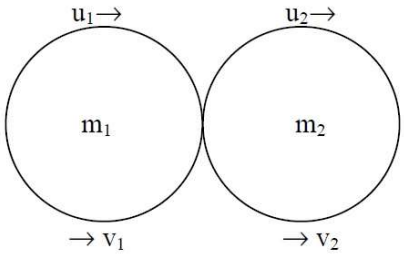

Figure 3.7. Schematic of directly collision between two bodies regarding to their velocities.

If two bodies of mass m_1 and m_2, move with velocities u_1 and u_2 in the directions inclined at angles α and β respectively to their common normal. Let v_1 and v_2 be their velocities in the direction inclined at angles θ and φ respectively after the collision (see Figure 3.8).

$$\frac{v_1 cos\theta - {}_2 cos\varphi}{u_1 cos \quad {}_2 cos\beta} = -\varepsilon \;\rightarrow\; v_1 cos\theta - v_2 cos\varphi = -\varepsilon(u_1 cos\alpha - u_2 cos\beta)\,. \tag{3.15}$$

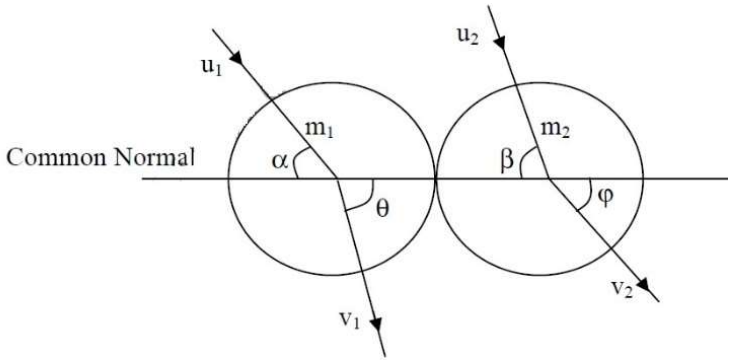

Figure 3.8. Schematic of oblique collision between two bodies.

The law on conservation of momentum for direct and oblique collisions are as follows:

$$m_1v_1 + m_2v_2 = m_1u_1 + m_2u_2 \qquad \text{(For Direct Collision)} \tag{3.16}$$

$$m_1v_1\cos\theta + m_2v_2\cos\varphi = m_1u_1\cos\alpha + m_2u_2\cos\beta \quad \text{(For Oblique Collision)} \tag{3.17}$$

3.7 Collision in one-dimension between two objects – center of mass reference frame

In this subsection we explain the velocity in the center of mass (CM) frame. The *x*-component of the velocity of the center of mass is.

$$v_{x.cm} = \frac{m_1 v_{1x.i} + m_2 v_{2x.i}}{m_1 + m_2}. \tag{3.18}$$

with respect to the center of mass, the *x*-components of the velocities of the objects are

$$v'_{1x.i} = v_{1x.i} - v_{x.cm} = (v_{1x.i} - v_{2x.i}) \frac{m_2}{m_1 + m_2} \tag{3.19}$$

$$v'_{2x.i} = v_{2x.i} - v_{x.cm} = (v_{2x.i} - v_{1x.i}) \frac{m_1}{m_1 + m_2}. \tag{3.20}$$

In the CM frame, the momentum of the system is zero before the collision and hence the momentum of the system is zero after the collision. For an elastic collision, the only way for both momentum and kinetic energy to be the same before and after the collision is either the objects have the same velocity or to reverse the direction of the velocities as shown in Figure 3.9.

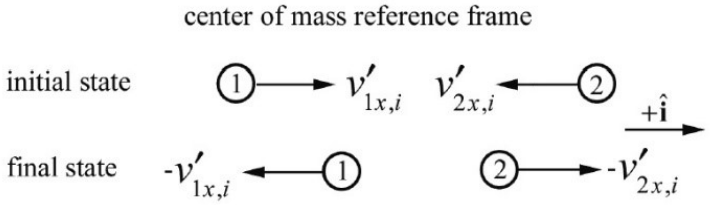

Figure 3.9. One-dimensional elastic collision in the centre of mass reference frame.

In the CM frame, the final *x*-components of velocities are

$$v'_{1x.f} = -v'_{1x.i} = (v_{2x.i} - v_{1x.i}) \frac{m_2}{m_1 + m_2} \tag{3.21}$$

$$v'_{2x.f} = -v'_{2x.i} = (v_{2x.i} - v_{1x.i}) \frac{m_1}{m_1 + m_2}. \tag{3.22}$$

Therefore, to calculate the momentum of bodies before and after the collision in center of mass frame, Equations (3.19) – (3.22) are used.

The final *x*-components of the velocities in the 'laboratory frame' are given by

$$v_{1x.f} = v'_{1x.f} + v_{x.cm} = v_{1x.i} \frac{m_1 - m_2}{m_1 + m_2} + v_{2x.i} \frac{2m_2}{m_1 + m_2}. \tag{3.23}$$

4. Monte Carlo simulation

Monte Carlo (MC) technique is a numerical method that uses random numbers to solve mathematical problems for which an analytical solution is not known. The first paper, “The Monte Carlo Method” by Metropolis and Ulam, has appeared in 1949 [27] even though some statistical problems had previously been solved using random numbers. Because simulation of random numbers is very time consuming, MC has only been implemented with the advent of computers.

4.1 Random numbers

At the heart of any Monte Carlo, a method is a random number generator: a procedure that produces an infinite stream

$$U1, U2, U3, \ldots \sim^{iid} \text{Dist}$$

of random variables that are independent and identically distributed (iid) according to some probability distribution Dist. When this distribution is the uniform distribution on the interval (0,1) (that is, Dist = U (0, 1)), the generator is said to be a uniform random number generator. Most computer languages already contain a built-in uniform random number generator. The user is typically requested only to input an initial number, called the seed, and upon invocation, the random number generator produces a sequence of independent uniform random variables on the interval (0, 1).

"The concept of an infinite iid sequence of random variables is a mathematical abstraction that may be impossible to implement on a computer. The best one can hope to achieve in practice is to produce a sequence of “random” numbers with statistical properties that are indistinguishable from those of a true sequence of iid random variables. Although physical generation methods based on universal background radiation or quantum mechanics seem to offer a stable source of such true randomness, the vast majority of current random number generators are based on simple algorithms that can be easily implemented on a computer. Such algorithms can usually be represented as a tuple (S, f, μ, U, g), where

- S is a finite set of states,
- f is a function from S to S,
- μ is a probability distribution on S,

- U is the output space; for a uniform random number generator U is the interval (0,1)
- g is a function from S to U " [28].

"A random number generator then has the following structure:

1. Initialize: Draw the seed S0 from the distribution μ on S. Set t = 1.
2. Transition: Set $S_t = f(S_{t-1})$.
3. Output: Set $U_t = g(S_t)$.
4. Repeat: Set t = t + 1 and return to Step 2" [28].

The algorithm produces a sequence U1, U2, U3, . . . of pseudorandom numbers. Starting from a particular seed, the sequence of states (and hence of random numbers) must repeat itself, because the state space is finite. The smallest number of steps taken before entering a previously visited state is called the random number generator period length [28].

What constitutes a good random number generator depends on many factors. It is always advisable to have a different types of random number generators available, as different applications may require different features of random generators. The following are some of the desirable or indeed essential properties of a good uniform random number generator [28]:

1. Pass the statistical tests: The ultimate goal is that the generator should produce a stream of uniform random numbers that are indistinguishable from a true uniform iid sequence. Although from a theoretical point of view this criterion is too inaccurate and even impossible, but from a practical point of view it means that the generator should pass a battery of simple statistical tests designed to detect deviations from uniformity and independence.
2. Theoretical support: A good generator should be based on sound mathematical principles that allow accurate analysis of the basic properties of the generator.
3. Reproducible: An important feature is that the random numbers streams are repeatable without the need to store a complete stream in memory. This is essential for testing and variance reduction techniques. Physical generation methods cannot be repeated unless the entire stream is recorded.
4. Fast and efficient: The generator should generate random numbers quickly and efficiently and requires little storage in computer memory. Many Monte Carlo techniques require billions or more random numbers to optimize and estimate. Current physical generation methods are no comparable in speed to simple algorithmic generators.
5. Large period: The period of a random number generator should be extremely large — on the order of 10^{50} — to avoid duplicate problems and dependencies. Most primitive algorithmic random number generators were fundamentally insufficient in this regard.

6. Multiple streams: In many applications, it is necessary to run several independent random streams in parallel. A good random number generator should have easy supplies for multiple independent streams.
7. Cheap and easy: A good random number generator should be cheap and not require expensive external equipment. In addition, it should be easy to install, implement, and run. In general, such a random number generator is also more easily portable on various computer platforms and architectures.
8. Not produce 0 or 1: A desirable property of a random number generator is that both 0 and 1 are removed from the random numbers sequence. This is to avoid division by 0 or other numerical complications.

Two categories of generators that have good overall performance are [28]:
1. Combined multiple recursive generators, some of which have excellent statistical properties, are simple, have large cycles, support for multiple streams, and are relatively fast.
2. Twisted general feedback shift register generators, some of which have very excellent matched distribution properties, are among the fastest generators available (due to their essentially binary implementation), and can have extremely long periods.
In general, a good uniform number generator has good overall performance, in terms of the criteria mentioned above, but does not perform best in all of these criteria. In choosing an appropriate generator, it pays to remember the following.
• Faster generators are not necessarily better (indeed, often the contrary is true).
• A small period is in general bad, but a larger period is not necessarily better.
• Good equidistributional is a necessary requirement for a good generator but not a sufficient requirement.

4.2 Random numbers generators

4.2.1 Linear congruential generators

A linear congruential generator (LCG) is a random number generator of the form of Algorithm, with state $S_t = X_t \in \{0, \ldots, m-1\}$ for some strictly positive integer m called the modulus, and state transitions

$$X_t = (aX_{t-1} + c) \bmod m, \quad t = 1, 2, \ldots, \tag{4.1}$$

where the multiplier a and the increment c are integers. Applying the modulo-m operator in (4.1) means that $aX_{t-1} + c$ is divided by m, and the remainder is taken as the value for X_t. When

$c = 0$, the generator is called a multiplicative congruential generator. I note that the multiplier and increment may be chosen in the set $\{0, \ldots, m-1\}$. Most existing implementations of LCGs are of this form — in general, the increment does not have a large impact on the quality of an LCG. The output function for an LCG is simply.

$$U_t = \frac{X_t}{m}. \tag{4.2}$$

4.2.2 Multiple-recursive generators

A multiple-recursive generator (MRG) of order k, is a random number generator of the form of Algorithm, with state $S_t = X_t = (X_{t-k+1}, \ldots, X_t) \in \{0, \ldots, m-1\}^k$ for some modulus m and state transitions defined by [28]:

$$X_t = (a_1 X_{t-1} + \cdots + a_k X_{t-k}) \bmod m, \quad t = k, k+1, \ldots, \tag{4.3}$$

where the multipliers $\{a_i, i = 1, \ldots, k\}$ lie in the set $\{0, \ldots, m-1\}$. The output function is often taken as

$$U_t = \frac{X_t}{m}. \tag{4.4}$$

The maximum period length for this generator is $m^k - 1$, which is obtained if (a) m is a prime number and (b) the polynomial $p(z) = z^k - \sum_{i=1}^{k-1} a_i z^{k-i}$ is primitive using modulo m arithmetic. To yield fast algorithms, all but a few of the $\{a_i\}$ should be 0.

4.2.3 Matrix congruential generators

An MRG can be interpreted and implemented as a matrix multiplicative congruential generator, which is a random number generator of the form of Algorithm, with state $S_t = X_t \in \{0, \ldots, m-1\}^k$ for some modulus m, and state transitions defined by [28]

$$X_t = (AX_{t-1}) \bmod m, \qquad t = 1, 2, \ldots, \tag{4.5}$$

where A is an invertible $k \times k$ matrix and X_t is a $k \times 1$ vector. The output function is often taken as

$$U_t = \frac{X_t}{m}. \tag{4.6}$$

Yielding a vector of uniform numbers in (0, 1). Hence, here the output space U for the algorithm is $(0, 1)^k$. For fast random number generation, the matrix A should be sparse.
To see that the multiple-recursive generation is a special case, take

$$A = \begin{pmatrix} 0 & 1 & \dots & 0 \\ \vdots & \vdots & \ddots & \vdots \\ 0 & 0 & \dots & 1 \\ a_k & a_{k-1} & & a_1 \end{pmatrix} \text{ and } \quad \mathrm{X}_t = \begin{pmatrix} X_t \\ X_{t+1} \\ \vdots \\ X_{t+k-1} \end{pmatrix}. \tag{4.7}$$

Obviously, the matrix multiplicative congruential generator is the k-dimensional generalization of the multiplicative congruential generator. A similar generalization of the multiplicative recursive generator — replacing the multipliers $\{a_i\}$ with matrices, and the scalars $\{X_t\}$ with vectors in (4.3) —yields the class of matrix multiplicative recursive generators.

It is worth noting that, in section 4.2, I explained the various random number generators, but I used a linear congruential generator (see subsection 4.2.2) to generate random numbers in my calculations.

4.3 Random variables

"The “Monte Carlo” name is derived from the city, with the same name, in the Principality of Monaco, well known for its casinos. This was because the roulette wheel was the simplest mechanical device for generating random numbers" [29, 30].

Even though “random variable” implies that one cannot predict its value, the distribution may well be known. The distribution of a random variable gives the probability of a given value [31]. The probability distribution of a discrete random variable is a list of probabilities associated with each of its possible values. It is also sometimes called the probability function or the probability mass function. (Valerie J. Easton and John H. McColl’s Statistics Glossary v1.1). A continuous random variable, x, take any values in a certain interval $(a\,,\, b)$. It is defined by the probability density function (pdf) $p(x)$ and the given interval. The probability of x_i falling in an arbitrary interval (a', b') is given by:

$$P\{a' \le x \le b'\} = \int_{a'}^{b'} p(x)dx\,. \tag{4.8}$$

The *pdf* has to satisfy the following two conditions:

1. $p(x) \ge 0$ for any $x \in (a, b)$

2. $\int_a^b p(x)dx = 1$

The expected value or mean, the second moment and the variance or central second moment of the random variable are respectively defined by [29]:

$$E[x] = \mu = \int_a^b xp(x)dx \tag{4.9}$$

$$E[x^2] = \int_a^b x^2 p(x)dx \tag{4.10}$$

$$Var[x] = \sigma^2 = E[(x-\mu)^2] = \int_a^b (x-\mu)^2 p(x)dx = E[x^2] - \mu^2 \,, \tag{4.11}$$

where σ is the standard deviation.

Consider now two continuous random variables *x* and *y*. We say that *x* and *y* are statistically independent if the distribution of *x* does not depend on *y* and vice-versa. Therefore, the joint probability density function $f_{xy}(x.y) = f_x(x)f_y(y)$.

The covariance and the correlation of two random variables [29]:

$$Cov\,[x.y] = E[(x - E[x])(y - E[y])] = E[xy] - E[x]E[y] \tag{4.12}$$

$$Corr\,[x.y] = \frac{Cov\,[x.y]}{\sqrt{Var\,[x]Var\,[y]}} \,. \tag{4.13}$$

If *x* and *y* are uncorrelated then their covariance and the correlation coefficient is zero, hence $E[xy] = E[x]E[y]$. Statistically independent random variables are always uncorrelated, but uncorrelated random variables can be dependent. Let *x* be uniformly distributed over [-1,1] and let $y = x^2$. The random variables are uncorrelated but are clearly not independent [32].

A sequence of truly random numbers is unpredictable and therefore unreproducible. Such a sequence can only be generated by a random physical process [31]. Practically it is very difficult to construct such a physical generator, which has to be fast enough and to connect it to a computer. To overcome this problem one can use pseudo-random numbers, which are computed according to a mathematical formulation, hence are reproducible and appear random to someone who does not know the algorithm [33].

John von Neumann has constructed the first pseudorandom generator called the mid-square method. Suppose we have a 4-digit number $x_1 = 0.9876$. We square it, $x_1^2 = 0.97535376$, obtaining this way an 8-digit number. We obtain x_2 by taking out the middle four digits, hence $x_2 = 0.5353$. Now square x_2 and so on. Unfortunately, the algorithm tends to produce a disproportionate frequency of small numbers [30].

One popular algorithm is the multiplicative congruential method suggested by D.H. Lehmer in 1949. Given a modulus *m*, a multiplier *a,* and a starting point x_1, the method generates successive pseudo-random numbers by the formula [31]:

$$x_i = ax_{i-1}Mod(m) \; . \tag{4.14}$$

5. Classical trajectory Monte Carlo method

Classical trajectory Monte Carlo method is a simulation for atomic collision. This model relies on the classical calculations of the trajectory of all bodies during the collision. In ion-atom collisions, where a large number of channels are coupled, the treatment of the collision systems quantum-mechanically is very challenging and difficult. In many cases, they cannot lead to satisfactory results. Full quantal calculations of cross sections usually require large-scale numerical computations, which are not easy when a large basis set is required, especially when highly excited states are involved. Therefore, there has always been an interest in constructing models for ion-atoms collisions based on classical mechanics, which can be evaluated rapidly.

The success of the CTMC method is that many-body interactions are exactly taken into account during the collisions on a classical level. In the last two decades, there has been a great revival of the CTMC calculations applied in atomic collisions involving three or more particles. This approximation is useful in treating atomic collisions where the quantum mechanical ones become very complicated or unfeasible [16]. The CTMC method is a non-perturbative method, where classical equations of motions are solved numerically [17, 34, 35] and the initial conditions are chosen randomly [17, 36, 37].

5.1 Three-body approximation

The three-body classical-trajectory Monte Carlo method was proposed by Abrines and Percival [38]. Later many scientists applied this calculation procedure among them in the earlier stage for example Olson and Salop [17] and Cohen [39]. It has been successfully applied to many problems [40, 41, 42]. This method is based on the numerical integration of the equation of motion for the three-body system. The Coulomb interactions, which include the projectile ion, the target nucleus, and an electron initially bound to the target nucleus, are included. The electron atom position and momentum distribution are described classically within a statistical distribution of the initial conditions. The method has the advantage that all possible processes can be included: excitation, ionization, and electron capture by the incident projectile. Becker and Mackellar [42] have improved the description of the atomic state using a micro canonical distribution corresponding to a given state in $|n, l\rangle$. Peach *et al*. [43] and Reinhold and Falcon [44] have each developed more elaborate methods to replace the Coulomb interactions with a model potential for the ionic cores. Specifically, Kohring et al. [45] and Pascale et al. [46] have also used the CTMC method for oriented atoms.

The physical picture is that the electron begins in a large, classical elliptical orbit. As the charged ion travels through the atom, the shape of the electron's orbit is then changed. The main interaction channels are defined as follows:

$$B^+ + A(n\,l\,m) = \begin{cases} B^+ + A^*(n'\,l'\,m') & \text{Excitation} \\ B^*(n'\,l'\,m') + A^+ & \text{Electron capture} \\ B^+ + A^+ + e^- & \text{Ionization} \end{cases} \tag{5.1}$$

where B^+ is a charged ion and A is a target atom with main quantum number n, orbital angular momentum l, and magnetic quantum number m. This system has been modeled successfully by considering the Coulomb forces among the three charged particles.

In the present work, the CTMC simulations were made in the three-body approximation. The three particles (target nucleus, target electron, and projectile) are characterized by their masses and charges. For the description of the interaction among the particles, Coulomb potential is used. Figure 5.1 shows the relative position vectors of the three-body collision system.

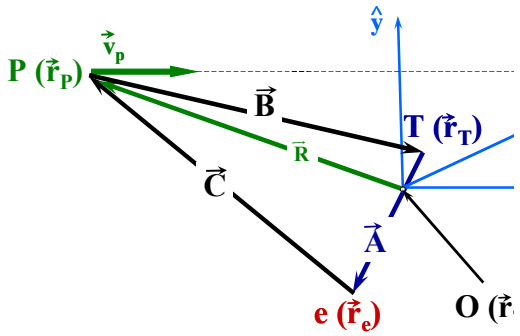

Figure 5.1. The relative position vectors of the particles involved in 3-body collisions. $\vec{A} = \vec{r}_e - \vec{r}_T$, $\vec{B} = \vec{r}_T - \vec{r}_p$ and $\vec{C} = \vec{r}_p - \vec{r}_e$, in such way that $\vec{A} + \vec{B} + \vec{C} = 0$. Also, $\vec{r}_{\mathrm{Te}}$ is the position vector of the center-of-mass of the target system, and b is the impact parameter.

5.2 Hamiltonian mechanics and equations of motion

The Hamiltonian equation for the three particles is written as:

$$H = T + V_{coul}, \tag{5.2}$$

where

$$T = \frac{\vec{P}_p^2}{2m_p} + \frac{\vec{P}_e^2}{2m_e} + \frac{\vec{P}_T^2}{2m_T} \tag{5.3}$$

$$V_{coul} = \frac{Z_p Z_e}{|\vec{r}_p - \vec{r}_e|} + \frac{Z_e Z_T}{|\vec{r}_e - \vec{r}_T|} + \frac{Z_p Z_T}{|\vec{r}_p - \vec{r}_T|}, \tag{5.4}$$

are total kinetic energy and Coulomb potential of interaction system. Also, $\vec{r}$, $\vec{p}$, Z and m are the position, momentum vector, the charge, and the mass of the given particles p; projectile, e; electron, T; target, respectively. The equations of motion taking into account the Hamiltonian equations are given as follows:

$$\dot{\vec{P}}_e = -\frac{\delta H}{\delta \vec{r}_e} = -\frac{Z_p Z_e}{|\vec{r}_p - \vec{r}_e|^3}(\vec{r}_p - \vec{r}_e) + \frac{Z_e Z_T}{|\vec{r}_e - \vec{r}_T|^3}(\vec{r}_e - \vec{r}_T) \tag{5.5}$$

$$\dot{\vec{P}}_T = -\frac{\delta H}{\delta \vec{r}_T} = -\frac{Z_p Z_T}{|\vec{r}_p - \vec{r}_T|^3}(\vec{r}_p - \vec{r}_T) - \frac{Z_e Z_T}{|\vec{r}_e - \vec{r}_T|^3}(\vec{r}_e - \vec{r}_T) \tag{5.6}$$

$$\dot{\vec{P}}_p = -\frac{\delta H}{\delta \vec{r}_p} = \frac{Z_p Z_e}{|\vec{r}_p - \vec{r}_e|^3}(\vec{r}_p - \vec{r}_e) + \frac{Z_p Z_T}{|\vec{r}_p - \vec{r}_T|^3}(\vec{r}_p - \vec{r}_T) \tag{5.7}$$

$$\dot{\vec{r}}_e = \frac{\partial H}{\partial \vec{P}_e} = N_e \vec{P}_e \tag{5.8}$$

$$\dot{\vec{r}}_T = \frac{\partial H}{\partial \vec{P}_T} = N_T \vec{P}_T \tag{5.9}$$

$$\dot{\vec{r}}_p = \frac{\partial H}{\partial \vec{P}_p} = N_p \vec{P}_p , \tag{5.10}$$

where $N_i = \frac{1}{m_i}$. Introducing the relative position vectors $\vec{A} = \vec{r}_e - \vec{r}_T$, $\vec{B} = \vec{r}_T - \vec{r}_p$ and $\vec{C} = \vec{r}_p - \vec{r}_e$, in such a way that $\vec{A} + \vec{B} + \vec{C} = \vec{0}$ (see Figure 5.1), the Equations (5.5) – (5.10) are reduced to the 12 coupled first-order differential equations as follows:

$$\ddot{\vec{A}} = \left\{\frac{N_e Z_p Z_e}{|\vec{A}+\vec{B}|^3} + \frac{(N_e+N_T) Z_e Z_T}{|\vec{A}|^3}\right\}\vec{A} + \left\{\frac{N_e Z_p Z_e}{|\vec{A}+\vec{B}|^3} - \frac{N_T Z_p Z_T}{|\vec{B}|^3}\right\}\vec{B} \tag{5.11}$$

$$\ddot{\vec{B}} = \left\{\frac{N_p Z_p Z_e}{|\vec{A}+\vec{B}|^3} - \frac{N_T Z_e Z_T}{|\vec{A}|^3}\right\}\vec{A} + \left\{\frac{(N_T+N_p) Z_p Z_T}{|\vec{B}|^3} + \frac{N_p Z_p Z_e}{|\vec{A}+\vec{B}|^3}\right\}\vec{B} . \tag{5.12}$$

These differential equations were integrated with respect to the time as an independent variable by the standard Runge-Kutta method for a given set of initial conditions [47].

5.3 Initial conditions in CTMC model

According to Equations (5.11) and (5.12), we need to consider and specify 12 initial values of initial conditions. These are the coordinates and the velocities of internal motion of (T, e) atomic system and the relative projectile ion – atomic center-of-mass motion. I note that all of these initial conditions are chosen randomly. I considered that the origin of our coordinate

system in the laboratory frame is the center-of-mass of the target atom, and the z-axis is parallel to the velocity vector of the projectile (see Figure 5.1). The distance between the projectile and the atomic centre of mass as well as the velocity of the projectile specifies the initial relative motion as follows:

$$\vec{R} = \begin{pmatrix} 0 \\ b \\ -\sqrt{R^2 - b^2} \end{pmatrix} \tag{5.13}$$

$$\dot{\vec{R}} = \begin{pmatrix} 0 \\ 0 \\ v_p \end{pmatrix}, \tag{5.14}$$

where v_p is the projectile velocity and is fixed during the CTMC simulations. To reproduce a uniform flux of incident particles, the impact parameter must be chosen. We can determine a maximum value of the impact parameter, $b_{\max}$, in such a way that the probabilities of the investigated processes must be zero or negligible above $b_{\max}$ in the CTMC calculations. The initial distance, R, between the projectile ion and target atom is chosen at sufficiently large internuclear separation, where the projectile ion and target atom interactions are negligible.

Finding the pairs of r and p for the initial condition of the target electron with respect to the target nuclei is an essential issue in classical calculations. If the potential between hydrogen and electron is net Coulomb potential, the initial r and p values are given as follows:

$$r_0 = \left|\frac{Z_e Z_T}{2E_b}\right| \tag{5.15}$$

$$p_0 = \sqrt{2|E_b|\mu_{te}}\,, \tag{5.16}$$

where E_b and μ_{te} denote the electron binding energy and reduced mass between target and electron, respectively. Potentials satisfying this condition represent the electron-core interaction.

In the CTMC model, a very important consideration is the classical description of the electron target position and momentum distributions. Abrines and Percival [38] have shown that it is possible to use Kepler's equation of planetary motion to represent hydrogen atoms with a randomly determined set of initial conditions. The sampling is completed by (i) fixing the binding energy E_0; (ii) choosing the eccentricity ϵ of the Columbic ellipse; (iii) solving Kepler's equation for the eccentric anomaly (eccentric angle) ξ in terms of the mean anomaly

α to establish the initial position and velocity on the ellipse; (iv) applying an Euler transformation with three random angles θ, ϕ and η to set up the arbitrary orientation of the ellipse. For a given quantal state, $|n\rangle$ is specified by the binding energy E_0 ($E_0 = -\frac{1}{2n^2}$ (a.u) for the hydrogen atom). The additional five random sampling parameters are ϵ, α and θ, ϕ, η is the eccentricity of the Kepler orbit, $\varepsilon^2 = 1 + 2E_0 l_c^2$, where l_c is the classical angular momentum. The classical angular momenta l_c are restricted to the interval $l \leq l_c \leq l + 1$, which is determined by the quantum mechanical angular momenta l. Thus, the eccentricity ε is chosen in the interval:

$$1 + 2E_0 l^2 \leq \varepsilon^2 \leq 1 + 2E_0 (l + 1)^2. \tag{5.17}$$

The angle α defines a starting point on the Kepler ellipse plane and it is a parameter of the orbit proportional to time. A random distribution of α corresponds to an equal probability of the atom having any phase in its periodic motion. ξ is the eccentric angle and is determined by solving Kepler's equation

$$\alpha = \xi - \varepsilon sin\xi. \tag{5.18}$$

The initial position and momentum of the electron on the orbit are fixed by a solution of Kepler's equation (5.18). The three Euler angles θ, ϕ, η fix the plane of the orbit in space.

The first rotation θ about the y axis gives the electron the proper z component of angular momentum. The second rotation ϕ about the angular momentum vector l fixes the z component of the Runge-Lenz vector A. The final rotation about the space fixed z-axis gives the randomly chosen η angle. These five parameters are distributed in the following ranges:

$$0 \leq \varepsilon^2 \leq 1, \quad 0 \leq \alpha \leq 2\pi, \quad -1 \leq \cos\theta \leq +1, \quad -\pi \leq \varphi \leq +\pi, \quad -\pi \leq \eta \leq +\pi$$

Figure 5.2 shows the geometrical structure of the collision system. The initial internal coordinates and momenta of the target electron are given by performing the rotation specified by the Euler angles θ, ϕ, and η [39].

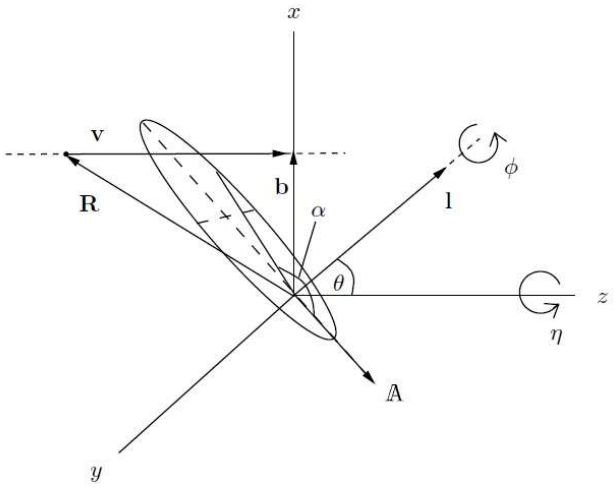

Figure 5.2. The geometry of the collision system. R is the internuclear vector, b is the impact parameter, and v is the ion velocity in the target frame chosen parallel with the magnetic field (*z*-axis), R = b + v*t*. An example of a Kepler ellipse with the angular momentum **l** and Runge-Lenz vector *A* is also shown. The angle α which defines a point on the Kepler ellipse plane and the three Euler angles θ, ϕ and η are indicated. The dashed lines indicate the major and minor axes.

5.4 Classical values

5.4.1 Classical principal quantum number

In the classical approaches, the classical principal (n_c) quantum number is defined by

$$n_c = Z_T Z_e \left(\frac{\mu_{Te}}{2U} \right)^{1/2}, \tag{5.19}$$

where μ_{Te} and U are the reduced mass of the target nucleus and the target electron, and electron binding energy, respectively. The classical values of n_c are quantized to a specific level n if they satisfy the relation [42]:

$$[(n-1)(n-1/2)n]^{1/3} \leq n_c \leq [(n+1)(n+1/2)n]^{1/3}. \tag{5.20}$$

5.4.2 Classical orbital angular momentum

The classical orbital angular momentum quantum number is given by

$$l_c = \sqrt{l_c^{x\,2} + l_c^{y\,2} + l_c^{z\,2}}, \tag{5.21}$$

$$l_c^x = m_e(x\dot{y} - y\dot{x}). \qquad l_c^y = m_e(x\dot{z} - z\dot{x}) \qquad l_c^z = m_e(y\dot{z} - z\dot{y}). \tag{5.22}$$

where x, y, and z are the Cartesian coordinates of the electron relative to the nucleus and $\dot{x}$, $\dot{y}$, and $\dot{z}$ are the corresponding velocities. Since l_c is uniformly distributed for a given n level, the quantal statistical weights are reproduced by choosing bin sizes such that [48]:

$$l \leq \frac{n}{n_c} l_c \leq l + 1, \tag{5.23}$$

where l is the quantum-mechanical orbital angular momentum.

5.4.3 Classical magnetic angular momentum

The projection of l_c onto the z-axis determines the classical magnetic angular momentum quantum number, m_c:

$$m_c = l_c^z. \tag{5.24}$$

The classical magnetic angular momentum quantum number is uniformly binned if it satisfies the relation [49]:

$$\frac{2m-1}{2l+1} \leq \frac{m_c}{l_c} \leq \frac{2m+1}{2l+1} \qquad m = -l.\, 1 - l. \ldots .\, l - 1.\, l. \tag{5.25}$$

5.5 Cross sections and statistical uncertainty

By evaluating the two-body total energies of the final state, it is now possible to classify the outcome of the ion-atom collision. If at the end of an individual trajectory, the electron is still bound to the target nucleus, it is the case of elastic collision of excitation; if the electron is found to be bound to the projectile ion, the reaction is cataloged as electron capture; and if the electron is bound to neither nucleus, it is cataloged as ionization. The cross sections for the various processes are proportional to the ratio of successful tries for that process to the number of trajectories calculated.

In physics, the cross section is a measure of the probability that a specific process will take place. The total cross sections is given by:

$$\sigma = \frac{2\pi b_{max}}{T_N} \sum_j b_j^{(i)}, \tag{5.26}$$

and the statistical uncertainty of the cross sections is defined by:

$$\Delta\sigma = \sigma\left(\frac{T_N - T_N^{(i)}}{T_N T_N^{(i)}}\right)^{1/2}, \tag{5.27}$$

where T_N is the total number of trajectories calculated for impact parameters less than b_{max}, $T_N^{(i)}$ is the number of trajectories that satisfy the criteria for the corresponding final channels (electron capture), and $b_j^{(i)}$ is the actual impact parameter for the trajectory corresponding electron capture processes.

6. Quasi-classical trajectory Monte Carlo model

The quasi-classical trajectory Monte Carlo model was proposed by Kirschbaum and Wilets in 1980 [50]. This model represents one step further towards a better description of the classical atomic collisions. According to QCTMC model, for atoms, a necessary condition for stability is that the electrons are not allowed to collapse to the symmetry point, i.e., to the nucleus. The effective potential enforcing this condition is motivated by the Heisenberg uncertainty principle $rp \geq \xi_H \hbar$, where r and p are the distance and momentum of an electron with respect to a nucleus and ξ_H is a constant. This condition is equivalent to the de Broglie description of the hydrogen atom. In addition, The Pauli constraint classically means that any two electrons having the same spins cannot occupy the same volume of phase space. We effect this by requiring that $r_{ij} p_{ij} \geq \xi_P$, where $\vec{r}_{ij}$ is the relative position and $\vec{p}_{ij}$ is the relative momentum of the *i*th and *j*th identical electrons, respectively, and ξ_P is another dimensionless constant which must be determined.

6.1 Model potential mimicking the Heisenberg and Pauli constrain

For more accurate classical simulation results, we must also consider the constraints of Heisenberg and Pauli principles. This approach was proposed by Kirschbaum and Wilets (KW) [50] in the dominant of the fermion molecular dynamic model (FMD). They added effective potentials, V_H and V_P, motivated by the Heisenberg and Pauli principles, to the pure Coulomb inter-particle potentials describing the atom. Thus,

$$H_{FMD} = H_0 + V_H + V_P \,, \tag{6.1}$$

where H_0 is the usual Hamiltonian containing the total kinetic energy of all bodies and Coulomb potential terms between all pairs of electrons and between the nucleus and electrons, respectively. The extra terms are

$$V_H = \sum_{n=a.b} \sum_{i=1}^{N} f(r_{ni} \,.\, p_{ni}; \xi_H \,.\, \alpha_H) \,, \tag{6.2}$$

and

$$V_p = \sum_{i=1}^{N} \sum_{j=i+1}^{N} f\left(r_{ij} \,.\, p_{ij}; \xi_p \,.\, \alpha_p\right) \delta_{s_i . s_j} \,, \tag{6.3}$$

where *a* and *b* denote the nuclei, while *i* and *j* index the electrons. Also, $r_{\alpha\beta} = r_\beta - r_\alpha$ is the relative distance of the two nuclei and the relative momenta are:

$$p_{\alpha\beta} = \frac{m_\alpha p_\beta - m_\beta p_\alpha}{m_\alpha + m_\beta}. \tag{6.4}$$

and $\delta_{s_i.s_j} = 1$ if the spins of the *i*th and *j*th electrons are the same and $\delta_{s_i.s_j} = 0$ if they are different. The constraining potentials are chosen of the form [50]:

$$f(r_{\lambda\nu}\,.\,p_{\lambda\nu};\xi\,.\,\alpha) = \frac{\xi}{4\alpha r_{\lambda\nu}^2 \mu_{\lambda\nu}} exp\left\{\alpha\left[1-\left(\frac{r_{\lambda\nu}p_{\lambda\nu}}{\xi}\right)^4\right]\right\}. \tag{6.5}$$

In this work, in the case of hydrogen as a one electron target I just take into account the Heisenberg constrain. Also, the Heisenberg potential between electron and both target and projectile nucleus is as follows:

$$f\left(\vec{r}_{pe}\,.\,\vec{P}_{pe};\varepsilon_H\,.\,\alpha_H\right) = \frac{{\xi_H}^2}{4\alpha_H \vec{r}_{pe}^2 \mu_{pe}} exp\left\{\alpha_H\left[1-\left(\frac{\vec{r}_{pe}\vec{P}_{pe}}{\xi_H}\right)^4\right]\right\} \tag{6.6}$$

$$f\left(\vec{r}_{Te}\,.\,\vec{P}_{Te};\varepsilon_H\,.\,\alpha_H\right) = \frac{{\xi_H}^2}{4\alpha_H \vec{r}_{Te}^2 \mu_{Te}} exp\left\{\alpha_H\left[1-\left(\frac{\vec{r}_{Te}\vec{P}_{Te}}{\xi_H}\right)^4\right]\right\}. \tag{6.7}$$

6.2 Equations of motion

The equations of motion taking into account the Hamiltonian described by Equation (6.1) is given by:

$$\ddot{\vec{A}} = \left[\frac{N_e Z_p Z_e}{\left|\vec{A}+\vec{B}\right|^3} + \frac{(N_e+N_T)Z_e Z_T}{\left|\vec{A}\right|^3} + \frac{{\xi_H}^2(N_e+N_T)^2}{2\alpha_H\left|\vec{A}\right|^4} e^{\alpha_H\left[1-\left(\frac{|\vec{A}||\vec{P}_{Te}|}{\xi_H}\right)^4\right]} + \frac{\vec{P}_{Te}^4(N_T+N_e)^2}{{\xi_H}^2} e^{\alpha_H\left[1-\left(\frac{|\vec{A}||\vec{P}_{Te}|}{\xi_H}\right)^4\right]} + \right.$$
$$\left. \frac{{\xi_H}^2 N_e(N_e+N_p)}{2\alpha_H\left|\vec{A}+\vec{B}\right|^4} e^{\alpha_H\left[1-\left(\frac{|\vec{A}+\vec{B}||\vec{P}_{ep}|}{\xi_H}\right)^4\right]} + \frac{\vec{P}_{ep}^4 N_e(N_e+N_p)}{{\xi_H}^2} e^{\alpha_H\left[1-\left(\frac{|\vec{A}+\vec{B}||\vec{P}_{ep}|}{\xi_H}\right)^4\right]}\right] \vec{A} + \left[\frac{N_e Z_p Z_e}{\left|\vec{A}+\vec{B}\right|^3} - \right.$$
$$\left. \frac{N_T Z_p Z_T}{\left|\vec{B}\right|^3} + \frac{{\xi_H}^2 N_e(N_e+N_p)}{2\alpha_H\left|\vec{A}+\vec{B}\right|^4} e^{\alpha_H\left[1-\left(\frac{|\vec{A}+\vec{B}||\vec{P}_{ep}|}{\xi_H}\right)^4\right]} + \frac{\vec{P}_{ep}^4 N_e(N_e+N_p)}{{\xi_H}^2} e^{\alpha_H\left[1-\left(\frac{|\vec{A}+\vec{B}||\vec{P}_{ep}|}{\xi_H}\right)^4\right]}\right] \vec{B} \tag{6.8}$$

$$\ddot{\vec{B}} = \left[\frac{N_p Z_p Z_e}{\left|\vec{A}+\vec{B}\right|^3} - \frac{N_T Z_e Z_T}{\left|\vec{A}\right|^3} - \frac{{\xi_H}^2 N_T (N_e+N_T)}{2\alpha_H \left|\vec{A}\right|^4} e^{\alpha_H \left[1-\left(\frac{|\vec{A}||\vec{P}_{Te}|}{\xi_H}\right)^4\right]} - \frac{\vec{P}_{Te}^4 N_T (N_e+N_T)}{{\xi_H}^2} e^{\alpha_H \left[1-\left(\frac{|\vec{A}||\vec{P}_{Te}|}{\xi_H}\right)^4\right]} + \right.$$
$$\left. \frac{{\xi_H}^2 N_p (N_e+N_p)}{2\alpha_H \left|\vec{A}+\vec{B}\right|^4} e^{\alpha_H \left[1-\left(\frac{|\vec{A}+\vec{B}||\vec{P}_{ep}|}{\xi_H}\right)^4\right]} + \frac{\vec{P}_{ep}^4 N_p (N_e+N_p)}{{\xi_H}^2} e^{\alpha_H \left[1-\left(\frac{|\vec{A}+\vec{B}||\vec{P}_{ep}|}{\xi_H}\right)^4\right]} \right] \vec{A} +$$
$$\left[\frac{(N_T+N_p) Z_p Z_T}{\left|\vec{B}\right|^3} + \frac{N_p Z_p Z_e}{\left|\vec{A}+\vec{B}\right|^3} + \frac{{\xi_H}^2 N_p (N_e+N_p)}{2\alpha_H \left|\vec{A}+\vec{B}\right|^4} e^{\alpha_H \left[1-\left(\frac{|\vec{A}+\vec{B}||\vec{P}_{ep}|}{\xi_H}\right)^4\right]} + \right.$$
$$\left. \frac{\vec{P}_{ep}^4 N_p (N_e+N_p)}{{\xi_H}^2} e^{\alpha_H \left[1-\left(\frac{|\vec{A}+\vec{B}||\vec{P}_{ep}|}{\xi_H}\right)^4\right]} \right] \vec{B} \,. \tag{6.9}$$

6.3 Initial conditions in QCTMC model

Since the Heisenberg correction term is added to the net Coulomb potential and kinetic energy between the electron and hydrogen atom, to find the allowed intervals for *r* and *p* for ground state hydrogen, I considered two conditions that *r* and *p* must satisfy. They are the followings:

$$\frac{|Z_e Z_T|}{2r} + f_H(r.p;\xi\,.\alpha) < 0.5 \tag{6.10}$$

$$\frac{p^2}{2\mu_{Te}} - \frac{1}{r} + f_H(r.p;\xi\,.\alpha) \approx -0.5\,, \tag{6.11}$$

where $f_H(r.p;\xi\,.\alpha)$ is the Heisenberg correction term (see Equation (6.5)) and 0.5 is the binding energy of the electron in ground state hydrogen. Figure 6.1 shows the allowed interval for *r* and *p* in which satisfies Equations (6.10) and (6.11). As I will explain in section 7.1, I found excellent agreements between our QCTMC results at α_H = 3.5, and ξ_H = 0.9354 and the previous ones in H^++H(1s) collisions. Therefore I used this combination of (α,ξ) to find the allowed interval in Figure 6.1.

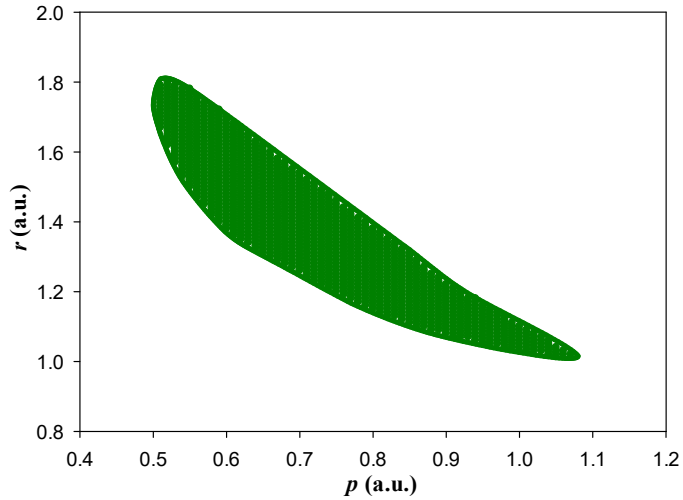

Figure 6.1. The allowed interval for r and p where $\alpha_H = 3.5$ and $\xi_H = 0.9354$.

The correction term is a function of the radial (r) and linear momentum (p) of the target electron (see Equation (6.5)). To define the initial conditions for r and p in the QCTMC model, I improved the initial conditions used in the standard 3-body CTMC model. In the first step, I showed the dependence of the Heisenberg correction term on the parameters r and p. Figure 6.2 shows the correction term dependence as a function of r (with some typical constant p) and p (with some typical constant r), respectively.

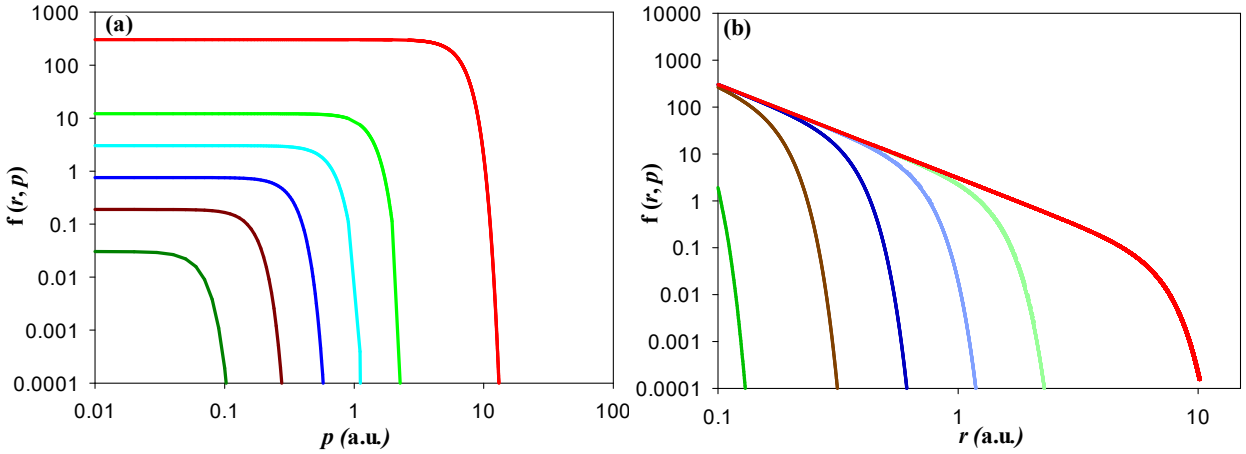

Figure 6.2. (a) Correction term dependence as a function of p, for the typical constant r = 0.1, 0.5, 1, 2, 4, 10 in atomic unit (from up to down), respectively. (b) Heisenberg constraining potential dependence as a function of r, for the typical constant p = 10, 4, 2, 1, 0.5, 0.1 in atomic unit (from left to right), respectively.

According to Figure 6.2, the dependence of the Heisenberg correction term on the p (when r is assumed to be constant) is unusual (see Figure 6.2 (a)). In this case, the function is constant before falling dramatically. On the other hand, the dependence of the correction term on the r (when p is assumed to be constant) is smooth (see Figure 6.2 (b)). Thus, I see a well-defined

function in this graph. Therefore, I performed the QCTMC model by using this condition to define the initial conditions.

By fixing the p parameter and finding the root of function F(r,p) (see Equation (6.12)), I specified the new initial conditions in the QCTMC model for r parameter in the allowed interval.

$$F(r.p) = \frac{p^2}{2\mu_{Te}} - \frac{1}{r} + f_H(r.p) + 0.5. \tag{6.12}$$

Figure 6.3 shows the dependence of function $F(r.p)$ according to r. I also consider that the obtained values for r and p in this part must be in the allowed interval (see Figure 6.1). According to Figure 6.2, I found that the initial conditions for the r parameter are around p = 1 a.u.

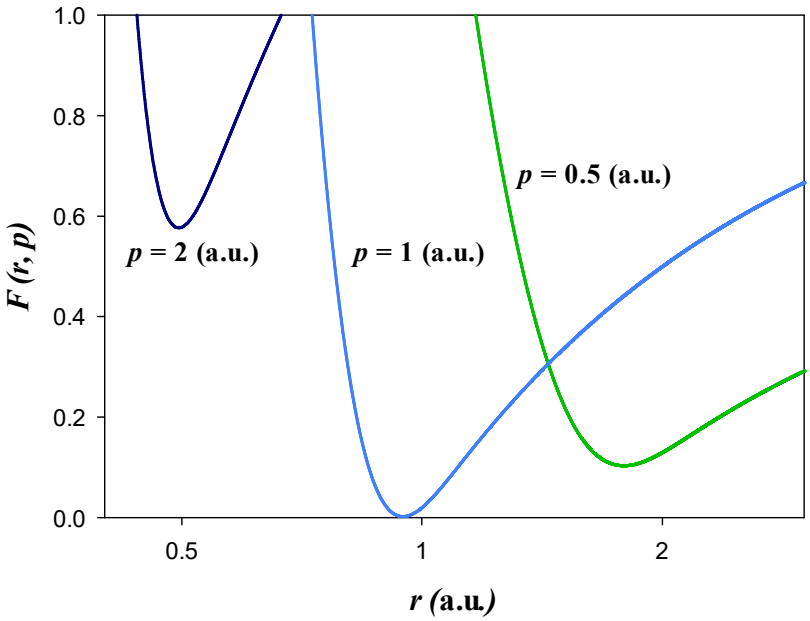

Figure 6.3. Dependence of function $F(r.p) = \frac{p^2}{2\mu_{Te}} - \frac{1}{r} + f_H(r.p) + 0.5$ according to r.

7. Results and discussion

To study the collision between H^+ + H(1s), and Be^{4+} + H(*nl*), I performed the standard three-body classical trajectory Monte Carlo, and quasi-classical trajectory Monte Carlo models. I took into account a classical simulation with an ensemble of 3×10^6 primary trajectories for each impact energy. The calculations are carried out in the projectile energy range, which is relevant to the interest of the fusion research when the target hydrogen atom is in the ground state and excited state. According to a large number of primary histories, the estimated uncertainties (see Equation (5.27)) of the cross sections are in general around 0.6%.

7.1 Interaction between H^+ and Hydrogen atom

The proton-hydrogen atom collision system is the simplest collision system in ion-atom collisions. This fundamental one-electron system has a great significance to test various theoretical descriptions where, luckily, a large number of experimental results are available for various channels like ionization, electron capture, excitation, and state-selective electron capture cross sections.

Therefore, I also used the H^++H collision system to evaluate the effects of the Heisenberg correction term on cross sections in the QCTMC model where the quantum features of the collision system is mimicking using the model potential in the Hamiltonian as was proposed by Kirschbaum and Wilets [50].

I note here that the collision processes between ions and atomic hydrogen also have considerable interest for the scientists working on fusion plasma research. Neutral beams of hydrogen atoms can be injected into tokamak plasmas to heat and fuel them [51], and they provide powerful plasma composition diagnostic tools through charge exchange recombination spectroscopy [52]. So accurate cross sections data are essential.

The proton-hydrogen collision system has been widely studied both theoretically and experimentally for various collision channels. Theoretically, Cohen calculated cross sections for all possible electronic rearrangements in H^++H using a quasi-classical-trajectory Monte Carlo energy-bounded approach (QTMC-EB) [53]. This model is proposed to extend the classical trajectory Monte Carlo model. Avazbaev *et al.* [54] used the semi-classical convergent close-coupling (SC-CCC) approach to study the cross sections for excitation, total and state-selective electron capture channels for a wide range of the proton impact energies from 1keV

to 1MeV. The latest research on the subject is the development of the quantum-mechanical convergent-close-coupling (QM-CCC) [55, 56].

The proton-hydrogen collision was also studied extensively experimentally. The ionization cross sections in H^++H collisions were obtained by Shah and Gilbody and Shah *et al.* in 1981 and 1987 [57, 58], where the authors claim that the experimental error on the level of 5% or better. The cross sections for electron capture between a proton and a hydrogen atom have been measured in the low projectile energies by McClure [59]. The collisional excitation of the proton-hydrogen system has been investigated at intermediate energies applying the optical method by Detleffsen *et al.* [60]. The state-selective electron capture is another interesting collision channel that has been considered for many years. The experimental data for cross sections of the state-selective electron capture into 2s and 2p states of the projectile in H^++H(1s) collision was published in Refs. [61-65].

7.1.1 Heisenberg dimensionless constant and adjustable hardness parameter

The Heisenberg correlation potential is sensitive to the choice of the two constants α and ξ. ξ_H and α_H are the dimensionless constant and adjustable hardness parameters, respectively, which must be determined. ξ_H is determined by our requiring $r_i p_i = \xi\hbar$ for the ground state of an atom. By considering atomic units $\hbar = m_e = e = 1$, Hamiltonian of a hydrogen atom is defined in the form of

$$H = \frac{p^2}{2} - \frac{1}{r} + \left[\frac{{\xi_H}^2}{4\alpha_H r^2}\right] exp\left\{\alpha_H\left[1 - \left(\frac{rp}{\xi_H}\right)^4\right]\right\}. \tag{7.1}$$

In the ground state the requirement is $\frac{\partial H}{\partial p} = 0$ and $\frac{\partial H}{\partial r} = 0$. This gives

$$p = \frac{1}{\xi_H\left(1+\frac{1}{2\alpha_H}\right)} \tag{7.2}$$

$$r = {\xi_H}^2\left(1 + \frac{1}{2\alpha_H}\right) \tag{7.3}$$

$$E = -\frac{1}{2{\xi_H}^2\left(1+\frac{1}{2\alpha_H}\right)}\ . \tag{7.4}$$

In the case of the hydrogen atom, the binding energy of the electron in the ground state is -0.5 a.u. Figure 7.1 shows the variations of ξ_H according to α_H for ground state hydrogen atom.

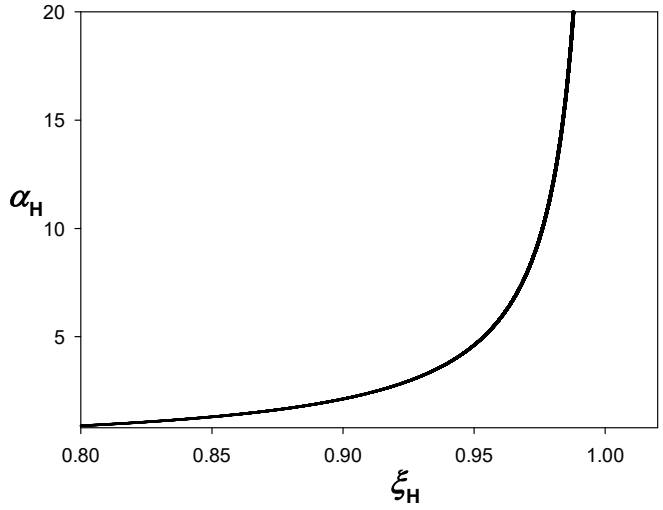

Figure 7.1. Variations of ξ_H according to α_H for ground state hydrogen atom.

7.1.2 Electron radial and momentum distribution

In the QCTMC model, Hamiltonian equations are numerically solved using a fourth-order Runge-Kutta integration method with an adaptive step size. For initialization procedures for the standard micro-canonical QCTMC model, I obtained the radial and momentum distribution of the electron. Figure 7.2 shows these distributions applying various combinations of α_H and ξ_H in comparison with the corresponding quantum-mechanics results.

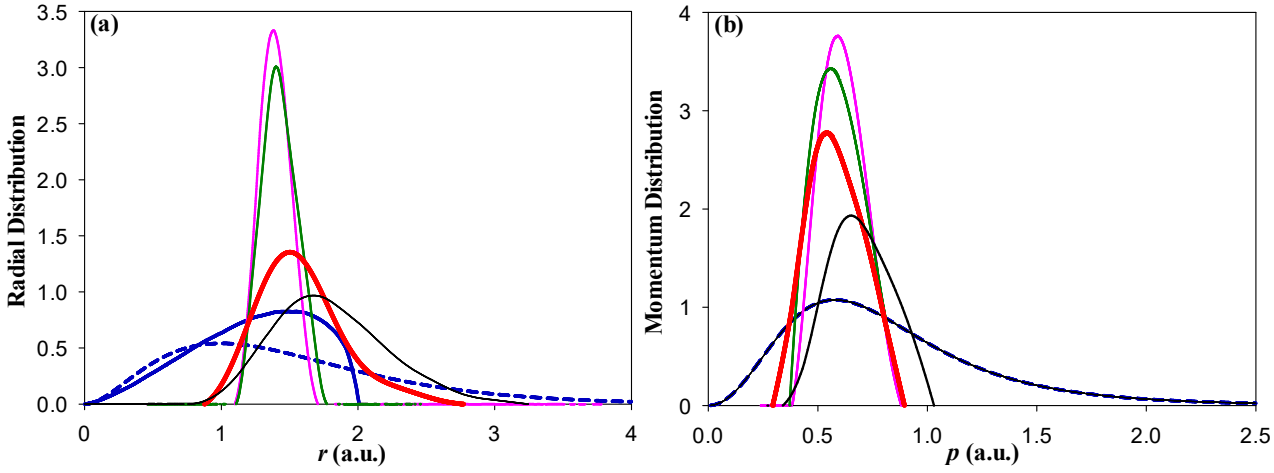

Figure 7.2. (a) Radial distribution and (b) Momentum distribution. Solid purple line: QCTMC (α_H = 3, ξ_H= 0.9258) results, solid green line: QCTMC (α_H = 3.2, ξ_H= 0.9299) results, solid red line: QCTMC (α_H = 3.5, ξ_H= 0.9354) results, solid black line: QCTMC (α_H = 4, ξ_H= 0.9428) results, solid blue line: CTMC results, dashed blue line: quantum-mechanics results.

According to Figure 7.2, one can see that the radial and momentum distributions are highly influenced by α_H and ξ_H. As discussed in Sec 6.3, I fixed the p and changed the r to find the initial condition in the QCTMC model. Therefore, it is expected that the momentum

distribution is not matched to the classical and quantum distributions (see Figure 7.2 (b)) but the QCTMC momentum distributions are still in the range of quantum-mechanical distribution. Figure 7.2 (a) shows that the standard classical radial distribution is terminated around $r = 2$. Since the Heisenberg constraint is one of the quantum-mechanics concepts I use in the classical simulation, I expect to see the quasi-classical radial distributions in the special quantum zone (beyond $r = 2$). This condition is seen for $\alpha_H \geq 3.5$. Therefore the suitable and reasonable range of α_H for the H^++H(1s) collision system is expected to be $\alpha_H \geq 3.5$. Furthermore, I note that the distributions are started from non-zero values because due to the Heisenberg constraint, the electron is not allowed to collapse to the nucleus.

To find the adequate combination of α_H and ξ_H for proton and ground state hydrogen collision system in the QCTMC model, I calculated the cross sections of ionization, electron capture, state-selective electron capture, and excitation channels as a function of incident energies and compared with the available quantum-mechanics approaches and experimental data.

7.1.3 Effects of Heisenberg correction term on three different schemes

In the QCTMC model, the effect of Heisenberg correlation potential on the particles in the collision is interesting. Therefore I tested three calculations schemes as follows:

1. Projectile-centered, where the correction term is taken into account between target electron and projectile
2. Target-centered, where the correction term is taken into account between the target electron the target nucleus
3. Combined one, i.e., target and projectile centered where the correction term is taken into account between target electron and both the target nucleus and projectile

Figure 7.3 shows my CTMC and QCTMC results corresponding to the three calculation schemes of the ionization and total electron capture cross sections in H^+ + H(1s) collision as a function of the impact energy. I compared the results with the QTMC-EB method and experimental data.

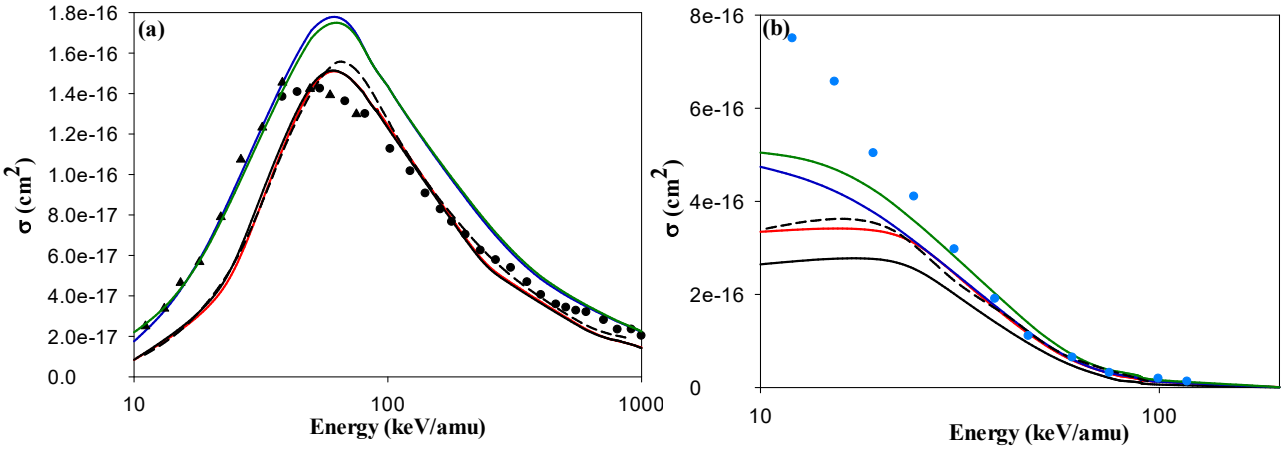

Figure 7.3. (a) Ionization and (b) Electron capture cross sections in H^+ +H(1s) collision as a function of impact energy. Solid red line: present CTMC results, solid green line: present target-centered QCTMC results, solid black line: present projectile-centered QCTMC results, solid blue line: present target and projectile centered QCTMC results, dashed line: QTMC-EB [53]. Experimental results are due to; black circles: Shah and Gilbody [57], black triangles: Shah, Eliot and Gilbody [58], blue circles: McClure [59].

According to Figure 7.3 (a), the present CTMC and projectile-centered QCTMC results are almost the same. Furthermore, it can be seen that the target-centered QCTMC results and the target-projectile-centered ones are almost the same. It means that due to the large distance between the electron and the projectile relative to the distance from the electron to the target nucleus, the Heisenberg correction term effect between the electron and the projectile is practically negligible. Therefore, I conclude that the correction term between the target electron and the projectile is ineffective in the ionization channel. According to the previous literature, both CTMC and projectile-centered QCTMC results are in good agreement with the QTMC-EB results of Cohen [53], and the experimental data are shown by Shah and Gilbody [57] at intermediate and high impact energies. Also, the target-centered QCTMC cross sections and target-projectile-centered QCTMC ones are in excellent agreement with the experimental data reported by Shah *et al.* [58] at low impact energies.

On the other hand, according to Figure 7.3 (b), the effects of correction term on three different calculation schemes are evidence in the electron capture channel. The correction term provides the repulsive force between the electron and both target and projectile cause to better transmit the electron to the projectile states in the electron capture channel. A better agreement is seen between experimental data and the QCTMC model, where the correction term is taken into account between the target electron and both the target nucleus and projectile at intermediate energies. It is worth noting that I used only the combination scheme as a justifiable cause in our calculations.

7.1.4 Ionization cross sections

Figure 7.4 shows the present CTMC and QCTMC results of the ionization channel (see Equation 7.5) in $H^+ + H(1s)$ as a function of impact energy. I considered α_H = 3, 3.5, 4, 4.5, 5 with corresponding ξ_H in the QCTMC model. The Comparison was made with the QTMC-EB method used by Cohen [53], and the experimental data have shown come from Shah and Gilbody [57] and Shah, Eliott, and Gilbody [58].

$$H^+ + H(1s) \rightarrow H^+ + H^+ + e^-. \tag{7.5}$$

It can be seen that the CTMC results are in good agreement with QTMC-EB results and experimental data of Shah and Gilbody [57] at intermediate and high energies. The Heisenberg correction term exerts a repulsive force on the electron. Due to the small distance between the electron and the target nucleus, the repulsive force between the electron and the target nucleus is much greater than the repulsive force between the electron and the projectile. Therefore, the ionization cross sections in the QCTMC model are higher than the CTMC ones in the whole range of impact energy. According to Figure 7.4, The QCTMC (α_H= 3, ξ_H= 0.9258) and QCTMC (α_H= 3.5, ξ_H= 0.9354) results match the experimental data of Shah, Eliott, and Gilbody [58] at low energies. Also, the QCTMC (α_H= 3, ξ_H= 0.9258) results are in good agreement with the experimental data of Shah and Gilbody [57] at high energies. However, one can see the close agreement between the QCTMC (α_H= 3.5, ξ_H= 0.9354) results and the experimental results due to Shah and Gilbody [57] at high energies.

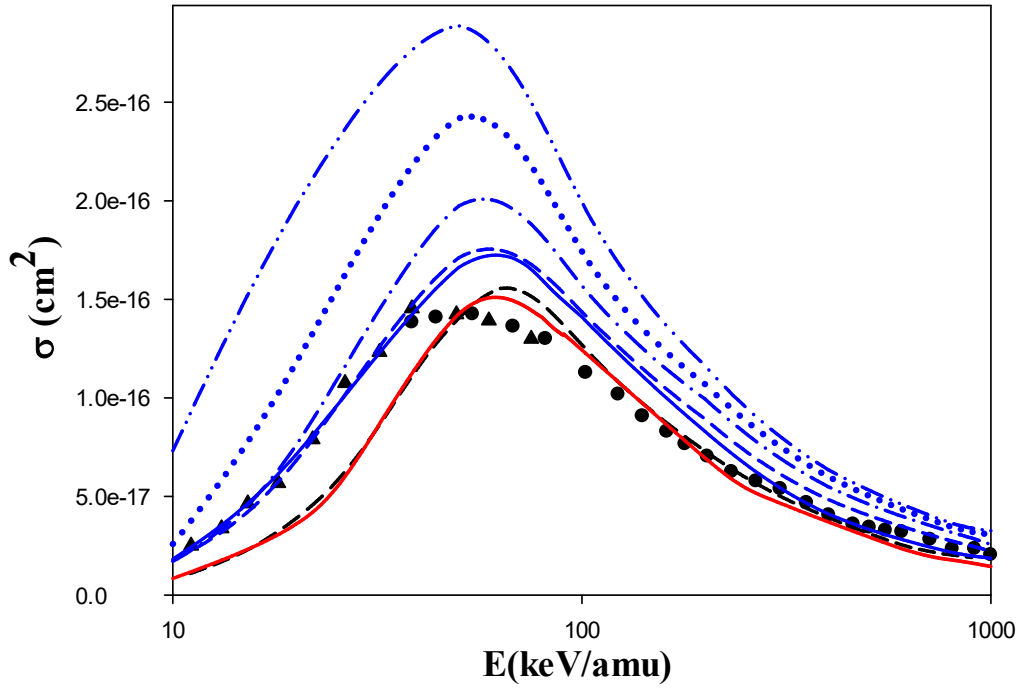

Figure 7.4. Ionization cross sections in $H^+ + H(1s)$ as a function of the impact energy. Solid red line: present CTMC results, solid blue line: present QCTMC (α_H = 3, ξ_H= 0.9258) results, dash blue line: present QCTMC (α_H = 3.5, ξ_H= 0.9354) results, dash-dot blue line: present QCTMC (α_H = 4, ξ_H= 0.9428) results, dotted blue line: present QCTMC (α_H = 4.5, ξ_H= 0.9486) results, dash-dot-dot blue line: present QCTMC (α_H = 5, ξ_H= 0.9534) results, dash black line: QTMC-EB results of Cohen [53]. Experimental results are due to; black circles: Shah and Gilbody [57], black triangles: Shah, Eliott, and Gilbody [58].

7.1.5 Total electron capture cross sections

I calculated the CTMC and QCTMC results of the total electron capture channel (see Equation 7.6) in $H^+ + H(1s)$ collision as a function of impact energy. I considered α_H = 3.5, 4, 4.5, 5 with ξ_H correspondence in the QCTMC model. I compared my results with the QTMC-EB method used by Cohen [53], and the experimental data shown come from McClure [59] (see Figure 7.5).

$$H^+ + H(1s) \rightarrow H(nl) + H^+ . \qquad (7.6)$$

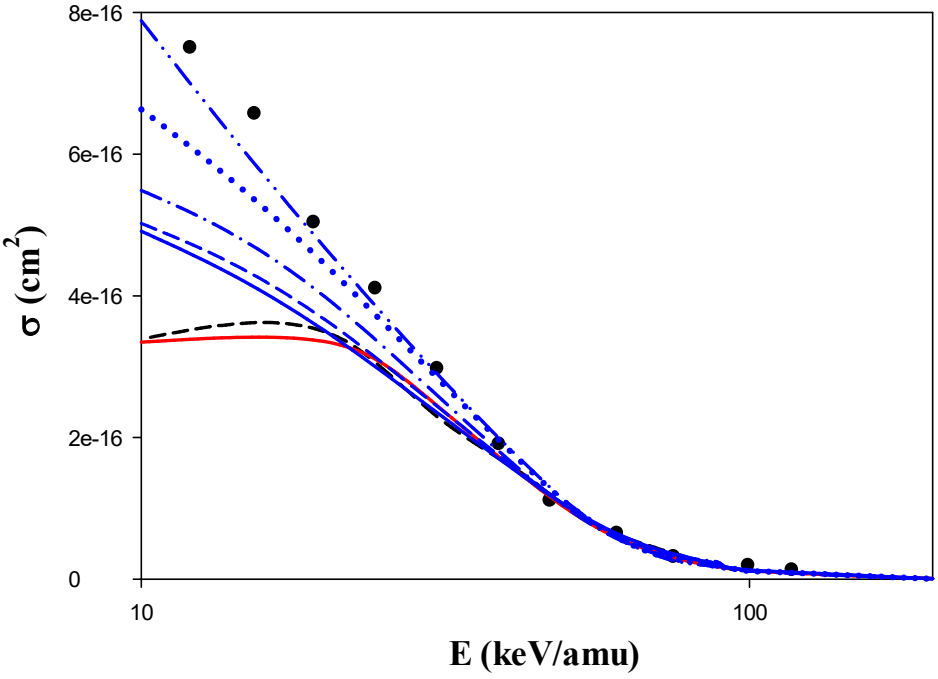

Figure 7.5. Total electron capture cross sections in H^+ + H(1s) collision as a function of the impact energy. Solid red line: present CTMC results, solid blue line: present QCTMC (α_H = 3, ξ_H= 0.9258) results, dash blue line: present QCTMC (α_H = 3.5, ξ_H= 0.9354) results, dash-dot blue line: present QCTMC (α_H = 4, ξ_H= 0.9428) results, dotted blue line: present QCTMC (α_H = 4.5, ξ_H= 0.9486) results, dash-dot-dot blue line: present QCTMC (α_H = 5, ξ_H= 0.9534) results, dashed black line: the QTMC-EB results of Cohen [53], circles: experimental results are due to McClure [59].

By considering the correction term to mimic the Heisenberg constrain, the repulsive force reduces the effects of the attractive Coulomb force between the electron and target nuclei. Therefore, the tendency of the electron to be placed at the states of the projectile increases. According to Figure 7.5, the QCTMC model increases the electron capture cross sections compared with CTMC and QTMC-EB methods at low and intermediate impact energies. The QCTMC (α_H= 5, ξ_H= 0.9535) results are very close to the experimental data.

7.1.6 Excitation cross sections

In the following, I show cross sections for H^+ induced $1s \rightarrow 2p$ transition (see Equation 7.7) in atomic hydrogen by using CTMC and QCTMC methods for α_H= 3, 3.5, 4, 4.5, 5 with ξ_H correspondence, respectively (see Figure 7.6). In addition, I compared my results with the SC-CCC method used by Avazbaev *et al.* [54], and the experimental data are shown by Morgan *et al.* [62], Detleffsen *et al.* [60], and Kondow *et al.* [65].

$$H^+ + H(1s) \rightarrow H^+ + H(2p)^*. \qquad (7.7)$$

According to Figure 7.6, the QCTMC results are higher than the CTMC ones. This behavior can be understood by explaining the effects of the correction term on the electron in the excitation channel. The effects of correction term to mimic the Heisenberg uncertainty principle reduce the effect of the attractive Coulomb force between the electron and the target nucleus. This is sufficient to increase the probability of excitation of the hydrogen atom. In terms of conformity with the experimental data and the SC-CCC theoretical results [54], the QCTMC (α_H= 3, ξ_H= 0.9258) and QCTMC (α_H= 3.5, ξ_H= 0.9354) results are very appropriate.

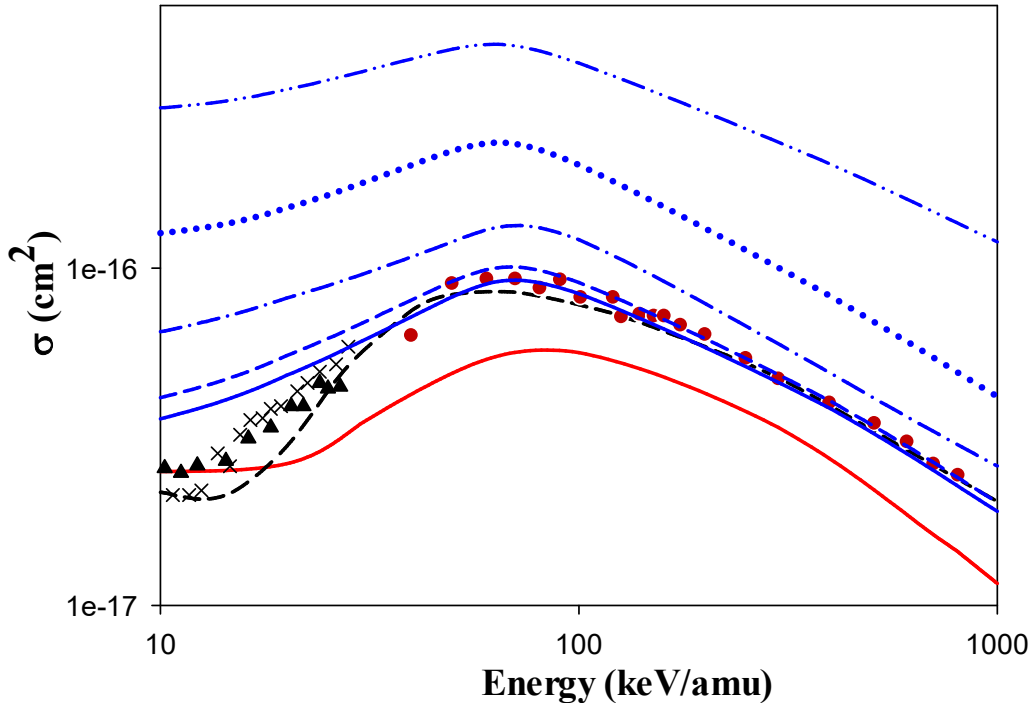

Figure 7.6. Excitation cross sections of $nl = 2p$ hydrogen level in $H^+ + H(1s)$ collision, as a function of the impact energy. Solid red line: present CTMC results, solid blue line: present QCTMC (α_H = 3, ξ_H= 0.9258) results, dash blue line: present QCTMC (α_H = 3.5, ξ_H= 0.9354) results, dash-dot blue line: present QCTMC (α_H = 4, ξ_H= 0.9428) results, dotted blue line: present QCTMC (α_H = 4.5, ξ_H= 0.9486) results, dash-dot-dot blue line: present QCTMC (α_H = 5, ξ_H= 0.9534) results, dashed line: SC-CCC [54]. Experimental results are due to; red circles: Detleffsen *et al.* [60], black triangles: Morgan *et al.* [62], crosses: Kondow *et al.* [65].

7.1.7 State-selective electron capture cross sections in H^++H(1s) collisions

I calculated the CTMC and QCTMC results of electron capture cross sections into 2s and 2p states of the projectile bound state (see Equation (7.8)). The calculations were obtained in the QCTMC model according to α_H= 3, 3.5, 4, 4.5 with ξ_H correspondence, respectively (see Figures 7.7 and 7.8).

$$H^+ + H(1s) \rightarrow H(nl) + H^+ . \qquad (7.8)$$

The comparison was made with the semi-classical convergent close-coupling (SC-CCC) method used by Avazbaev *et al.* [54], and the experimental data are due to Bayfield [61], Morgan *et al.* [62], Hill *et al.* [63], Ryding *et al.* [64], Kondow *et al.* [65] and Stebbings *et al* [66].

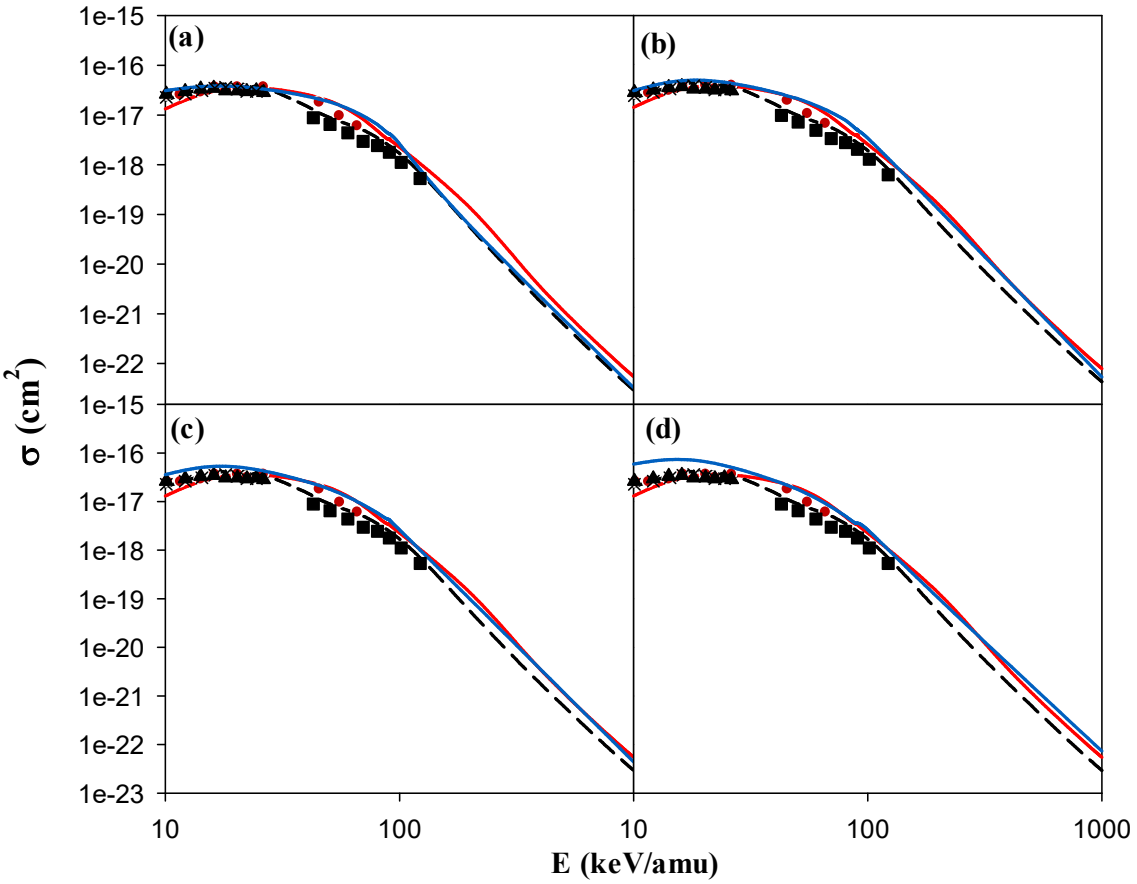

Figure 7.7. Electron capture cross sections into 2s state of the projectile in H^+ + H(1s) collision as a function of the impact energy. Solid red line: present CTMC results, solid blue line: present QCTMC results for: a) α_H = 3, ξ_H= 0.9258, b) α_H = 3.5, ξ_H= 0.9354, c) α_H = 4, ξ_H= 0.9428, d) α_H = 4.5, ξ_H= 0.9486 , dash line: SC-CCC results of Avazbaev *et al.* [54]. Experimental results are due to; red circles: Bayfield [61], black triangles: Morgan *et al.* [62], crosses: Hill *et al*. [63], black squares: Ryding *et al.* [64].

According to Figure 7.7, the QCTMC model improves the results at low energies significantly. At the low energies, the QCTMC (α_H= 3, ξ_H= 0.9258) and QCTMC (α_H= 3.5, ξ_H= 0.9354) results agree with the experimental data of Morgan *et al.* [62]. Also, between impact energies 100- 1000 keV, the QCTMC (α_H= 3, ξ_H= 0.9258) and QCTMC (α_H= 3.5, ξ_H= 0.9354) results match the SC-CCC [54] method.

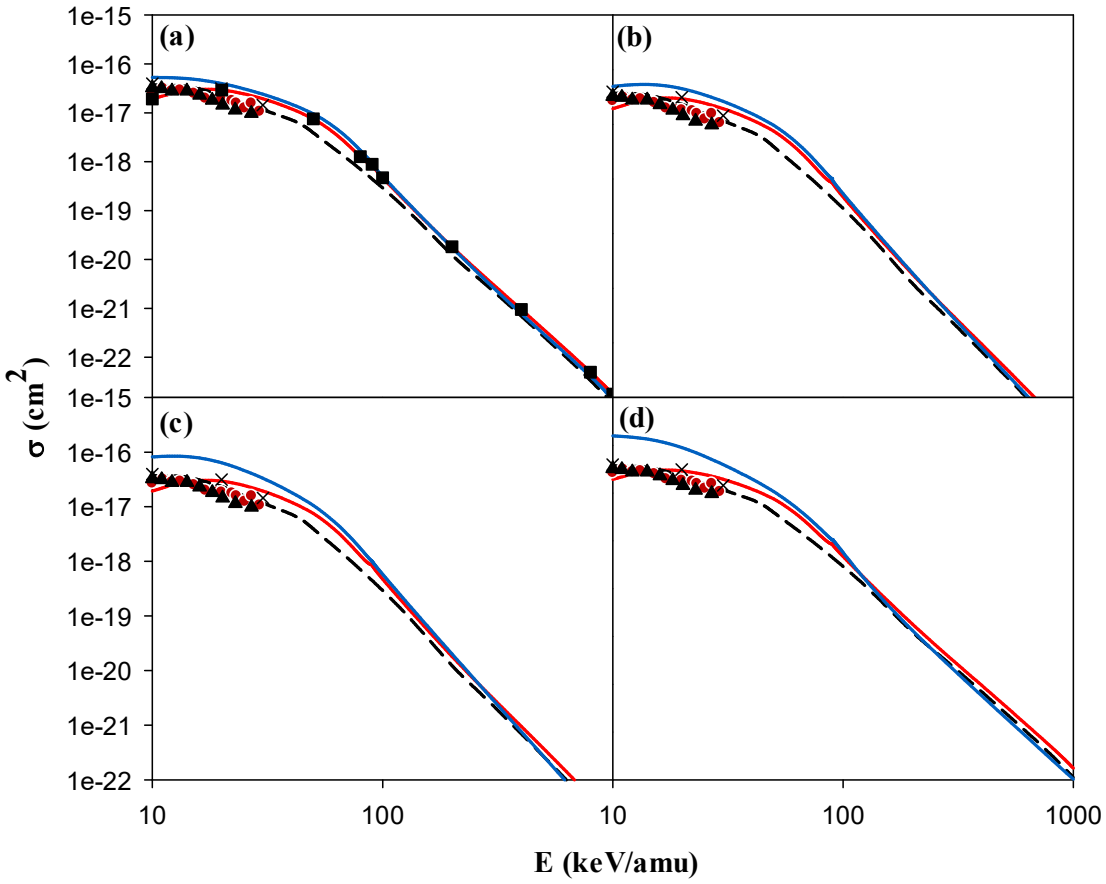

Figure 7.8. Electron capture cross sections into the 2p state of the projectile in H^+ + H(1s) collision as a function of the impact energy. Solid red line: present CTMC results, solid blue line: present QCTMC results for: : a) α_H = 3, ξ_H= 0.9258, b) α_H = 3.5, ξ_H= 0.9354, c) α_H = 4, ξ_H= 0.9428, d) α_H = 4.5, ξ_H= 0.9486, dashed line: SC-CCC [54]. Experimental results are due to; red circles: Kondow [65], black triangles: Morgan *et al.* [62], crosses: Stebbings *et al.* [66].

Figure 7.8 shows that the QCTMC (α_H= 3, ξ_H= 0.9258) and QCTMC (α_H= 3.5, ξ_H= 0.9354) results are close to the experimental data at low energies. In addition, good agreement is seen with the SC-CCC theoretical method [54] at high energies.

As seen in Figures 7.4, 7.5, 7.6, 7.7, and 7.8, I conclude that the results by considering the QCTMC method significantly improve the cross sections as a function of the impact energies. I also observed the effects of α_H and ξ_H on the displacement of cross sections for proton and ground state hydrogen collision systems. Since one combination of α_H and ξ_H in Heisenberg potential function should be chosen for collision systems, by investigating the electron radial and momentum distribution and analyzing the experimental data for various final channels, I found that the constants α_H= 3.5 and ξ_H = 0.9354 in the QCTMC model are reasonable in H^+ + H(1s) collisions.

7.1.8 State-selective electron capture cross sections in H^++H (*nl*) collisions

Collisions between the ions and excited state hydrogen are also the interesting topics for fusion research. Due to the very hot temperature inside the plasma, the majority of the hydrogens atoms are in the excited state. Therefore, cross section calculations for excited state hydrogen as a target is important. I calculated the state-selective electron capture cross sections between excited state hydrogen into the different subshells of H^+ using the CTMC model (Tables 7.1-7.9). I took into account 1×10^6 trajectories for each impact energy. Dashes indicate omitted entries because the cross sections are less than the order of 10^{-21} cm^2.

Table 7.1. *nl* state-selective cross sections (in cm^2) for H^++H(2s).

E (keV/u)	2s	2p	3s	3p	3d	4s	4p	4d	4f
10	2.54(-16)[b]	4.65(-16)	1.21(-16)	1.79(-16)	7.19(-17)	6.15(-17)	7.30(-17)	3.36(-17)	5.01(-18)
20	5.80(-17)	8.94(-17)	2.65(-17)	2.46(-17)	8.44(-18)	1.15(-17)	1.02(-17)	4.82(-18)	1.93(-19)
30	1.90(-17)	2.68(-17)	7.47(-18)	7.97(-18)	1.66(-18)	3.24(-18)	3.46(-18)	8.29(-19)	2.39(-20)
40	8.91(-18)	1.05(-17)	2.96(-18)	3.16(-18)	2.57(-19)	1.42(-18)	1.46(-18)	2.05(-19)	-
50	4.46(-18)	5.09(-18)	1.64(-18)	1.55(-18)	7.30(-20)	7.47(-19)	6.53(-19)	2.01(-20)	-
60	2.74(-18)	2.66(-18)	9.12(-19)	8.16(-19)	8.44(-21)	4.23(-19)	3.51(-19)	-	-
70	1.61(-18)	1.40(-18)	5.61(-19)	3.71(-19)	-	2.39(-19)	1.61(-19)	-	-
80	9.68(-19)	7.40(-19)	3.66(-19)	2.09(-19)	-	1.44(-19)	8.95(-20)	-	-
90	6.91(-19)	3.87(-19)	2.50(-19)	1.14(-19)	-	9.74(-20)	3.78(-20)	-	-
100	4.28(-19)	2.53(-19)	1.52(-19)	6.14(-20)	-	6.39(-20)	1.94(-20)	-	-

[b] $a(-x) = a \times 10^{-x}$

Table 7.2. *nl* state-selective cross sections (in cm^2) for H^++H(2p).

E (keV/u)	2s	2p	3s	3p	3d	4s	4p	4d	4f
10	2.79(-16)[b]	1.38(-15)	1.34(-16)	5.12(-16)	2.65(-16)	7.09(-17)	1.88(-16)	6.90(-17)	7.77(-18)
20	4.45(-17)	2.09(-16)	2.83(-17)	9.78(-17)	9.78(-17)	1.84(-17)	4.27(-17)	6.90(-18)	8.79(-20)
30	1.11(-17)	4.18(-17)	7.01(-18)	1.81(-17)	1.96(-18)	4.51(-18)	8.05(-18)	6.73(-19)	-
40	4.33(-18)	1.09(-17)	2.54(-18)	4.37(-18)	2.07(-19)	1.34(-18)	1.99(-18)	1.08(-19)	-
50	2.05(-18)	3.58(-18)	1.15(-18)	1.47(-18)	3.27(-20)	5.62(-19)	5.94(-19)	1.57(-20)	-
60	1.03(-18)	1.16(-18)	5.47(-19)	4.78(-19)	-	2.66(-19)	2.03(-19)	-	-
70	5.59(-19)	4.25(-19)	3.00(-19)	1.62(-19)	-	1.38(-19)	7.37(-20)	-	-
80	3.52(-19)	2.44(-19)	1.17(-19)	8.32(-19)	-	7.23(-20)	2.26(-20)	-	-
90	1.61(-19)	8.97(-20)	7.77(-20)	9.64(-21)	-	5.43(-20)	-	-	-
100	1.21(-19)	2.82(-20)	4.65(-20)	1.02(-20)	-	2.12(-20)	-	-	-

[b] $a(-x) = a \times 10^{-x}$

Table 7.3. *nl* state-selective cross sections (in cm^2) for H^++H(3s).

E (keV/u)	2s	2p	3s	3p	3d	4s	4p	4d	4f
10	1.12(-16)[b]	2.37(-16)	7.22(-17)	1.18(-16)	7.83(-17)	4.05(-17)	5.37(-17)	3.30(-17)	1.43(-17)
20	2.23(-17)	4.57(-17)	1.16(-17)	1.37(-17)	6.52(-18)	5.68(-18)	5.90(-18)	4.17(-18)	3.70(-19)
30	7.54(-18)	1.40(-17)	3.64(-18)	3.87(-18)	1.27(-18)	1.67(-18)	1.40(-18)	6.81(-19)	-
40	3.12(-18)	5.37(-18)	1.48(-18)	1.37(-18)	2.49(-19)	5.32(-19)	6.84(-19)	1.26(-19)	-
50	1.62(-18)	2.30(-18)	6.44(-19)	6.62(-19)	5.07(-20)	3.33(-19)	3.06(-19)	3.60(-20)	-
60	8.59(-19)	1.10(-18)	3.05(-19)	3.48(-19)	-	1.59(-19)	1.31(-19)	-	-
70	5.05(-19)	5.22(-19)	1.60(-19)	1.67(-19)	-	9.72(-20)	6.15(-20)	-	-
80	3.11(-19)	2.76(-19)	1.12(-19)	8.46(-20)	-	4.69(-20)	4.55(-20)	-	-
90	2.13(-19)	1.61(-19)	7.57(-20)	4.49(-20)	-	2.68(-20)	2.18(-20)	-	-
100	1.38(-19)	1.01(-19)	5.31(-20)	3.08(-20)	-	2.11(-20)	1.36(-20)	-	-

[b] $a(-x) = a \times 10^{-x}$

Table 7.4. *nl* state-selective cross sections (in cm^2) for H^++H(3p).

E (keV/u)	2s	2p	3s	3p	3d	4s	4p	4d	4f
10	8.02(-17)[b]	4.11(-16)	6.99(-17)	2.17(-16)	2.36(-16)	4.15(-17)	1.13(-16)	8.38(-17)	3.44(-17)
20	1.18(-17)	7.36(-17)	8.99(-18)	2.91(-17)	1.49(-17)	6.44(-18)	1.36(-17)	7.59(-18)	2.00(-19)
30	3.68(-18)	1.73(-17)	2.63(-18)	7.06(-18)	1.77(-18)	1.44(-18)	2.89(-18)	8.21(-19)	-
40	1.75(-18)	5.03(-18)	9.84(-19)	2.31(-18)	1.73(-19)	5.35(-19)	9.41(-19)	7.31(-20)	-
50	9.91(-19)	1.75(-18)	3.67(-19)	6.82(-19)	-	2.52(-19)	2.85(-19)	-	-
60	4.14(-19)	6.07(-19)	2.31(-19)	2.00(-19)	-	1.00(-19)	9.61(-20)	-	-
70	1.90(-19)	1.93(-16)	9.71(-20)	7.28(-20)	-	4.36(-20)	4.91(-20)	-	-
80	1.21(-19)	7.65(-20)	7.87(-20)	2.21(-20)	-	3.00(-20)	-	-	-
90	6.26(-20)	4.43(-20)	2.21(-20)	1.89(-20)	-	2.72(-20)	-	-	-
100	4.35(-20)	1.73(-20)	2.64(-20)	-	-	-	-	-	-

[b] $a(-x) = a \times 10^{-x}$

Table 7.5. *nl* state-selective cross sections (in cm^2) for H^++H(3d).

E (keV/u)	2s	2p	3s	3p	3d	4s	4p	4d	4f
10	1.77(-17)[b]	1.58(-16)	2.84(-17)	1.63(-16)	3.74(-16)	2.35(-17)	1.27(-16)	2.27(-16)	3.88(-17)
20	2.99(-18)	1.14(-17)	2.47(-18)	1.43(-17)	7.16(-18)	2.13(-18)	2.84(-18)	4.69(-18)	2.87(-19)
30	8.04(-19)	1.63(-18)	6.37(-19)	2.23(-18)	3.95(-19)	6.02(-19)	1.22(-18)	2.04(-19)	-
40	1.70(-19)	1.13(-19)	1.16(-19)	8.13(-20)	2.13(-20)	8.33(-20)	4.54(-20)	2.15(-20)	-
50	1.67(-20)	2.90(-20)	3.34(-20)	-	-	-	-	-	-

[b] $a(-x) = a \times 10^{-x}$

Table 7.6. *nl* state-selective cross sections (in cm^2) for H^++H(4s).

E (keV/u)	2s	2p	3s	3p	3d	4s	4p	4d	4f
10	5.33(-17)[b]	1.21(-16)	3.91(-17)	7.67(-17)	5.54(-17)	2.61(-17)	3.72(-17)	2.02(-17)	1.18(-17)
20	1.01(-17)	2.37(-17)	5.48(-18)	7.09(-18)	4.17(-18)	3.32(-18)	2.84(-18)	2.08(-18)	2.23(-19)
30	3.14(-18)	6.88(-18)	1.76(-18)	2.00(-18)	7.83(-19)	8.50(-19)	7.90(-19)	3.90(-19)	-
40	1.26(-18)	2.32(-18)	6.45(-19)	6.45(-19)	1.34(-19)	3.07(-19)	2.93(-19)	5.71(-20)	-
50	6.33(-19)	9.54(-19)	2.83(-19)	3.74(-19)	-	1.10(-19)	1.78(-19)	-	-
60	3.85(-19)	4.65(-19)	1.44(-19)	1.50(-19)	-	6.42(-20)	4.86(-20)	-	-
70	2.32(-19)	2.34(-19)	8.17(-20)	8.11(-20)	-	2.04(-20)	4.04(-20)	-	-
80	1.38(-19)	1.43(-19)	3.54(-20)	4.94(-20)	-	2.71(-20)	1.96(-20)	-	-
90	9.07(-20)	8.53(-20)	2.93(-20)	1.88(-20)	-	1.14(-20)	-	-	-
100	6.35(-20)	3.84(-20)	1.54(-20)	1.96(-20)	-	1.11(-20)	-	-	-

[b] $a(-x) = a \times 10^{-x}$

Table 7.7. *nl* state-selective cross sections (in cm^2) for H^++H(4p).

E (keV/u)	2s	2p	3s	3p	3d	4s	4p	4d	4f
10	3.13(-17)[b]	1.80(-16)	3.84(-17)	1.17(-16)	1.45(-16)	2.63(-17)	6.96(-17)	4.85(-17)	3.13(-17)
20	5.09(-18)	3.35(-17)	4.52(-18)	1.37(-17)	9.81(-18)	3.32(-18)	7.35(-18)	4.01(-18)	3.13(-19)
30	1.64(-18)	7.92(-18)	1.08(-18)	3.09(-18)	1.22(-18)	6.38(-19)	1.59(-18)	7.36(-19)	-
40	8.16(-19)	2.23(-18)	4.24(-19)	1.08(-18)	1.76(-19)	2.14(-19)	5.92(-19)	1.32(-19)	-
50	4.21(-19)	8.00(-19)	1.73(-19)	2.92(-19)	-	7.01(-20)	2.01(-19)	-	-
60	2.45(-19)	2.31(-19)	8.82(-20)	1.13(-19)	-	5.98(-20)	7.63(-20)	-	-
70	1.01(-19)	1.02(-19)	4.80(-20)	5.33(-20)	-	2.76(-20)	-	-	-
80	4.21(-20)	1.10(-20)	1.54(-20)	5.74(-21)	-	-	-	-	-
90	4.27(-20)	1.99(-20)	1.28(-20)	9.51(-21)	-	-	-	-	-
100	8.68(-21)	3.48(-21)	4.29(-21)	-	-	-	-	-	-

[b] $a(-x) = a \times 10^{-x}$

Table 7.8. *nl* state-selective cross sections (in cm^2) for H^++H(4d).

E (keV/u)	2s	2p	3s	3p	3d	4s	4p	4d	4f
10	9.54(-18)[b]	7.41(-17)	9.99(-18)	6.28(-17)	1.89(-16)	9.21(-18)	5.05(-17)	9.63(-17)	3.94(-17)
20	2.00(-18)	7.47(-18)	1.81(-18)	8.05(-18)	4.93(-18)	1.32(-18)	4.88(-18)	3.54(-18)	2.07(-19)
30	5.88(-19)	1.47(-18)	5.90(-19)	1.53(-18)	3.46(-19)	3.40(-19)	1.06(-18)	1.37(-19)	-
40	2.14(-19)	1.05(-19)	7.72(-20)	2.06(-19)	2.64(-20)	9.44(-20)	1.22(-19)	-	-
50	3.16(-21)	8.66(-21)	-	-	-	-	-	-	-

[b] $a(-x) = a \times 10^{-x}$

Table 7.9. *nl* state-selective cross sections (in cm^2) for H^++H(4f).

E (keV/u)	2s	2p	3s	3p	3d	4s	4p	4d	4f
10	2.77(-18)[b]	5.55(-18)	5.14(-18)	2.60(-17)	3.95(-17)	4.70(-18)	2.40(-17)	5.11(-17)	1.65(-17)
20	6.55(-20)	1.16(-19)	2.09(-19)	1.07(-18)	4.15(-19)	2.19(-19)	1.24(-18)	3.07(-19)	-

[b] $a(-x) = a \times 10^{-x}$

7.1.9 Trajectories

Trajectories of particles in collisions are an instructive and exciting way to show the behaviour of the projectile ion, electron target, and target nucleus.

Ionization

Figure 7.9 shows trajectories of the ionization channel in the *y-z* lab frame coordinate system without and with considering the Heisenberg correction term, respectively. The trajectories were obtained at 70 keV/amu impact energy. The target electron experiences the attractive Coulomb force from both of target and projectile positive charge. On the other hand, the presence of a correction term in the QCTMC model causes continuous changes in the sum of the forces acting on the electron. Therefore, it can be seen the distortion in electron trajectory (see Figure 7.9 (b)). Also, target repulsion becomes more apparent with the addition of the Heisenberg correction term.

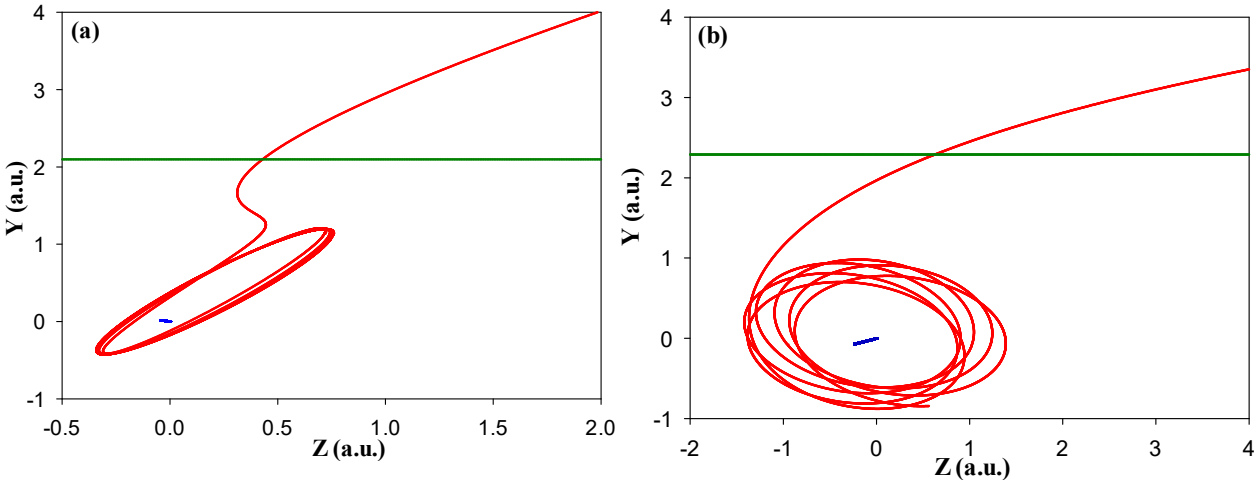

Figure 7.9. Ionization trajectories in the y-z lab frame (a) without considering the correction term, (b) with considering the correction term, at the typical 70 keV/amu impact energy. Solid red line: electron trajectory, solid green line: projectile trajectory, solid blue line: target trajectory.

Electron capture

For the illustration of the electron capture channel, Figure 7.10 represents the trajectories in the *x-z* projectile frame for electron, target, and projectile without and with considering the Heisenberg correction term. The presence of the Heisenberg repulsive force causes slight distortion in the electron trajectory before the electron is placed into the states of the projectile.

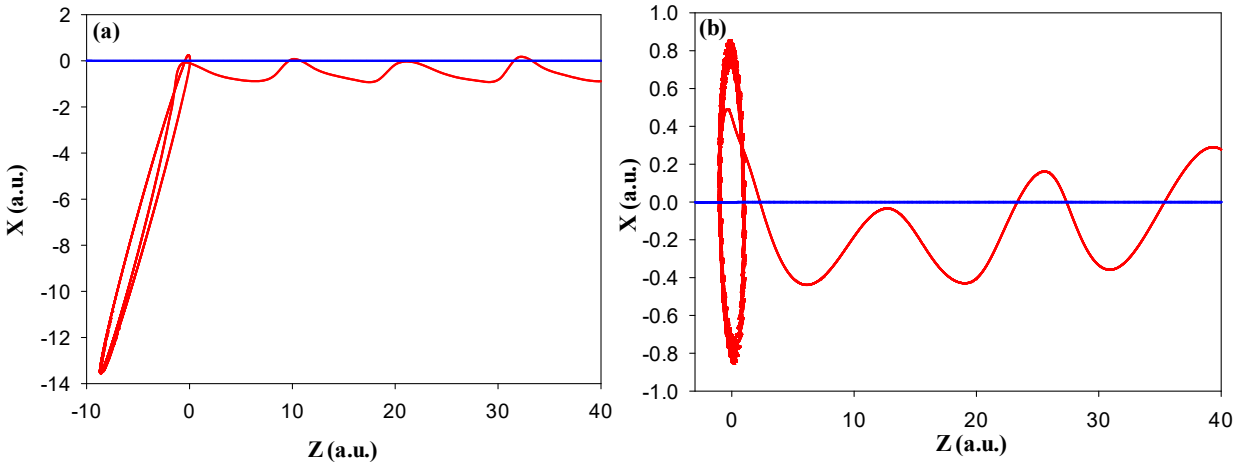

Figure 7.10. Electron capture trajectories in the x-z projectile frame (a) without considering the correction term, (b) with considering the correction term at the typical 70 keV/amu impact energy. Solid red line: electron trajectory, solid blue line: target trajectory.

Excitation

To better understand the excitation channel without and with considering the Heisenberg correction term, I have shown the electron, projectile, and target trajectories in the *x-z* lab frame coordinate system in Figure 7.11. The trajectories were obtained at 70 keV/amu impact energy. The effect of the correction term adds a repulsive force to the classical calculations. Competition between attractive Coulomb force and repulsive Heisenberg force distorts the trajectory of the electron in the excitation channel.

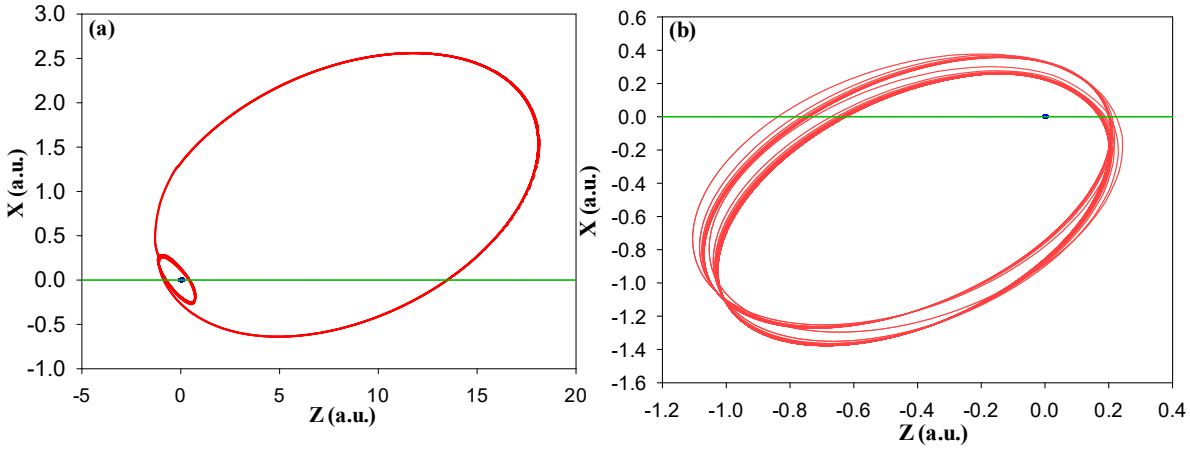

Figure 7.11. Excitation trajectories in the x-z lab frame (a) without considering the correction term, (b) with considering the correction term at the typical 70 keV/amu impact energy. Solid red line: electron trajectory, solid green line: projectile trajectory, solid blue line: target trajectory.

7.2 Interaction between Be^{4+} and ground state hydrogen

The calculation of cross section in collision Be^{4+} and hydrogen atom for ionization, electron capture, and excitation channels have been studied using different quantum-mechanical approaches such as atomic orbital close coupling (AOCC) [37, 67], adiabatic super promotion model [68], the molecular orbital expansion of the solution of the time-dependent Schrödinger equation [69], symmetric Eikonal approximation [70], and classical methods [16].

7.2.1 Three different schema

At first, I tested three calculation schemes during our simulations since the Heisenberg correlation potential may influence the obtained results significantly. These are the following: 1) target-centered, where the correction term is taken into account between the target electron the target nucleus, 2) projectile-centered, where the correction term is taken into account between the target electron the projectile. 3) combined one, i.e., target and projectile centered when the correction term is taken into account between target electron and both the target nucleus and projectile.

As an example, Figure 7.12 shows my CTMC and QCTMC results corresponding to the three calculation schema of the electron capture cross sections into the 4s state of the projectile in Be^{4+} + H (1s) collision as a function of the impact energy. It can be seen that the effects of the correction term at lower energies are significant. While for the case of target-centered, the cross sections at lower incident energies are increasing compared to the standard CTMC results for the case of projectile-centered they are decreasing. The combination of the use of target- and projectile-centered corrections results increases the cross sections and I obtained good

agreement between my QCTMC results and previous full quantum mechanical results in the entire impact energy range. One can have the same definition for other collision channels, as well. Therefore, in the following, for the calculation of the cross sections for various collision channels, I will use only the combination scheme.

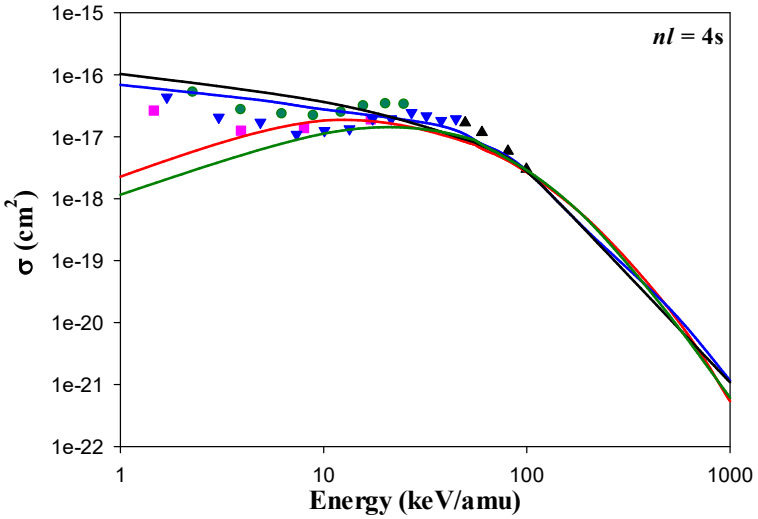

Figure 7.12. Electron capture cross sections into the 4s state of the projectile in Be^{4+} + H (1s) collision as a function of the impact energy. Solid red line: present CTMC results, solid black line: present *target-centered* QCTMC results, solid green line: present *projectile-centered* QCTMC results, solid blue line: present *target and projectile centered* QCTMC results, pink squares: AOCC results of Fritsch [9], green circles: QMOCC results of Harel *et al.* [8], black triangles: BCCIS results of Das *et al.* [15], blue inverse triangles: OEDM results of Errea *et al.* [14].

7.2.2 Impact parameter dependent probabilities

Figure 7.13 shows the present CTMC and QCTMC results with the three calculation schemes of the electron capture probabilities into the specific n = 3, 4 and nl = 3d, 4s states of the projectile at 10 keV/amu impact energy in Be^{4+} + H(1s) as a function of impact parameter. The impact parameter dependent electron capture probabilities, *bP(b)*, were fitted by a Gaussian function. The peak maxima of the Gaussian fitting is also shown in Figure 7.13. I note that the area under the curves is proportional to the state-selective electron capture cross sections. I found that the probability of electron capture is higher in target-centered QCTMC and lower in projectile-centered QCTMC model compared with the standard CTMC model. This behavior can be understood with the explanation of the acting forces between the interacting particles, $F = -{dU}/{dr}$. The attractive force between an electron and both of proton and positive projectile ion, is due to the Coulomb interaction and repulsive force is due to the Heisenberg correction term as follow:

$$F_{Heisenberg} = -\left(\frac{{\xi_H}^2}{2\alpha_H r^3} + \frac{rp^4}{{\xi_H}^2}\right) exp\left\{\alpha_H\left[1-\left(\frac{rp}{\xi_H}\right)^4\right]\right\}. \quad (7.9)$$

The attractive Coulomb force acts between the electron and positively charged, target and projectile, in the same way in all schemes. This force, most of the time of the collision, is much larger than $F_{Heisenberg}$. On the other hand, in the target-centered scheme, the repulsive force, $F_{Heisenberg}$, is toward the projectile, but on the contrary, this repulsive force is towards the target in projectile-centered mode. I note that this repulsive force, of course, does not show up in the standard CTMC model. According to the sum of the forces, the electron has the highest attraction to the projectile in the target-centered QCTMC and the least attraction to the projectile in the projectile-centered QCTMC. With this scenario, the case of CTMC is placed between the above two modes. Therefore, the probability of electron capture in projectile-centered QCTMC, CTMC, and target-centered QCTMC modes increases, respectively.

Another noteworthy point is that the peak maxima in CTMC and QCTMC projectile-centered cases are very close to each other and locate in lower impact parameters. This is also true in QCTMC target-centered and QCTMC combined target- and projectile-centered cases, except that the peak maxima are at higher impact parameters.

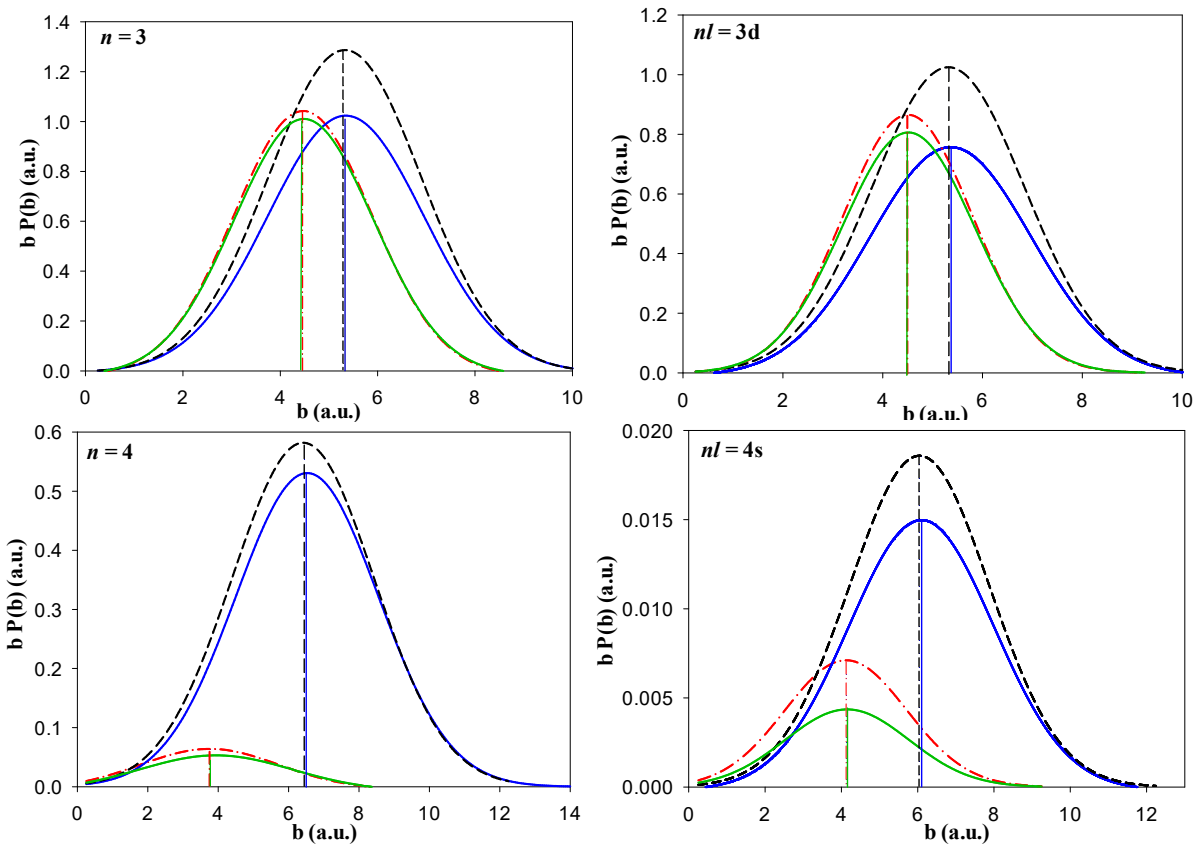

Figure 7.13. Probability for electron capture into n = 3, 4 and nl = 3d, 4s states of the projectile (multiplied by impact parameter) in Be^{4+} + H(1s), as a function of the impact parameter, at 10 keV/amu impact energy. Dash-dotted red line: present CTMC results, dash black line: present target-centered QCTMC results, solid green line: present projectile-centered QCTMC results, solid blue line: combination of target-projectile-centered.

7.2.3 Ionization cross sections

Figure 7.14 shows the cross section for the ionization channel (see Equation 7.10) obtained by both the CTMC and QCTMC methods as a function of projectile energy in the energy range between 10 and 1000 keV/amu. The results of the present CTMC models are compared with previous results. My results with the CTMC method match the data of Olson [17] for the entire energy range. At the same time, my results show lower cross section data than that obtained by Krstic and Radmilovic [68] for lower projectile energies. Applying the effective potentials, V_H, to mimic the Heisenberg principles in our simulations, the cross section data are a little increased compared to the standard CTMC results.

$$Be^{4+} + H(1s) \rightarrow Be^{4+} + H^{+} + e^{-}. \qquad (7.10)$$

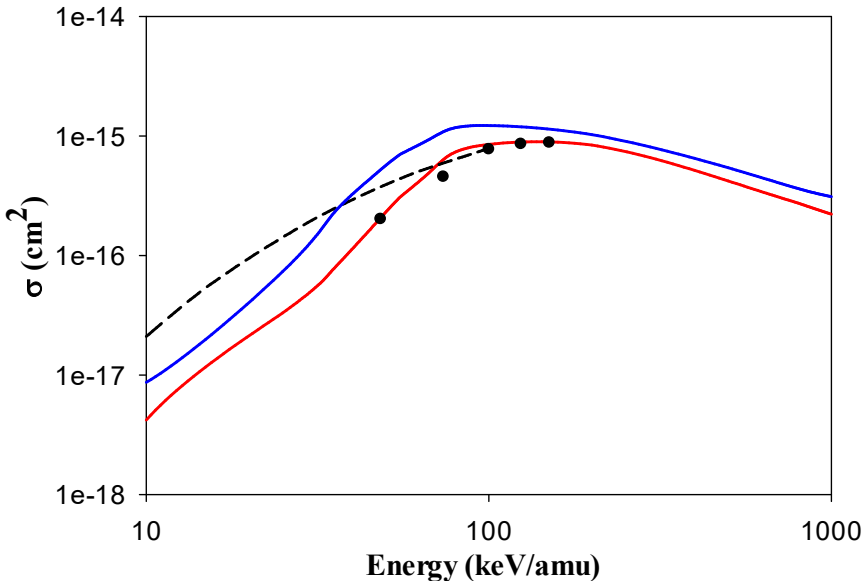

Figure 7.14. Cross section for ionization of H(1s) by Be^{4+} as a function of projectile energy. Solid red line: present CTMC results, solid blue line: present QCTMC results, dash line: adiabatic superpromotion results of Krstic *et al*. [68], black circles: CTMC results of Olson *et al*. [17].

7.2.4 Total electron capture cross sections

The exact knowledge of electron capture cross sections in collisions between Be ions and hydrogen atoms is very interesting for fusion research [64] (see Sections 2.5 and 2.6). Due to the experimental difficulties, the experimental results for electron capture cross sections in Be^{4+} + H collisions are entirely lacking, but those were studied intensively theoretically in the past years.

The total electron capture cross sections have been studied using various models and methods such as applying the quantum-mechanical molecular orbital close-coupling (QMOCC) [8], the atomic orbital close-coupling (AOCC) [9], the hyper spherical close-coupling (HSCC) [10] models, using the solution of the time dependent Schrödinger equation (TDSE) [11], the lattice time dependent Schrödinger equation (LTDSE) [12], the classical over barrier model (COBM) [13] and the classical trajectory Monte Carlo method [73, 74]. I have calculated the total cross section of CX to the projectile bound states *nl* according to CTMC and QCTMC methods for the process:

$$Be^{4+} + H(1s) \rightarrow Be^{3+}(nl) + H^{+}. \qquad (7.11)$$

The comparisons were made with all available methods such as the solution of time-dependent Schrödinger equations, molecular-orbital-close coupling (MOCC), and atomic-orbital-close coupling (AOCC) calculations (see Figure 7.15).

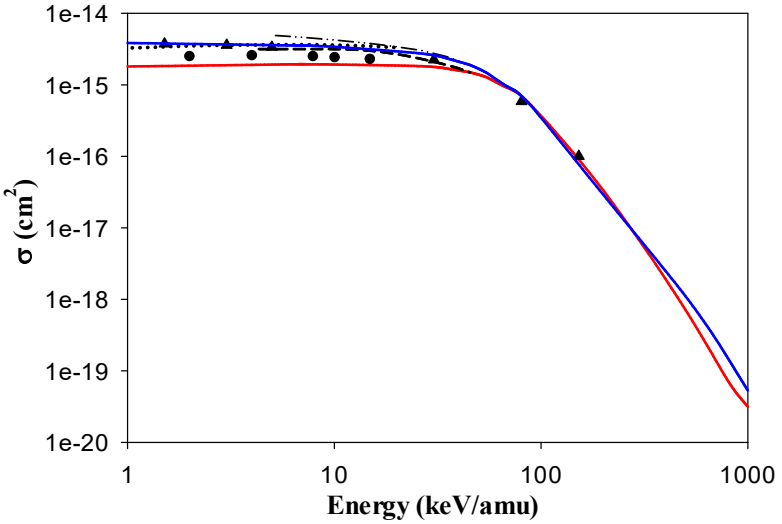

Figure 7.15. Total cross section for electron capture in Be^{4+} + H(1s) collision, as a function of the impact energy. Solid red line: present CTMC results, solid blue line: present QCTMC results, dash line: TDSE results of Ludde *et al*. [75], dash-double-dot line: AOCC results of Bransden *et al*. [76], dotes: MOCC results of Harel *et al*. [77], circles: TDSE results of Kimura *et al*. [69], triangles: QMOCC results of Qu *et al*. [67].

I found a significant improvement in the cross section using the QCTMC method compared to the standard CTMC model. I also found excellent agreement between my QCTMC results and the previous data by Qu *et al*. [67], Ludde *et al*. [80], Bransden *et al*. [76], and Harel *et al*. [77].

7.2.5 State-selective electron capture cross sections

The partial electron capture cross sections in collisions between Be and hydrogen atom have been also studied using different quantum-mechanical methods such as QMOCC [8,78], AOCC [9], one-electron diatomic molecule (OEDM) [14], and boundary corrected continuum intermediate state (BCCIS) [15] models. It is worth noting that all the results have been published for projectile energy below 100 keV/amu. The calculation of the principal quantum number, n, dependent cross sections has been studied by Jorge *et al*. [79] by solving the time-dependent Schrödinger equation with the GridTDSE package (GTDSE) numerically in the broad energy range between 1 keV/amu and 500 keV/amu.

Quantum mechanical models are known to be potent candidates performing the simulations but the analysis of equations to describe atomic collisions in many cases is very complicated and time consuming. Therefore, classical theories like the trajectory Monte Carlo method can be a good alternative.

Figure 7.16 shows the present CTMC and QCTMC results of the electron capture into $n = 2$ state of the projectile in Be^{4+}+H(1s) as a function of the impact energy. My present results are compared with the quantum-mechanical approaches based on the AOCC [9], MOCC [8], OEDM [14], CDW [80], and BCCIS [15]. To evaluate the validity of my CTMC results, I also showed the CTMC results of Schultz *et al.* [74] for comparison.

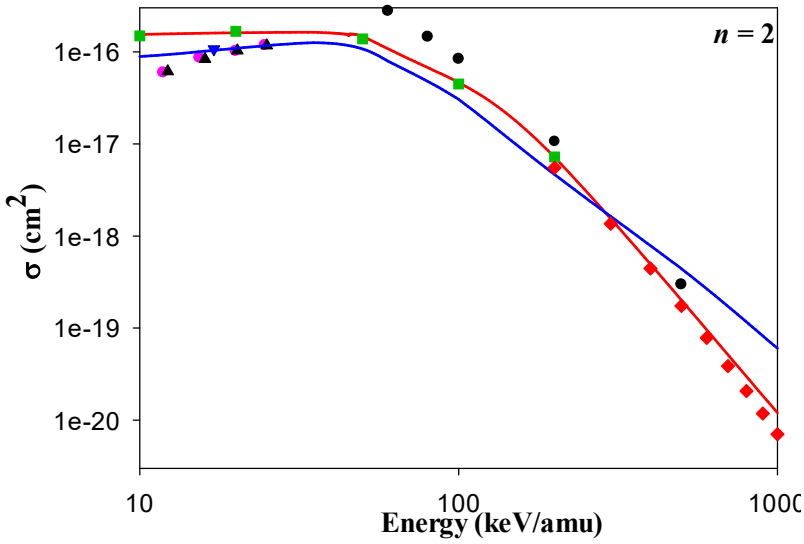

Figure 7.16. Electron capture cross sections into the $n = 2$ state of the projectile in Be^{4+} + H(1s) collision as a function of the impact energy. Solid red line: present CTMC results, solid blue line: present QCTMC results, blue inverse triangle: AOCC results of Fritsch *et al.* [9], pink circles: MOCC results of Harel *et al.* [8], black triangles: OEDM results of Errea *et al.* [14], red diamonds: CDW results of Belkic *et al.* [80], black circles: BCCIS results of Das *et al.* [15], green squares: CTMC results of Schultz *et al.* [74].

I found that the QCTMC results are significantly closer to the quantum-mechanics results like the AOCC results of Fritsch *et al*. [9], OEDM results of Errea *et al.* [14], and the MOCC results of Harel *et al.* [8] compared with the CTMC ones at low energies. The present CTMC cross sections below 300 keV/amu impact energy are higher than the QCTMC cross sections, and the two curves with and without correction term intersect at around 300 keV/amu. The correction term exerts the repulsive force between the electron and both of target nucleus and the projectile. This repulsive force is less than the attractive Coulomb force between the electron and target nucleus but affects the charge transfer process. At low impact energy, the projectile spent more time at the vicinity of the target, and the repulsive force causes to increases the probability of the electron capture channel. The correction term loses its effect at higher impact energies, and the standard CTMC method described the cross sections reasonably well. According to Figure 7.17, the present CTMC results are in excellent agreement with the CDW results of Belkic *et al.* [80] and with the BCCIS results of Das *et al.* [15] at higher impact energies. On the other hand, the QCTMC results give reasonable cross sections at lower impact energies.

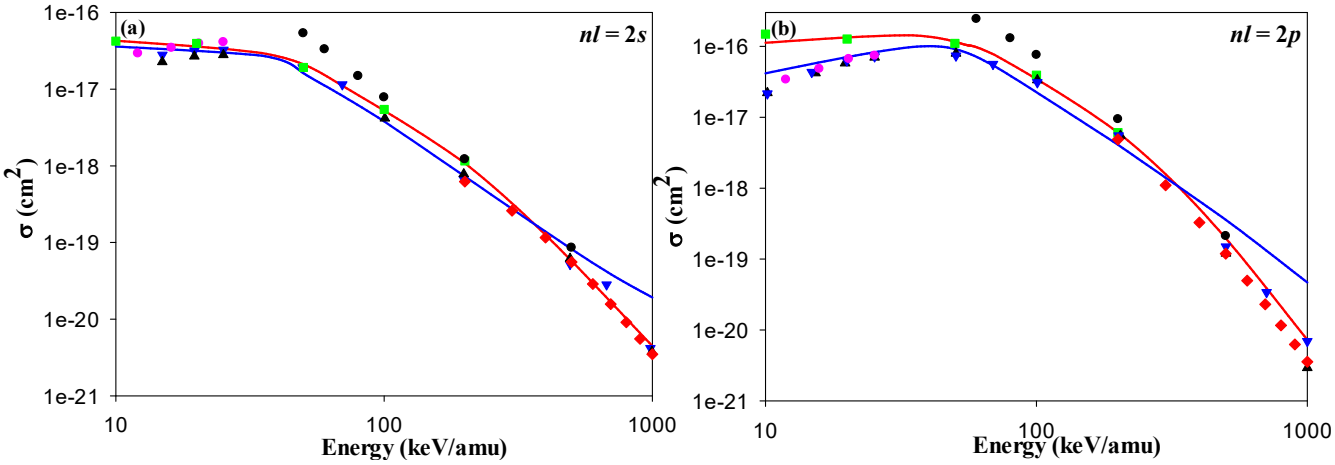

Figure 7.17. Electron capture cross sections into (a) 2s, (b) 2p states of the projectile in Be^{4+} + H(1s) collisions as a function of the impact energy. Solid red line: present CTMC results, solid blue line: present QCTMC results, blue inverse triangles: AOCC results of Minami *et al.* [12], pink circles: MOCC results of Harel *et al.* [8], black triangles: LTDSE results of Minami *et al.* [12], red diamonds: CDW results of Belkic *et al.* [80], black circles: BCCIS results of Das *et al.* [15], green squares: CTMC results of Schultz *et al.* [74].

Figure 7.17 (a) shows the electron capture cross sections into the 2s state of the projectile in Be^{4+}+H(1s) as a function of the impact energy. The LTDSE results of Minami *et al.* [12] are in good agreement with the present QCTMC results. Also, the AOCC results of Minami *et al.* [12] agreed with QCTMC results at low and intermediate impact energies. The present CTMC

and QCTMC results are very close to each other at low impact energies and they are in agreement with the MOCC results of Harel *et al.* [14]. The BCCIS results of Das *et. al* [15] have a better agreement with the present CTMC results at intermediate and high impact energies than the present QCTMC results. In addition, one can see the exact matching between the CDW results of Belkic [80] and the present CTMC results at high impact energies.

Figure 7.17 (b) shows the electron capture cross sections into the 2p state of the projectile in Be^{4+}+H(1s) as a function of the impact energy. The QCTMC results at low impact energies drop more than the CTMC ones, which agrees with quantum-mechanical approaches such as MOCC [8] and LTDSE [12]. The QCTMC cross sections are greater than CTMC ones beyond the energy of about 300 keV/amu. In addition, the present CTMC results are in good agreement with the obtained results based on CDW approximation [80] and with the BCCIS [15] at higher impact energies.

Figure 7.18 shows the present CTMC and QCTMC results of the electron capture cross sections into the n = 3, 4, 5 states of the projectile in Be^{4+} + H(1s) collision as a function of the impact energy. The present classical results are compared with Fritsch [9], Harel *et al.* [8], and Das *et al.* [15], as well. The QCTMC results are higher than the CTMC ones at low and intermediate impact energies. This difference is more significant in n = 4 and n = 5 states. The best matching between the present CTMC and QCTMC is seen at high energies. In n = 3 and n = 5 states, the present QCTMC results agree well with the available quantum-mechanical approaches such as; QMOCC [8], AOCC [9], and BCCIS [15].

The standard statistical error at 1000 keV/amu impact energy is around 4% in CTMC and QCTMC, respectively. Figure 7.18 also shows the cross sections for higher states where no previous data are available.

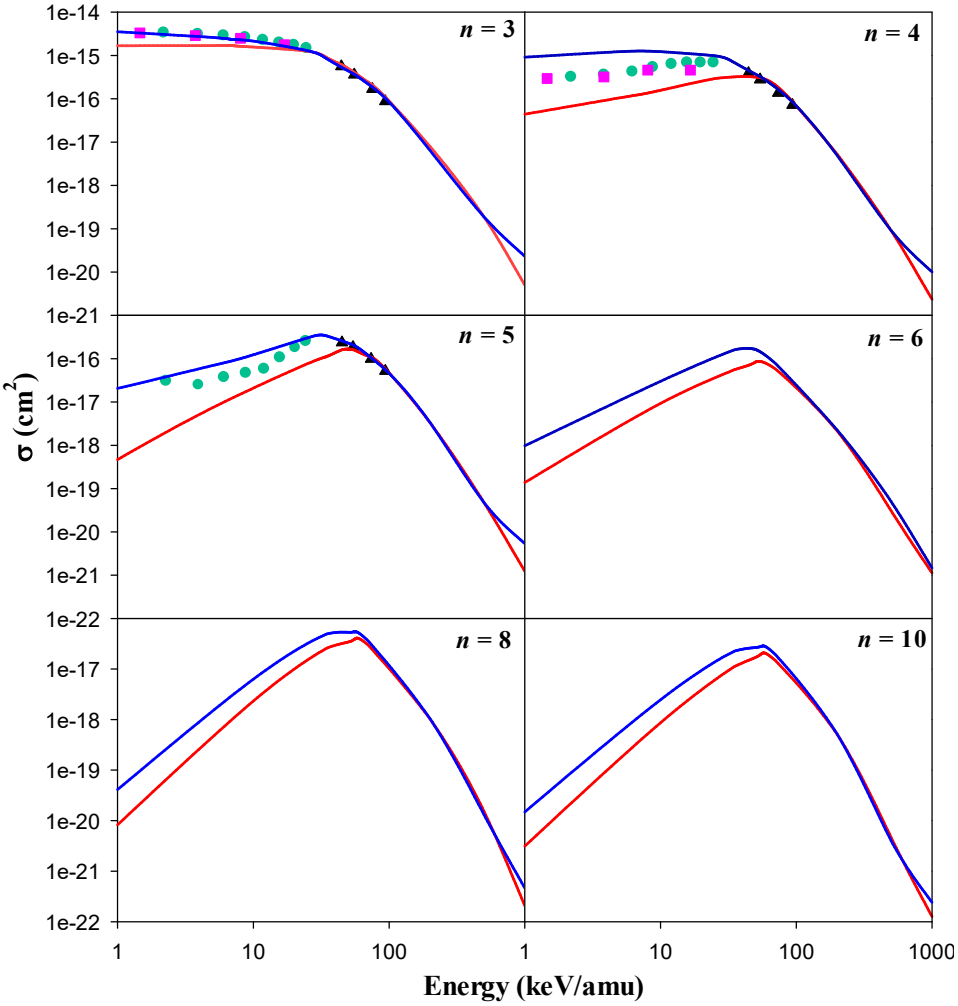

Figure 7.18. Electron capture cross sections into the n = 3, 4, 5 states of the projectile in Be^{4+} + H(1s) collision as a function of the impact energy. Solid red line: present CTMC results, solid blue line: present QCTMC results, pink squares: AOCC results of Fritsch [9], green circles: QMOCC results of Harel *et al.* [8], black triangles: BCCIS results of Das *et al.* [15]. Also, electron capture cross sections into n = 6, 8, 10 states are recommended.

Figure 7.19 shows my CTMC and QCTMC results of the electron capture cross sections into 3s, 3p, and 3d states of the projectile in Be^{4+}+H(1s) as a function of the impact energy. The comparison is made with Fritsch [9], Harel *et al* [8], Das *et al.* [15], and Errea *et al*. [14]. The QCTMC model significantly improves the cross sections compared to the CTMC at low and intermediate impact energies. Moreover, the unique agreement is obtained between the present QCTMC results and 1) QMOCC results [8] in the 3s state, 2) OEDM [14], and BCCIS results [15] in 3p state 3) QMOCC [8], AOCC [9], OEDM [14], and BCCIS [15] results in 3d state of the Be^{3+} at energies lower than 100 keV/amu, respectively.

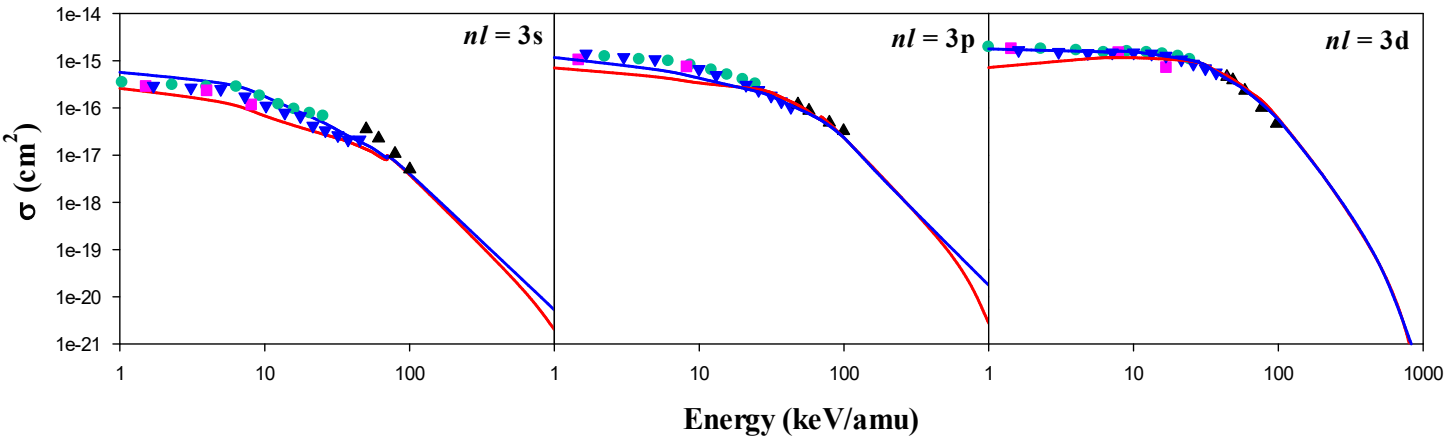

Figure 7.19. Electron capture cross sections into 3s, 3p, and 3d states of the projectile in Be^{4+} + H(1s) collision as a function of the impact energy. Solid red line: present CTMC results, solid blue line: present QCTMC results, pink squares: AOCC results of Fritsch [9], green circles: QMOCC results of Harel *et al.* [8], black triangles: BCCIS results of Das *et al.* [15], blue inverse triangles: OEDM results of Errea *et al.* [14].

Figure 7.20 represents my CTMC and QCTMC results of the electron capture cross sections into 4s, 4p, 4d, and 4f states of the projectile in Be^{4+}+H(1s) as a function of the impact energy. I have compared the present classical results with the quantum-mechanical approaches such as QMOCC [8], AOCC [9], OEDM [14], and BCCIS [15]. The QCTMC model remarkably increases the cross sections compared with the CTMC at low and intermediate energies. The difference between the present CTMC and QCTMC results at low energies gradually increases from 4s to 4f states. It can be seen that my CTMC results have the best agreement with the AOCC results of Fritsch [9] in 4s and 4p states. Moreover, the QCTMC cross sections in 4s and 4p states have better agreement with the QMOCC results of Harel *et al.* [8] and the OEDM results of Errea *et al.* [14]. However, both present classical results are in excellent agreement with the BCCIS results of Das *et al.* [15] at intermediate energies. The standard statistical error for 4s, 4p, 4d, and 4f states is around 1.6% in the range of 1-500 keV/amu impact energies. At the same time, for the projectile energy range of 500-1000 keV/amu, the estimated uncertainties are around 4%.

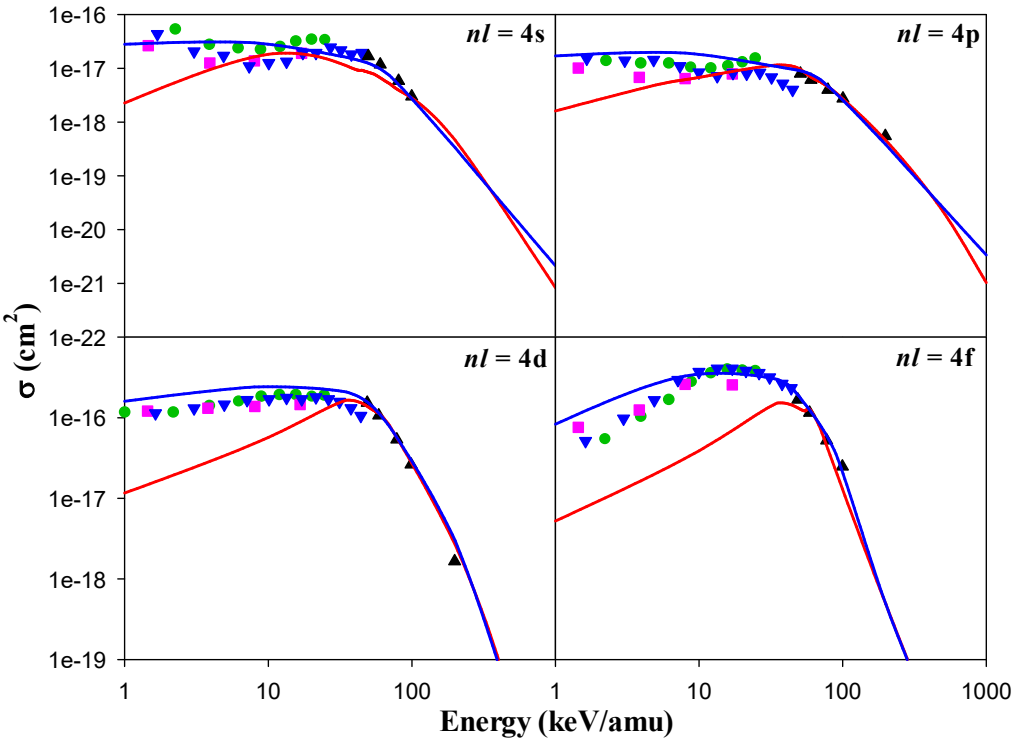

Figure 7.20. Electron capture cross sections into 4s, 4p, 4d, and 4f states of the projectile in Be^{4+} + H(1s) collision, as a function of the impact energy. Solid red line: present CTMC results, solid blue line: present QCTMC results, pink squares: AOCC results of Fritsch [9], green circles: QMOCC results of Harel *et al.* [8], black triangles: BCCIS results of Das *et al.* [15], blue inverse triangles: OEDM results of Errea *et al.* [14].

Figure 7.21 shows the present CTMC and QCTMC results of the electron capture cross sections into 5s, 5p, 5d, and 5f states of the projectile in Be^{4+}+H(1s) as a function of the impact energy. The obtained results are compared with QMOCC [8], BCCIS [15], and OEDM [14] methods, as well. According to Figure 7.21, the QCTMC method outstandingly enhances the cross sections compare to the CTMC results at impact energies lower than about 60 keV/amu. Good agreements are obtained between the present QCTMC results with the OEDM results of Errea *et al.* [14] and the QMOCC results of Harel *et al.* [8] in 5s, 5d, and 5f states of the projectile. The present CTMC and QCTMC results in all 5*l*-states agree well with the BCCIS results of Das *et al.* [15] at intermediate energies. The QCTMC and CTMC cross sections are approximately matched at the impact energies greater than 100 keV/amu.

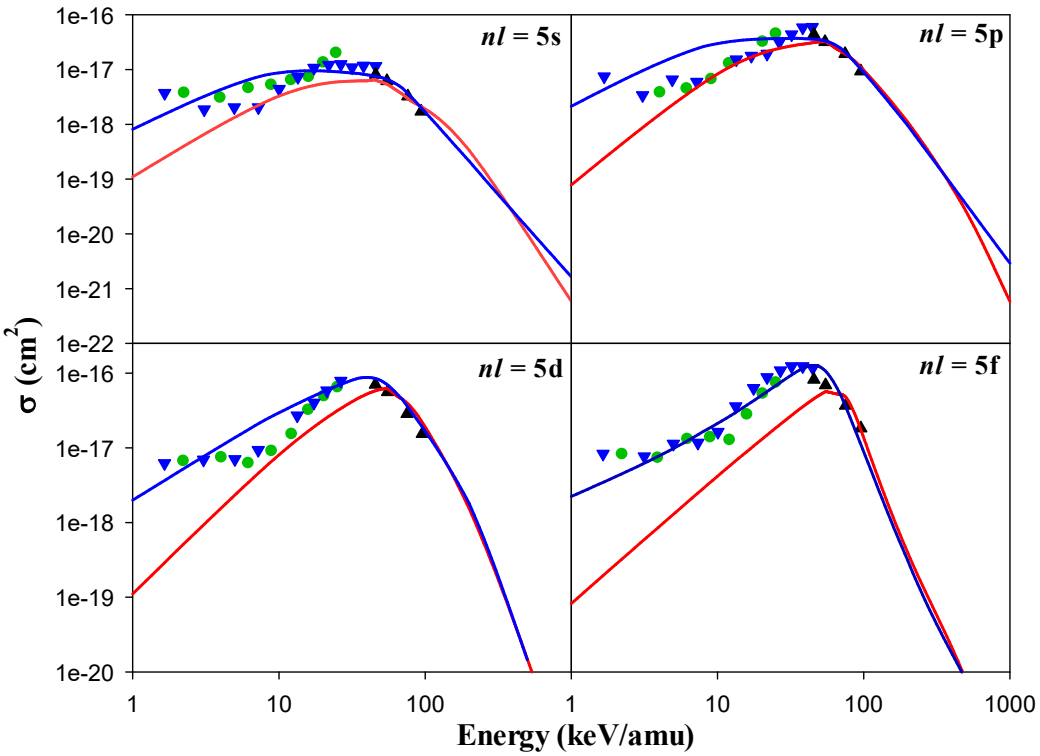

Figure 7.21. Electron capture cross sections into 5s, 5p, 5d, and 5f states of the projectile in Be^{4+} + H(1s) collision, as a function of the impact energy. Solid red line: present CTMC results, solid blue line: present QCTMC results, green circles: QMOCC results of Harel *et al.* [8], black triangles: BCCIS results of Das *et al.* [15], blue inverse triangles: OEDM results of Errea *et al.* [14]

According to Figures 7.18 - 7.21, the present CTMC and QCTMC results of the electron capture cross sections into specific states of the projectile in Be^{4+}+H(1s) are given for several typical impact energies in Table 7.10. As I already mentioned, the QCTMC cross sections are larger compared to CTMC ones at lower incident energies. However, as the energy increases, this difference gradually decreases so that at very high energies, this difference is negligible. To explain this behavior physically, I focus on the force between the electron and the hydrogen nucleus. Typically, the net Coulomb force is applied between two bodies, which is inversely related to the square of the distance between them. Heisenberg correction term (see Equation 6.5) generates a repulsive force in the opposite direction to the Coulomb force. In this case, the attraction force between the electron and the target nucleus decreases, increasing the electron reactivity with the projectile ion in the electron capture channel. In addition, the long-distance of the projectile to the electron practically reduces this repulsive force effect on the calculations (see Figure 7.12).

On the other hand, the passing projectile ion at low energies causes the extension of the interaction time. Therefore, the effect of these factors increases the cross section at low energies in the QCTMC model. Also, the interaction time is shorter at high energies. Furthermore, due

to the small Heisenberg repulsive force, the correction term gradually loses its effects; therefore, the CTMC and QCTMC results are approximately the same.

Table 7.10. The present CTMC and QCTMC results of the electron capture cross sections into specific states of the projectile in Be^{4+}+H(1s).

Energy (keV/amu)	Model	Cross Section (in 10^{-16} cm^2)					
		3s	3d	4s	4d	5s	5d
1	CTMC	2.608	7.175	0.022	0.116	0.001	0.001
	QCTMC	5.698	17.81	0.686	3.370	0.017	0.056
5	CTMC	1.326	11.09	0.135	0.314	0.012	0.019
	QCTMC	3.343	15.74	0.385	3.844	0.061	0.170
10	CTMC	0.681	11.61	0.183	0.571	0.033	0.081
	QCTMC	1.757	15.46	0.276	3.364	0.084	0.316
35	CTMC	0.209	6.780	0.112	1.652	0.062	0.464
	QCTMC	0.288	6.469	0.158	2.275	0.087	1.024
55	CTMC	0.117	3.109	0.077	1.220	0.054	0.623
	QCTMC	0.144	2.787	0.089	1.161	0.055	0.658
70	CTMC	0.081	1.793	0.052	0.797	0.036	0.450
	QCTMC	0.089	1.576	0.062	0.705	0.039	0.401
90	CTMC	0.052	0.879	0.033	0.401	0.022	0.263
	QCTMC	0.040	0.569	0.028	0.405	0.023	0.212
200	CTMC	0.007	0.039	0.005	0.024	0.003	0.015
	QCTMC	0.004	0.039	0.003	0.028	0.002	0.0187

7.2.6 Principal quantum number dependent cross sections for electron capture

For a better intuitive understanding of the electron capture cross sections relative to the projectile energy level, the *n*- and *l*- level distribution is very useful. Figure 7.22 shows the electron capture *n*-level distribution in a collision between Be^{4+} and ground state hydrogen atom at 50, 100, 200, and 500 keV/amu impact energies by CTMC and QCTMC models. I considered 1×10^6 trajectories for each impact energy. The maximum electron capture cross section in both models takes place in $n = 3$ state of the projectile at 50, and 100 keV/amu impact energy. It can be seen that the probability of the electron capture is higher in $n = 2$ state of the projectile at 200, and 500 keV/amu impact energies. Also, in $n = 1$ state of the projectile, the QCTMC cross sections is higher than the CTMC ones at typical impact energies. According to Figure 7.22, the QCTMC results are approximately matched with CTMC ones at 100, 200, and 500 keV/amu impact energies in $n \geq 4$ states. This means that the effect of the Heisenberg correction term is gradually reduced at higher energies at larger *n* levels.

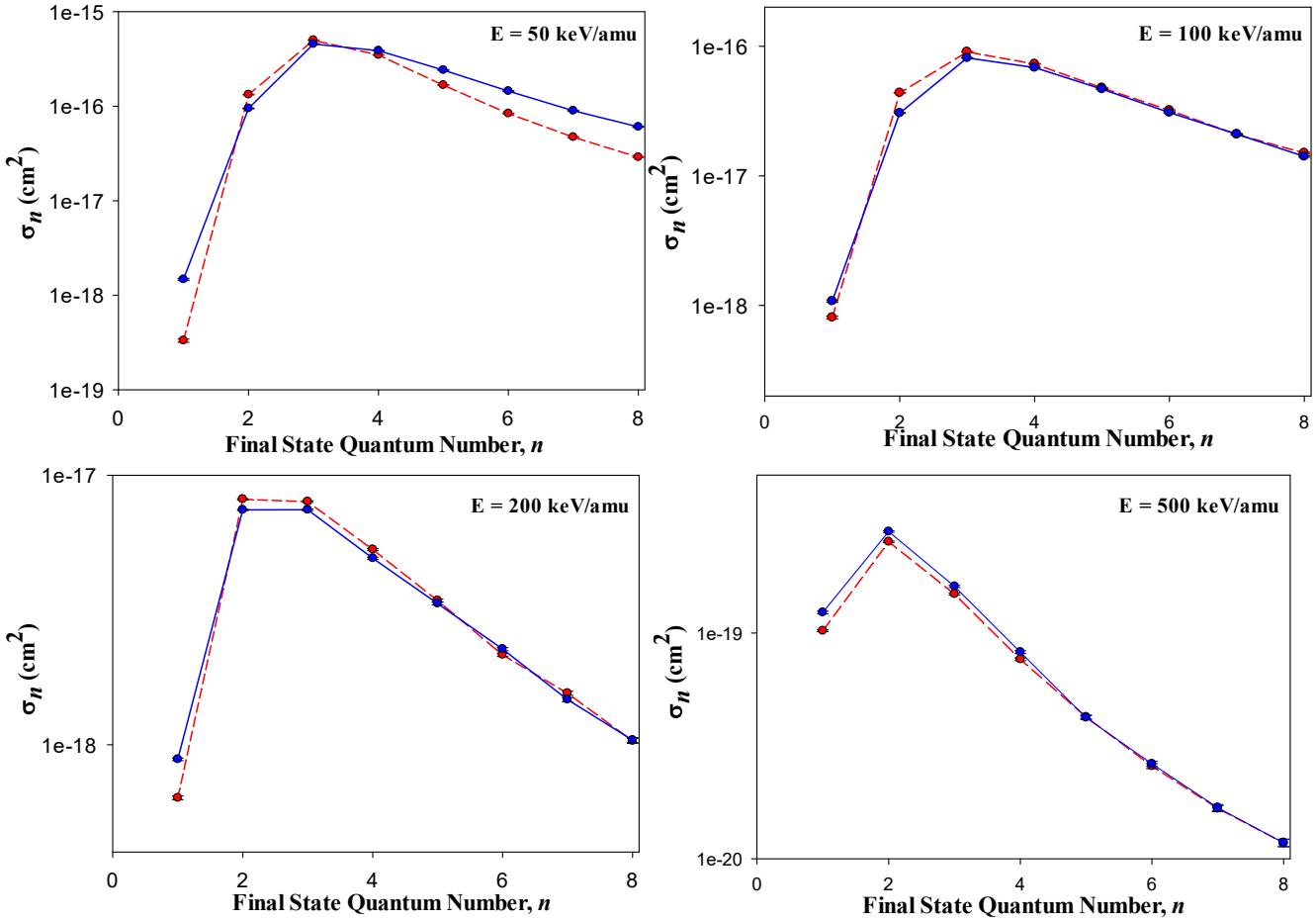

Figure 7.22. Electron capture cross sections to product n levels at 50, 100, 200 and 500 keV/amu impact energies in the Be^{4+} + H(1s) collision system. Solid blue line: present CTMC results, dash red line: present QCTMC results.

7.2.7 Angular quantum number dependent cross sections for electron capture

Figure 7.23 shows the electron capture l-level distribution in a collision between Be^{4+} and ground state hydrogen atom at 50, 100, 200, and 500 keV/amu impact energies by CTMC and QCTMC models. It can be seen that in the higher impact energy, the CTMC results are in better agreement with the QCTMC ones. In fact, at higher impact energies, the effect of the Heisenberg correction term is negligible. Also, for both CTMC and QCTMC models, the most probability of collision in electron capture channel according to nl states of the projectile is the same at each impact energy. According to Figure 7.23, the maximum of electron capture cross sections is seen in nl=3d state at 50, 100 keV/amu impact energy and nl=2p state at 200, 500 keV/amu impact energy.

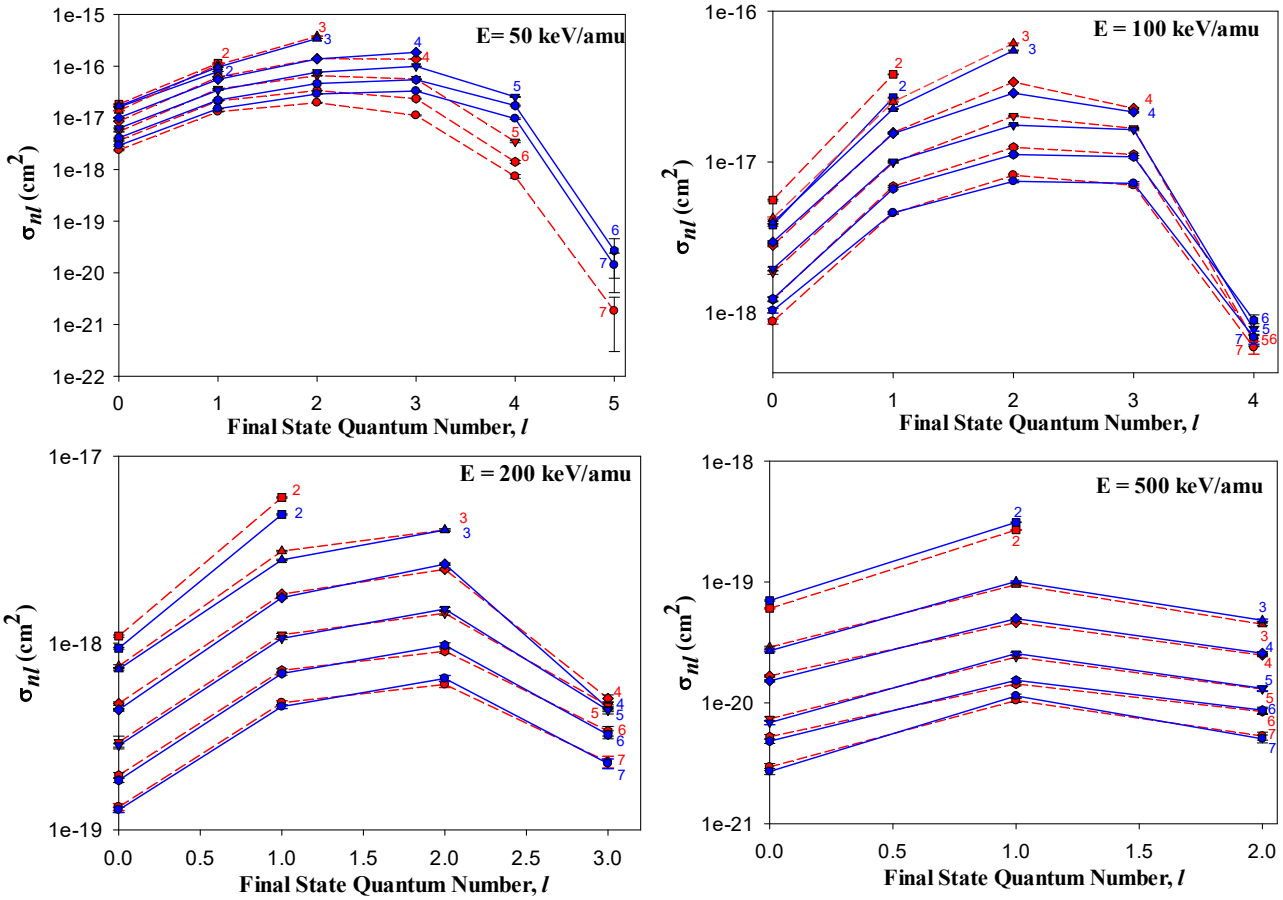

Figure 7.23. Electron capture into nl levels at 50, 100, 200 and 500 keV/amu impact energies in Be^{4+} + H(1s) collision system. Solid red line: present CTMC results, dash red line: present QCTMC results. The numbers depict the n level while x axis gives the orbital-angular-momentum quantum number l.

7.2.8 Excitation cross sections

In the following, I show cross sections for Be^{4+} induced $1s \rightarrow 2s$ and $1s \rightarrow 2p$ transitions in atomic hydrogen by using CTMC and QCTMC methods. The excitation process is given as follows:

$$Be^{4+} + H(1s) \rightarrow \quad Be^{4+} + H(n,l)^{*}. \tag{7.12}$$

I considered the excitation of hydrogen atom by beryllium from 1s state to 2s and 2p excited states. Hence, the hydrogen's electron is then described by the quantum numbers $n = 2$ and $l =$ 0,1 which corresponds to spherical (s) or polar (p) orbital-angular-momentum, respectively. Figure 7.24 shows the excitation cross section in Be^{+4} + H(1s) collisions as a function of projectile energy for $H(1s) \rightarrow H(2s)$ (see Figure 7.25 (a)) and $H(1s) \rightarrow H(2p)$ (see Figure 7.24 (b)) transition states, respectively. The comparisons were made with the corresponding

results based on adiabatic superpromotion model [68], symmetric Eikonal approximation [70] as well as AOCC calculations [9].

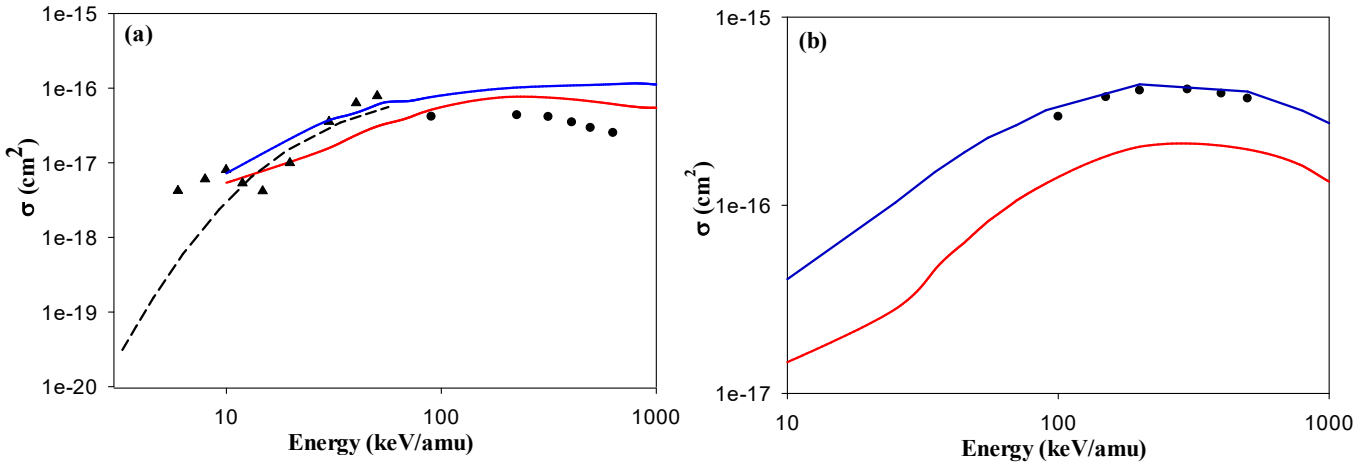

Figure 7.24. Cross section for the excitation of (a) $nl = 2s$ and (b) $nl = 2p$ hydrogen subshells in Be^{4+} + H(1s) collision, as a function of the impact energy. Solid red line: present CTMC results, solid blue line: present QCTMC results, dash line: adiabatic superpromotion results of Krstic *et al*. [68], triangles: AOCC results of Fritsch *et al*. [9], circles: symmetric Eikonal approximation results of Olivera [70].

I note that, while in the previous works, the obtained excitation cross sections are from H(1s) to H($n = 2$), while in this work, I show cross sections into H(2s) and H(2p) subshells. As shown in Figure 7.24, both CTMC and QCTMC methods are useful to describe the excitation cross section for H(1s) to H(2s) transition state. Furthermore, using the QCTMC model it is seen that the cross sections are shifted to higher values compared to the CTMC data. It is noticeable that the data obtained by the QCTMC model are in good agreement with the data reported by the symmetric Eikonal approximation results [70].

7.2.9 Trajectories

Ionization

For the illustration of the ionization channel in the CTMC method, Figure 7.25 shows typical trajectories in the y–z coordinate system (a) and y position as a function of time (b) for three bodies (projectile, electron, and target) in the lab frame, respectively. The trajectories were obtained at 900 keV/amu projectile impact.

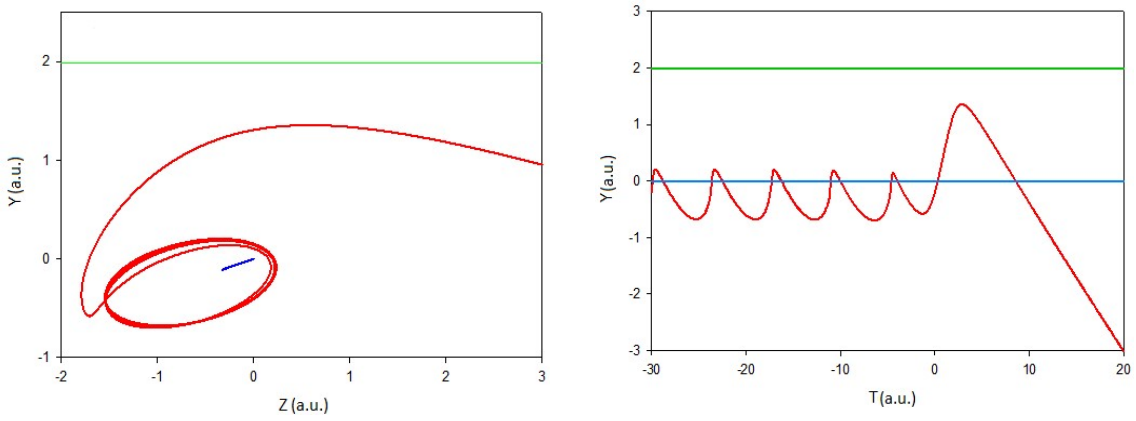

(a) (b)

Figure 7.25. (a) Trajectories in the *y-z* lab frame, (b) *y* position as a function of time for the electron (red line), projectile (green line) and target (blue line) for ionization channel for Be^{4+} + projectile with E = 900 keV/amu.

Electron capture

Figure 7.26 shows typical classical trajectories for the electron capture channel in CTMC method. The trajectory calculations were performed at 900 keV/amu impact energy.

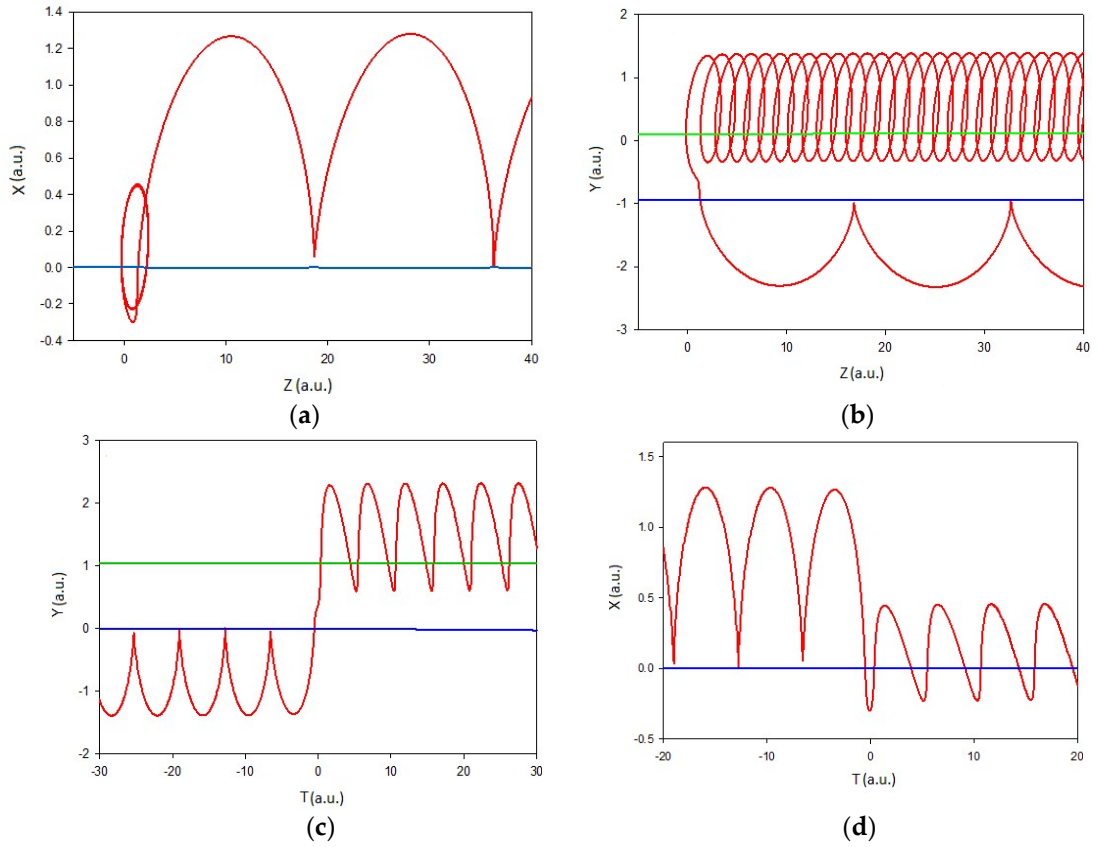

(**a**) (**b**)

(**c**) (**d**)

Figure 7.26. (a) Trajectories in the *x-z* projectile frame, (b) Trajectories in the *y-z* center-of-mass frame, (c) *y* position as a function of time in the lab frame, (d) *x* position as a function of time in the projectile frame for the electron (red line), projectile (green line) and target (blue line) for electron capture channel for Be^{4+} with E = 900 keV/amu.

Excitation

Figure 7.27 (a) and 7.27 (b) show the *y* position as a function of time and 3D trajectory in the lab frame, using the CTMC method for three bodies (projectile, electron, and target), respectively. These Figures correspond to a projectile with 900 keV/amu impact energy.

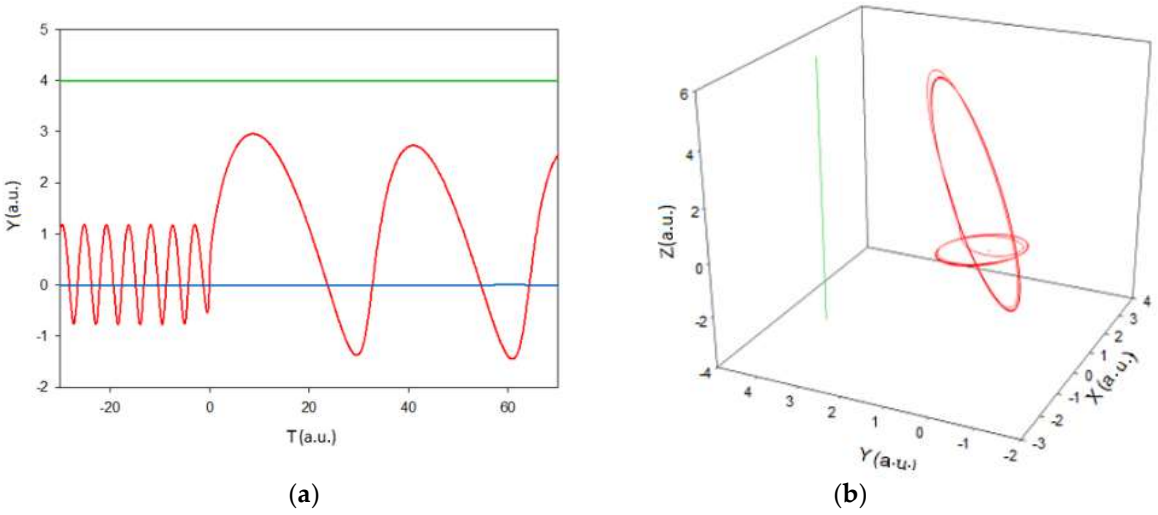

(**a**) (**b**)

Figure 7.27. (a) *y* position trajectory as a function of time in the lab frame, (b) 3D trajectory in the lab frame for the electron (red line), projectile (green line) and target (blue line) for the excitation channel 1s → 2s,2p for Be^{4+} with E = 900 keV/amu.

7.3 Interaction between Be^{4+} and excited state hydrogen

Cornelius *et al.* [81] and Hoekstra *et al.* [49] have calculated the electron capture cross sections into the final states *n*, in collisions of Be^{4+} with an excited hydrogen atom (H(*n* = 2)) by the classical trajectory Monte Carlo method. Igenbergs *et al.* [37] and Shimakura *et al.* [82] have studied the electron capture cross sections in Be^{4+} - H(*n* = 2) collision system in the framework of atomic-orbital close-coupling (AOCC) and molecular orbital close-coupling (MOCC) methods, respectively. Errea *et al.* [14] have computed the total and *n*-partial cross sections at low impact energies for electron capture in Be^{4+}+ H(1s, 2s) collisions using quantum-mechanical and semi-classical approaches.

In this section, I focus on the electron capture cross sections in collisions between Be^{4+} and excited state hydrogen atoms, H(*n,l,m*). I calculated the state-selective cross sections from H(2s, 2p*m*) to Be^{3+}(2*l*, 3*l*, 4*l*) states as a function of the projectile energy. I used the 3-body classical trajectory Monte Carlo method for impact energies between 10 to 200 keV/amu. Since there is no experimental data in Be^{4+} and H(2*lm*) collision system, I compare my results with the previous theoretical results.

7.3.1 Total electron capture cross sections

The electron capture process is defined by equation:

$$Be^{4+} + H(2lm) \rightarrow Be^{3+}(nl) + H^{+}. \quad (7.13)$$

For the determination of the state selective electron capture cross sections, I calculated 5×10^6 individual trajectories for each collision energy. Figure 7.28 shows my results of the total electron capture cross sections in Be^{4+}+H(2s). The comparison was made with the quantum-mechanical results based on the AOCC method [37] and the semi-classical approach [14] for H(2s). I also show the results for H(n = 2) target based on the classical simulation [49] and on the AOCC model [37].

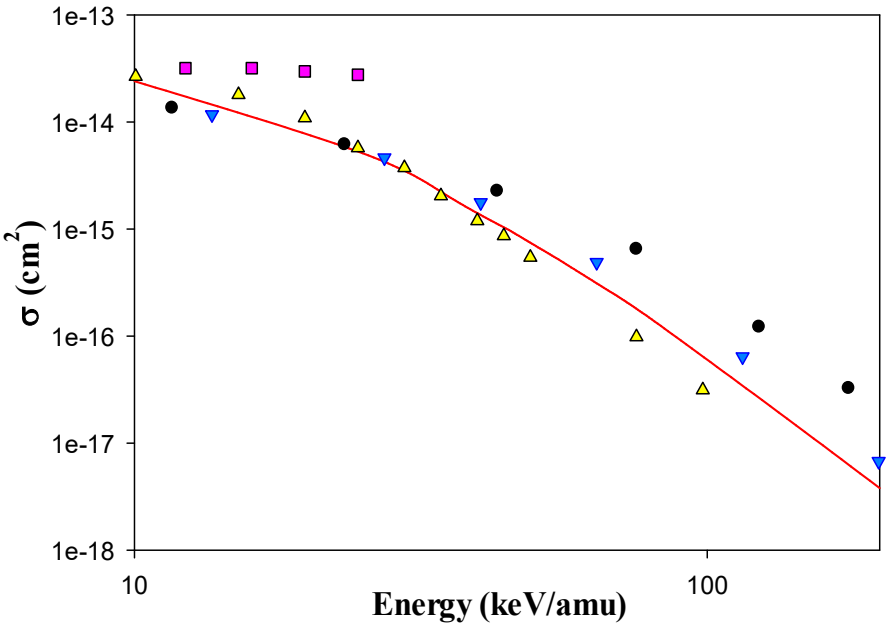

Figure 7.28. Total cross sections for electron capture in Be^{4+} + H(2s) collision as a function of the impact energy. Solid red line: present CTMC results, pink squares: semi-classical results of Errea *et al.* for H(2s) target [14], black circles: AOCC results of Igenbergs *et al.* for H(2s) target [37], blue inverse triangles: AOCC results of Igenbergs *et al.* for H(n = 2) target [37], yellow triangles: CTMC results of Hoekstra *et al.* for H(n = 2) target [49].

At low energies, my CTMC cross sections from H(2s) state into the Be bound states are in good agreement with the results of Igenbergs *et al.* [37]. At the same time at higher energies, my CTMC cross section data are significantly smaller than the data of Igenbergs *et al.* [37] and closer to the cross sections calculated from H (n = 2) state by Hoekstra *et al.* [49] and Igenbergs *et al.* [37]. I note that all cross sections calculated using the semiclassical approach [14] are higher than any other results.

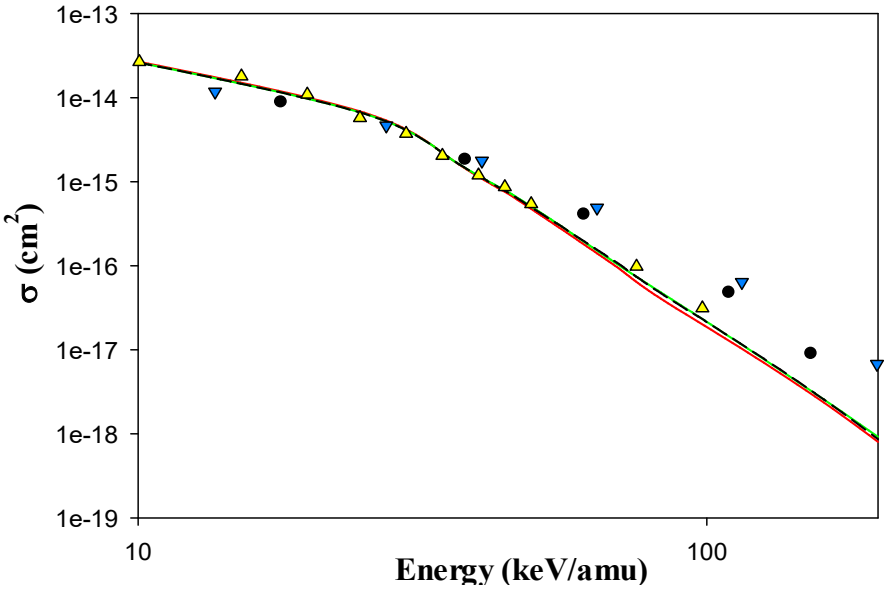

Figure 7.29. Total cross sections for electron capture in Be^{4+} + H($2p_m$) collision as a function of the impact energy. Solid red line: present CTMC results for H($2p_0$) target, Solid green line: present CTMC results for H($2p_{+1}$) target, Solid black dash line: present CTMC results for H($2p_{-1}$) target, black circles: AOCC results of Igenbergs *et al.* for H(2p) target [37], blue inverse triangles: AOCC results of Igenbergs *et al.* for H(n = 2) target [37], yellow triangles: CTMC results of Hoekstra *et al.* for H(n = 2) target [49].

Figure 7.29 shows the total electron capture cross sections from H(2*lm*) corresponding to orbital quantum numbers *l=2* and magnetic quantum numbers *m* (-1, 0, 1), respectively. My results compared to different theoretical approach, namely an atomic orbital close coupling for H(2p) and H(n = 2) as the target [37] and CTMC for H(n = 2) [49]. The cross sections from H(n = 2) are matched to present cross sections from H(2*2m*) below 100 keV/amu impact energies. Also, at low impact energies, the AOCC results of Igenbergs *et al.* [37] for H(2p) target are in good agreement with our H(2*lm*) results. My results show that the cross sections corresponding from the H($2p_0$), H($2p_{+1}$), and H($2p_{-1}$) states almost coincide with each other, and the differences are hardly visible.

7.3.2 State-selective cross sections

My CTMC results for *nl* state-selective electron capture cross section in Be^{4+} + H (2s, $2p_0$, $2p_{+1}$, $2p_{-1}$) collisions for different subshells of Be^{4+} are given in Tables 7.11-7.14.

Table 7.11. *nl* state-selective cross sections (in cm^2) for Be^{4+} + H(2s).

E (keV/u)	2s	2p	3s	3p	3d	4s	4p	4d	4f
10	1.86(-19)[b]	2.78(-19)	5.70(-18)	1.26(-17)	2.58(-17)	4.97(-17)	2.15(-16)	3.52(-16)	4.55(-16)
25	4.73(-19)	1.17(-18)	7.51(-18)	2.32(-17)	4.24(-17)	1.13(-17)	5.70(-17)	1.70(-16)	2.73(-16)
35	6.43(-19)	1.72(-18)	4.36(-18)	1.95(-17)	3.43(-17)	5.97(-18)	2.55(-17)	6.72(-17)	1.56(-16)
45	5.92(-19)	2.16(-18)	2.57(-18)	1.24(-17)	2.68(-17)	2.96(-18)	1.25(-17)	3.22(-17)	8.83(-17)
55	4.75(-19)	1.94(-18)	1.69(-18)	8.08(-18)	2.28(-17)	1.57(-18)	7.27(-18)	1.88(-17)	4.86(-17)
70	4.21(-19)	1.82(-18)	7.79(-19)	4.91(-18)	1.43(-17)	8.71(-19)	4.02(-18)	9.00(-18)	2.32(-17)
90	2.99(-19)	1.53(-18)	4.29(-19)	2.68(-18)	7.95(-18)	4.76(-19)	1.75(-18)	3.89(-18)	8.86(-18)
200	8.64(-20)	4.24(-19)	8.89(-20)	2.50(-19)	6.98(-19)	2.41(-20)	1.19(-19)	3.19(-19)	1.74(-19)

[b] $a(-x) = a \times 10^{-x}$

Table 7.12. *nl* state-selective cross sections (in cm^2) for Be^{4+} + H($2p_0$).

E (keV/u)	2s	2p	3s	3p	3d	4s	4p	4d	4f
10	1.24(-19)[b]	3.71(-19)	5.34(-18)	1.51(-17)	2.90(-17)	4.04(-17)	1.23(-16)	2.09(-16)	4.26(-16)
25	5.05(-19)	1.38(-18)	5.07(-18)	1.81(-17)	3.56(-17)	5.24(-18)	2.18(-17)	6.03(-17)	1.49(-16)
35	6.44(-19)	2.22(-18)	3.02(-18)	1.26(-17)	3.02(-17)	2.58(-18)	1.07(-17)	2.84(-17)	6.99(-17)
45	9.11(-19)	2.37(-18)	1.18(-18)	7.40(-18)	1.95(-17)	1.43(-18)	5.47(-18)	1.49(-17)	3.01(-17)
55	7.99(-19)	2.05(-18)	9.36(-19)	3.92(-18)	1.26(-17)	8.63(-19)	3.86(-18)	8.91(-18)	1.39(-17)
70	6.19(-19)	2.01(-18)	4.49(-19)	2.14(-18)	6.65(-18)	4.28(-19)	1.63(-18)	4.03(-18)	5.47(-18)
90	2.09(-19)	1.39(-18)	2.49(-19)	9.55(-19)	2.78(-18)	2.11(-19)	9.12(-19)	2.15(-18)	1.77(-18)
200	6.09(-21)	1.26(-19)	2.29(-20)	9.35(-20)	7.14(-20)	2.16(-20)	7.45(-20)	5.84(-20)	3.56(-20)

[b] $a(-x) = a \times 10^{-x}$

Table 7.13. *nl* state-selective cross sections (in cm^2) for Be^{4+} + H($2p_{+1}$).

E (keV/u)	2s	2p	3s	3p	3d	4s	4p	4d	4f
10	1.24(-19)[b]	2.74(-19)	6.83(-18)	1.70(-17)	3.32(-17)	4.45(-17)	1.50(-16)	2.73(-16)	4.94(-16)
25	7.99(-19)	1.75(-18)	7.07(-18)	2.42(-17)	4.51(-17)	6.44(-18)	2.78(-17)	8.27(-17)	1.70(-16)
35	9.05(-19)	2.57(-18)	3.79(-18)	1.55(-17)	3.31(-17)	2.51(-18)	1.35(-17)	3.58(-17)	7.95(-17)
45	7.76(-19)	2.69(-18)	1.54(-18)	9.17(-18)	2.25(-17)	1.60(-18)	7.45(-18)	1.94(-17)	3.67(-17)
55	7.47(-19)	2.61(-18)	1.22(-18)	5.14(-18)	1.50(-17)	8.97(-19)	4.72(-18)	1.01(-17)	1.75(-17)
70	4.82(-19)	1.97(-18)	5.35(-19)	2.86(-18)	7.26(-18)	4.22(-19)	2.00(-18)	5.56(-18)	6.91(-18)
90	3.41(-19)	1.50(-18)	3.02(-19)	1.22(-18)	3.32(-18)	2.54(-19)	1.04(-18)	2.22(-18)	2.00(-18)
200	3.67(-20)	1.89(-19)	1.61(-20)	1.11(-19)	1.00(-19)	6.63(-21)	3.53(-20)	6.83(-20)	4.86(-20)

[b] $a(-x) = a \times 10^{-x}$

Table 7.14. *nl* state-selective cross sections (in cm^2) for Be^{4+} + H($2p_{-1}$).

E (keV/u)	2s	2p	3s	3p	3d	4s	4p	4d	4f
10	1.23(-19)[b]	2.15(-19)	7.55(-18)	1.72(-17)	3.35(-17)	4.60(-17)	1.48(-16)	2.75(-16)	4.85(-16)
25	5.74(-19)	1.86(-18)	6.79(-18)	2.35(-17)	4.43(-17)	6.21(-18)	2.68(-17)	7.98(-17)	1.76(-16)
35	7.83(-19)	2.72(-18)	3.38(-18)	1.53(-17)	3.30(-17)	2.80(-18)	1.31(-17)	3.57(-17)	8.05(-17)
45	9.87(-19)	2.56(-18)	1.88(-18)	9.64(-18)	2.12(-17)	1.22(-18)	7.91(-18)	1.88(-17)	3.78(-17)
55	8.81(-19)	2.62(-18)	1.01(-18)	5.60(-18)	1.42(-17)	9.86(-19)	4.16(-18)	1.04(-17)	1.69(-17)
70	4.96(-19)	1.95(-18)	5.02(-19)	2.76(-18)	7.89(-18)	6.25(-19)	2.05(-18)	4.97(-18)	6.54(-18)
90	3.08(-19)	1.47(-18)	2.44(-19)	1.42(-18)	3.11(-18)	2.74(-19)	9.35(-19)	1.96(-18)	1.95(-18)
200	3.00(-20)	1.66(-19)	1.09(-20)	1.11(-19)	6.48(-20)	1.59(-20)	4.16(-20)	6.31(-20)	5.80(-21)

[b] $a(-x) = a \times 10^{-x}$

Furthermore, my CTMC results for *nl* state-selective electron capture cross section in Be^{4+} + H ($3l$, $4l$) collisions for different subshells of Be^{4+} are given in Tables 7.15-7.21.

Table 7.15. *nl* state-selective cross sections (in cm^2) for Be^{4+} + H(3s).

E (keV/u)	2s	2p	3s	3p	3d	4s	4p	4d	4f
10	-	-	4.26(-19)[b]	1.41(-18)	1.83(-18)	4.25(-18)	1.29(-17)	2.09(-17)	3.53(-17)
20	-	-	6.40(-19)	2.03(-18)	4.48(-18)	2.41(-18)	9.48(-18)	1.76(-17)	3.34(-17)
30	4.88(-20)	2.10(-19)	7.53(-19)	1.82(-18)	4.39(-18)	1.01(-18)	5.45(-18)	1.54(-17)	2.22(-17)
40	9.04(-20)	3.90(-19)	3.61(-19)	1.84(-18)	3.62(-18)	7.88(-19)	3.83(-18)	8.93(-18)	1.75(-17)
50	8.82(-20)	3.12(-19)	2.12(-19)	1.38(-18)	3.50(-18)	5.74(-19)	2.04(-18)	5.39(-18)	1.20(-17)
60	6.38(-20)	3.25(-19)	2.90(-19)	1.31(-18)	2.96(-18)	3.62(-19)	1.30(-18)	3.33(-18)	7.00(-18)
70	8.40(-20)	2.72(-19)	2.25(-19)	8.55(-19)	2.63(-18)	2.48(-19)	9.89(-19)	2.12(-18)	5.13(-18)
80	7.11(-20)	3.33(-19)	1.66(-19)	7.03(-19)	2.27(-18)	1.42(-19)	6.56(-19)	1.54(-18)	3.42(-18)
90	5.68(-20)	2.86(-19)	1.18(-19)	5.99(-19)	1.74(-18)	1.04(-19)	5.14(-19)	1.10(-18)	2.25(-18)
100	4.19(-20)	3.13(-19)	1.00(-19)	5.53(-19)	1.42(-18)	8.87(-20)	3.70(-19)	8.12(-19)	1.53(-18)

[b] $a(-x) = a \times 10^{-x}$

Table 7.16. *nl* state-selective cross sections (in cm^2) for Be^{4+} + H(3p).

E (keV/u)	2s	2p	3s	3p	3d	4s	4p	4d	4f
10	-	-	5.92(-19)[b]	1.38(-18)	2.25(-18)	5.71(-18)	1.34(-17)	2.08(-17)	3.67(-17)
20	-	1.30(-19)	9.68(-19)	2.57(-18)	5.30(-18)	2.71(-18)	9.71(-18)	2.55(-17)	3.37(-17)
30	1.16(-19)	1.69(-19)	9.04(-19)	2.60(-18)	4.83(-18)	1.12(-18)	3.62(-18)	1.14(-17)	2.32(-17)
40	1.68(-19)	3.29(-19)	5.84(-19)	2.34(-18)	4.64(-18)	4.05(-19)	1.66(-18)	5.58(-18)	1.36(-17)
50	1.75(-19)	3.58(-19)	3.94(-19)	1.72(-18)	3.95(-18)	2.31(-19)	9.09(-19)	2.64(-18)	7.58(-18)
60	1.18(-19)	4.19(-19)	1.88(-19)	1.02(-18)	3.18(-18)	1.54(-19)	5.14(-19)	1.47(-18)	4.25(-18)
70	1.35(-19)	4.32(-19)	1.28(-19)	6.57(-19)	2.33(-18)	8.86(-20)	3.95(-19)	9.60(-19)	2.49(-18)
80	1.00(-19)	4.63(-19)	6.36(-20)	5.05(-19)	1.61(-18)	7.90(-20)	2.99(-19)	6.94(-19)	1.48(-18)
90	6.23(-20)	3.98(-19)	4.83(-20)	3.26(-19)	1.07(-18)	4.49(-20)	1.99(-19)	5.26(-19)	8.33(-19)
100	7.47(-20)	3.11(-19)	4.39(-20)	2.52(-19)	7.79(-19)	4.48(-20)	1.72(-19)	4.32(-19)	4.31(-19)

[b] $a(-x) = a \times 10^{-x}$

Table 7.17. *nl* state-selective cross sections (in cm^2) for Be^{4+} + H(3d).

E (keV/u)	2s	2p	3s	3p	3d	4s	4p	4d	4f
10	-	-	7.16(-19)[b]	1.00(-18)	2.54(-18)	5.69(-18)	1.62(-17)	2.13(-17)	3.96(-17)
20	9.73(-20)	9.63(-20)	1.22(-18)	2.58(-18)	5.67(-18)	2.08(18)	8.64(-18)	1.68(-17)	2.89(-17)
30	1.00(-19)	2.80(-19)	7.44(-19)	2.18(-18)	4.62(-18)	7.66(-19)	2.53(-18)	6.20(-18)	1.41(-17)
40	1.26(-19)	2.40(-19)	3.99(-19)	1.34(-18)	2.78(-18)	2.96(-19)	1.26(-18)	2.41(-18)	5.16(-18)
50	7.89(-20)	3.18(-19)	1.73(-19)	6.55(-19)	1.56(-18)	9.75(-20)	6.11(-19)	1.24(-18)	2.01(18)
60	4.83(-20)	2.14(-19)	8.44(-20)	3.25(-19)	7.57(-19)	1.22(-19)	3.40(-19)	5.44(-19)	7.89(-19)
70	3.30(-20)	1.94(-19)	4.36(-20)	2.07(-19)	4.67(-19)	5.12(-20)	1.81(-19)	2.89(-19)	3.47(-19)
80	3.40(-20)	1.05(-19)	3.08(-20)	1.08(-19)	2.71(-19)	4.24(-20)	7.94(-20)	1.70(-19)	1.76(-19)
90	1.83(-20)	8.08(-20)	1.97(-20)	7.47(-20)	1.43(-19)	2.90(-20)	6.95(-20)	1.47(-19)	5.95(-20)
100	1.58(-20)	5.81(-20)	2.97(-20)	5.02(-20)	8.03(-20)	1.78(-20)	4.36(-20)	7.66(-20)	1.85(-20)

[b] $a(-x) = a \times 10^{-x}$

Table 7.18. *nl* state-selective cross sections (in cm^2) for Be^{4+} + H(4s).

E (keV/u)	2s	2p	3s	3p	3d	4s	4p	4d	4f
10	-	-	-	-	7.16(-19)[b]	8.98(-19)	2.46(-18)	3.28(-18)	6.07(-18)
20	-	-	1.31(-19)	6.10(-19)	1.23(-18)	4.59(-19)	1.84(-18)	4.38(-18)	8.80(-18)
30	-	-	1.39(-19)	4.70(-19)	1.47(-18)	2.27(-19)	1.05(-18)	3.29(-18)	5.21(-18)
40	2.39(-20)	1.21(-19)	9.58(-20)	3.95(-19)	1.01(-18)	2.32(-19)	8.36(-19)	2.16(-18)	4.32(-18)
50	4.30(-20)	1.26(-19)	9.94(-20)	3.33(-19)	1.08(-18)	9.74(-20)	6.75(-19)	1.73(-18)	2.95(-18)
60	3.06(-20)	1.31(-19)	4.89(-20)	3.38(-19)	7.69(-19)	1.34(-19)	5.92(-19)	1.11(-18)	2.22(-18)
70	1.00(-20)	6.22(-20)	5.58(-20)	2.90(-19)	7.36(-19)	3.96(-20)	3.62(-19)	8.91(-19)	1.52(-18)
80	2.44(-20)	1.32(-19)	6.01(-20)	2.10(-19)	5.45(-19)	8.11(-20)	3.03(-19)	6.20(-19)	9.55(-19)
90	1.56(-20)	7.98(-20)	1.97(-20)	2.00(-19)	4.24(-19)	2.10(-20)	2.62(-19)	4.14(-19)	7.55(-19)
100	1.60(-20)	5.96(-20)	3.21(-20)	1.37(-19)	4.24(-19)	3.05(-20)	1.55(-19)	3.11(-19)	4.85(-19)

[b] $a(-x) = a \times 10^{-x}$

Table 7.19. *nl* state-selective cross sections (in cm^2) for Be^{4+} + H(4p).

E (keV/u)	2s	2p	3s	3p	3d	4s	4p	4d	4f
10	-	-	1.87(-19)[b]	2.67(-19)	4.59(-19)	6.63(-19)	2.16(-18)	3.37(-18)	7.14(-18)
20	-	-	2.81(-19)	5.32(-19)	1.16(-18)	9.57(-19)	2.99(-18)	5.18(-18)	8.39(-18)
30	-	-	1.31(-19)	7.48(-19)	1.58(-18)	3.91(-19)	1.69(-18)	4.98(-18)	7.13(-18)
40	1.48(-20)	1.04(-19)	2.43(-19)	7.02(-19)	1.34(-18)	1.58(-19)	8.46(-19)	2.24(-18)	5.45(-18)
50	2.71(-20)	1.34(-19)	1.44(-19)	7.13(-19)	1.46(-18)	5.70(-20)	3.61(-19)	1.00(-18)	3.37(-18)
60	7.64(-20)	1.07(-19)	7.47(-20)	3.92(-19)	1.29(-18)	5.43(-20)	2.26(-19)	5.01(-19)	2.03(-18)
70	4.27(-20)	1.38(-19)	4.10(-20)	2.77(-19)	9.28(-19)	1.59(-20)	1.34(-20)	4.08(-19)	1.24(-18)
80	4.67(-20)	1.20(-19)	1.96(-20)	1.95(-19)	7.84(-19)	2.63(-20)	1.42(-19)	2.24(-19)	7.32(-19)
90	3.68(-20)	1.80(-19)	2.66(-20)	1.20(-19)	5.93(-19)	1.38(-20)	1.00(-19)	1.80(-19)	4.63(-19)
100	2.05(-20)	1.39(-19)	1.42(-20)	1.23(-19)	4.11(-19)	1.76(-20)	4.92(-20)	1.53(-19)	1.98(-19)

[b] $a(-x) = a \times 10^{-x}$

Table 7.20. *nl* state-selective cross sections (in cm^2) for Be^{4+} + H(4d).

E (keV/u)	2s	2p	3s	3p	3d	4s	4p	4d	4f
10	-	-	1.22(-19)[b]	1.48(-19)	6.02(-19)	6.47(-19)	3.12(-18)	4.89(-18)	6.95(-18)
20	-	-	3.33(-19)	7.01(-19)	1.16(-18)	9.67(-19)	3.82(-18)	5.31(-18)	9.67(-18)
30	-	8.44(-20)	3.43(-19)	8.84(-19)	1.47(-18)	1.72(-19)	1.11(-18)	3.23(-18)	6.26(-18)
40	-	1.11(-19)	2.97(-19)	7.36(-19)	1.39(-18)	1.25(-19)	4.82(-19)	1.11(-18)	2.72(-18)
50	4.86(-20)	1.47(-19)	1.30(-19)	4.27(-19)	1.00(-18)	6.14(-20)	2.87(-19)	6.06(-19)	1.46(-18)
60	3.40(-20)	1.41(-19)	5.32(-20)	1.98(-19)	5.46(-19)	3.93(-20)	1.60(-19)	2.95(-19)	6.02(-19)
70	3.81(-20)	8.29(-20)	4.61(-20)	1.19(-19)	3.44(-19)	3.91(-20)	1.07(-19)	2.03(-19)	2.77(-19)
80	1.56(-20)	7.62(-20)	1.44(-20)	6.33(-20)	1.72(-19)	1.52(-20)	5.37(-20)	1.22(-19)	1.22(-19)
90	1.56(-20)	6.04(-20)	1.03(-20)	5.04(-20)	1.29(-19)	1.51(-20)	3.35(-20)	9.38(-20)	4.91(-20)
100	1.02(-20)	5.36(-20)	1.06(-20)	2.49(-20)	6.73(-20)	1.36(-20)	1.81(-20)	5.45(-20)	1.79(-20)

[b] $a(-x) = a \times 10^{-x}$

Table 7.21. *nl* state-selective cross sections (in cm^2) for Be^{4+} + H(4f).

E (keV/u)	2s	2p	3s	3p	3d	4s	4p	4d	4f
10	-	-	1.93(-19)[b]	3.42(-19)	6.70(-19)	1.45(-18)	3.77(-18)	6.09(-18)	8.98(-18)
20	-	-	2.40(-19)	5.92(-19)	1.19(-18)	7.19(-19)	1.87(-18)	3.85(-18)	6.59(-18)
30	-	4.89(-20)	1.43(-19)	4.24(-19)	8.34(-19)	1.14(-19)	4.14(-19)	1.12(-18)	2.26(-18)
40	-	4.74(-20)	7.48(-20)	1.00(-19)	3.32(-19)	5.07(-20)	1.93(-19)	3.05(-19)	5.73(-19)
50	-	3.12(-20)	2.06(-20)	3.85(-20)	1.56(-19)	2.83(-20)	5.84(-20)	6.89(-20)	2.54(-19)
60	-	-	-	2.08(-20)	6.64(-20)	1.62(-20)	3.28(-20)	3.95(-20)	5.93(-20)
70	-	-	-	-	2.43(-20)	-	-	1.27(-20)	2.30(-20)
80	-	-	-	-	-	-	-	-	-
90									
100									

[b] $a(-x) = a \times 10^{-x}$

7.4 State-selective electron capture cross sections between fully striped ions and H(1s)

Recently, elements with nuclear charges $Z \leq 8$ are found in the core of tokamak plasmas [83]. Due to the high temperature and density in the core, these elements are fully ionized. When an energetic neutral hydrogen beam is injected into the plasma, electron capture from H atoms by bare ions of the core of tokamak plasma produces hydrogen-like ions in excited states. Therefore, it is essential to know electron capture cross sections in collisions between bare ions and hydrogen atoms.

The state-selective electron capture cross sections for bare ions A^{Z+} with $1 \leq Z \leq 8$ colliding with H(1s) for each value of the final quantum numbers n, l, m have been obtained using

molecular approach [8], continuum distorted wave method (CDW) [80] and boundary corrected continuum intermediate states method (BCIS) [84].

Due to the significant effects of classical models especially QCTMC model on state-selective electron capture cross sections (see sections 7.1.7 and 7.2.5), I motivated to present a state-selective electron capture cross sections database in A^{Z+} with $1 \leq Z \leq 8$ and ground-state hydrogen atom. The CTMC and QCTMC models were employed for impact energies between 10 and 200 keV/amu. The projectile ions are H^{+}, He^{2+}, Li^{3+}, Be^{4+}, B^{5+}, C^{6+}, N^{7+}, and O^{8+} (see appendix A).

8. Summary

The collision processes between ions and atomic hydrogen are interesting in fusion plasma research. Due to the high temperature and density in the core plasma, the elements are fully ionized. According to these facts, the accurate knowledge of the inelastic scattering cross sections such as ionization, electron capture, state-selective electron capture, and excitation for collisions between bare ions and hydrogen atoms is essential. Therefore, the main objective of my PhD research work was the investigation of bare ions interaction with hydrogen atom. I especially focus on the interaction between Be^{4+} and hydrogen atom collisions, because beryllium is known as one of the most important impurities in the fusion reactor chamber. During my theoretical works, I used both the classical trajectory Monte Carlo and the Quasi-Classical Monte Carlo models. The main results of my research works are as follows:

I have shown an intensive study of the interaction between a proton and a ground state hydrogen atom. Calculations were performed employing a standard three-body CTMC and a QCTMC models where the Heisenberg correction term is added to the Hamiltonian of the collision system to mimic the Heisenberg uncertainty principle. The projectile energy range was between 10 and 1000 keV/amu. Firstly, I obtained the initial conditions for distance (r) and linear momentum (p) of the target electron in the QCTMC model. Secondly, I presented ionization and total electron capture cross sections in three calculation schemes in H^+ + H(1s) collision. These were the followings: 1) projectile-centered, when the correction term is taken into account between target electron and projectile, 2) target-centered, when the correction term is taken into account between target electron and target nucleus, 3) combined one, i.e., when the correction term is taken into account between the target electron and both the target nucleus and projectile. My QCTMC results in different schemes were compared with the results of the 3-body CTMC model. I found that the effect of the correction term between the target electron and projectile is not noticeable in the ionization channel. However, the correction term between the particles plays an important role in calculations in the electron capture channel. Finally, I obtained the relevant range for two important constants in the Heisenberg constraining function, i.e., α_H and ξ_H, by analyzing the radial and momentum distributions of the target electron. By comparing the present radial distribution with the quantum-mechanics ones, I found that the reasonable range of α_H for ground state hydrogen as a target is expected to be $\alpha_H \geq 3.5$ [85]. To find the optimized, best combination of α_H and ξ_H, I calculated the cross

sections for various channels such as; ionization, total electron capture, low-level excitation, and state-selective electron capture to the projectile bound state. My results were compared with previous quantum-mechanical and experimental results. I found excellent agreements between my QCTMC (α_H= 3.5, ξ_H = 0.9354) results and previous ones in H^++H(1s) collision.

Cross sections for ionization, electron capture, and low-level excitation channels were simulated for a Be^{4+}+H(1s) collision system using the classical trajectory Monte Carlo method and quasi-classical trajectory Monte Carlo method of Kirschbaum and Wilets [50]. I estimate uncertainties of 0.6%. I draw the conclusion that the classical treatment can describe the cross sections reasonably. Since there is no experimental data for the mentioned collision system, I compared my results with the previous literature based on other methods, such as applying the atomic orbital close-coupling (AOCC), quantum-mechanical molecular orbital close-coupling (MOCC), adiabatic superpromotion model, and symmetric Eikonal approximation. I found that my calculations are in good agreement with previous results.

I calculated the electron capture cross sections into n = 2, and nl = 2s, 2p states of the projectile in the collision between Be^{4+} and ground state hydrogen atom in wide impact energies range based on CTMC and QCTMC models. CTMC cannot compete with quantum calculation in many aspects because of lacking the quantum feature of the collisions. Therefore, I developed a three-body quasi-classical Monte Carlo model taking into account the quantum features of the collision system, where the Heisenberg correction term is added to the standard three-body classical trajectory Monte Carlo model. For the determination of the cross sections 5×10^6 trajectories were calculated for each impact energy. The comparison was made with the available quantum-mechanical approaches such as MOCC, AOCC, one-electron diatomic molecule (OEDM), boundary corrected continuum intermdiate state (BCCIS), continuum distorted wave (CDW), and previous classical simulations. I found that the QCTMC method can reasonably describe the state-selective cross sections in a wide projectile energy range. My calculations provide a fast and reliable estimation of fusion related state-selective cross sections both in low and higher energies. I have shown that the QCTMC model may have an alternative to the quantum-mechanical models, especially at low impact energies providing the same results with maybe low computation efforts.

The electron capture cross sections into n = 3, 4, 5, 6, 8, 10 and nl = 3l, 4l, 5l states of the projectile have been presented in Be^{4+} + H(1s) in the framework of CTMC and QCTMC

methods. For the determination of the cross sections 10^7 trajectories were calculated for each impact energy. I found that the QCTMC cross sections are higher than the CTMC ones at low energies. I have used the previous AOCC, QMOCC, BCCIS, and OEDM quantum-mechanical approaches for comparison with my present data. Including the potential correction term to mimic the Heisenberg uncertainty principle in the classical Hamiltonian, I have shown that my QCTMC electron capture cross sections into the projectile states, n = 3, 5 and nl = 3s, 3p, 3d, 4s, 4p, 5s, 5d, 5f are in excellent agreement with quantum-mechanical results. I believe that my model, with its simplicity, can be an alternative way to calculate accurate cross sections and maybe can replace the results of the quantum-mechanical models, where the quantum mechanical calculations become complicated.

A three-body classical trajectory Monte Carlo method was performed to calculate the nl state-selective electron capture cross sections in Be^{4+}+ H($2lm$) collisions in the energy range between 10 and 200 keV/amu [86]. 5×10^6 individual trajectories for each collision energy have been calculated. The state-selective cross sections for electron capture into Be^{3+}(nl) (nl = 2s, 2p, 3s, 3p, 3d, 4s, 4p, 4d, 4f) states as a function of impact energy were presented. As a result of a large number of classical trajectories, the uncertainty of the cross sections is less than 1 %. Due to the lack of experimental data for the investigated collision system, I compared my results with the theoretical approaches. I found that the CTMC method can able to describe reasonably the cross sections of the electron capture channel from the excited states of H atom.

I presented a state-selective electron capture cross sections database from the ground state hydrogen atom. A standard three-body classical trajectory Monte Carlo and quasi-classical trajectory Monte Carlo models were employed for impact energies between 10 and 200 keV/amu. The projectile ions are H^+, He^{2+}, Li^{3+}, Be^{4+}, B^{5+}, C^{6+}, N^{7+}, and O^{8+}. The cross sections are tabulated for each value of the final quantum numbers n, l, m, summed over m for the given n and l and over l and m for the given n. The maximum quantum number n_{max} is set to 4 for H^+, He^{2+} and Li^{3+}, as well as to 5 for Be^{4+}, B^{5+}, C^{6+}, N^{7+} and O^{8+}, respectively.

Összefoglalás

Ionok és atomi hidrogén ütközési folyamatai érdekesek a fúziós plazmakutatásban. Mivel a fúziós plázmában magas hőmérséklet és sűrűség urlkodik, az elemek teljesen ionizáltak a palzmában. Ezek fényében nyilvánvaló, hogy elengedhetetlen a rugalmatlan szórás keresztmetszeteinek pontos ismerete, mint az ionizáció, gerjesztés, elektronbefogás, állapotszelektív elektronbefogás eseteire csupasz ionok és hidrogénatomok közötti ütközésekben. Ezért PhD munkám fő célja a csupasz ionok hidrogénatommal való kölcsönhatásának vizsgálata volt. Különös figyelmet fordítottam a Be^{4+} és a hidrogénatom ütközések közötti kölcsönhatásra, mivel a berillium a fúziós reaktor kamrájának egyik legfontosabb szennyezőjeként ismert. Elméleti munkáim során a klasszikus pályájú Monte Carlo (CTMC – classical trajectory Monte Carlo) és a kvázi- klasszikus pályájú Monte Carlo (QCTMC – quasi-classical trajectory Monte Carlo) modelleket egyaránt alkalmaztam. Kutatásaim főbb eredményei a következők:

Kiterjedt vizsgálatokat folytattam proton és alap állapotú hidrogénatom közötti kölcsönhatások vizsgálatára. A számításokat klasszikus közelítésben végeztem el mind a standard CTMC mind pedig a QCTMC modellek alkalmazásával. A QCTMC modell a standard CTMC modell továbbfejlesztett változata, ahol az ütközések kvantumjellemzőinek utánzását Kirschbaum és Wilets [50] által javasolt modellpotenciáll biztosítja. Egy I elektronos rendszerre ez a Heisenberg bizonytalanság elvét jelenti. Szamításaim során a lövedék energiatartománya 10 és 1000 keV/amu között volt. Munkám során először meghatároztam a QCTMC modellben alkalmazható kezdeti kötött alapállapotú elektronra vonatkozó radiális elektron távolság és momentum eloszlásait. A megfelelő kezdeti állapot meghatározása után kiszámítottam az ionizációs és a teljes elektronbefogási keresztmetszeteket három számítási sémában $H^+ + H$ (1s) ütközésben. Ezek a következők voltak: 1) lövedék-központú, amikor a korrekciós kifejezést a cél elektron és a lövedék között vesszük figyelembe, 2) célatomközpontú, amikor a korrekciós kifejezést a cél elektron és a célatom magja között vesszük figyelembe, 3) valamint a kombinált esetben, azaz amikor a korrekciós kifejezést figyelembefigyelembe vesszük a cél elektron és mind a célatommag, mind a lövedék között. A QCTMC modell különböző közelítéseiben kapott számítási eredményeimet a korrekció nélküli háromtest CTMC modell eredményeivel hasonlítottam össze. Azt tapasztaltam, hogy a cél elektron és a lövedék közötti korrekciós kifejezés hatása alig észrevehető az ionizációs hatáskeresztmetszetekben. A részecskék közötti korrekciós kifejezés azonban fontos szerepet

játszik az elektronbefogási csatorna hataskeresztmetszet számításaira. Ezen tapasztalatok alapján a Heisenberg korlátozó elvet utánzó függvény két fontos állandójának (α_H, ξ_H) meghatároztam a számításokban alkalmazható lehetséges tartományát. Összehasonlítva a QCTMC modell radiális eloszlást a kvantummechanikai eloszlással, azt találtam, hogy alapállaptú hidrogénre a választható α_H tartománya várhatóan $\alpha_H \geq 3.5$. A legjobb α_H és ξ_H kombináció megtalálásához különböző végállapotú csatornák (ionizáció, teljes elektronbefogás, alacsony szintű gerjesztés és állapotszelektív elektronbefogás a lövedékhez kötött állapotba) hatáskeresztmetszeteit számítottam ki. Eredményeink összehasonlításra kerültek a korábbi kvantummechanikai és kísérleti eredményekkel. Megmutattam, hogy kiváló egyezés tapasztalható a QCTMC modell eredményei és a korábbi adatok között, amikor α_H = 3,5, ξ_H = 0,9354.

Be^{4+}+H (1s) ütközési rendszerre kiszámítottam a gerjesztési, ionizációs, és a töltés cserére vonatkó hataáskerestmetsezetek. A számításokat CTMC és QCTMC közelítésben végeztem el. Arra a következtetésre jutok, hogy a klasszikus kezelés ésszerűen le tudja írni a keresztmetszeteket. Mivel az említett ütközési rendszerre kísérleti adatok nincsenek, eredményeinket a korábbi elméleti munkákkal (AOCC – atomic orbital close-coupling, QMOCC – quantum-mechanical molecular orbital close-coupling) vetettem össze. Azt talaltam, hogy számításaink összhangban vannak a korábbi eredményekkel.

Be^{4+} és alapállapotú hidrogénatom ütközésében, széles ütközési energiatartományban CTMC és a QCTMC modellek alapján kiszámítottam az elektronbefogási hatáskeresztmetszeteket n = 2 -re és nl = 2s, 2p-s állapotokra. Eredményeimet a rendelkezésre álló kvantummechanikai megközelítésekkel végeztett számításokkal, mint például a MOCC – molecular orbital close-coupling, az AOCC, az OEDM – one-electron diatomic molecule, a BCCIS – boundary corrected continuum intermdiate state, a CDW – continuum distorted wave és a korábbi klasszikus szimulációk hasonlítottam össze. Azt tapasztaltam, hogy a QCTMC módszer nagyon jól le tudja írni az állapotszelektív keresztmetszeteket széles lövedékenergia-tartományban. Számításaink gyors és megbízható becslést nyújtanak a fúzióval kapcsolatos állapotszelektív keresztmetszetekre mind alacsony, mind magasabb energiájú lövedék energiák esetében. Megmutattuk, hogy a QCTMC modell egy lehetséges alternatívája lehet a kvantummechanikai modelleknek, különösen alacsony energiákon, amelyek ugyanazokat az eredményeket biztosítják, sokkal alacsony számítási erőfeszítésekkel.

CTMC és QCTMC modellben a lövedék n = 3, 4, 5, 6, 8, 10 és nl = 3l, 4l, 5l állapotaiba történő befogási hatáskeresztmetszeteket számítottam ki Be^{4+} + H(1s) ütközésben. A hatáskeresztmetszetek meghatározásához 10^7 pályát számítottam ki minden egyes ütközési energiára vonatkozóan. Azt tapasztaltam, hogy a QCTMC keresztmetszetek kisebb energiákon nagyobbak, mint a CTMC model eredményei. A korábbi AOCC, QMOCC, BCCIS és OEDM kvantummechanikai eredményeket használtuk a jelenlegi adatainkkal való összehasonlításhoz. Megmutattam, hogy a QCTMC modell kereteiben számolt, a lövedék n = 3, 5 és nl = 3s, 3p, 3d, 4s, 4p, 5s, 5d, 5f állapotaiba történő állapotszelektív hatáskeresztmetszeteink kiváló egyezésben vannak a kvantummechanikai eredményekkel. Hisszük, hogy modellünk egyszerűségével alternatív módja lehet a pontos keresztmetszetek kiszámításának, és talán helyettesítheti a kvantummechanikai modellek eredményeit, ahol a kvantummechanikai számítások bonyolulttá válnak.

nl állapotszelektív elektronbefogási hatáskeresztmetszeteket határoztam meg CTMC módszerrel Be^{4+}+ H(2lm) ütközési rendszerre 10 és 200 keV/amu közötti energiatartományban. Minden ütközési energiára 5×10^6 egyedi pályát számítottam ki. Az ütközési energia függvényében a Be^{3+}(nl) (nl = 2s, 2p, 3s, 3p, 3d, 4s, 4p, 4d, 4f) állapotokra vonatkazó hatáskeresztmetszet értékeket adtam meg. A klasszikus pályák nagy száma miatt a keresztmetszetek bizonytalansága kevesebb, mint 1 %. A vizsgált ütközési rendszer kísérleti adatainak hiánya miatt, eredményeinket korábbi elméleti munkák eredményeivel hasonlítottuk össze. Azt találtuk, hogy a CTMC módszer képes leírni az elektronbefogási csatorna keresztmetszeteit a H atom gerjesztett állapotából.

Kiszámítottam és létrehoztam egy állapotszelektív elektronbefogási keresztmetszeti adatbázist. A számításokat CTMC és QCTMC közelítésben végeztem el 10 és 200 keV/amu közötti ütközési energiatartományban. A lövedék ionok: H^+, He^{2+}, Li^{3+}, Be^{4+}, B^{5+}, C^{6+}, N^{7+}, és O^{8+}. A hatáskeresztmetszetek az n, l, m végső kvantumszámok minden értékéhez táblázatosan adtam meg.

9. Outlook

The data presented in my PhD thesis strongly support the nuclear fusion power research. I have shown that the classical models especially the quasi-classical trajectory Monte Carlo model can describe the ion-atom collisions reasonably well. Eventually, the collision between beryllium and atomic hydrogen could be more interesting for fusion research where the beryllium is a disturbance impurity into the ITER. The classical simulation, as well as the initial conditions, are correctly established and caused to obtain outstanding results in the QCTMC model. The importance of these results is evident from the fact that many scientists have shown a desire to compare their quantum-mechanical results with our classical ones.

In accordance with my thesis, it is clear that there are still many open activities. Here I would like to specify a few of them:

a) I plan to create one database for the ionization cross sections in a collision between fully stripped ions and ground state hydrogen by using classical approaches.
b) The calculation of cross sections in the collision between the bare ions and excited state hydrogen is also an interesting subject in fusion research. Therefore, I plan to complete my calculations in these collision systems.
c) I plan to have a comprehensive study on the differential cross sections by considering the classical treatment of the collision.
d) I try to perform the classical treatment in the collision between bare ions and He atom using the QCTMC model. For this purpose, the 4-body classical trajectory Monte Carlo method is used. In addition, I should consider the Heisenberg correction term and Pauli constraint to define the reasonable collision cross sections.

10. Acknowledgement

I would like to appreciate all people who helped and encourage me to realize this thesis during my year as a PhD student. First, I am indebted to my supervisor Dr. Károly Tőkési for directing my thesis and for his unique guidance in my research.

I would like to thank all the officials of the Institute for Nuclear Research (Atomki) who provided a calm and friendly environment for my research.

I would like to express this project has been carried out within the framework of the EURO fusion Consortium and has received funding from the Euratom research and training program 2014-2018 and 2019-2020 under grant agreement No 633053.

Most importantly, I express my sincere gratitude to my family, especially my wife. It would not have been possible for me to continue this activity without her sacrifices and support. I am proud to present this dissertation to my wife.

Bibliography

[1] R.A. Pitts, S. Carpentier, F. Escourbiac, T. Hirai, V. Komarov, A.S. Kukushin, S. Lisgo, A. Loarte, M. Merola, R. Mitteau, A.R. Raffray, M. Shimada, and P.C. Stangeby, J. Nucl. Mater. **415** (2011) S957.

[2] M.M. Nasiri, J. Fusion Energy, **35** (2016) 621.

[3] D. Perrault, Fusion Eng. Des. **146** (2019) 130.

[4] D. J. Campbell et. al. J. Fusion Energy, **38** (2019) 11.

[5] C. Liu, J. Zhang, H. Yang, Z. L. Wang, C. Liang, Z.B. Zhoe, L. Cao, D.M. Yao, and X. Gao, J. Fusion Energy, **33** (2014) 422.

[6] J. Chen, et. al, J. Fusion Energy, **40** (2021) 10.

[7] J. Hackman, and J. Uhlenbusch, J. Nucl. Mater. **128/129** (1984) 418.

[8] C. Harel, H. Jouin, and B. Pons, At. Data. Nucl. Data Tables. **68** (1998) 279.

[9] W. Fritsch, and C.D. Lin, Phys. Rev. A. **29** (1984) 3039.

[10] A.T. Le, M. Hesse, and C.D. lin, J. Phys. B. **36** (2003) 3281.

[11] H.J. Lüdde, and R.M. Dreizler, J. Phys. B. **15** (1982) 2713.

[12] T. Minami, M.S. Pindzola, T-G Lee, and D.R. Schultz, J. Phys. B: At. Mol. Opt. Phys. **39** (2006) 2877.

[13] F. Sattin, Phys. Rev. A**. 62** (2000) 042711.

[14] L.F. Errea, C. Harel, H. Jouin, L. Méndez, B. Pons, and A. Riera, J. Phys. B. **31** (1998) 3527

[15] M. Das, M. Purkait, and C.R. Mandal, Phys. Rev. A. **57** (1998) 3573.

[16] R.E. Olson, C.O. Reinhold, and D.R. Schultz, In Proceedings of the 4th Workshop on High-Energy Ion-Atom Collision Processes, Debrecen, Hungary, 17–19 September 1990.

[17] R.E. Olson, and A. Salop, Phys. Rev. A. **16 (**1977) 531.

[18] S. Zhang, L. Tang, Q. He, J. Zhang, and H. Zhang, J. Fusion Energy, **36** (2017) 58.

[19] D. Perrault, Nuclear fusion reactors, edition property of IRSN 31, avenue de la Division Leclerc 92260 Fontenay-aux-Roses, France, www.irsn.fr

[20] A.Y. Chirkov, J. Fusion Energy, **32** (2013) 208.

[21] D. Xia, D. Sin, Z. Wang, C. Liu, L. Jiang, W. Wang, W. Ba, and G. Zhuang, J. Fusion Energy, **34** (2015) 1314.

[22] Nuclear Engineering, https://www.neimagazine.com/features/featurefabricating-iters-first-wall-4551656.

[23] H.R. Yousefi, and Masuqata, J. Fusion Energy, **30** (2011) 490.

[24] R. Majumdar, and M.A. Bourham, J. Fusion Energy, **35** (2016) 795.

[25] L.A. Klyuchnikov, V.A. Krupin, M.R. Nurgaliev, K.V. Korobov, A.R.Nemets, A.Yu. Dnestrovskij, S.N. Tugarinov, S.V. Serov, and N.N. Naumenko, Rev. Sci. Instrum. 87 (2016) 053506.

[26] Y. Yu, et. al, J. Fusion Energy, **40** (2021) 13.

[27] N.C. Metropolis, and S.M. Ulam, J. Amer. Stat. Assoc. **44** (1949) 335.

[28] D.P. Kroese, Monte Carlo Method, Department of mathematics, University of Queensland, http://www.maths.uq.edu.au/~kroese

[29] G.A. Terejanu, Tutorial on Monte Carlo Techniques, Department of computer science and engineering, University at Buffalo, https://cse.sc.edu/~terejanu/files/tutorialMC.pdf

[30] I.M. Sobol, CRC Press, (1994).

[31] F. James, Rep. Prog. Phys. **43** (1980) 1147.

[32] D. Johnson, http://cnx.org/content/m11248/latest/, (2005).

[33] S. Weinzierl, Technical report, NIKHEF Theory group, (2000).

[34] K. Tőkési, and G. Hock, Nucl. Instrum Meth. Phys. Res. B. **86 (**1994) 201.

[35] K. Tőkési, and G. Hock, Phys. B: At. Mol. Phys. **29 (1996)** L119.

[36] I. Ziaeian, and K. Tőkési, Atoms Journal **8** (2020) 27.

[37] K. Igenbergs, J. Schweinzer, F. Aumayr, J. Phys. B: At. Mol. Opt. Phys. **42** (2009) 2352.

[38] R. Abrines and I. C. Percival. Proc. Phys. Soc. **88** (1966) 861.

[39] J. S. Cohen. Phys. Rev. A. **26** (1982) 3008.

[40] R. E. Olson. J. Phys. B: At. Mol. Opt. Phys. **13** (1980) 483.

[41] D. Banks, R. S. Barnes, and J. Wilson. J. Phys. **9** (1976) 141.

[42] R.C. Becker, and A.D. MacKellar, J. Phys. B: At. Mol. Phys. **17** (1984) 3923.

[43] G. Peach, S. L. Willis, and M. R. C. McDowell. J. Phys. B: At. Mol. **18** (1985) 3921.

[44] C. O. Reinhold and C. A. Falcon. Phys. Rev. A. **33** (1986) 3859.

[45] G. A. Kohring, A. E. Wetmore, and R. E. Olson. Phys. Rev. A. **28** (1983) 2526.

[46] J. Pascale, R.E. Olson, and C. O. Reinhold. Phys. Rev. A. **42** (1990) 5305.

[47] K. Tőkési, and Á. Kövér, J. Phys. B. **33** (2000) 3067.

[48] R.E. Olson, Phys. Rev. A. **24** (1981) 1726.

[49] R. Hoekstra, H. Anderson, F. W. Bliek, M. von. Hellermann, C. F. Maggi, R. E. Olson, and H. P. Summers, Plasma Phys. Control. Fusion. **40** (1998) 1541.

[50] C.L. Kirschbaun, and L. Wilet, Phys. Rev. A. **21** (1980) 834.

[51] H. Anderson, M.G. von Hellermann, R. Hoekstra, L.D. Horton, A.C. Howman, R.W.T. Konig, R. Martin, R.E. Olson, and H.P. Summers. Plasma Phys. Control. Fusion. **42** (2000) 781.

[52] R.C. Isler, Plasma Phys. Control. Fusion **36** (1994) 171.

[53] J.S. Cohen, Phys. Rev. A**. 54** (1996) 573.

[54] S.K. Avazbaev, A.S. Kadyrov, I.B. Abdurakhmanov, D.V. Fursa, and I. Bray, Phys. Rev. A **93** (2016) 022710.

[55] I.B. Abdurakhmanov, A.S. Kadyrov, and I. Bray, J. Phys. B: At. Mol. Opt. Phys **49** (2016) 115203

[56] N.W. Antonio, C.T. Plowman, I.B. Abdurakhmanov, I. Bray, and A.S. Kadyrov, J. Phys. B: At. Mol. Opt. Phys **54** (2021) 175201.

[57] M.B. Shah and H.B. Gilbody, J. Phys. B **14** (1981) 2361.

[58] M.B. Shah, D.S. Elliott, and H.B. Gilbody J. Phys B **20** (1987) 2481.

[59] G.W. McClure, Phys. Rev**.** A **148** (1966) 47.

[60] D. Detleffsen, M. Anton, A. Werner, and K.H. Schartner, J. *Phys.* B **27** (1994) 4195.

[61] J.E. Bayfield Phys. Rev **185** (1969) 105.

[62] T.J. Morgan, J. Geddes, and H.B. Gilbody J. Phys. B **6** (1973) 2118.

[63] J. Hill, J, Geddes, and H.B. Gilbody J. Phys. B **12** (1979) L341.

[64] G. Ryding, A.B. Wittkower, and H.B. Gilbody Proc. Phys. Soc. London **89** (1966) 547.

[65] T. Kondow, R.J. Girnius, Y.P. Chong, and W.L. Fite, Phys. Rev. A **10** (1974) 1167.

[66] R.F. Stebbings, R.A. Young, C.L. Oxley, and H. Ehrhardt, Phys. Rev. A **138** (1965) 1312.

[67] Y.Z. Qu, L. Liu, C.H. Liu, T.C. Li, J.G. Wang, and R.K. Janev, In Proceedings of the 8th International Conference on Atomic and Molecular Data and Their Applications, NIST, Cambridge, MA, USA, 30 September –4 October (2012) 232–241.

[68] P.S. Krstic, and M. Radmilovic, J. Nuclear Fusion, **3** (1992) 113.

[69] M. Kimura, and W.R. Thorson, J. Phys. B At. Mol. Phys. **16** (1983) 1471.

[70] G.H. Olivera, C.A. Ramirez, and R.D. Rivarola, Physica Scripta **T62** (1996) 84.

[71] M. Mattioli, C.De Michelis, and A.L. Pecquet, Nucl. Fusion. **38** (1998) 1629.

[72] A. Loarte, *et al.* Nucl. Fusion. **47** (2007) S203.

[73] C. Illescas, and Riera, Phys. Rev. A. **60** (1999) 4546.

[74] D.R. Schultz, P.S. Krsti, and C.O. Reinhold, Physica Scripta. **T62** (1996) 69.

[75] H.J. Ludde, and R.M. Dreizler, J. Phys. B At. Mol. Phys, **15** (1982) 2713.

[76] B.H. Bransden, C.W. Newby, and C.J. Noble, J. Phys. B At. Mol. Phys **13** (1980) 4245.

[77] C. Harel, and A. Salin, J. Phys. B At. Mol. Phys **10** (1977) 3511.

[78] C. Harel, H. Jouin, B. Pons, L.F. Errea, L. Méndez, and A. Riera, Phys. Rev. A. **55** (1997) 287.

[79] A. Jorge, J. Suárez, C. Illescas, L.F. Errea, L. Méndez, Phys. Rev. A. **94** (2016) 032707.

[80] D. Belkic, R. Gayet, and A. Salin, At. Data. Nucl. Data Tables. **51** (1992) 59.

[81] K.R. Cornelius, K. Wojtkowski, and R.E. Olson, J. Phys. B: At. Mol. Opt. Phys. **33** (2000) 2017.

[82] N. Shimakura, N. Kobayashi, M. Honma, T. Nakano, and H. Kubo, Journal of Physics: Conference Series, **163** (2009) 012045.

[83] R. K. Janev, IAEA Report INDC(NDS)-225/MS (1989)

[84] D. Delibasic. N. Milojevic, I. Mancev, and D. Belkic, At. Data. Nucl. Data Tables **139**, (2021)101417

[85] I. Ziaeian, and K. Tőkési, Sci. Rep **11** (2021) 20164.

[86] I. Ziaeian, and K. Tőkési, Eur. Phys. J. D. **75** (2021) 138.

Appendix A

State-selective electron capture cross sections in collision between fully striped ions and ground state hydrogen atom- classical treatment of the collision

EXPLANATION OF TABLES

TABLE I. Cross Sections for Electron Capture from H(1s) by H^{+}

TABLE II. Cross Sections for Electron Capture from H(1s) by He^{2+}

TABLE III. Cross Sections for Electron Capture from H(1s) by Li^{3+}

TABLE IV. Cross Sections for Electron Capture from H(1s) by Be^{4+}

TABLE V. Cross Sections for Electron Capture from H(1s) by B^{5+}

TABLE VI. Cross Sections for Electron Capture from H(1s) by C^{6+}

TABLE VII. Cross Sections for Electron Capture from H(1s) by N^{7+}

TABLE VIII. Cross Sections for Electron Capture from H(1s) by O^{8+}

For each projectile, we give a set of data corresponding to the impact energy range 10 – 200 keV/amu. For a given *n*, we give first the sum over all values of *l* and *m* on the line with a space in the *l* and *m* columns. For a given *n* and *l*, we give first the sum over *m* on the line with a space in the *m* column. As the initial state has a zero value of *m*, the cross sections are independent of the sign of *m*. Due to the same cross sections for the +*m* and -*m* states, we give only one value in the table in the *m* column. The second column points to the Heisenberg correction term, labelled ‘with’ and ‘without’ and the third column represents the correspondence cross sections.

Final state n	l	m	correction	Cross sections (cm^2)
2			with	Cross section for electron capture into $n = 2$ summed over all l and m with considering Heisenberg correction term.
			without	Cross section for electron capture into $n = 2$ summed over all l and m without considering Heisenberg correction term.
2	0	0	with	Cross section for electron capture into $n = 2$, $l = 0$, $m = 0$ with considering Heisenberg correction term.
			without	Cross section for electron capture into $n = 2$, $l = 0$, $m = 0$ without considering Heisenberg correction term.
2	1		with	Cross section for electron capture into $n = 2$, $l = 1$, summed over all m with considering Heisenberg correction term.
			without	Cross section for electron capture into $n = 2$, $l = 1$, summed over all m without considering Heisenberg correction term.
2	1	0	with	Cross section for electron capture into $n = 2$, $l = 1$, $m = 0$ with considering Heisenberg correction term
			without	Cross section for electron capture into $n = 2$, $l = 1$, $m = 0$ without considering Heisenberg correction term
2	1	1	with	Cross section for electron capture into $n = 2$, $l = 1$, $\|m\| = 1$ with considering Heisenberg correction term
			without	Cross section for electron capture into $n = 2$, $l = 1$, $\|m\| = 1$ without considering Heisenberg correction term

All cross sections are in cm^2.

To increase the calculation's accuracy, we took into account 15×10^6 trajectories for each impact energy. Dashes indicate omitted entries because the cross sections are less than the order of 10^{-21} cm^2.

TABLE I. Cross Sections for Electron Capture and statistical error values (in parenthesis) from H(1s) by H^+

See page 93 for Explanation of Tables

$H^+ + H(1s) \rightarrow H(nlm) + H^+$

Final state			correction	Energy (keV/amu)			
n	*l*	*m*		10	20	30	40
1	0	0	with	3.82E-16 (3.32E-19)	2.45E-16 (1.79E-19)	1.44E-16 (1.27E-19)	8.81E-17 (9.72E-20)
			without	2.94E-16 (1.96E-19)	2.53E-16 (1.67E-19)	1.66E-16 (1.20E-19)	9.84E-17 (8.90E-20)
2			with	7.84E-17 (1.55E-19)	9.21E-17 (1.19E-19)	7.60E-17 (9.82E-20)	4.90E-17 (7.59E-20)
			without	3.30E-17 (6.03E-20)	6.43E-17 (8.87E-20)	6.14E-17 (8.42E-20)	4.42E-17 (6.86E-20)
2	0	0	with	2.86E-17 (9.65E-20)	4.67E-17 (8.79E-20)	4.38E-17 (7.72E-20)	3.04E-17 (6.30E-20)
			without	1.33E-17 (4.10E-20)	3.49E-17 (7.12E-20)	4.02E-17 (7.21E-20)	3.07E-17 (6.06E-20)
2	1		with	4.98E-17 (1.24E-19)	4.53E-17 (8.23E-20)	3.22E-17 (6.32E-20)	1.86E-17 (4.44E-20)
			without	1.97E-17 (4.52E-20)	2.94E-17 (5.63E-20)	2.12E-17 (4.66E-20)	1.35E-17 (3.47E-20)
2	1	0	with	2.72E-17 (9.72E-20)	2.37E-17 (6.17E-20)	1.68E-17 (4.81E-20)	1.02E-17 (3.53E-20)
			without	1.11E-17 (3.41E-20)	1.47E-17 (4.05E-20)	9.76E-18 (3.28E-20)	6.29E-18 (2.53E-20)
2	1	1	with	1.12E-17 (5.65E-20)	1.08E-17 (3.95E-20)	7.65E-18 (2.97E-20)	4.13E-18 (1.97E-20)
			without	4.34E-18 (2.13E-20)	7.35E-18 (2.82E-20)	5.69E-18 (2.37E-20)	3.59E-18 (1.72E-20)
3			with	7.33E-18 (4.55E-20)	1.38E-17 (4.69E-20)	1.58E-17 (4.69E-20)	1.23E-17 (3.92E-20)
			without	3.52E-18 (1.83E-20)	9.42E-18 (3.39E-20)	1.26E-17 (3.90E-20)	1.12E-17 (3.58E-20)
3	0	0	with	1.61E-18 (2.29E-20)	5.65E-18 (3.24E-20)	9.44E-18 (3.94E-20)	8.35E-18 (3.60E-20)
			without	8.15E-19 (9.42E-21)	3.31E-18 (2.13E-20)	7.67E-18 (3.24E-20)	7.94E-18 (3.27E-20)
3	1		with	3.89E-18 (3.42E-20)	6.87E-18 (3.30E-20)	5.93E-18 (2.66E-20)	3.79E-18 (1.85E-20)
			without	1.78E-18 (1.39E-20)	4.52E-18 (2.41E-20)	4.49E-18 (2.20E-20)	3.17E-18 (1.64E-20)
3	1	0	with	2.33E-18 (2.76E-20)	3.98E-18 (2.57E-20)	3.08E-18 (1.96E-20)	1.92E-18 (1.34E-20)
			without	9.70E-19 (1.03E-20)	2.82E-18 (1.96E-20)	2.17E-18 (1.58E-20)	1.38E-18 (1.09E-20)
3	1	1	with	7.87E-19 (1.45E-20)	1.45E-18 (1.49E-20)	1.43E-18 (1.28E-20)	9.32E-19 (9.13E-21)
			without	3.99E-19 (6.58E-21)	8.59E-19 (1.01E-20)	1.16E-18 (1.09E-20)	9.03E-19 (8.73E-21)
3	2		with	1.83E-18 (2.06E-20)	1.28E-18 (1.14E-20)	4.11E-19 (5.56E-21)	1.36E-19 (3.00E-21)
			without	9.23E-19 (8.09E-21)	1.59E-18 (1.21E-20)	4.20E-19 (5.59E-21)	9.17E-20 (2.44E-21)
3	2	0	with	9.34E-19 (1.45E-20)	5.15E-19 (7.01E-21)	1.88E-19 (3.56E-21)	6.77E-20 (2.02E-21)
			without	5.49E-19 (6.26E-21)	5.93E-19 (7.02E-21)	1.38E-19 (2.88E-21)	2.94E-20 (1.21E-21)
3	2	1	with	4.05E-19 (9.74E-21)	3.38E-19 (5.93E-21)	1.05E-19 (2.93E-21)	3.11E-20 (1.48E-21)
			without	1.80E-19 (3.56E-21)	4.83E-19 (6.85E-21)	1.16E-19 (3.08E-21)	2.35E-20 (1.29E-21)
3	2	2	with	3.37E-20 (2.94E-21)	3.69E-20 (2.09E-21)	1.05E-20 (1.08E-21)	1.84E-21 (4.76E-22)
			without	6.57E-21 (7.86E-22)	2.05E-20 (1.45E-21)	2.53E-20 (1.58E-21)	6.27E-21 (7.66E-22)

TABLE I. Cross Sections for Electron Capture and statistical error values (in parenthesis) from H(1s) by H^+

See page 93 for Explanation of Tables

Final state			correction	Energy (keV/amu)			
n	*l*	*m*		10	20	30	40
4			with	2.22E-18 (2.46E-20)	4.95E-18 (2.82E-20)	6.04E-18 (2.93E-20)	5.02E-18 (2.53E-20)
			without	1.10E-18 (1.01E-20)	3.31E-18 (2.00E-20)	4.64E-18 (2.38E-20)	4.46E-18 (2.27E-20)
4	0	0	with	4.71E-19 (1.27E-20)	1.48E-18 (1.64E-20)	3.13E-18 (2.29E-20)	3.25E-18 (2.28E-20)
			without	2.13E-19 (4.73E-21)	8.76E-19 (1.07E-20)	2.43E-18 (1.82E-20)	2.94E-18 (2.02E-20)
4	1		with	9.71E-19 (1.70E-20)	2.61E-18 (2.12E-20)	2.62E-18 (1.84E-20)	1.69E-18 (1.27E-20)
			without	4.66E-19 (7.05E-21)	1.54E-18 (1.44E-20)	1.94E-18 (1.51E-20)	1.46E-18 (1.15E-20)
4	1	0	with	5.66E-19 (1.34E-20)	1.69E-18 (1.76E-20)	1.44E-18 (1.40E-20)	8.60E-19 (9.12E-21)
			without	2.55E-19 (5.21E-21)	1.07E-18 (1.25E-20)	1.03E-18 (1.13E-20)	6.68E-19 (7.85E-21)
4	1	1	with	1.92E-19 (7.26E-21)	4.55E-19 (8.51E-21)	5.91E-19 (8.47E-21)	4.19E-19 (6.36E-21)
			without	1.07E-19 (3.39E-21)	2.40E-19 (5.32E-21)	4.58E-19 (7.12E-21)	3.99E-19 (5.94E-21)
4	2		with	6.30E-19 (1.22E-20)	8.08E-19 (9.63E-21)	2.92E-19 (4.87E-21)	9.17E-20 (2.46E-21)
			without	3.29E-19 (5.20E-21)	8.11E-19 (8.87E-21)	2.70E-19 (4.54E-21)	5.92E-20 (1.93E-21)
4	2	0	with	3.24E-19 (8.79E-21)	3.46E-19 (6.22E-21)	1.42E-19 (3.30E-21)	4.68E-20 (1.68E-21)
			without	1.86E-19 (3.88E-21)	3.59E-19 (5.91E-21)	9.42E-20 (2.50E-21)	2.18E-20 (1.04E-21)
4	2	1	with	1.37E-19 (5.62E-21)	2.17E-19 (5.04E-21)	6.52E-20 (2.36E-21)	1.97E-20 (1.17E-21)
			without	6.81E-20 (2.38E-21)	2.19E-19 (4.58E-21)	7.68E-20 (2.51E-21)	1.46E-20 (1.01E-21)
4	2	2	with	9.25E-21 (1.45E-21)	9.66E-21 (1.12E-21)	7.23E-21 (8.89E-22)	1.15E-21 (3.46E-22)
			without	3.32E-21 (5.07E-22)	4.45E-21 (6.79E-22)	1.12E-20 (1.01E-21)	4.48E-21 (6.40E-22)
4	3		with	1.49E-19 (5.14E-21)	4.47E-20 (2.12E-21)	-	-
			without	9.40E-20 (2.36E-21)	8.16E-20 (2.73E-21)	-	-
4	3	0	with	7.76E-20 (3.61E-21)	2.00E-20 (1.34E-21)	-	-
			without	5.42E-20 (1.76E-21)	3.12E-20 (1.51E-21)	-	-
4	3	1	with	3.23E-20 (2.48E-21)	1.23E-20 (1.16E-21)	-	-
			without	1.93E-20 (1.11E-21)	2.40E-20 (1.61E-21)	-	-
4	3	2	with	-	-	-	-
			without	-	-	-	-
4	3	3	with	-	-	-	-
			without	-	-	-	-

TABLE I. Cross Sections for Electron Capture and statistical error values (in parenthesis) from H(1s) by H^+

See page 93 for Explanation of Tables

$H^+ + H(1s) \rightarrow H(nlm) + H^+$

Final state			correction	Energy (keV/amu)			
n	*l*	*m*		50	60	70	80
1	0	0	with	5.23E-17 (6.89E-20)	3.34E-17 (4.56E-20)	2.32E-17 (3.45E-20)	1.52E-17 (2.61E-20)
			without	5.73E-17 (6.21E-20)	3.56E-17 (4.09E-20)	2.25E-17 (3.15E-20)	1.51E-17 (2.08E-20)
2			with	2.95E-17 (5.44E-20)	1.86E-17 (3.64E-20)	1.30E-17 (2.76E-20)	9.06E-18 (2.18E-20)
			without	2.66E-17 (4.80E-20)	1.63E-17 (3.14E-20)	9.83E-18 (2.36E-20)	6.18E-18 (1.51E-20)
2	0	0	with	1.97E-17 (4.69E-20)	1.35E-17 (3.23E-20)	9.80E-18 (2.49E-20)	7.15E-18 (2.01E-20)
			without	1.92E-17 (4.32E-20)	1.22E-17 (2.83E-20)	7.55E-18 (2.12E-20)	4.89E-18 (1.37E-20)
2	1		with	9.84E-18 (2.91E-20)	5.17E-18 (1.76E-20)	3.19E-18 (1.26E-20)	1.90E-18 (8.96E-21)
			without	7.39E-18 (2.28E-20)	4.04E-18 (1.43E-20)	2.27E-18 (1.07E-20)	1.28E-18 (6.56E-21)
2	1	0	with	5.62E-18 (2.39E-20)	3.14E-18 (1.49E-20)	1.97E-18 (1.07E-20)	1.22E-18 (7.78E-21)
			without	3.73E-18 (1.72E-20)	2.11E-18 (1.11E-20)	1.25E-18 (8.53E-21)	7.25E-19 (5.31E-21)
2	1	1	with	2.12E-18 (1.24E-20)	1.01E-18 (7.03E-21)	6.01E-19 (4.92E-21)	3.46E-19 (3.41E-21)
			without	1.80E-18 (1.07E-20)	9.67E-19 (6.61E-21)	5.05E-19 (4.68E-21)	2.74E-19 (2.79E-21)
3			with	8.16E-18 (2.95E-20)	5.16E-18 (1.97E-20)	3.62E-18 (1.50E-20)	2.63E-18 (1.20E-20)
			without	7.44E-18 (2.61E-20)	4.72E-18 (1.73E-20)	2.93E-18 (1.32E-20)	1.85E-18 (8.47E-21)
3	0	0	with	6.15E-18 (2.86E-20)	4.14E-18 (1.92E-20)	3.02E-18 (1.47E-20)	2.27E-18 (1.19E-20)
			without	5.70E-18 (2.51E-20)	3.81E-18 (1.68E-20)	2.41E-18 (1.27E-20)	1.56E-18 (8.15E-21)
3	1		with	1.97E-18 (1.15E-20)	1.02E-18 (6.85E-21)	5.98E-19 (4.74E-21)	3.53E-19 (3.32E-21)
			without	1.71E-18 (1.01E-20)	9.10E-19 (6.05E-21)	5.12E-19 (4.44E-21)	2.90E-19 (2.76E-21)
3	1	0	with	1.01E-18 (8.52E-21)	5.55E-19 (5.30E-21)	3.34E-19 (3.74E-21)	2.05E-19 (2.67E-21)
			without	7.81E-19 (6.84E-21)	4.14E-19 (4.11E-21)	2.46E-19 (3.15E-21)	1.46E-19 (2.01E-21)
3	1	1	with	4.82E-19 (5.57E-21)	2.30E-19 (3.11E-21)	1.30E-19 (2.06E-21)	7.28E-20 (1.40E-21)
			without	4.64E-19 (5.21E-21)	2.49E-19 (3.16E-21)	1.30E-19 (2.19E-21)	7.34E-20 (1.37E-21)
3	2		with	4.18E-20 (1.48E-21)	1.01E-20 (5.33E-22)	2.66E-21 (2.39E-22)	1.07E-21 (1.54E-22)
			without	2.05E-20 (1.01E-21)	5.26E-21 (4.09E-22)	1.57E-21 (2.18E-22)	6.27E-22 (1.11E-22)
3	2	0	with	1.90E-20 (9.18E-22)	4.81E-21 (3.35E-22)	1.25E-21 (1.46E-22)	-
			without	7.19E-21 (5.20E-22)	2.15E-21 (2.33E-22)	6.93E-22 (1.31E-22)	-
3	2	1	with	1.17E-20 (8.61E-22)	2.41E-21 (2.76E-22)	5.82E-22 (1.30E-22)	-
			without	5.78E-21 (5.64E-22)	1.34E-21 (2.23E-22)	4.18E-22 (1.21E-22)	-
3	2	2	with	-	-	-	-
			without	-	-	-	-

TABLE I. Cross Sections for Electron Capture and statistical error values (in parenthesis) from H(1s) by H^+

See page 93 for Explanation of Tables

Final State			correction	Energy (keV/amu)			
n	*l*	*m*		50	60	70	80
4			with	3.38E-18 (1.91E-20)	2.14E-18 (1.27E-20)	1.48E-18 (9.59E-21)	1.09E-18 (7.74E-21)
			without	3.06E-18 (1.68E-20)	2.00E-18 (1.14E-20)	1.23E-18 (8.61E-21)	7.73E-19 (5.48E-21)
4	0	0	with	2.47E-18 (1.84E-20)	1.69E-18 (1.25E-20)	1.23E-18 (9.47E-21)	9.42E-19 (7.74E-21)
			without	2.25E-18 (1.61E-20)	1.58E-18 (1.10E-20)	1.01E-18 (8.41E-21)	6.48E-19 (5.32E-21)
4	1		with	8.76E-19 (7.75E-21)	4.39E-19 (4.50E-21)	2.47E-19 (2.99E-21)	1.43E-19 (2.07E-21)
			without	7.95E-19 (6.94E-21)	4.13E-19 (4.08E-21)	2.20E-19 (2.84E-21)	1.25E-19 (1.77E-21)
4	1	0	with	4.45E-19 (5.61E-21)	2.35E-19 (3.42E-21)	1.36E-19 (2.32E-21)	8.34E-20 (1.66E-21)
			without	3.65E-19 (4.72E-21)	1.95E-19 (2.82E-21)	1.01E-19 (1.94E-21)	5.89E-20 (1.23E-21)
4	1	1	with	2.15E-19 (3.76E-21)	9.81E-20 (2.03E-21)	5.52E-20 (1.33E-21)	2.84E-20 (8.59E-22)
			without	2.14E-19 (3.62E-21)	1.09E-19 (2.10E-21)	5.81E-20 (1.46E-21)	3.34E-20 (9.05E-22)
4	2		with	2.76E-20 (1.23E-21)	9.19E-21 (5.41E-22)	2.92E-21 (2.72E-22)	-
			without	1.19E-20 (7.82E-22)	3.05E-21 (3.20E-22)	7.69E-22 (1.54E-22)	-
4	2	0	with	1.46E-20 (8.55E-22)	4.53E-21 (3.60E-22)	1.45E-21 (1.79E-22)	-
			without	4.82E-21 (4.40E-22)	1.08E-21 (1.64E-22)	2.66E-22 (8.03E-23)	-
4	2	1	with	6.08E-21 (6.05E-22)	2.32E-21 (2.92E-22)	7.96E-22 (1.56E-22)	-
			without	3.18E-21 (4.37E-22)	1.22E-21 (2.35E-22)	1.77E-22 (7.93E-23)	-
4	2	2	with	-	-	-	-
			without	-	-	-	-
4	3		with	-	-	-	-
			without	-	-	-	-
4	3	0	with	-	-	-	-
			without	-	-	-	-
4	3	1	with	-	-	-	-
			without	-	-	-	-
4	3	2	with	-	-	-	-
			without	-	-	-	-
4	3	3	with	-	-	-	-
			without	-	-	-	-

TABLE I. Cross Sections for Electron Capture and statistical error values (in parenthesis) from H(1s) by H^+

See page 93 for Explanation of Tables

$H^+ + H(1s) \rightarrow H(nlm) + H^+$

Final state			correction	Energy (keV/amu)			
n	*l*	*m*		90	100	150	200
1	0	0	with	9.13E-18 (1.80E-20)	6.11E-18 (1.26E-20)	1.14E-18 (2.68E-21)	2.67E-19 (1.47E-21)
			without	1.04E-17 (1.68E-20)	7.50E-18 (1.32E-20)	1.85E-18 (3.32E-21)	6.54E-19 (2.29E-21)
2			with	5.54E-18 (1.53E-20)	3.63E-18 (1.06E-20)	6.02E-19 (2.11E-21)	1.21E-19 (1.04E-21)
			without	4.05E-18 (1.19E-20)	2.71E-18 (9.00E-21)	5.14E-19 (1.98E-21)	1.45E-19 (1.22E-21)
2	0	0	with	4.55E-18 (1.44E-20)	3.03E-18 (1.00E-20)	5.37E-19 (2.02E-21)	1.05E-19 (9.69E-22)
			without	3.28E-18 (1.08E-20)	2.25E-18 (8.26E-21)	4.63E-19 (1.88E-21)	1.36E-19 (1.18E-21)
2	1		with	9.92E-19 (5.68E-21)	5.90E-19 (3.84E-21)	6.48E-20 (6.26E-22)	1.68E-20 (3.84E-22)
			without	7.70E-19 (4.99E-21)	4.61E-19 (3.59E-21)	5.16E-20 (6.33E-22)	9.13E-21 (3.26E-22)
2	1	0	with	6.59E-19 (5.04E-21)	4.07E-19 (3.41E-21)	5.24E-20 (5.74E-22)	1.55E-20 (3.69E-22)
			without	4.46E-19 (4.10E-21)	2.66E-19 (2.92E-21)	3.14E-20 (5.18E-22)	5.36E-21 (2.57E-22)
2	1	1	with	1.67E-19 (2.04E-21)	9.10E-20 (1.33E-21)	6.13E-21 (1.77E-22)	5.99E-22 (7.06E-23)
			without	1.65E-19 (2.12E-21)	9.72E-20 (1.53E-21)	9.64E-21 (2.53E-22)	2.03E-21 (1.51E-22)
3			with	1.67E-18 (8.65E-21)	1.08E-18 (5.95E-21)	1.78E-19 (1.17E-21)	3.43E-20 (5.57E-22)
			without	1.21E-18 (6.61E-21)	8.21E-19 (5.06E-21)	1.50E-19 (1.08E-21)	4.18E-20 (6.60E-22)
3	0	0	with	1.48E-18 (8.64E-21)	9.73E-19 (5.93E-21)	1.64E-19 (1.15E-21)	3.01E-20 (5.26E-22)
			without	1.04E-18 (6.36E-21)	7.22E-19 (4.88E-21)	1.40E-19 (1.05E-21)	3.98E-20 (6.43E-22)
3	1		with	1.91E-19 (2.14E-21)	1.08E-19 (1.39E-21)	1.35E-20 (2.64E-22)	4.27E-21 (1.86E-22)
			without	1.67E-19 (2.06E-21)	9.87E-20 (1.48E-21)	1.01E-20 (2.63E-22)	2.00E-21 (1.53E-22)
3	1	0	with	1.13E-19 (1.76E-21)	6.69E-20 (1.15E-21)	1.03E-20 (2.31E-22)	3.83E-21 (1.75E-22)
			without	8.52E-20 (1.52E-21)	5.09E-20 (1.09E-21)	5.01E-21 (1.84E-22)	1.01E-21 (1.05E-22)
3	1	1	with	3.97E-20 (9.03E-22)	2.02E-20 (5.62E-22)	1.61E-21 (9.06E-23)	2.38E-22 (4.87E-23)
			without	3.97E-20 (9.76E-22)	2.36E-20 (1.09E-21)	2.45E-21 (1.28E-22)	5.10E-22 (7.78E-23)
3	2		with	-	-	-	-
			without	-	-	-	-
3	2	0	with	-	-	-	-
			without	-	-	-	-
3	2	1	with	-	-	-	-
			without	-	-	-	-
3	2	2	with	-	-	-	-
			without	-	-	-	-

TABLE I. Cross Sections for Electron Capture and statistical error values (in parenthesis) from H(1s) by H^+

See page 93 for Explanation of Tables

Final State			correction	Energy (keV/amu)			
n	*l*	*m*		90	100	150	200
4			with	7.14E-19 (5.67E-21)	4.67E-19 (3.96E-21)	7.56E-20 (7.71E-22)	1.49E-20 (3.71E-22)
			without	5.00E-19 (4.25E-21)	3.46E-19 (3.30E-21)	6.29E-20 (7.01E-22)	1.70E-20 (4.22E-22)
4	0	0	with	6.36E-19 (5.72E-21)	4.22E-19 (3.96E-21)	7.03E-20 (7.58E-22)	1.32E-20 (3.52E-22)
			without	4.30E-19 (4.12E-21)	3.07E-19 (3.21E-21)	5.90E-20 (6.84E-22)	1.64E-20 (4.12E-22)
4	1		with	7.82E-20 (1.32E-21)	4.49E-20 (8.84E-22)	5.30E-21 (1.66E-22)	1.72E-21 (1.18E-22)
			without	7.03E-20 (1.29E-21)	3.94E-20 (9.14E-22)	3.90E-21 (1.58E-22)	6.69E-22 (8.95E-23)
4	1	0	with	4.56E-20 (1.07E-21)	2.72E-20 (7.20E-22)	3.87E-21 (1.41E-22)	1.57E-21 (1.12E-22)
			without	3.41E-20 (9.11E-22)	2.01E-20 (6.63E-22)	1.89E-21 (1.10E-22)	2.52E-22 (4.95E-23)
4	1	1	with	1.68E-20 (5.75E-22)	9.07E-21 (3.76E-22)	7.46E-22 (6.44E-23)	1.05E-22 (3.31E-23)
			without	1.90E-20 (6.67E-22)	9.66E-21 (4.52E-22)	1.03E-21 (8.17E-23)	3.31E-22 (6.91E-23)
4	2		with	-	-	-	-
			without	-	-	-	-
4	2	0	with	-	-	-	-
			without	-	-	-	-
4	2	1	with	-	-	-	-
			without	-	-	-	-
4	2	2	with	-	-	-	-
			without	-	-	-	-
4	3		with	-	-	-	-
			without	-	-	-	-
4	3	0	with	-	-	-	-
			without	-	-	-	-
4	3	1	with	-	-	-	-
			without	-	-	-	-
4	3	2	with	-	-	-	-
			without	-	-	-	-
4	3	3	with	-	-	-	-
			without	-	-	-	-

TABLE II. Cross Sections for Electron Capture and statistical error values (in parenthesis) from H(1s) by He^{2+}

See page 93 for Explanation of Tables

$He^{2+} + H(1s) \rightarrow He^{+}(nlm) + H^{+}$

Final state			correction	Energy (keV/amu)			
n	*l*	*m*		10	20	30	40
1	0	0	with	6.53E-17 (1.12E-19)	6.10E-17 (1.03E-19)	5.50E-17 (8.58E-20)	4.80E-17 (7.43E-20)
			without	4.50E-17 (7.37E-20)	4.90E-17 (7.98E-20)	5.40E-17 (7.91E-20)	5.15E-17 (7.28E-20)
2			with	1.15E-15 (5.35E-19)	8.75E-16 (3.98E-19)	5.78E-16 (3.08E-19)	3.66E-16 (2.44E-19)
			without	7.32E-16 (3.55E-19)	6.87E-16 (3.18E-19)	5.04E-16 (2.74E-19)	3.34E-16 (2.26E-19)
2	0	0	with	2.35E-16 (2.64E-19)	1.29E-16 (1.62E-19)	8.49E-17 (1.17E-19)	6.03E-17 (9.01E-20)
			without	1.43E-16 (1.59E-19)	1.01E-16 (1.21E-19)	7.22E-17 (9.98E-20)	5.22E-17 (8.20E-20)
2	1		with	9.16E-16 (5.11E-19)	7.46E-16 (3.92E-19)	4.93E-16 (3.02E-19)	3.05E-16 (2.39E-19)
			without	5.90E-16 (3.48E-19)	5.86E-16 (3.19E-19)	4.31E-16 (2.71E-19)	2.82E-16 (2.20E-19)
2	1	0	with	4.35E-16 (3.93E-19)	3.59E-16 (3.09E-19)	2.45E-16 (2.39E-19)	1.55E-16 (1.89E-19)
			without	3.05E-16 (2.83E-19)	3.14E-16 (2.61E-19)	2.37E-16 (2.19E-19)	1.56E-16 (1.76E-19)
2	1	1	with	2.40E-16 (2.83E-19)	1.93E-16 (2.17E-19)	1.24E-16 (1.59E-19)	7.50E-17 (1.18E-19)
			without	1.42E-16 (1.79E-19)	1.36E-16 (1.66E-19)	9.73E-17 (1.36E-19)	6.28E-17 (1.06E-19)
3			with	1.05E-16 (1.64E-19)	1.41E-16 (2.06E-19)	1.62E-16 (2.07E-19)	1.40E-16 (1.86E-19)
			without	3.75E-17 (7.64E-20)	7.11E-17 (1.17E-19)	1.10E-16 (1.51E-19)	1.12E-16 (1.52E-19)
3	0	0	with	1.87E-17 (6.68E-20)	2.67E-17 (8.09E-20)	2.78E-17 (7.36E-20)	2.53E-17 (6.52E-20)
			without	8.63E-18 (3.92E-20)	2.41E-17 (7.07E-20)	3.19E-17 (7.67E-20)	2.69E-17 (6.54E-20)
3	1		with	6.09E-17 (1.32E-19)	9.10E-17 (1.73E-19)	1.08E-16 (1.75E-19)	9.28E-17 (1.57E-19)
			without	1.86E-17 (5.66E-20)	3.03E-17 (8.54E-20)	6.60E-17 (1.25E-19)	7.33E-17 (1.30E-19)
3	1	0	with	3.68E-17 (1.12E-19)	5.08E-17 (1.32E-19)	5.69E-17 (1.32E-19)	4.69E-17 (1.20E-19)
			without	8.35E-18 (4.05E-20)	1.94E-17 (6.81E-20)	4.06E-17 (9.80E-20)	4.27E-17 (1.02E-19)
3	1	1	with	1.20E-17 (5.35E-20)	2.01E-17 (8.06E-20)	2.57E-17 (8.39E-20)	2.29E-17 (7.49E-20)
			without	5.15E-18 (2.85E-20)	5.46E-18 (3.68E-20)	1.27E-17 (5.54E-20)	1.53E-17 (5.84E-20)
3	2		with	2.59E-17 (7.73E-20)	2.36E-17 (8.79E-20)	2.59E-17 (1.00E-19)	2.20E-17 (9.41E-20)
			without	1.02E-17 (3.61E-20)	1.66E-17 (4.89E-20)	1.19E-17 (4.98E-20)	1.15E-17 (5.77E-20)
3	2	0	with	7.99E-18 (4.29E-20)	9.29E-18 (5.58E-20)	1.16E-17 (6.67E-20)	1.11E-17 (6.79E-20)
			without	3.83E-18 (2.24E-20)	7.97E-18 (3.20E-20)	5.98E-18 (3.52E-20)	6.20E-18 (4.30E-20)
3	2	1	with	7.19E-18 (4.16E-20)	6.60E-18 (4.70E-20)	6.77E-18 (5.26E-20)	5.27E-18 (4.60E-20)
			without	2.33E-18 (1.71E-20)	4.12E-18 (2.61E-20)	2.79E-18 (2.47E-20)	2.62E-18 (2.75E-20)
3	2	2	with	1.74E-18 (1.91E-20)	5.50E-19 (1.14E-20)	3.25E-19 (8.49E-21)	1.75E-19 (6.28E-21)
			without	9.17E-19 (1.08E-20)	1.80E-19 (5.09E-21)	1.51E-19 (4.65E-21)	7.40E-20 (3.17E-21)

TABLE II. Cross Sections for Electron Capture and statistical error values (in parenthesis) from H(1s) by He^{2+}

See page 93 for Explanation of Tables

Final state			correction	Energy (keV/amu)			
n	*l*	*m*		10	20	30	40
4			with	1.56E-17 (5.88E-20)	3.12E-17 (1.01E-19)	4.79E-17 (1.17E-19)	5.16E-17 (1.17E-19)
			without	7.45E-18 (3.22E-20)	1.48E-17 (5.38E-20)	2.94E-17 (8.00E-20)	3.87E-17 (9.13E-20)
4	0	0	with	2.14E-18 (2.06E-20)	9.69E-18 (5.46E-20)	1.31E-17 (5.43E-20)	1.27E-17 (4.85E-20)
			without	1.16E-18 (1.31E-20)	4.56E-18 (3.07E-20)	1.42E-17 (5.48E-20)	1.48E-17 (5.17E-20)
4	1		with	7.64E-18 (4.55E-20)	1.65E-17 (7.92E-20)	3.07E-17 (1.00E-19)	3.49E-17 (1.04E-19)
			without	2.70E-18 (2.08E-20)	5.48E-18 (3.66E-20)	1.17E-17 (5.36E-20)	2.12E-17 (7.36E-20)
4	1	0	with	4.17E-18 (3.68E-20)	9.27E-18 (6.09E-20)	1.64E-17 (7.48E-20)	1.78E-17 (7.84E-20)
			without	1.21E-18 (1.46E-20)	3.66E-18 (3.03E-20)	7.01E-18 (4.07E-20)	1.22E-17 (5.64E-20)
4	1	1	with	1.72E-18 (1.97E-20)	3.60E-18 (3.60E-20)	7.15E-18 (4.76E-20)	8.58E-18 (4.92E-20)
			without	7.53E-19 (1.06E-20)	9.30E-19 (1.48E-20)	2.41E-18 (2.50E-20)	4.57E-18 (3.38E-20)
4	2		with	4.73E-18 (3.12E-20)	4.44E-18 (3.50E-20)	3.92E-18 (3.39E-20)	4.03E-18 (3.64E-20)
			without	2.91E-18 (2.03E-20)	3.21E-18 (2.41E-20)	3.18E-18 (2.48E-20)	2.62E-18 (2.39E-20)
4	2	0	with	1.66E-18 (1.87E-20)	2.02E-18 (2.32E-20)	1.81E-18 (2.28E-20)	2.03E-18 (2.57E-20)
			without	9.80E-19 (1.20E-20)	1.89E-18 (1.81E-20)	1.68E-18 (1.77E-20)	1.39E-18 (1.73E-20)
4	2	1	with	1.25E-18 (1.59E-20)	1.15E-18 (1.81E-20)	1.01E-18 (1.78E-20)	9.66E-19 (1.82E-20)
			without	7.68E-19 (1.03E-20)	6.18E-19 (1.08E-20)	7.20E-19 (1.23E-20)	5.92E-19 (1.16E-20)
4	2	2	with	2.59E-19 (7.12E-21)	6.11E-20 (3.67E-21)	5.53E-20 (3.37E-21)	4.45E-20 (3.00E-21)
			without	2.00E-19 (5.27E-21)	3.16E-20 (2.06E-21)	2.88E-20 (1.98E-21)	2.52E-20 (1.83E-21)
4	3		with	1.09E-18 (1.21E-20)	6.24E-19 (1.03E-20)	2.59E-19 (6.22E-21)	7.85E-20 (3.41E-21)
			without	6.83E-19 (7.56E-21)	1.57E-18 (1.36E-20)	3.74E-19 (6.45E-21)	6.98E-20 (2.54E-21)
4	3	0	with	3.17E-19 (5.99E-21)	1.85E-19 (4.89E-21)	9.03E-20 (3.21E-21)	2.60E-20 (1.73E-21)
			without	2.42E-19 (4.28E-21)	6.06E-19 (7.55E-21)	1.29E-19 (3.37E-21)	2.62E-20 (1.38E-21)
4	3	1	with	2.89E-19 (6.47E-21)	1.50E-19 (5.37E-21)	5.96E-20 (3.17E-21)	2.04E-20 (1.82E-21)
			without	1.47E-19 (3.47E-21)	4.21E-19 (7.60E-21)	9.57E-20 (3.48E-21)	1.74E-20 (1.37E-21)
4	3	2	with	9.38E-20 (4.01E-21)	7.27E-20 (3.99E-21)	2.14E-20 (2.09E-21)	6.02E-21 (1.16E-21)
			without	7.69E-20 (2.98E-21)	7.37E-20 (3.37E-21)	3.02E-20 (2.09E-21)	4.41E-21 (7.68E-22)
4	3	3	with	1.52E-21 (4.06E-22)	-	-	-
			without	1.94E-22 (4.45E-23)	-	-	-

TABLE II. Cross Sections for Electron Capture and statistical error values (in parenthesis) from H(1s) by He^{2+}

See page 93 for Explanation of Tables

$He^{2+} + H(1s) \rightarrow He^{+}(nlm) + H^{+}$

Final state			correction	Energy (keV/amu)			
n	*l*	*m*		50	60	70	80
1	0	0	with	3.75E-17 (5.54E-20)	2.85E-17 (4.69E-20)	2.17E-17 (3.66E-20)	1.73E-17 (3.05E-20)
			without	4.26E-17 (6.08E-20)	3.35E-17 (4.55E-20)	2.57E-17 (3.89E-20)	1.95E-17 (3.15E-20)
2			with	2.32E-16 (1.66E-19)	1.52E-16 (1.30E-19)	1.01E-16 (9.37E-20)	6.81E-17 (7.14E-20)
			without	2.16E-16 (1.71E-19)	1.39E-16 (1.15E-19)	9.03E-17 (8.96E-20)	5.98E-17 (6.71E-20)
2	0	0	with	4.21E-17 (6.04E-20)	2.93E-17 (4.73E-20)	2.05E-17 (3.46E-20)	1.45E-17 (2.67E-20)
			without	3.84E-17 (6.40E-20)	2.80E-17 (4.51E-20)	2.01E-17 (3.62E-20)	1.44E-17 (2.79E-20)
2	1		with	1.90E-16 (1.63E-19)	1.23E-16 (1.28E-19)	8.04E-17 (9.22E-20)	5.36E-17 (7.02E-20)
			without	1.78E-16 (1.65E-19)	1.11E-16 (1.11E-19)	7.01E-17 (8.56E-20)	4.54E-17 (6.39E-20)
2	1	0	with	1.01E-16 (1.31E-19)	6.72E-17 (1.04E-19)	4.51E-17 (7.63E-20)	3.04E-17 (5.82E-20)
			without	9.98E-17 (1.33E-19)	6.33E-17 (9.05E-20)	4.03E-17 (7.01E-20)	2.64E-17 (5.25E-20)
2	1	1	with	4.47E-17 (7.69E-20)	2.78E-17 (5.79E-20)	1.76E-17 (4.03E-20)	1.16E-17 (3.03E-20)
			without	3.89E-17 (7.64E-20)	2.39E-17 (4.97E-20)	1.49E-17 (3.74E-20)	9.47E-18 (2.75E-20)
3			with	1.02E-16 (1.31E-19)	6.97E-17 (1.02E-19)	4.85E-17 (7.42E-20)	3.32E-17 (5.60E-20)
			without	9.03E-17 (1.27E-19)	6.42E-17 (8.95E-20)	4.35E-17 (7.00E-20)	2.94E-17 (5.21E-20)
3	0	0	with	1.97E-17 (4.60E-20)	1.40E-17 (3.64E-20)	9.90E-18 (2.69E-20)	7.12E-18 (2.10E-20)
			without	2.07E-17 (5.16E-20)	1.51E-17 (3.61E-20)	1.08E-17 (2.88E-20)	7.66E-18 (2.20E-20)
3	1		with	6.83E-17 (1.14E-19)	4.76E-17 (8.97E-20)	3.41E-17 (6.63E-20)	2.36E-17 (5.04E-20)
			without	6.00E-17 (1.10E-19)	4.24E-17 (7.76E-20)	2.84E-17 (6.06E-20)	1.92E-17 (4.52E-20)
3	1	0	with	3.51E-17 (8.85E-20)	2.50E-17 (7.01E-20)	1.87E-17 (5.28E-20)	1.32E-17 (4.05E-20)
			without	3.36E-17 (8.61E-20)	2.36E-17 (6.17E-20)	1.59E-17 (4.86E-20)	1.08E-17 (3.68E-20)
3	1	1	with	1.67E-17 (5.32E-20)	1.12E-17 (4.11E-20)	7.72E-18 (2.97E-20)	5.18E-18 (2.21E-20)
			without	1.32E-17 (4.98E-20)	9.33E-18 (3.45E-20)	6.29E-18 (2.67E-20)	4.21E-18 (1.97E-20)
3	2		with	1.37E-17 (6.36E-20)	8.10E-18 (4.75E-20)	4.53E-18 (3.16E-20)	2.47E-18 (2.15E-20)
			without	9.51E-18 (5.30E-20)	6.65E-18 (3.89E-20)	4.27E-18 (3.08E-20)	2.58E-18 (2.24E-20)
3	2	0	with	7.36E-18 (4.72E-20)	4.51E-18 (3.60E-20)	2.68E-18 (2.45E-20)	1.50E-18 (1.69E-20)
			without	5.14E-18 (3.96E-20)	3.65E-18 (2.93E-20)	2.36E-18 (2.33E-20)	1.47E-18 (1.72E-20)
3	2	1	with	3.17E-18 (3.04E-20)	1.77E-18 (2.20E-20)	9.38E-19 (1.42E-20)	4.85E-19 (9.43E-21)
			without	2.14E-18 (2.50E-20)	1.50E-18 (1.83E-20)	9.44E-19 (1.43E-20)	5.63E-19 (1.03E-20)
3	2	2	with	6.80E-20 (3.28E-21)	2.72E-20 (2.03E-21)	8.68E-21 (1.01E-21)	3.67E-21 (5.73E-22)
			without	3.55E-20 (2.12E-21)	1.96E-20 (1.38E-21)	9.58E-21 (9.49E-22)	5.18E-21 (6.43E-22)

TABLE II. Cross Sections for Electron Capture and statistical error values (in parenthesis) from H(1s) by He^{2+}

See page 93 for Explanation of Tables

Final State			correction	Energy (keV/amu)			
n	*l*	*m*		50	60	70	80
4			with	4.33E-17 (8.94E-20)	3.10E-17 (7.10E-20)	2.24E-17 (5.24E-20)	1.55E-17 (3.95E-20)
			without	3.64E-17 (8.32E-20)	2.84E-17 (6.16E-20)	2.03E-17 (4.96E-20)	1.39E-17 (3.70E-20)
4	0	0	with	1.03E-17 (3.55E-20)	7.35E-18 (2.81E-20)	5.25E-18 (2.08E-20)	3.80E-18 (1.63E-20)
			without	1.17E-17 (4.09E-20)	8.47E-18 (2.85E-20)	5.98E-18 (2.25E-20)	4.15E-18 (1.70E-20)
4	1		with	2.97E-17 (8.05E-20)	2.15E-17 (6.41E-20)	1.58E-17 (4.75E-20)	1.09E-17 (3.56E-20)
			without	2.26E-17 (7.20E-20)	1.81E-17 (5.41E-20)	1.30E-17 (4.36E-20)	8.84E-18 (3.24E-20)
4	1	0	with	1.53E-17 (6.18E-20)	1.13E-17 (4.98E-20)	8.62E-18 (3.74E-20)	6.03E-18 (2.81E-20)
			without	1.25E-17 (5.56E-20)	9.95E-18 (4.23E-20)	7.16E-18 (3.45E-20)	4.88E-18 (2.59E-20)
4	1	1	with	7.21E-18 (3.75E-20)	5.08E-18 (2.94E-20)	3.58E-18 (2.14E-20)	2.43E-18 (1.58E-20)
			without	5.03E-18 (3.28E-20)	4.05E-18 (2.42E-20)	2.92E-18 (1.94E-20)	1.98E-18 (1.43E-20)
4	2		with	3.30E-18 (2.96E-20)	2.17E-18 (2.36E-20)	1.32E-18 (1.65E-20)	7.77E-19 (1.17E-20)
			without	2.12E-18 (2.20E-20)	1.74E-18 (1.85E-20)	1.28E-18 (1.62E-20)	8.65E-19 (1.28E-20)
4	2	0	with	1.83E-18 (2.21E-20)	1.23E-18 (1.79E-20)	7.68E-19 (1.26E-20)	4.70E-19 (9.15E-21)
			without	1.17E-18 (1.66E-20)	9.75E-19 (1.41E-20)	7.42E-19 (1.25E-20)	4.99E-19 (9.89E-21)
4	2	1	with	7.09E-19 (1.38E-20)	4.64E-19 (1.10E-20)	2.71E-19 (7.51E-21)	1.57E-19 (5.26E-21)
			without	4.64E-19 (1.04E-20)	3.75E-19 (8.52E-21)	2.67E-19 (7.37E-21)	1.78E-19 (5.76E-21)
4	2	2	with	2.59E-20 (1.97E-21)	1.00E-20 (1.19E-21)	4.68E-21 (6.90E-22)	1.73E-21 (3.77E-22)
			without	1.55E-20 (1.34E-21)	7.28E-21 (7.85E-22)	4.43E-21 (6.15E-22)	1.40E-21 (2.93E-22)
4	3		with	1.73E-20 (1.38E-21)	3.47E-21 (6.45E-22)	-	-
			without	1.13E-20 (8.80E-22)	1.80E-21 (2.85E-22)	-	-
4	3	0	with	3.52E-21 (4.93E-22)	-	-	-
			without	4.15E-21 (4.66E-22)	-	-	-
4	3	1	with	5.20E-21 (7.75E-22)	-	-	-
			without	2.17E-21 (3.95E-22)	-	-	-
4	3	2	with	1.72E-21 (5.44E-22)	-	-	-
			without	1.36E-21 (3.93E-22)	-	-	-
4	3	3	with	-	-	-	-
			without	-	-	-	-

TABLE II. Cross Sections for Electron Capture and statistical error values (in parenthesis) from H(1s) by He^{2+}

See page 93 for Explanation of Tables

$He^{2+} + H(1s) \rightarrow He^{+}(nlm) + H^{+}$

Final state			correction	Energy (keV/amu)			
n	*l*	*m*		90	100	150	200
1	0	0	with	1.35E-17 (2.48E-20)	1.07E-17 (1.81E-20)	3.60E-18 (6.02E-21)	1.56E-18 (3.90E-21)
			without	1.52E-17 (2.31E-20)	1.17E-17 (1.87E-20)	4.05E-18 (7.23E-21)	1.70E-18 (4.42E-21)
2			with	4.78E-17 (5.54E-20)	3.48E-17 (3.88E-20)	6.78E-18 (1.01E-20)	1.93E-18 (5.18E-21)
			without	4.08E-17 (4.55E-20)	2.83E-17 (3.48E-20)	6.21E-18 (1.06E-20)	1.91E-18 (5.52E-21)
2	0	0	with	1.06E-17 (2.11E-20)	8.02E-18 (1.50E-20)	1.91E-18 (4.43E-21)	6.62E-19 (2.64E-21)
			without	1.06E-17 (1.96E-20)	7.76E-18 (1.53E-20)	2.17E-18 (5.31E-21)	8.02E-19 (3.06E-21)
2	1		with	3.72E-17 (5.43E-20)	2.68E-17 (3.79E-20)	4.87E-18 (9.48E-21)	1.27E-18 (4.62E-21)
			without	3.02E-17 (4.31E-20)	2.05E-17 (3.28E-20)	4.04E-18 (9.75E-21)	1.11E-18 (4.92E-21)
2	1	0	with	2.15E-17 (4.53E-20)	1.58E-17 (3.19E-20)	3.08E-18 (8.03E-21)	8.48E-19 (3.93E-21)
			without	1.78E-17 (3.55E-20)	1.22E-17 (2.71E-20)	2.50E-18 (8.16E-21)	7.11E-19 (4.16E-21)
2	1	1	with	7.86E-18 (2.30E-20)	5.51E-18 (1.57E-20)	8.93E-19 (3.73E-21)	2.07E-19 (1.75E-21)
			without	6.19E-18 (1.83E-20)	4.15E-18 (1.37E-20)	7.68E-19 (3.92E-21)	1.97E-19 (1.91E-21)
3			with	2.29E-17 (4.23E-20)	1.71E-17 (3.00E-20)	3.16E-18 (7.32E-21)	8.37E-19 (3.65E-21)
			without	1.99E-17 (3.48E-20)	1.35E-17 (2.60E-20)	2.72E-18 (7.43E-21)	7.70E-19 (3.66E-21)
3	0	0	with	5.29E-18 (1.66E-20)	4.12E-18 (1.20E-20)	9.72E-19 (3.34E-21)	3.28E-19 (1.95E-21)
			without	5.47E-18 (1.52E-20)	3.91E-18 (1.16E-20)	9.99E-19 (3.77E-21)	3.45E-19 (2.09E-21)
3	1		with	1.65E-17 (3.88E-20)	1.23E-17 (2.78E-20)	2.17E-18 (6.85E-21)	5.09E-19 (3.26E-21)
			without	1.29E-17 (3.03E-20)	8.76E-18 (2.28E-20)	1.66E-18 (6.68E-21)	4.21E-19 (3.23E-21)
3	1	0	with	9.47E-18 (3.16E-20)	7.20E-18 (2.28E-20)	1.36E-18 (5.82E-21)	3.34E-19 (2.75E-21)
			without	7.36E-18 (2.48E-20)	5.07E-18 (1.88E-20)	1.01E-18 (5.60E-21)	2.66E-19 (2.75E-21)
3	1	1	with	3.48E-18 (1.66E-20)	2.56E-18 (1.17E-20)	4.04E-19 (2.68E-21)	8.72E-20 (1.25E-21)
			without	2.74E-18 (1.29E-20)	1.84E-18 (9.58E-21)	3.24E-19 (2.68E-21)	7.79E-20 (1.26E-21)
3	2		with	1.11E-18 (1.29E-20)	6.78E-19 (8.36E-21)	1.72E-20 (7.47E-22)	3.97E-22 (9.94E-23)
			without	1.52E-18 (1.42E-20)	8.71E-19 (9.89E-21)	5.85E-20 (1.64E-21)	3.54E-21 (3.54E-22)
3	2	0	with	6.83E-19 (1.02E-20)	4.32E-19 (6.73E-21)	1.37E-20 (6.72E-22)	-
			without	8.84E-19 (1.10E-20)	5.15E-19 (7.74E-21)	3.86E-20 (1.36E-21)	-
3	2	1	with	2.14E-19 (5.59E-21)	1.23E-19 (3.51E-21)	1.83E-21 (2.40E-22)	-
			without	3.12E-19 (6.36E-21)	1.74E-19 (4.35E-21)	8.64E-21 (6.17E-22)	-
3	2	2	with	2.21E-21 (4.33E-22)	-	-	-
			without	3.47E-21 (4.45E-22)	-	-	-

TABLE II. Cross Sections for Electron Capture and statistical error values (in parenthesis) from H(1s) by He^{2+}

See page 93 for Explanation of Tables

Final State			correction	Energy (keV/amu)			
n	*l*	*m*		90	100	150	200
4			with	1.07E-17 (2.98E-20)	8.03E-18 (2.12E-20)	1.52E-18 (5.15E-21)	3.97E-19 (2.56E-21)
			without	9.44E-18 (2.46E-20)	6.55E-18 (1.85E-20)	1.28E-18 (5.19E-21)	3.53E-19 (2.51E-21)
4	0	0	with	2.82E-18 (1.28E-20)	2.26E-18 (9.43E-21)	5.20E-19 (2.52E-21)	1.72E-19 (1.47E-21)
			without	2.95E-18 (1.16E-20)	2.11E-18 (8.86E-21)	5.05E-19 (2.75E-21)	1.67E-19 (1.49E-21)
4	1		with	7.59E-18 (2.72E-20)	5.57E-18 (1.93E-20)	9.93E-19 (4.75E-21)	2.24E-19 (2.22E-21)
			without	5.95E-18 (2.14E-20)	4.13E-18 (1.62E-20)	7.53E-19 (4.62E-21)	1.85E-19 (2.19E-21)
4	1	0	with	4.30E-18 (2.18E-20)	3.22E-18 (1.56E-20)	6.13E-19 (3.98E-21)	1.43E-19 (1.84E-21)
			without	3.34E-18 (1.74E-20)	2.35E-18 (1.33E-20)	4.54E-19 (3.84E-21)	1.15E-19 (1.83E-21)
4	1	1	with	1.66E-18 (1.19E-20)	1.18E-18 (8.23E-21)	1.91E-19 (1.91E-21)	3.97E-20 (8.80E-22)
			without	1.30E-18 (9.22E-21)	8.91E-19 (6.96E-21)	1.49E-19 (1.88E-21)	3.44E-20 (8.61E-22)
4	2		with	3.01E-19 (6.18E-21)	1.91E-19 (4.11E-21)	4.45E-21 (3.11E-22)	-
			without	5.39E-19 (8.45E-21)	3.09E-19 (5.91E-21)	1.98E-20 (9.56E-22)	-
4	2	0	with	1.91E-19 (4.91E-21)	1.19E-19 (3.20E-21)	3.53E-21 (2.82E-22)	-
			without	3.22E-19 (6.67E-21)	1.86E-19 (4.66E-21)	1.38E-20 (8.23E-22)	-
4	2	1	with	5.32E-20 (2.56E-21)	3.75E-20 (1.89E-21)	-	-
			without	1.04E-19 (3.64E-21)	6.11E-20 (2.60E-21)	-	-
4	2	2	with	-	-	-	-
			without	-	-	-	-
							-
4	3		with	-	-	-	-
			without	-	-	-	-
4	3	0	with	-	-	-	-
			without	-	-	-	-
4	3	1	with	-	-	-	-
			without	-	-	-	-
4	3	2	with	-	-	-	-
			without	-	-	-	-
4	3	3	with	-	-	-	-
			without	-	-	-	-

TABLE III. Cross Sections for Electron Capture and statistical error values (in parenthesis) from H(1s) by Li^{3+}

See page 93 for Explanation of Tables

$Li^{3+} + H(1s) \rightarrow Li^{2+}(nlm) + H^{+}$

Final state			correction	Energy (keV/amu)			
n	*l*	*m*		10	20	30	40
1	0	0	with	9.59E-19 (7.29E-21)	1.15E-18 (7.83E-21)	1.41E-18 (8.96E-21)	1.60E-18 (8.57E-21)
			without	5.56E-19 (5.86E-21)	1.26E-18 (9.19E-21)	1.91E-18 (1.16E-20)	2.73E-18 (1.27E-20)
2			with	8.74E-16 (5.72E-19)	7.37E-16 (4.49E-19)	5.40E-16 (3.54E-19)	3.74E-16 (2.52E-19)
			without	8.72E-16 (4.63E-19)	7.15E-16 (3.78E-19)	5.35E-16 (3.14E-19)	3.75E-16 (2.36E-19)
2	0	0	with	2.37E-16 (3.27E-19)	1.28E-16 (2.03E-19)	7.43E-17 (1.38E-19)	4.72E-17 (8.95E-20)
			without	1.17E-16 (1.57E-19)	7.43E-17 (1.14E-19)	5.26E-17 (9.59E-20)	3.75E-17 (7.18E-20)
2	1		with	6.37E-16 (5.00E-19)	6.09E-16 (4.20E-19)	4.66E-16 (3.37E-19)	3.27E-16 (2.41E-19)
			without	7.54E-16 (4.65E-19)	6.41E-16 (3.79E-19)	4.82E-16 (3.09E-19)	3.38E-16 (2.30E-19)
2	1	0	with	2.55E-16 (3.28E-19)	2.44E-16 (2.82E-19)	1.88E-16 (2.25E-19)	1.35E-16 (1.63E-19)
			without	3.03E-16 (3.28E-19)	2.52E-16 (2.63E-19)	2.03E-16 (2.13E-19)	1.49E-16 (1.59E-19)
2	1	1	with	1.91E-16 (2.91E-19)	1.82E-16 (2.47E-19)	1.39E-16 (1.96E-19)	9.60E-17 (1.37E-19)
			without	2.24E-16 (2.71E-19)	1.94E-16 (2.26E-19)	1.40E-16 (1.81E-19)	9.47E-17 (1.30E-19)
3			with	1.27E-15 (7.04E-19)	9.85E-16 (5.66E-19)	6.99E-16 (4.89E-19)	4.85E-16 (3.50E-19)
			without	4.44E-16 (3.55E-19)	5.66E-16 (3.71E-19)	5.26E-16 (3.62E-19)	4.12E-16 (2.92E-19)
3	0	0	with	5.83E-17 (1.38E-19)	4.28E-17 (1.11E-19)	3.37E-17 (9.70E-20)	2.66E-17 (7.15E-20)
			without	4.17E-17 (1.01E-19)	2.81E-17 (7.67E-20)	2.62E-17 (7.00E-20)	2.07E-17 (5.53E-20)
3	1		with	3.49E-16 (3.60E-19)	2.36E-16 (2.71E-19)	1.97E-16 (2.37E-19)	1.55E-16 (1.75E-19)
			without	1.53E-16 (2.01E-19)	1.61E-16 (1.97E-19)	1.82E-16 (1.99E-19)	1.47E-16 (1.58E-19)
3	1	0	with	2.16E-16 (3.08E-19)	1.45E-16 (2.15E-19)	1.17E-16 (1.86E-19)	8.85E-17 (1.36E-19)
			without	8.70E-17 (1.69E-19)	1.03E-16 (1.57E-19)	1.09E-16 (1.56E-19)	8.40E-17 (1.21E-19)
3	1	1	with	6.67E-17 (1.50E-19)	4.54E-17 (1.23E-19)	4.00E-17 (1.09E-19)	3.32E-17 (8.19E-20)
			without	3.29E-17 (8.62E-20)	2.89E-17 (8.80E-20)	3.64E-17 (9.33E-20)	3.17E-17 (7.54E-20)
3	2		with	8.60E-16 (6.70E-19)	7.06E-16 (5.37E-19)	4.68E-16 (4.63E-19)	3.03E-16 (3.32E-19)
			without	2.49E-16 (3.02E-19)	3.77E-16 (3.34E-19)	3.18E-16 (3.32E-19)	2.44E-16 (2.72E-19)
3	2	0	with	3.32E-16 (4.45E-19)	2.68E-16 (3.47E-19)	1.80E-16 (2.98E-19)	1.17E-16 (2.16E-19)
			without	1.10E-16 (2.20E-19)	1.76E-16 (2.34E-19)	1.44E-16 (2.29E-19)	1.09E-16 (1.86E-19)
3	2	1	with	2.39E-16 (3.79E-19)	2.05E-16 (3.09E-19)	1.36E-16 (2.58E-19)	8.80E-17 (1.81E-19)
			without	6.21E-17 (1.53E-19)	9.62E-17 (1.78E-19)	8.16E-17 (1.75E-19)	6.32E-17 (1.42E-19)
3	2	2	with	2.43E-17 (9.95E-20)	1.36E-17 (7.82E-20)	8.43E-18 (6.13E-20)	5.01E-18 (4.10E-20)
			without	7.28E-18 (4.00E-20)	4.23E-18 (3.60E-20)	5.14E-18 (4.10E-20)	4.53E-18 (3.53E-20)

TABLE III. Cross Sections for Electron Capture and statistical error values (in parenthesis) from H(1s) by Li^{3+}

See page 93 for Explanation of Tables

Final state			correction	Energy (keV/amu)			
n	*l*	*m*		10	20	30	40
4			with	1.01E-16 (1.80E-19)	1.48E-16 (2.73E-19)	2.06E-16 (3.02E-19)	2.04E-16 (2.55E-19)
			without	3.69E-17 (8.58E-20)	5.06E-17 (1.25E-19)	1.07E-16 (1.81E-19)	1.44E-16 (1.86E-19)
4	0	0	with	1.08E-17 (5.49E-20)	1.16E-17 (6.55E-20)	1.33E-17 (6.18E-20)	1.25E-17 (5.13E-20)
			without	5.69E-18 (3.39E-20)	9.37E-18 (5.49E-20)	1.33E-17 (5.39E-20)	1.20E-17 (4.39E-20)
4	1		with	4.04E-17 (1.20E-19)	5.72E-17 (1.63E-19)	7.07E-17 (1.56E-19)	6.80E-17 (1.27E-19)
			without	1.48E-17 (5.60E-20)	1.96E-17 (9.02E-20)	4.96E-17 (1.21E-19)	6.38E-17 (1.12E-19)
4	1	0	with	2.56E-17 (1.09E-19)	3.77E-17 (1.34E-19)	4.37E-17 (1.23E-19)	3.97E-17 (9.88E-20)
			without	5.97E-18 (3.94E-20)	1.25E-17 (7.36E-20)	3.19E-17 (9.51E-20)	3.97E-17 (8.80E-20)
4	1	1	with	7.39E-18 (4.37E-20)	9.74E-18 (6.72E-20)	1.35E-17 (6.90E-20)	1.43E-17 (5.75E-20)
			without	4.43E-18 (2.91E-20)	3.53E-18 (3.71E-20)	8.89E-18 (5.34E-20)	1.21E-17 (5.01E-20)
4	2		with	3.30E-17 (1.07E-19)	6.58E-17 (2.00E-19)	1.00E-16 (2.43E-19)	1.00E-16 (2.08E-19)
			without	1.18E-17 (5.01E-20)	1.35E-17 (6.93E-20)	3.88E-17 (1.27E-19)	6.13E-17 (1.51E-19)
4	2	0	with	1.37E-17 (6.98E-20)	2.84E-17 (1.31E-19)	4.29E-17 (1.59E-19)	4.10E-17 (1.35E-19)
			without	3.91E-18 (3.02E-20)	7.03E-18 (4.85E-20)	1.93E-17 (8.84E-20)	2.94E-17 (1.05E-19)
4	2	1	with	8.89E-18 (5.55E-20)	1.83E-17 (1.07E-19)	2.75E-17 (1.28E-19)	2.84E-17 (1.11E-19)
			without	3.40E-18 (2.68E-20)	3.11E-18 (3.49E-20)	9.51E-18 (6.41E-20)	1.51E-17 (7.56E-20)
4	2	2	with	7.19E-19 (1.36E-20)	4.09E-19 (1.41E-20)	1.27E-18 (2.51E-20)	1.33E-18 (2.22E-20)
			without	4.97E-19 (9.39E-21)	8.80E-20 (4.77E-21)	3.08E-19 (1.03E-20)	7.68E-19 (1.52E-20)
4	3		with	1.66E-17 (6.82E-20)	1.32E-17 (8.27E-20)	2.14E-17 (1.26E-19)	2.34E-17 (1.19E-19)
			without	4.60E-18 (2.69E-20)	8.16E-18 (3.74E-20)	4.95E-18 (3.74E-20)	6.86E-18 (5.14E-20)
4	3	0	with	4.48E-18 (3.21E-20)	4.10E-18 (4.60E-20)	7.58E-18 (7.30E-20)	9.45E-18 (7.61E-20)
			without	1.37E-18 (1.44E-20)	3.23E-18 (2.15E-20)	2.29E-18 (2.54E-20)	3.40E-18 (3.64E-20)
4	3	1	with	4.69E-18 (3.72E-20)	3.74E-18 (4.58E-20)	6.08E-18 (6.93E-20)	6.31E-18 (6.22E-20)
			without	1.21E-18 (1.36E-20)	2.11E-18 (2.03E-20)	1.19E-18 (1.90E-20)	1.67E-18 (2.57E-20)
4	3	2	with	1.36E-18 (2.17E-20)	7.74E-19 (1.76E-20)	7.88E-19 (2.18E-20)	6.39E-19 (1.81E-20)
			without	3.95E-19 (8.81E-21)	3.28E-19 (8.24E-21)	1.66E-19 (5.76E-21)	7.86E-20 (4.15E-21)
4	3	3	with	7.97E-20 (5.80E-21)	3.43E-20 (3.74E-21)	1.52E-20 (2.32E-21)	-
			without	2.29E-20 (2.11E-21)	6.55E-21 (1.18E-21)	5.60E-21 (1.02E-21)	-

TABLE III. Cross Sections for Electron Capture and statistical error values (in parenthesis) from H(1s) by Li^{3+}

See page 93 for Explanation of Tables

$$Li^{3+} + H(1s) \rightarrow Li^{2+}(nlm) + H^{+}$$

Final state			correction	Energy (keV/amu)			
n	*l*	*m*		50	60	70	80
1	0	0	with	1.85E-18 (9.01E-21)	2.12E-18 (9.42E-21)	2.29E-18 (8.47E-21)	2.37E-18 (8.32E-21)
			without	3.46E-18 (1.41E-20)	4.05E-18 (1.46E-20)	4.42E-18 (1.46E-20)	4.29E-18 (1.23E-20)
2			with	2.59E-16 (1.96E-19)	1.78E-16 (1.53E-19)	1.29E-16 (1.09E-19)	9.02E-17 (8.54E-20)
			without	2.60E-16 (1.92E-19)	1.83E-16 (1.51E-19)	1.31E-16 (1.19E-19)	9.34E-17 (8.35E-20)
2	0	0	with	3.26E-17 (6.60E-20)	2.27E-17 (4.89E-20)	1.70E-17 (3.36E-20)	1.21E-17 (2.53E-20)
			without	2.73E-17 (5.90E-20)	2.04E-17 (4.68E-20)	1.55E-17 (1.55E-17)	1.19E-17 (2.64E-20)
2	1		with	2.26E-16 (1.89E-19)	1.55E-16 (1.48E-19)	1.12E-16 (1.07E-19)	7.82E-17 (8.43E-20)
			without	2.33E-16 (1.86E-19)	1.62E-16 (1.46E-19)	1.16E-16 (1.15E-19)	8.15E-17 (8.07E-20)
2	1	0	with	9.53E-17 (1.30E-19)	6.65E-17 (1.04E-19)	4.89E-17 (7.67E-20)	3.48E-17 (6.19E-20)
			without	1.07E-16 (1.29E-19)	7.76E-17 (1.03E-19)	5.70E-17 (8.26E-20)	4.14E-17 (5.89E-20)
2	1	1	with	6.53E-17 (1.04E-19)	4.42E-17 (7.91E-20)	3.16E-17 (5.57E-20)	2.17E-17 (4.29E-20)
			without	6.31E-17 (1.02E-19)	4.25E-17 (7.79E-20)	2.93E-17 (5.97E-20)	2.01E-17 (4.08E-20)
3			with	3.27E-16 (2.67E-19)	2.25E-16 (2.05E-19)	1.55E-16 (1.41E-19)	1.08E-16 (1.09E-19)
			without	3.03E-16 (2.47E-19)	2.10E-16 (1.94E-19)	1.44E-16 (1.49E-19)	9.92E-17 (1.02E-19)
3	0	0	with	2.05E-17 (5.62E-20)	1.61E-17 (4.46E-20)	1.21E-17 (3.05E-20)	9.32E-18 (2.39E-20)
			without	1.62E-17 (4.77E-20)	1.27E-17 (3.90E-20)	9.84E-18 (3.13E-20)	7.84E-18 (2.28E-20)
3	1		with	1.14E-16 (1.37E-19)	8.25E-17 (1.08E-19)	5.89E-17 (7.60E-20)	4.29E-17 (6.06E-20)
			without	1.09E-16 (1.32E-19)	7.87E-17 (1.04E-19)	5.62E-17 (8.16E-20)	4.02E-17 (5.73E-20)
3	1	0	with	6.13E-17 (1.03E-19)	4.14E-17 (7.88E-20)	2.78E-17 (5.46E-20)	1.97E-17 (4.37E-20)
			without	6.09E-17 (1.00E-19)	4.34E-17 (7.89E-20)	3.08E-17 (6.21E-20)	2.22E-17 (4.41E-20)
3	1	1	with	2.62E-17 (6.63E-20)	2.06E-17 (5.37E-20)	1.55E-17 (3.84E-20)	1.16E-17 (3.06E-20)
			without	2.43E-17 (6.31E-20)	1.76E-17 (4.95E-20)	1.27E-17 (3.86E-20)	9.03E-18 (2.66E-20)
3	2		with	1.93E-16 (2.55E-19)	1.26E-16 (1.96E-19)	8.39E-17 (1.35E-19)	5.55E-17 (1.03E-19)
			without	1.77E-16 (2.30E-19)	1.19E-16 (1.79E-19)	7.78E-17 (1.38E-19)	5.11E-17 (9.43E-20)
3	2	0	with	7.66E-17 (1.69E-19)	5.21E-17 (1.32E-19)	3.60E-17 (9.15E-20)	2.51E-17 (7.14E-20)
			without	7.83E-17 (1.57E-19)	5.25E-17 (1.22E-19)	3.47E-17 (9.44E-20)	2.29E-17 (6.50E-20)
3	2	1	with	5.53E-17 (1.36E-19)	3.53E-17 (1.03E-19)	2.31E-17 (7.02E-20)	1.47E-17 (5.25E-20)
			without	4.61E-17 (1.19E-19)	3.09E-17 (9.21E-20)	2.01E-17 (7.00E-20)	1.33E-17 (4.78E-20)
3	2	2	with	2.77E-18 (2.89E-20)	1.57E-18 (2.05E-20)	9.17E-19 (1.32E-20)	5.05E-19 (9.22E-21)
			without	3.33E-18 (2.99E-20)	2.23E-18 (2.31E-20)	1.39E-18 (1.71E-20)	8.95E-19 (1.15E-20)

TABLE III. Cross Sections for Electron Capture and statistical error values (in parenthesis) from H(1s) by Li^{3+}

See page 93 for Explanation of Tables

Final State			correction	Energy (keV/amu)			
n	*l*	*m*		50	60	70	80
4			with	1.67E-16 (2.14E-19)	1.22E-16 (1.67E-19)	8.65E-17 (1.15E-19)	6.32E-17 (9.02E-20)
			without	1.39E-16 (1.80E-19)	1.11E-16 (1.51E-19)	8.05E-17 (1.19E-19)	5.77E-17 (8.35E-20)
4	0	0	with	1.10E-17 (4.37E-20)	9.18E-18 (3.52E-20)	7.32E-18 (2.49E-20)	5.73E-18 (1.95E-20)
			without	1.00E-17 (3.86E-20)	7.95E-18 (3.19E-20)	6.10E-18 (2.54E-20)	4.87E-18 (1.85E-20)
4	1		with	5.67E-17 (1.06E-19)	4.31E-17 (8.50E-20)	3.17E-17 (6.05E-20)	2.40E-17 (4.89E-20)
			without	5.62E-17 (1.01E-19)	4.27E-17 (8.15E-20)	3.10E-17 (6.43E-20)	2.25E-17 (4.54E-20)
4	1	0	with	3.15E-17 (8.18E-20)	2.21E-17 (6.32E-20)	1.53E-17 (4.41E-20)	1.11E-17 (3.55E-20)
			without	3.34E-17 (7.82E-20)	2.45E-17 (6.27E-20)	1.74E-17 (4.95E-20)	1.25E-17 (3.50E-20)
4	1	1	with	1.26E-17 (4.92E-20)	1.05E-17 (4.10E-20)	8.23E-18 (2.98E-20)	6.43E-18 (2.44E-20)
			without	1.14E-17 (4.58E-20)	9.08E-18 (3.74E-20)	6.77E-18 (2.95E-20)	5.00E-18 (2.07E-20)
4	2		with	8.19E-17 (1.78E-19)	5.90E-17 (1.42E-19)	4.20E-17 (1.01E-19)	3.06E-17 (8.05E-20)
			without	6.50E-17 (1.52E-19)	5.36E-17 (1.29E-19)	3.89E-17 (1.03E-19)	2.75E-17 (7.29E-20)
4	2	0	with	3.33E-17 (1.17E-19)	2.45E-17 (9.49E-20)	1.81E-17 (6.77E-20)	1.39E-17 (5.55E-20)
			without	3.07E-17 (1.06E-19)	2.47E-17 (8.92E-20)	1.77E-17 (7.11E-20)	1.25E-17 (5.02E-20)
4	2	1	with	2.34E-17 (9.43E-20)	1.65E-17 (7.42E-20)	1.15E-17 (5.22E-20)	8.09E-18 (4.10E-20)
			without	1.63E-17 (7.63E-20)	1.36E-17 (6.51E-20)	9.99E-18 (5.21E-20)	7.13E-18 (3.69E-20)
4	2	2	with	1.06E-18 (1.86E-20)	7.10E-19 (1.42E-20)	4.52E-19 (9.53E-21)	2.63E-19 (6.78E-21)
			without	9.22E-19 (1.65E-20)	8.10E-19 (1.45E-20)	6.00E-19 (1.16E-20)	4.20E-19 (8.13E-21)
4	3		with	1.74E-17 (9.77E-20)	1.06E-17 (7.19E-20)	5.51E-18 (4.34E-20)	2.85E-18 (2.94E-20)
			without	7.65E-18 (5.80E-20)	6.49E-18 (5.17E-20)	4.56E-18 (4.11E-20)	2.90E-18 (2.76E-20)
4	3	0	with	7.72E-18 (6.58E-20)	4.91E-18 (4.94E-20)	2.63E-18 (3.03E-20)	1.45E-18 (2.12E-20)
			without	3.75E-18 (4.08E-20)	3.19E-18 (3.65E-20)	2.25E-18 (2.91E-20)	1.44E-18 (1.96E-20)
4	3	1	with	4.48E-18 (4.95E-20)	2.67E-18 (3.60E-20)	1.33E-18 (2.13E-20)	6.80E-19 (1.43E-20)
			without	1.88E-18 (2.89E-20)	1.59E-18 (2.55E-20)	1.11E-18 (2.02E-20)	7.31E-19 (1.38E-20)
4	3	2	with	3.57E-19 (1.29E-20)	1.63E-19 (8.31E-21)	7.72E-20 (4.76E-21)	2.68E-20 (2.67E-21)
			without	7.45E-20 (4.96E-21)	6.11E-20 (4.58E-21)	3.83E-20 (3.51E-21)	1.90E-20 (2.04E-21)
4	3	3	with	-	-	-	-
			without	-	-	-	-

TABLE III. Cross Sections for Electron Capture and statistical error values (in parenthesis) from H(1s) by Li^{3+}

See page 93 for Explanation of Tables

$$Li^{3+} + H(1s) \rightarrow Li^{2+}(nlm) + H^{+}$$

Final state			correction	Energy (keV/amu)			
n	*l*	*m*		90	100	150	200
1	0	0	with	2.37E-18 (7.95E-21)	2.31E-18 (7.45E-21)	1.78E-18 (4.29E-21)	1.31E-18 (3.03E-21)
			without	4.26E-18 (1.15E-20)	3.83E-18 (1.04E-20)	2.34E-18 (5.85E-21)	1.33E-18 (3.30E-21)
2			with	6.57E-17 (6.83E-20)	4.97E-17 (5.59E-20)	1.26E-17 (1.80E-20)	4.18E-18 (8.18E-21)
			without	6.94E-17 (6.56E-20)	5.59E-20 (5.20E-20)	1.43E-17 (1.86E-20)	5.11E-18 (8.09E-21)
2	0	0	with	8.96E-18 (1.97E-20)	6.82E-18 (1.58E-20)	1.73E-18 (4.97E-21)	5.79E-19 (2.40E-21)
			without	9.47E-18 (2.10E-20)	7.41E-18 (1.70E-20)	2.61E-18 (6.52E-21)	1.08E-18 (3.03E-21)
2	1		with	5.67E-17 (6.79E-20)	4.29E-17 (5.59E-20)	1.09E-17 (1.80E-20)	3.61E-18 (8.01E-21)
			without	6.00E-17 (6.33E-20)	4.33E-17 (5.02E-20)	1.17E-17 (1.79E-20)	4.03E-18 (7.77E-21)
2	1	0	with	2.57E-17 (5.06E-20)	2.00E-17 (4.24E-20)	5.79E-18 (1.41E-20)	2.11E-18 (6.37E-21)
			without	3.12E-17 (4.68E-20)	2.30E-17 (3.76E-20)	6.66E-18 (1.39E-20)	2.41E-18 (6.20E-21)
2	1	1	with	1.55E-17 (3.39E-20)	1.15E-17 (2.74E-20)	2.55E-18 (8.19E-21)	7.44E-19 (3.49E-21)
			without	1.44E-17 (3.13E-20)	1.02E-17 (2.44E-20)	2.51E-18 (8.10E-21)	8.11E-19 (3.37E-21)
3			with	7.58E-17 (8.44E-20)	5.52E-17 (6.67E-20)	1.14E-17 (1.85E-20)	3.26E-18 (7.89E-21)
			without	6.94E-17 (7.74E-20)	4.89E-17 (5.97E-20)	1.09E-17 (1.81E-20)	3.33E-18 (7.13E-21)
3	0	0	with	7.01E-18 (1.86E-20)	5.36E-18 (1.48E-20)	1.33E-18 (4.41E-21)	3.98E-19 (2.00E-21)
			without	6.24E-18 (1.82E-20)	4.89E-18 (1.46E-20)	1.57E-18 (5.25E-21)	6.01E-19 (2.34E-21)
3	1		with	3.11E-17 (4.83E-20)	2.36E-17 (3.93E-20)	6.07E-18 (1.30E-20)	2.08E-18 (6.31E-21)
			without	2.94E-17 (4.45E-20)	2.15E-17 (3.53E-20)	5.63E-18 (1.22E-20)	1.92E-18 (5.39E-21)
3	1	0	with	1.40E-17 (3.48E-20)	1.05E-17 (2.85E-20)	2.90E-18 (9.85E-21)	1.13E-18 (4.97E-21)
			without	1.64E-17 (3.46E-20)	1.20E-17 (2.77E-20)	3.25E-18 (9.69E-21)	1.13E-18 (4.32E-21)
3	1	1	with	8.63E-18 (2.45E-20)	6.50E-18 (1.98E-20)	1.58E-18 (6.18E-21)	4.66E-19 (2.80E-21)
			without	6.49E-18 (2.03E-20)	4.75E-18 (1.59E-20)	1.19E-18 (5.34E-21)	3.92E-19 (2.33E-21)
3	2		with	3.76E-17 (7.97E-20)	2.63E-17 (6.25E-20)	4.03E-18 (1.53E-20)	7.90E-19 (5.27E-21)
			without	3.38E-17 (7.07E-20)	2.24E-17 (5.42E-20)	3.73E-18 (1.51E-20)	8.09E-19 (5.18E-21)
3	2	0	with	1.75E-17 (5.61E-20)	1.26E-17 (4.46E-20)	2.10E-18 (1.13E-20)	4.60E-19 (4.08E-21)
			without	1.53E-17 (4.89E-20)	1.03E-17 (3.77E-20)	1.82E-18 (1.08E-20)	4.28E-19 (3.84E-21)
3	2	1	with	9.76E-18 (4.01E-20)	6.69E-18 (3.10E-20)	9.51E-19 (7.29E-21)	1.67E-19 (2.38E-21)
			without	8.64E-18 (3.54E-20)	5.75E-18 (2.72E-20)	9.17E-19 (7.39E-21)	1.85E-19 (2.43E-21)
3	2	2	with	2.90E-19 (6.59E-21)	1.62E-19 (4.60E-21)	7.25E-21 (6.04E-22)	-
			without	5.44E-19 (8.24E-21)	3.44E-19 (6.11E-21)	3.32E-20 (1.26E-21)	-

TABLE III. Cross Sections for Electron Capture and statistical error values (in parenthesis) from H(1s) by Li^{3+}

See page 93 for Explanation of Tables

Final State			correction	Energy (keV/amu)			
n	*l*	*m*		90	100	150	200
4			with	4.52E-17 (7.00E-20)	3.33E-17 (5.54E-20)	6.85E-18 (1.48E-20)	1.89E-18 (6.17E-21)
			without	4.09E-17 (6.34E-20)	2.89E-17 (4.90E-20)	6.24E-18 (1.42E-20)	1.79E-18 (5.39E-21)
4	0	0	with	4.34E-18 (1.51E-20)	3.28E-18 (1.20E-20)	8.18E-19 (3.55E-21)	2.35E-19 (1.54E-21)
			without	3.83E-18 (1.46E-20)	2.98E-18 (1.18E-20)	9.13E-19 (4.10E-21)	3.33E-19 (1.78E-21)
4	1		with	1.77E-17 (3.91E-20)	1.34E-17 (3.15E-20)	3.49E-18 (1.01E-20)	1.17E-18 (4.87E-21)
			without	1.65E-17 (3.53E-20)	1.20E-17 (2.79E-20)	3.03E-18 (9.21E-21)	9.78E-19 (3.94E-21)
4	1	0	with	8.18E-18 (2.85E-20)	6.13E-18 (2.29E-20)	1.68E-18 (7.62E-21)	6.38E-19 (3.86E-21)
			without	9.20E-18 (2.76E-20)	6.69E-18 (2.20E-20)	1.74E-18 (7.39E-21)	5.75E-19 (3.18E-21)
4	1	1	with	4.75E-18 (1.93E-20)	3.65E-18 (1.57E-20)	8.97E-19 (4.78E-21)	2.65E-19 (2.15E-21)
			without	3.62E-18 (1.58E-20)	2.65E-18 (1.24E-20)	6.40E-19 (3.96E-21)	2.03E-19 (1.68E-21)
4	2		with	2.17E-17 (6.36E-20)	1.58E-17 (5.10E-20)	2.54E-18 (1.28E-20)	4.85E-19 (4.34E-21)
			without	1.89E-17 (5.56E-20)	1.30E-17 (4.33E-20)	2.27E-18 (1.23E-20)	4.79E-19 (4.12E-21)
4	2	0	with	1.02E-17 (4.44E-20)	7.57E-18 (3.60E-20)	1.36E-18 (9.53E-21)	2.89E-19 (3.40E-21)
			without	8.69E-18 (3.87E-20)	6.04E-18 (3.02E-20)	1.11E-18 (8.83E-21)	2.48E-19 (3.02E-21)
4	2	1	with	5.63E-18 (3.20E-20)	4.02E-18 (2.54E-20)	5.82E-19 (6.01E-21)	9.81E-20 (1.92E-21)
			without	4.84E-18 (2.79E-20)	3.30E-18 (2.16E-20)	5.59E-19 (6.02E-21)	1.13E-19 (1.97E-21)
4	2	2	with	1.62E-19 (5.01E-21)	1.09E-19 (3.87E-21)	5.56E-21 (5.42E-22)	-
			without	2.66E-19 (5.87E-21)	1.81E-19 (4.56E-21)	2.04E-20 (1.01E-21)	-
4	3		with	1.44E-18 (1.97E-20)	7.89E-19 (1.37E-20)	3.15E-21 (5.32E-22)	-
			without	1.68E-18 (1.93E-20)	9.71E-19 (1.38E-20)	2.80E-20 (1.56E-21)	-
4	3	0	with	7.51E-19 (1.44E-20)	4.24E-19 (1.01E-20)	-	-
			without	8.84E-19 (1.41E-20)	5.18E-19 (1.01E-20)	-	-
4	3	1	with	3.32E-19 (9.39E-21)	1.78E-19 (6.46E-21)	-	-
			without	3.91E-19 (9.24E-21)	2.25E-19 (6.57E-21)	-	-
4	3	2	with	-	-	-	-
			without	-	-	-	-
4	3	3	with	-	-	-	-
			without	-	-	-	-

TABLE IV. Cross Sections for Electron Capture and statistical error values (in parenthesis) from H(1s) by Be^{4+}

See page 93 for Explanation of Tables

$Be^{4+} + H(1s) \rightarrow Be^{3+}(nlm) + H^{+}$

Final state			correction	Energy (keV/amu)			
n	*l*	*m*		10	20	30	40
1	0	0	with	2.57E-19 (3.37E-21)	3.59E-19 (4.10E-21)	4.17E-19 (4.40E-21)	4.41E-19 (3.91E-21)
			without	3.48E-20 (1.96E-21)	6.57E-20 (1.88E-21)	1.09E-19 (2.39E-21)	1.61E-19 (2.68E-21)
2			with	1.10E-16 (2.14E-19)	1.32E-16 (2.29E-19)	1.48E-16 (2.10E-19)	1.31E-16 (1.61E-19)
			without	1.46E-16 (1.81E-19)	1.66E-16 (1.97E-19)	1.79E-16 (1.93E-19)	1.61E-16 (1.62E-19)
2	0	0	with	4.46E-17 (1.53E-19)	4.42E-17 (1.47E-19)	3.29E-17 (1.11E-19)	2.25E-17 (7.26E-20)
			without	3.91E-17 (9.18E-20)	3.59E-17 (9.37E-20)	3.26E-17 (8.78E-20)	2.48E-17 (6.84E-20)
2	1		with	6.51E-17 (1.55E-19)	8.74E-17 (1.81E-19)	1.15E-16 (1.82E-19)	1.09E-16 (1.46E-19)
			without	1.07E-16 (1.59E-19)	1.31E-16 (1.76E-19)	1.47E-16 (1.75E-19)	1.36E-16 (1.49E-19)
2	1	0	with	2.13E-17 (8.23E-20)	2.76E-17 (9.74E-20)	3.44E-17 (9.49E-20)	3.33E-17 (7.55E-20)
			without	3.52E-17 (9.00E-20)	3.04E-17 (1.10E-19)	4.51E-17 (9.17E-20)	4.57E-17 (8.13E-20)
2	1	1	with	2.23E-17 (9.58E-20)	3.04E-17 (1.10E-19)	4.03E-17 (1.12E-19)	3.78E-17 (9.07E-20)
			without	3.59E-17 (9.51E-20)	4.68E-17 (1.10E-19)	5.16E-17 (1.11E-19)	4.53E-17 (9.27E-20)
3			with	2.25E-15 (1.08E-18)	1.74E-15 (8.19E-19)	1.14E-15 (6.53E-19)	7.59E-16 (4.58E-19)
			without	1.57E-15 (6.60E-19)	1.45E-15 (5.81E-19)	1.06E-15 (5.18E-19)	7.31E-16 (4.04E-19)
3	0	0	with	1.62E-16 (3.30E-19)	7.08E-17 (1.86E-19)	4.15E-17 (1.24E-19)	2.78E-17 (8.10E-20)
			without	6.83E-17 (1.31E-19)	3.18E-17 (8.23E-20)	2.40E-17 (7.22E-20)	1.80E-17 (5.70E-20)
3	1		with	4.66E-16 (5.04E-19)	2.96E-16 (3.48E-19)	2.03E-16 (2.67E-19)	1.46E-16 (1.83E-19)
			without	3.39E-16 (3.16E-19)	2.87E-16 (2.67E-19)	2.16E-16 (2.29E-19)	1.54E-16 (1.71E-19)
3	1	0	with	2.23E-16 (3.55E-19)	1.59E-16 (2.55E-19)	1.13E-16 (2.01E-19)	8.11E-17 (1.39E-19)
			without	1.83E-16 (2.52E-19)	1.67E-16 (2.08E-19)	1.20E-16 (1.73E-19)	8.31E-17 (1.27E-19)
3	1	1	with	1.21E-16 (2.67E-19)	6.87E-17 (1.75E-19)	4.50E-17 (1.29E-19)	3.25E-17 (8.75E-20)
			without	7.82E-17 (1.49E-19)	5.97E-17 (1.28E-19)	4.79E-17 (1.12E-19)	3.56E-17 (8.44E-20)
3	2		with	1.62E-15 (1.03E-18)	1.37E-15 (7.97E-19)	9.00E-16 (6.31E-19)	5.86E-16 (4.44E-19)
			without	1.17E-15 (6.69E-19)	1.13E-15 (5.95E-19)	8.17E-16 (5.15E-19)	5.59E-16 (3.96E-19)
3	2	0	with	5.48E-16 (6.38E-19)	4.54E-16 (4.90E-19)	3.01E-16 (3.79E-19)	1.99E-16 (2.68E-19)
			without	3.88E-16 (4.40E-19)	3.94E-16 (3.89E-19)	2.91E-16 (3.26E-19)	2.04E-16 (2.48E-19)
3	2	1	with	4.24E-16 (5.84E-19)	3.94E-16 (4.74E-19)	2.68E-16 (3.72E-19)	1.77E-16 (2.58E-19)
			without	3.11E-16 (3.86E-19)	3.08E-16 (3.51E-19)	2.23E-16 (2.96E-19)	1.52E-16 (2.22E-19)
3	2	2	with	1.13E-16 (2.90E-19)	6.48E-17 (2.04E-19)	3.16E-17 (1.34E-19)	1.63E-17 (7.99E-20)
			without	7.74E-17 (1.74E-19)	6.04E-17 (1.56E-19)	4.03E-17 (1.26E-19)	2.56E-17 (9.00E-20)

TABLE IV. Cross Sections for Electron Capture and statistical error values (in parenthesis) from H(1s) by Be^{4+}

See page 93 for Explanation of Tables

Final state			correction	Energy (keV/amu)			
n	*l*	*m*		10	20	30	40
4			with	7.81E-16 (6.74E-19)	7.06E-16 (6.67E-19)	6.73E-16 (6.15E-19)	5.43E-16 (4.61E-19)
			without	1.54E-16 (2.03E-19)	2.04E-16 (2.92E-19)	3.67E-16 (3.69E-19)	4.03E-16 (3.42E-19)
4	0	0	with	2.51E-17 (1.06E-19)	1.94E-17 (9.10E-20)	1.83E-17 (8.59E-20)	1.47E-17 (6.42E-20)
			without	1.72E-17 (6.51E-20)	9.07E-18 (6.38E-20)	1.10E-17 (5.03E-20)	1.05E-17 (4.34E-20)
4	1		with	1.17E-16 (2.44E-19)	8.19E-17 (2.06E-19)	8.26E-17 (1.81E-19)	7.31E-17 (1.38E-19)
			without	4.27E-17 (1.04E-19)	3.55E-17 (1.30E-19)	7.06E-17 (1.36E-19)	7.74E-17 (1.20E-19)
4	1	0	with	7.94E-17 (2.18E-19)	5.69E-17 (1.71E-19)	5.47E-17 (1.48E-19)	4.74E-17 (1.13E-19)
			without	2.50E-17 (9.04E-20)	2.32E-17 (1.05E-19)	4.92E-17 (1.12E-19)	4.98E-17 (9.62E-20)
4	1	1	with	1.90E-17 (8.66E-20)	1.26E-17 (8.29E-20)	1.40E-17 (7.45E-20)	1.28E-17 (5.69E-20)
			without	8.79E-18 (4.12E-20)	6.14E-18 (5.42E-20)	1.08E-17 (5.59E-20)	1.38E-17 (5.22E-20)
4	2		with	2.37E-16 (3.64E-19)	2.45E-16 (3.73E-19)	2.36E-16 (3.44E-19)	1.94E-16 (2.63E-19)
			without	5.55E-17 (1.30E-19)	7.77E-17 (1.89E-19)	1.51E-16 (2.42E-19)	1.61E-16 (2.23E-19)
4	2	0	with	1.16E-16 (2.62E-19)	1.13E-16 (2.47E-19)	1.06E-16 (2.30E-19)	8.42E-17 (1.73E-19)
			without	2.44E-17 (9.17E-20)	3.82E-17 (1.26E-19)	6.97E-17 (1.60E-19)	7.08E-17 (1.46E-19)
4	2	1	with	5.76E-17 (1.79E-19)	6.39E-17 (2.00E-19)	6.23E-17 (1.83E-19)	5.27E-17 (1.40E-19)
			without	1.45E-17 (6.48E-20)	1.87E-17 (9.92E-20)	3.80E-17 (1.27E-19)	4.15E-17 (1.17E-19)
4	2	2	with	3.05E-18 (3.89E-20)	2.00E-18 (3.78E-20)	2.78E-18 (3.87E-20)	2.49E-18 (3.02E-20)
			without	1.08E-18 (1.58E-20)	9.64E-19 (2.25E-20)	2.48E-18 (3.33E-20)	3.52E-18 (3.37E-20)
4	3		with	4.01E-16 (5.58E-19)	3.60E-16 (5.64E-19)	3.36E-16 (5.42E-19)	2.61E-16 (4.08E-19)
			without	3.82E-17 (1.08E-19)	8.14E-17 (1.78E-19)	1.35E-16 (2.89E-19)	1.55E-16 (2.85E-19)
4	3	0	with	1.42E-16 (3.39E-19)	1.19E-16 (3.27E-19)	1.12E-16 (3.13E-19)	8.71E-17 (2.39E-19)
			without	1.21E-17 (6.27E-20)	3.38E-17 (1.11E-19)	5.48E-17 (1.86E-19)	6.04E-17 (1.80E-19)
4	3	1	with	1.09E-16 (3.01E-19)	9.86E-17 (3.02E-19)	9.22E-17 (2.92E-19)	7.25E-17 (2.18E-19)
			without	1.02E-17 (5.60E-20)	2.08E-17 (9.41E-20)	3.46E-17 (1.49E-19)	3.99E-17 (1.46E-19)
4	3	2	with	2.03E-17 (1.17E-19)	2.14E-17 (1.38E-19)	1.94E-17 (1.30E-19)	1.42E-17 (9.46E-20)
			without	2.66E-18 (2.67E-20)	2.93E-18 (3.42E-20)	5.39E-18 (5.49E-20)	7.32E-18 (5.99E-20)
4	3	3	with	8.72E-19 (2.36E-20)	1.81E-19 (1.01E-20)	9.21E-20 (6.79E-21)	6.81E-20 (5.35E-21)
			without	2.81E-19 (9.01E-21)	5.41E-20 (3.74E-21)	2.96E-20 (2.62E-21)	1.82E-20 (1.77E-21)

TABLE IV. Cross Sections for Electron Capture and statistical error values (in parenthesis) from H(1s) by Be^{4+}

See page 93 for Explanation of Tables

Final state			correction	Energy (keV/amu)			
n	*l*	*m*		10	20	30	40
5			with	8.13E-17 (1.91E-19)	1.31E-16 (3.39E-19)	2.14E-16 (3.78E-19)	2.46E-16 (3.33E-19)
			without	2.75E-17 (7.58E-20)	3.46E-17 (1.25E-19)	8.10E-17 (1.96E-19)	1.44E-16 (2.16E-19)
5	0	0	with	7.03E-18 (5.02E-20)	6.30E-18 (6.65E-20)	7.80E-18 (5.68E-20)	7.81E-18 (4.76E-20)
			without	4.20E-18 (2.83E-20)	4.19E-18 (4.71E-20)	5.21E-18 (4.08E-20)	6.12E-18 (3.36E-20)
5	1		with	2.47E-17 (1.07E-19)	2.77E-17 (1.46E-19)	3.58E-17 (1.25E-19)	3.73E-17 (1.01E-19)
			without	8.00E-18 (4.01E-20)	1.03E-17 (7.82E-20)	2.00E-17 (9.22E-20)	3.56E-17 (8.54E-20)
5	1	0	with	1.67E-17 (1.01E-19)	2.09E-17 (1.27E-19)	2.59E-17 (1.06E-19)	2.52E-17 (8.43E-20)
			without	4.43E-18 (3.39E-20)	7.08E-18 (6.66E-20)	1.29E-17 (7.48E-20)	2.48E-17 (7.03E-20)
5	1	1	with	3.98E-18 (3.52E-20)	3.46E-18 (5.20E-20)	4.95E-18 (4.71E-20)	6.05E-18 (4.00E-20)
			without	1.80E-18 (1.69E-20)	1.65E-18 (2.98E-20)	3.52E-18 (3.81E-20)	5.37E-18 (3.46E-20)
5	2		with	2.33E-17 (1.11E-19)	4.85E-17 (2.09E-19)	7.53E-17 (2.19E-19)	8.30E-17 (1.85E-19)
			without	7.75E-18 (4.32E-20)	1.04E-17 (7.91E-20)	3.42E-17 (1.35E-19)	5.69E-17 (1.49E-19)
5	2	0	with	1.18E-17 (8.15E-20)	2.45E-17 (1.48E-19)	3.56E-17 (1.49E-19)	3.81E-17 (1.25E-19)
			without	3.33E-18 (2.96E-20)	5.36E-18 (5.61E-20)	1.60E-17 (9.03E-20)	2.63E-17 (1.01E-19)
5	2	1	with	5.32E-18 (5.19E-20)	1.19E-17 (1.05E-19)	1.93E-17 (1.13E-19)	2.16E-17 (9.61E-20)
			without	1.97E-18 (2.12E-20)	2.47E-18 (3.93E-20)	8.77E-18 (7.01E-20)	1.44E-17 (7.63E-20)
5	2	2	with	2.72E-19 (9.67E-21)	1.14E-19 (8.83E-21)	4.86E-19 (1.70E-20)	7.88E-19 (1.76E-20)
			without	2.40E-19 (7.01E-21)	6.29E-20 (5.10E-21)	3.47E-19 (1.31E-20)	1.02E-18 (1.90E-20)
5	3		with	1.64E-17 (8.76E-20)	4.17E-17 (2.10E-19)	8.16E-17 (2.84E-19)	9.92E-17 (2.61E-19)
			without	5.48E-18 (3.55E-20)	5.53E-18 (4.92E-20)	2.01E-17 (1.08E-19)	4.35E-17 (1.56E-19)
5	3	0	with	5.83E-18 (4.89E-20)	1.49E-17 (1.26E-19)	2.85E-17 (1.68E-19)	3.44E-17 (1.53E-19)
			without	1.74E-18 (1.98E-20)	2.50E-18 (3.14E-20)	8.77E-18 (7.02E-20)	1.83E-17 (1.02E-19)
5	3	1	with	4.78E-18 (4.88E-20)	1.24E-17 (1.16E-19)	2.26E-17 (1.51E-19)	2.76E-17 (1.40E-19)
			without	1.57E-18 (1.89E-20)	1.36E-18 (2.56E-20)	5.10E-18 (5.56E-20)	1.11E-17 (7.94E-20)
5	3	2	with	4.88E-19 (1.76E-20)	1.06E-18 (3.17E-20)	3.93E-18 (5.97E-20)	4.89E-18 (5.67E-20)
			without	2.57E-19 (8.01E-21)	1.30E-19 (7.95E-21)	5.83E-19 (1.70E-20)	1.40E-18 (2.64E-20)
5	3	3	with	5.22E-20 (5.27E-21)	1.34E-20 (2.69E-21)	1.24E-20 (2.30E-21)	-
			without	5.88E-20 (4.15E-21)	1.27E-20 (1.79E-21)	6.55E-21 (1.20E-21)	-
5	4		with	9.78E-18 (5.98E-20)	6.24E-18 (6.65E-20)	1.36E-17 (1.24E-19)	1.89E-17 (1.31E-19)
			without	2.09E-18 (1.85E-20)	4.14E-18 (2.84E-20)	1.51E-18 (2.07E-20)	2.30E-18 (3.38E-20)
5	4	0	with	2.42E-18 (2.49E-20)	1.60E-18 (3.32E-20)	4.08E-18 (6.57E-20)	6.21E-18 (7.56E-20)
			without	5.57E-19 (8.85E-21)	1.41E-18 (1.48E-20)	6.07E-19 (1.32E-20)	1.16E-18 (2.44E-20)
5	4	1	with	2.70E-18 (3.31E-20)	1.62E-18 (3.56E-20)	3.68E-18 (6.69E-20)	5.10E-18 (6.86E-20)
			without	5.51E-19 (9.48E-21)	1.03E-18 (1.50E-20)	3.59E-19 (1.05E-20)	5.40E-19 (1.66E-20)
5	4	2	with	8.98E-19 (2.09E-20)	6.92E-19 (2.06E-20)	1.14E-18 (3.53E-20)	1.12E-18 (3.07E-20)
			without	1.95E-19 (6.35E-21)	3.12E-19 (8.78E-21)	8.13E-20 (4.35E-21)	3.55E-20 (3.12E-21)
5	4	3	with	-	6.35E-20 (5.87E-21)	2.41E-20 (3.37E-21)	1.05E-20 (2.15E-21)
			without	-	3.19E-20 (2.88E-21)	1.80E-20 (2.09E-21)	3.52E-21 (8.08E-22)
5	4	4	with	-	-	-	-
			without	-	-	-	-

TABLE IV. Cross Sections for Electron Capture and statistical error values (in parenthesis) from H(1s) by Be^{4+}

See page 93 for Explanation of Tables

$Be^{4+} + H(1s) \rightarrow Be^{3+}(nlm) + H^{+}$

Final state			correction	Energy (keV/amu)			
n	*l*	*m*		50	60	70	80
1	0	0	with	4.50E-19 (3.87E-21)	4.76E-19 (3.72E-21)	6.47E-19 (4.21E-21)	5.61E-19 (3.39E-21)
			without	2.29E-19 (3.18E-21)	3.07E-19 (3.54E-21)	3.91E-19 (3.86E-21)	4.93E-19 (4.18E-21)
2			with	1.07E-16 (1.40E-19)	8.46E-17 (1.15E-19)	8.40E-17 (1.09E-19)	5.26E-17 (7.34E-20)
			without	1.33E-16 (1.44E-19)	1.07E-16 (1.22E-19)	8.52E-17 (1.02E-19)	6.85E-17 (8.60E-20)
2	0	0	with	1.59E-17 (5.58E-20)	1.17E-17 (4.18E-20)	1.11E-17 (3.70E-20)	6.80E-18 (2.36E-20)
			without	1.86E-17 (5.69E-20)	1.40E-17 (4.54E-20)	1.07E-17 (3.67E-20)	8.52E-18 (3.01E-20)
2	1		with	9.12E-17 (1.30E-19)	7.29E-17 (1.08E-19)	7.29E-17 (1.03E-19)	4.58E-17 (7.01E-20)
			without	1.14E-16 (1.33E-19)	9.31E-17 (1.14E-19)	7.45E-17 (9.61E-20)	5.99E-17 (8.11E-20)
2	1	0	with	2.84E-17 (6.84E-20)	2.33E-17 (5.82E-20)	2.40E-17 (5.74E-20)	1.54E-17 (3.99E-20)
			without	4.11E-17 (7.53E-20)	3.51E-17 (6.61E-20)	2.97E-17 (5.74E-20)	2.50E-17 (4.97E-20)
2	1	1	with	3.14E-17 (8.01E-20)	2.48E-17 (6.58E-20)	2.44E-17 (6.18E-20)	1.52E-17 (4.14E-20)
			without	3.66E-17 (8.13E-20)	2.91E-17 (6.85E-20)	2.23E-17 (5.65E-20)	1.75E-17 (4.68E-20)
3			with	5.14E-16 (3.70E-19)	3.51E-16 (2.81E-19)	3.06E-16 (2.44E-19)	1.74E-16 (1.57E-19)
			without	5.01E-16 (3.36E-19)	3.46E-16 (2.66E-19)	2.42E-16 (2.11E-19)	1.73E-16 (1.67E-19)
3	0	0	with	1.97E-17 (6.42E-20)	1.41E-17 (4.83E-20)	1.31E-17 (4.26E-20)	7.92E-18 (2.71E-20)
			without	1.35E-17 (4.82E-20)	1.02E-17 (3.91E-20)	7.97E-18 (3.26E-20)	6.28E-18 (2.68E-20)
3	1		with	1.09E-16 (1.48E-19)	8.13E-17 (1.14E-19)	7.66E-17 (1.01E-19)	4.61E-17 (6.53E-20)
			without	1.08E-16 (1.38E-19)	7.69E-17 (1.09E-19)	5.60E-17 (8.66E-20)	4.22E-17 (6.98E-20)
3	1	0	with	6.02E-17 (1.12E-19)	4.44E-17 (8.55E-20)	4.08E-17 (7.46E-20)	2.38E-17 (4.69E-20)
			without	5.74E-17 (1.02E-19)	4.10E-17 (8.05E-20)	3.01E-17 (6.41E-20)	2.30E-17 (5.20E-20)
3	1	1	with	2.44E-17 (7.08E-20)	1.84E-17 (5.49E-20)	1.79E-17 (5.00E-20)	1.12E-17 (3.28E-20)
			without	2.52E-17 (6.81E-20)	1.80E-17 (5.34E-20)	1.30E-17 (4.23E-20)	9.64E-18 (3.37E-20)
3	2		with	3.85E-16 (3.59E-19)	2.55E-16 (2.74E-19)	2.17E-16 (2.42E-19)	1.20E-16 (1.56E-19)
			without	3.80E-16 (3.26E-19)	2.59E-16 (2.57E-19)	1.78E-16 (2.03E-19)	1.24E-16 (1.61E-19)
3	2	0	with	1.32E-16 (2.18E-19)	8.87E-17 (1.70E-19)	7.66E-17 (1.54E-19)	4.36E-17 (1.02E-19)
			without	1.42E-16 (2.03E-19)	9.83E-17 (1.61E-19)	6.88E-17 (1.28E-19)	4.88E-17 (1.02E-19)
3	2	1	with	1.18E-16 (2.05E-19)	7.83E-17 (1.54E-19)	6.60E-17 (1.34E-19)	3.62E-17 (8.42E-20)
			without	1.03E-16 (1.79E-19)	7.02E-17 (1.40E-19)	4.84E-17 (1.09E-19)	3.35E-17 (8.55E-20)
3	2	2	with	8.74E-18 (5.60E-20)	4.96E-18 (3.84E-20)	3.91E-18 (3.21E-20)	2.07E-18 (1.97E-20)
			without	1.60E-17 (6.93E-20)	1.00E-17 (5.19E-20)	6.39E-18 (3.90E-20)	4.14E-18 (2.95E-20)

TABLE IV. Cross Sections for Electron Capture and statistical error values (in parenthesis) from H(1s) by Be^{4+}

See page 93 for Explanation of Tables

Final State			correction	Energy (keV/amu)			
n	*l*	*m*		50	60	70	80
4			with	4.03E-16 (3.80E-19)	2.89E-16 (2.92E-19)	2.56E-16 (2.53E-19)	1.48E-16 (1.62E-19)
			without	3.45E-16 (3.12E-19)	2.64E-16 (2.59E-19)	1.94E-16 (2.09E-19)	1.40E-16 (1.66E-19)
4	0	0	with	1.17E-17 (5.31E-20)	9.30E-18 (4.20E-20)	8.98E-18 (3.78E-20)	5.64E-18 (2.45E-20)
			without	8.39E-18 (3.83E-20)	6.74E-18 (3.25E-20)	5.28E-18 (2.71E-20)	4.17E-18 (2.24E-20)
4	1		with	6.09E-17 (1.19E-19)	4.92E-17 (9.51E-20)	4.87E-17 (8.63E-20)	3.08E-17 (5.65E-20)
			without	6.22E-17 (1.05E-19)	4.63E-17 (8.55E-20)	3.47E-17 (6.95E-20)	2.64E-17 (5.67E-20)
4	1	0	with	3.89E-17 (9.67E-20)	3.07E-17 (7.68E-20)	2.95E-17 (6.82E-20)	1.78E-17 (4.34E-20)
			without	3.79E-17 (8.24E-20)	2.74E-17 (6.64E-20)	2.03E-17 (5.38E-20)	1.54E-17 (4.39E-20)
4	1	1	with	1.10E-17 (4.96E-20)	9.29E-18 (4.07E-20)	9.63E-18 (3.82E-20)	6.51E-18 (2.61E-20)
			without	1.22E-17 (4.69E-20)	9.49E-18 (3.89E-20)	7.19E-18 (3.16E-20)	5.46E-18 (2.56E-20)
4	2		with	1.48E-16 (2.22E-19)	1.08E-16 (1.75E-19)	9.76E-17 (1.59E-19)	5.78E-17 (1.05E-19)
			without	1.38E-16 (2.00E-19)	1.07E-16 (1.66E-19)	8.00E-17 (1.35E-19)	5.89E-17 (1.10E-19)
4	2	0	with	5.93E-17 (1.41E-19)	3.97E-17 (1.07E-19)	3.37E-17 (9.49E-20)	1.94E-17 (6.32E-20)
			without	5.93E-17 (1.30E-19)	4.52E-17 (1.07E-19)	3.33E-17 (8.68E-20)	2.45E-17 (7.08E-20)
4	2	1	with	4.21E-17 (1.21E-19)	3.25E-17 (9.75E-20)	3.07E-17 (8.97E-20)	1.84E-17 (5.90E-20)
			without	3.59E-17 (1.05E-19)	2.80E-17 (8.71E-20)	2.11E-17 (7.09E-20)	1.54E-17 (5.69E-20)
4	2	2	with	1.97E-18 (2.60E-20)	1.49E-18 (2.09E-20)	1.40E-18 (1.92E-20)	8.57E-19 (1.28E-20)
			without	3.50E-18 (3.25E-20)	2.91E-18 (2.78E-20)	2.24E-18 (2.30E-20)	1.67E-18 (1.87E-20)
4	3		with	1.82E-16 (3.34E-19)	1.23E-16 (2.54E-19)	1.01E-16 (2.18E-19)	5.41E-17 (1.35E-19)
			without	1.37E-16 (2.62E-19)	1.04E-16 (2.16E-19)	7.44E-17 (1.73E-19)	5.04E-17 (1.35E-19)
4	3	0	with	6.18E-17 (2.00E-19)	4.34E-17 (1.55E-19)	3.68E-17 (1.34E-19)	2.06E-17 (8.49E-20)
			without	5.22E-17 (1.64E-19)	3.96E-17 (1.35E-19)	2.82E-17 (1.08E-19)	1.93E-17 (8.48E-20)
4	3	1	with	5.10E-17 (1.77E-19)	3.39E-17 (1.34E-19)	2.77E-17 (1.14E-19)	1.47E-17 (7.07E-20)
			without	3.57E-17 (1.35E-19)	2.67E-17 (1.11E-19)	1.92E-17 (8.86E-20)	1.30E-17 (6.87E-20)
4	3	2	with	9.39E-18 (7.44E-20)	5.89E-18 (5.43E-20)	4.30E-18 (4.38E-20)	2.00E-18 (2.53E-20)
			without	6.89E-18 (5.70E-20)	5.52E-18 (4.83E-20)	3.81E-18 (3.78E-20)	2.53E-18 (2.90E-20)
4	3	3	with	3.66E-20 (3.90E-21)	1.55E-20 (2.37E-21)	-	-
			without	9.52E-21 (1.32E-21)	6.73E-21 (1.25E-21)	-	-

TABLE IV. Cross Sections for Electron Capture and statistical error values (in parenthesis) from H(1s) by Be^{4+}

See page 93 for Explanation of Tables

Final state			correction	Energy (keV/amu)			
n	*l*	*m*		50	60	70	80
5			with	2.22E-16 (3.04E-19)	1.74E-16 (2.43E-19)	1.62E-16 (2.15E-19)	9.55E-17 (1.38E-19)
			without	1.65E-16 (2.25E-19)	1.47E-16 (2.02E-19)	1.19E-16 (1.71E-19)	8.91E-17 (1.39E-19)
5	0	0	with	6.77E-18 (4.24E-20)	5.72E-18 (3.46E-20)	5.77E-18 (3.14E-20)	3.73E-18 (2.06E-20)
			without	5.38E-18 (3.10E-20)	4.40E-18 (2.67E-20)	3.50E-18 (2.24E-20)	2.80E-18 (1.87E-20)
5	1		with	3.42E-17 (9.26E-20)	2.93E-17 (7.68E-20)	3.02E-17 (7.13E-20)	1.93E-17 (4.67E-20)
			without	3.55E-17 (8.06E-20)	2.84E-17 (6.79E-20)	2.21E-17 (5.68E-20)	1.69E-17 (4.64E-20)
5	1	0	with	2.26E-17 (7.70E-20)	1.91E-17 (6.34E-20)	1.90E-17 (5.76E-20)	1.15E-17 (3.66E-20)
			without	2.31E-17 (6.48E-20)	1.77E-17 (5.38E-20)	1.34E-17 (4.47E-20)	1.02E-17 (3.66E-20)
5	1	1	with	5.78E-18 (3.70E-20)	5.09E-18 (3.09E-20)	5.57E-18 (3.02E-20)	3.90E-18 (2.08E-20)
			without	6.20E-18 (3.43E-20)	5.37E-18 (2.97E-20)	4.34E-18 (2.49E-20)	3.35E-18 (2.04E-20)
5	2		with	7.41E-17 (1.68E-19)	5.85E-17 (1.36E-19)	5.48E-17 (1.25E-19)	3.30E-17 (8.28E-20)
			without	6.45E-17 (1.48E-19)	5.70E-17 (1.28E-19)	4.57E-17 (1.07E-19)	3.43E-17 (8.70E-20)
5	2	0	with	3.19E-17 (1.10E-19)	2.29E-17 (8.62E-20)	1.96E-17 (7.63E-20)	1.12E-17 (5.02E-20)
			without	2.97E-17 (9.98E-20)	2.56E-17 (8.54E-20)	2.00E-17 (7.05E-20)	1.47E-17 (5.70E-20)
5	2	1	with	2.04E-17 (8.88E-20)	1.72E-17 (7.43E-20)	1.69E-17 (6.90E-20)	1.04E-17 (4.61E-20)
			without	1.60E-17 (7.54E-20)	1.45E-17 (6.60E-20)	1.19E-17 (5.56E-20)	8.97E-18 (4.50E-20)
5	2	2	with	7.93E-19 (1.70E-20)	6.80E-19 (1.43E-20)	6.71E-19 (1.35E-20)	4.51E-19 (9.37E-21)
			without	1.33E-18 (2.07E-20)	1.26E-18 (1.88E-20)	1.06E-18 (1.61E-20)	8.35E-19 (1.34E-20)
5	3		with	8.97E-17 (2.41E-19)	7.01E-17 (1.97E-19)	6.35E-17 (1.77E-19)	3.65E-17 (1.14E-19)
			without	5.64E-17 (1.75E-19)	5.37E-17 (1.61E-19)	4.44E-17 (1.38E-19)	3.32E-17 (1.13E-19)
5	3	0	with	3.08E-17 (1.43E-19)	2.48E-17 (1.19E-19)	2.32E-17 (1.09E-19)	1.38E-17 (7.10E-20)
			without	2.29E-17 (1.13E-19)	2.13E-17 (1.02E-19)	1.75E-17 (8.77E-20)	1.29E-17 (7.12E-20)
5	3	1	with	2.52E-17 (1.28E-19)	1.93E-17 (1.03E-19)	1.75E-17 (9.31E-20)	9.85E-18 (5.93E-20)
			without	1.44E-17 (8.91E-20)	1.39E-17 (8.24E-20)	1.14E-17 (7.04E-20)	8.66E-18 (5.77E-20)
5	3	2	with	4.23E-18 (5.11E-20)	3.22E-18 (4.11E-20)	2.63E-18 (3.50E-20)	1.43E-18 (2.18E-20)
			without	2.23E-18 (3.34E-20)	2.34E-18 (3.23E-20)	2.03E-18 (2.83E-20)	1.51E-18 (2.29E-20)
5	3	3	with	1.33E-20 (2.31E-21)	-	-	-
			without	5.99E-21 (9.85E-22)	-	-	-
5	4		with	1.70E-17 (1.22E-19)	1.08E-17 (8.95E-20)	7.28E-18 (6.96E-20)	3.02E-18 (3.79E-20)
			without	3.60E-18 (4.69E-20)	3.71E-18 (4.66E-20)	3.08E-18 (4.06E-20)	1.99E-18 (3.09E-20)
5	4	0	with	6.30E-18 (7.50E-20)	4.44E-18 (5.81E-20)	3.03E-18 (4.52E-20)	1.34E-18 (2.55E-20)
			without	1.74E-18 (3.26E-20)	1.74E-18 (3.19E-20)	1.44E-18 (2.79E-20)	9.56E-19 (2.15E-20)
5	4	1	with	4.61E-18 (6.35E-20)	2.74E-18 (4.51E-20)	1.88E-18 (3.53E-20)	7.36E-19 (1.86E-20)
			without	8.84E-19 (2.33E-20)	9.37E-19 (2.35E-20)	7.49E-19 (2.00E-20)	4.82E-19 (1.51E-20)
5	4	2	with	8.03E-19 (2.52E-20)	4.13E-19 (1.68E-20)	2.26E-19 (1.17E-20)	8.21E-20 (6.03E-21)
			without	4.06E-20 (4.54E-21)	5.54E-20 (5.57E-21)	6.00E-20 (5.57E-21)	3.09E-20 (3.78E-21)
5	4	3	with	-	-	-	-
			without	-	-	-	-
5	4	4	with	-	-	-	-
			without	-	-	-	-

TABLE IV. Cross Sections for Electron Capture and statistical error values (in parenthesis) from H(1s) by Be^{4+}

See page 93 for Explanation of Tables

$Be^{4+} + H(1s) \rightarrow Be^{3+}(nlm) + H^{+}$

Final state			correction	Energy (keV/amu)			
n	*l*	*m*		90	100	150	200
1	0	0	with	6.12E-19 (3.44E-21)	6.64E-19 (3.36E-21)	7.92E-19 (2.50E-21)	8.00E-19 (2.82E-21)
			without	5.72E-19 (4.52E-21)	6.29E-19 (4.08E-21)	6.69E-19 (2.88E-21)	5.73E-19 (2.89E-21)
2			with	4.15E-17 (6.18E-20)	3.29E-17 (5.03E-20)	1.13E-17 (1.86E-20)	4.64E-18 (1.23E-20)
			without	5.51E-17 (7.52E-20)	4.36E-17 (5.58E-20)	1.63E-17 (2.08E-20)	7.10E-18 (1.39E-20)
2	0	0	with	5.21E-18 (1.88E-20)	4.01E-18 (1.45E-20)	1.29E-18 (4.72E-21)	5.54E-19 (3.39E-21)
			without	6.82E-18 (2.56E-20)	5.40E-18 (1.87E-20)	2.23E-18 (6.70E-21)	1.07E-18 (4.51E-21)
2	1		with	3.63E-17 (5.96E-20)	2.89E-17 (4.89E-20)	9.99E-18 (1.85E-20)	4.09E-18 (1.20E-20)
			without	4.83E-17 (7.11E-20)	3.82E-17 (5.30E-20)	1.41E-17 (2.00E-20)	6.03E-18 (1.34E-20)
2	1	0	with	1.26E-17 (3.50E-20)	1.04E-17 (2.98E-20)	4.39E-18 (1.29E-20)	2.09E-18 (8.87E-21)
			without	2.10E-17 (4.47E-20)	1.73E-17 (3.41E-20)	7.11E-18 (1.38E-20)	3.25E-18 (9.70E-21)
2	1	1	with	1.18E-17 (3.44E-20)	9.18E-18 (2.77E-20)	2.81E-18 (9.53E-21)	1.00E-18 (5.78E-21)
			without	1.36E-17 (4.03E-20)	1.05E-17 (2.95E-20)	3.50E-18 (1.03E-20)	1.39E-18 (6.54E-21)
3			with	1.25E-16 (1.25E-19)	9.13E-17 (9.65E-20)	2.19E-17 (2.88E-20)	6.64E-18 (1.67E-20)
			without	1.24E-16 (1.38E-19)	9.06E-17 (9.87E-20)	2.35E-17 (2.94E-20)	7.91E-18 (1.66E-20)
3	0	0	with	6.00E-18 (2.16E-20)	4.62E-18 (1.68E-20)	1.29E-18 (4.73E-21)	4.13E-19 (2.78E-21)
			without	5.04E-18 (2.30E-20)	4.13E-18 (1.73E-20)	1.68E-18 (6.06E-21)	7.48E-19 (3.88E-21)
3	1		with	3.46E-17 (5.24E-20)	2.61E-17 (4.11E-20)	6.68E-18 (1.29E-20)	2.18E-18 (8.12E-21)
			without	3.22E-17 (5.87E-20)	2.48E-17 (4.29E-20)	8.05E-18 (1.43E-20)	3.15E-18 (9.00E-21)
3	1	0	with	1.71E-17 (3.69E-20)	1.23E-17 (2.83E-20)	2.71E-18 (8.67E-21)	9.35E-19 (5.63E-21)
			without	1.78E-17 (4.40E-20)	1.39E-17 (3.23E-20)	4.66E-18 (1.09E-20)	1.85E-18 (6.93E-21)
3	1	1	with	8.71E-18 (2.68E-20)	6.90E-18 (2.14E-20)	1.98E-18 (6.84E-21)	6.27E-19 (4.19E-21)
			without	7.19E-18 (2.79E-20)	5.47E-18 (2.02E-20)	1.70E-18 (6.55E-21)	6.51E-19 (4.09E-21)
3	2		with	8.48E-17 (1.26E-19)	6.06E-17 (9.74E-20)	1.40E-17 (2.91E-20)	4.05E-18 (1.61E-20)
			without	8.71E-17 (1.33E-19)	6.16E-17 (9.46E-20)	1.38E-17 (2.84E-20)	4.01E-18 (1.58E-20)
3	2	0	with	3.16E-17 (8.29E-20)	2.31E-17 (6.50E-20)	5.75E-18 (1.96E-20)	1.80E-18 (1.11E-20)
			without	3.50E-17 (8.53E-20)	2.51E-17 (6.12E-20)	6.00E-18 (1.91E-20)	1.84E-18 (1.09E-20)
3	2	1	with	2.51E-17 (6.66E-20)	1.77E-17 (5.13E-20)	3.96E-18 (1.51E-20)	1.10E-18 (8.18E-21)
			without	2.33E-17 (6.98E-20)	1.65E-17 (4.93E-20)	3.62E-18 (1.45E-20)	1.02E-18 (7.91E-21)
3	2	2	with	1.47E-18 (1.57E-20)	9.93E-19 (1.18E-20)	1.78E-19 (3.11E-21)	3.00E-20 (1.34E-21)
			without	2.73E-18 (2.34E-20)	1.82E-18 (1.61E-20)	2.99E-19 (3.99E-21)	6.63E-20 (1.89E-21)

TABLE IV. Cross Sections for Electron Capture and statistical error values (in parenthesis) from H(1s) by Be^{4+}

See page 93 for Explanation of Tables

Final State			correction	Energy (keV/amu)			
n	*l*	*m*		90	100	150	200
4			with	1.08E-16 (1.28E-19)	7.80E-17 (9.75E-20)	1.76E-17 (2.70E-20)	4.96E-18 (1.48E-20)
			without	1.01E-16 (1.37E-19)	7.26E-17 (9.69E-20)	1.71E-17 (2.70E-20)	5.28E-18 (1.43E-20)
4	0	0	with	4.53E-18 (2.01E-20)	3.43E-18 (1.53E-20)	9.95E-19 (4.27E-21)	3.06E-19 (2.37E-21)
			without	3.39E-18 (1.94E-20)	2.73E-18 (1.44E-20)	1.09E-18 (5.01E-21)	4.63E-19 (3.10E-21)
4	1		with	2.42E-17 (4.61E-20)	1.81E-17 (3.56E-20)	4.72E-18 (1.09E-20)	1.43E-18 (6.41E-21)
			without	2.03E-17 (4.81E-20)	1.56E-17 (3.50E-20)	4.87E-18 (1.14E-20)	1.82E-18 (6.92E-21)
4	1	0	with	1.34E-17 (3.44E-20)	9.43E-18 (2.58E-20)	1.97E-18 (7.44E-21)	5.88E-19 (4.38E-21)
			without	1.19E-17 (3.74E-20)	9.11E-18 (2.72E-20)	2.88E-18 (9.01E-21)	1.09E-18 (5.46E-21)
4	1	1	with	5.44E-18 (2.20E-20)	4.35E-18 (1.75E-20)	1.38E-18 (5.71E-21)	4.20E-19 (3.33E-21)
			without	4.22E-18 (2.17E-20)	3.25E-18 (1.58E-20)	9.93E-19 (4.99E-21)	3.66E-19 (3.04E-21)
4	2		with	4.40E-17 (8.86E-20)	3.31E-17 (7.07E-20)	9.06E-18 (2.36E-20)	2.90E-18 (1.41E-20)
			without	4.31E-17 (9.23E-20)	3.16E-17 (6.71E-20)	7.93E-18 (2.17E-20)	2.49E-18 (1.27E-20)
4	2	0	with	1.50E-17 (5.41E-20)	1.16E-17 (4.38E-20)	3.59E-18 (1.54E-20)	1.29E-18 (9.69E-21)
			without	1.78E-17 (5.94E-20)	1.31E-17 (4.34E-20)	3.42E-18 (1.45E-20)	1.12E-18 (8.70E-21)
4	2	1	with	1.39E-17 (4.92E-20)	1.03E-17 (3.88E-20)	2.64E-18 (1.25E-20)	7.93E-19 (7.21E-21)
			without	1.15E-17 (4.80E-20)	8.41E-18 (3.48E-20)	2.09E-18 (1.11E-20)	6.40E-19 (6.40E-21)
4	2	2	with	6.20E-19 (1.03E-20)	4.36E-19 (7.84E-21)	9.81E-20 (2.34E-21)	2.09E-20 (1.12E-21)
			without	1.16E-18 (1.52E-20)	8.40E-19 (1.09E-20)	1.72E-19 (3.07E-21)	4.16E-20 (1.52E-21)
4	3		with	3.57E-17 (1.04E-19)	2.33E-17 (7.67E-20)	2.78E-18 (1.64E-20)	3.18E-19 (5.78E-21)
			without	3.39E-17 (1.09E-19)	2.26E-17 (7.49E-20)	3.18E-18 (1.75E-20)	5.12E-19 (7.10E-21)
4	3	0	with	1.42E-17 (6.67E-20)	9.75E-18 (5.03E-20)	1.35E-18 (1.16E-20)	1.80E-19 (4.35E-21)
			without	1.29E-17 (6.80E-20)	8.78E-18 (4.74E-20)	1.33E-18 (1.15E-20)	2.43E-19 (4.95E-21)
4	3	1	with	9.59E-18 (5.39E-20)	6.15E-18 (3.93E-20)	6.78E-19 (8.08E-21)	6.86E-20 (2.67E-21)
			without	8.94E-18 (5.59E-20)	5.90E-18 (3.83E-20)	8.19E-19 (8.86E-21)	1.24E-19 (3.49E-21)
4	3	2	with	1.19E-18 (1.85E-20)	6.05E-19 (1.19E-20)	3.18E-20 (1.69E-21)	-
			without	1.63E-18 (2.28E-20)	1.03E-18 (1.53E-20)	9.85E-20 (2.90E-21)	-
4	3	3	with	-	-	-	-
			without	-	-	-	-

TABLE IV. Cross Sections for Electron Capture and statistical error values (in parenthesis) from H(1s) by Be^{4+}

See page 93 for Explanation of Tables

Final state			correction	Energy (keV/amu)			
n	*l*	*m*		90	100	150	200
5			with	7.13E-17 (1.10E-19)	5.15E-17 (8.32E-20)	1.18E-17 (2.28E-20)	3.26E-18 (1.22E-20)
			without	6.56E-17 (1.16E-19)	4.81E-17 (8.24E-20)	1.11E-17 (2.26E-20)	3.34E-18 (1.17E-20)
5	0	0	with	3.05E-18 (1.70E-20)	2.34E-18 (1.30E-20)	7.08E-19 (3.68E-21)	2.09E-19 (1.98E-21)
			without	2.26E-18 (1.61E-20)	1.85E-18 (1.21E-20)	7.17E-19 (4.14E-21)	2.99E-19 (2.53E-21)
5	1		with	1.55E-17 (3.86E-20)	1.17E-17 (2.96E-20)	3.07E-18 (8.98E-21)	9.27E-19 (5.18E-21)
			without	1.29E-17 (3.91E-20)	9.93E-18 (2.86E-20)	3.02E-18 (9.17E-21)	1.12E-18 (5.53E-21)
5	1	0	with	8.76E-18 (2.93E-20)	6.18E-18 (2.18E-20)	1.27E-18 (6.12E-21)	3.82E-19 (3.58E-21)
			without	7.68E-18 (3.07E-20)	5.88E-18 (2.25E-20)	1.79E-18 (7.31E-21)	6.72E-19 (4.40E-21)
5	1	1	with	3.39E-18 (1.79E-20)	2.74E-18 (1.43E-20)	9.03E-19 (4.71E-21)	2.75E-19 (2.70E-21)
			without	2.61E-18 (1.73E-20)	2.00E-18 (1.25E-20)	6.22E-19 (3.98E-21)	2.27E-19 (2.39E-21)
5	2		with	2.58E-17 (7.03E-20)	1.97E-17 (5.60E-20)	5.64E-18 (1.89E-20)	1.81E-18 (1.14E-20)
			without	2.54E-17 (7.32E-20)	1.89E-17 (5.35E-20)	4.71E-18 (1.72E-20)	1.46E-18 (9.95E-21)
5	2	0	with	8.88E-18 (4.29E-20)	6.93E-18 (3.44E-20)	2.24E-18 (1.23E-20)	8.09E-19 (7.84E-21)
			without	1.08E-17 (4.79E-20)	8.01E-18 (3.51E-20)	2.05E-18 (1.15E-20)	6.48E-19 (6.76E-21)
5	2	1	with	8.15E-18 (3.90E-20)	6.07E-18 (3.07E-20)	1.64E-18 (1.01E-20)	4.86E-19 (5.78E-21)
			without	6.70E-18 (3.77E-20)	5.04E-18 (2.76E-20)	1.23E-18 (8.66E-21)	3.80E-19 (5.02E-21)
5	2	2	with	3.52E-19 (7.85E-21)	2.57E-19 (6.12E-21)	6.14E-20 (1.88E-21)	1.23E-20 (8.71E-22)
			without	6.41E-19 (1.14E-20)	4.54E-19 (8.07E-21)	1.01E-19 (2.38E-21)	2.42E-20 (1.17E-21)
5	3		with	2.55E-17 (9.02E-20)	1.73E-17 (6.77E-20)	2.39E-18 (1.56E-20)	3.10E-19 (5.83E-21)
			without	2.39E-17 (9.35E-20)	1.67E-17 (6.60E-20)	2.67E-18 (1.64E-20)	4.58E-19 (6.84E-21)
5	3	0	with	1.01E-17 (5.73E-20)	7.15E-18 (4.40E-20)	1.16E-18 (1.10E-20)	1.72E-19 (4.37E-21)
			without	9.31E-18 (5.91E-20)	6.66E-18 (4.24E-20)	1.13E-18 (1.08E-20)	2.10E-19 (4.69E-21)
5	3	1	with	6.88E-18 (4.67E-20)	4.55E-18 (3.46E-20)	5.84E-19 (7.70E-21)	6.68E-20 (2.71E-21)
			without	6.21E-18 (4.77E-20)	4.32E-18 (3.36E-20)	6.79E-19 (8.23E-21)	1.19E-19 (3.47E-21)
5	3	2	with	8.56E-19 (1.60E-20)	4.81E-19 (1.09E-20)	3.19E-20 (1.73E-21)	1.17E-21 (3.38E-22)
			without	1.08E-18 (1.89E-20)	7.10E-19 (1.29E-20)	8.41E-20 (2.73E-21)	7.84E-21 (8.36E-22)
5	3	3	with	-	-	-	-
			without	-	-	-	-
5	4		with	1.32E-18 (2.37E-20)	5.69E-19 (1.42E-20)	-	-
			without	1.16E-18 (2.32E-20)	6.43E-19 (1.46E-20)	-	-
5	4	0	with	6.01E-19 (1.61E-20)	2.73E-19 (9.92E-21)	-	-
			without	5.82E-19 (1.65E-20)	3.27E-19 (1.04E-20)	-	-
5	4	1	with	3.38E-19 (1.20E-20)	1.51E-19 (7.29E-21)	-	-
			without	2.93E-19 (1.16E-20)	1.66E-19 (7.38E-21)	-	-
5	4	2	with	2.84E-20 (3.32E-21)	-	-	-
			without	1.27E-20 (2.36E-21)	-	-	-
5	4	3	with	-	-	-	-
			without	-	-	-	-
5	4	4	with	-	-	-	-
			without	-	-	-	-

TABLE V. Cross Sections for Electron Capture and statistical error values (in parenthesis) from H(1s) by B^{5+}

See page 93 for Explanation of Tables

$B^{5+} + H(1s) \rightarrow B^{4+}(nlm) + H^{+}$

Final state			correction	Energy (keV/amu)			
n	*l*	*m*		10	20	30	40
1	0	0	with	9.57E-20 (1.80E-21)	1.57E-19 (2.46E-21)	1.95E-19 (2.82E-21)	2.19E-19 (2.69E-21)
			without	2.28E-20 (2.70E-21)	1.01E-20 (1.07E-21)	1.30E-20 (9.22E-22)	1.73E-20 (9.06E-22)
2			with	6.93E-18 (3.82E-20)	9.61E-18 (4.70E-20)	1.42E-17 (5.90E-20)	1.94E-17 (5.95E-20)
			without	1.18E-17 (4.36E-20)	2.03E-17 (6.28E-20)	2.98E-17 (7.41E-20)	3.60E-17 (7.33E-20)
2	0	0	with	2.44E-18 (2.43E-20)	4.26E-18 (3.55E-20)	5.49E-18 (4.08E-20)	5.85E-18 (3.72E-20)
			without	4.12E-18 (2.59E-20)	5.52E-18 (3.40E-20)	7.33E-18 (3.95E-20)	8.31E-18 (3.97E-20)
2	1		with	4.49E-18 (2.98E-20)	5.34E-18 (3.23E-20)	8.73E-18 (4.37E-20)	1.35E-17 (4.75E-20)
			without	7.66E-18 (3.51E-20)	1.48E-17 (5.31E-20)	2.24E-17 (6.32E-20)	2.77E-17 (6.26E-20)
2	1	0	with	1.23E-18 (1.41E-20)	1.24E-18 (1.32E-20)	1.82E-18 (1.66E-20)	3.00E-18 (1.83E-20)
			without	2.58E-18 (1.92E-20)	4.41E-18 (2.68E-20)	6.63E-18 (3.09E-20)	8.75E-18 (3.13E-20)
2	1	1	with	1.66E-18 (1.90E-20)	2.09E-18 (2.17E-20)	3.53E-18 (2.98E-20)	5.32E-18 (3.25E-20)
			without	2.58E-18 (2.11E-20)	5.43E-18 (3.38E-20)	8.29E-18 (4.10E-20)	9.87E-18 (4.05E-20)
3			with	1.09E-15 (8.59E-19)	1.06E-15 (7.15E-19)	8.04E-16 (5.74E-19)	5.73E-16 (4.22E-19)
			without	1.39E-15 (7.16E-19)	1.20E-15 (5.94E-19)	8.81E-16 (5.09E-19)	6.28E-16 (3.95E-19)
3	0	0	with	1.45E-16 (3.64E-19)	7.30E-17 (2.19E-19)	3.92E-17 (1.37E-19)	2.35E-17 (8.46E-20)
			without	6.21E-17 (1.39E-19)	3.84E-17 (1.03E-19)	2.62E-17 (8.70E-20)	1.77E-17 (6.41E-20)
3	1		with	2.72E-16 (4.40E-19)	2.24E-16 (3.39E-19)	1.60E-16 (2.61E-19)	1.11E-16 (1.79E-19)
			without	3.31E-16 (3.56E-19)	2.86E-16 (3.03E-19)	2.03E-16 (2.53E-19)	1.43E-16 (1.88E-19)
3	1	0	with	9.75E-17 (2.53E-19)	9.80E-17 (2.18E-19)	7.63E-17 (1.79E-19)	5.46E-17 (1.26E-19)
			without	1.54E-16 (2.54E-19)	1.34E-16 (2.09E-19)	9.54E-17 (1.73E-19)	6.80E-17 (1.30E-19)
3	1	1	with	8.81E-17 (2.63E-19)	6.31E-17 (1.89E-19)	4.16E-17 (1.37E-19)	2.83E-17 (9.26E-20)
			without	8.83E-17 (1.87E-19)	7.56E-17 (1.63E-19)	5.38E-17 (1.36E-19)	3.74E-17 (9.95E-20)
3	2		with	6.76E-16 (6.93E-19)	7.63E-16 (6.31E-19)	6.05E-16 (5.18E-19)	4.39E-16 (3.89E-19)
			without	9.97E-16 (6.85E-19)	8.72E-16 (5.63E-19)	6.52E-16 (4.71E-19)	4.67E-16 (3.62E-19)
3	2	0	with	2.14E-16 (3.83E-19)	2.12E-16 (3.35E-19)	1.64E-16 (2.65E-19)	1.23E-16 (2.02E-19)
			without	2.41E-16 (3.63E-19)	2.18E-16 (2.94E-19)	1.78E-16 (2.48E-19)	1.36E-16 (1.93E-19)
3	2	1	with	1.59E-16 (3.53E-19)	2.11E-16 (3.49E-19)	1.79E-16 (2.99E-19)	1.34E-16 (2.26E-19)
			without	2.37E-16 (3.65E-19)	2.12E-16 (3.03E-19)	1.63E-16 (2.53E-19)	1.19E-16 (1.95E-19)
3	2	2	with	7.19E-17 (2.47E-19)	6.40E-17 (2.11E-19)	4.14E-17 (1.56E-19)	2.40E-17 (1.01E-19)
			without	1.41E-16 (2.73E-19)	1.15E-16 (2.32E-19)	7.40E-17 (1.82E-19)	4.64E-17 (1.29E-19)

TABLE V. Cross Sections for Electron Capture and statistical error values (in parenthesis) from H(1s) by B^{5+}

See page 93 for Explanation of Tables

Final state			correction	Energy (keV/amu)			
n	*l*	*m*		10	20	30	40
4			with	2.71E-15 (1.36E-18)	1.91E-15 (1.05E-18)	1.32E-15 (8.62E-19)	9.15E-16 (6.27E-19)
			without	9.46E-16 (6.52E-19)	1.05E-15 (6.57E-19)	9.94E-16 (6.18E-19)	7.99E-16 (5.04E-19)
4	0	0	with	5.21E-17 (1.83E-19)	3.26E-17 (1.27E-19)	2.33E-17 (1.02E-19)	1.68E-17 (7.22E-20)
			without	2.55E-17 (9.01E-20)	9.64E-18 (6.68E-20)	1.17E-17 (5.38E-20)	1.02E-17 (4.57E-20)
4	1		with	1.96E-16 (3.50E-19)	1.16E-16 (2.54E-19)	9.32E-17 (2.07E-19)	7.32E-17 (1.51E-19)
			without	8.65E-17 (1.67E-19)	6.92E-17 (1.54E-19)	9.79E-17 (1.62E-19)	8.31E-17 (1.33E-19)
4	1	0	with	1.08E-16 (2.58E-19)	7.06E-17 (1.94E-19)	5.84E-17 (1.64E-19)	4.53E-17 (1.20E-19)
			without	5.33E-17 (1.41E-19)	4.94E-17 (1.25E-19)	6.61E-17 (1.32E-19)	5.14E-17 (1.04E-19)
4	1	1	with	4.39E-17 (1.71E-19)	2.28E-17 (1.19E-19)	1.75E-17 (9.09E-20)	1.39E-17 (6.61E-20)
			without	1.66E-17 (6.70E-20)	9.86E-18 (6.66E-20)	1.59E-17 (6.83E-20)	1.59E-17 (5.92E-20)
4	2		with	6.57E-16 (6.91E-19)	4.79E-16 (5.07E-19)	3.33E-16 (3.92E-19)	2.34E-16 (2.82E-19)
			without	2.28E-16 (3.13E-19)	2.65E-16 (3.14E-19)	2.84E-16 (3.10E-19)	2.24E-16 (2.46E-19)
4	2	0	with	2.75E-16 (4.56E-19)	2.03E-16 (3.22E-19)	1.38E-16 (2.50E-19)	9.66E-17 (1.81E-19)
			without	1.02E-16 (2.21E-19)	1.21E-16 (2.05E-19)	1.21E-16 (1.99E-19)	9.19E-17 (1.56E-19)
4	2	1	with	1.70E-16 (3.63E-19)	1.29E-16 (2.81E-19)	9.21E-17 (2.16E-19)	6.48E-17 (1.54E-19)
			without	5.81E-17 (1.57E-19)	6.80E-17 (1.70E-19)	7.53E-17 (1.69E-19)	5.95E-17 (1.33E-19)
4	2	2	with	2.10E-17 (1.34E-19)	9.13E-18 (8.18E-20)	5.60E-18 (5.54E-20)	3.57E-18 (3.69E-20)
			without	4.98E-18 (4.51E-20)	4.14E-18 (5.11E-20)	5.96E-18 (5.10E-20)	6.19E-18 (4.42E-20)
4	3		with	1.80E-15 (1.29E-18)	1.28E-15 (1.01E-18)	8.71E-16 (8.38E-19)	5.92E-16 (6.08E-19)
			without	6.06E-16 (6.12E-19)	7.04E-16 (6.19E-19)	6.01E-16 (6.11E-19)	4.82E-16 (4.97E-19)
4	3	0	with	5.38E-16 (7.49E-19)	3.84E-16 (5.67E-19)	2.69E-16 (4.72E-19)	1.83E-16 (3.44E-19)
			without	2.14E-16 (3.91E-19)	2.49E-16 (3.76E-19)	2.04E-16 (3.67E-19)	1.60E-16 (2.94E-19)
4	3	1	with	4.52E-16 (6.99E-19)	3.37E-16 (5.49E-19)	2.34E-16 (4.55E-19)	1.63E-16 (3.29E-19)
			without	1.60E-16 (3.27E-19)	1.82E-16 (3.34E-19)	1.54E-16 (3.23E-19)	1.22E-16 (2.59E-19)
4	3	2	with	1.76E-16 (4.35E-19)	1.12E-16 (3.32E-19)	6.65E-17 (2.48E-19)	4.10E-17 (1.68E-19)
			without	3.53E-17 (1.38E-19)	4.50E-17 (1.67E-19)	4.44E-17 (1.70E-19)	3.84E-17 (1.42E-19)
4	3	3	with	4.82E-18 (6.45E-20)	1.06E-18 (2.84E-20)	4.58E-19 (1.82E-20)	2.77E-19 (1.24E-20)
			without	1.21E-18 (2.13E-20)	3.05E-19 (1.14E-20)	3.97E-19 (1.36E-20)	5.01E-19 (1.43E-20)

TABLE V. Cross Sections for Electron Capture and statistical error values (in parenthesis) from H(1s) by B^{5+}

See page 93 for Explanation of Tables

Final state			correction	Energy (keV/amu)			
n	*l*	*m*		10	20	30	40
5			with	3.53E-16 (4.93E-19)	4.62E-16 (6.58E-19)	5.82E-16 (6.59E-19)	5.44E-16 (5.43E-19)
			without	8.04E-17 (1.56E-19)	9.91E-17 (2.48E-19)	2.19E-16 (3.55E-19)	3.41E-16 (3.61E-19)
5	0	0	with	1.36E-17 (8.79E-20)	9.05E-18 (7.58E-20)	1.05E-17 (6.87E-20)	9.25E-18 (5.76E-20)
			without	8.67E-18 (4.83E-20)	4.33E-18 (5.51E-20)	4.19E-18 (4.04E-20)	5.58E-18 (3.30E-20)
5	1		with	5.15E-17 (1.87E-19)	3.60E-17 (1.64E-19)	4.21E-17 (1.42E-19)	3.97E-17 (1.15E-19)
			without	1.74E-17 (6.93E-20)	1.50E-17 (1.06E-19)	2.19E-17 (9.09E-20)	4.15E-17 (9.17E-20)
5	1	0	with	3.85E-17 (1.75E-19)	2.71E-17 (1.39E-19)	3.08E-17 (1.22E-19)	2.79E-17 (9.82E-20)
			without	1.20E-17 (6.40E-20)	1.04E-17 (9.05E-20)	1.65E-17 (7.68E-20)	3.04E-17 (7.79E-20)
5	1	1	with	6.47E-18 (5.54E-20)	4.45E-18 (6.17E-20)	5.54E-18 (5.19E-20)	5.89E-18 (4.32E-20)
			without	2.66E-18 (2.28E-20)	2.27E-18 (3.94E-20)	2.68E-18 (3.53E-20)	5.54E-18 (3.48E-20)
5	2		with	7.59E-17 (2.37E-19)	9.13E-17 (2.56E-19)	1.13E-16 (2.38E-19)	1.03E-16 (1.94E-19)
			without	2.10E-17 (8.16E-20)	2.71E-17 (1.46E-19)	5.37E-17 (1.59E-19)	8.26E-17 (1.60E-19)
5	2	0	with	4.30E-17 (1.79E-19)	4.84E-17 (1.81E-19)	5.64E-17 (1.65E-19)	4.97E-17 (1.33E-19)
			without	1.14E-17 (6.21E-20)	1.28E-17 (1.00E-19)	2.59E-17 (1.05E-19)	4.00E-17 (1.08E-19)
5	2	1	with	1.59E-17 (1.10E-19)	2.13E-17 (1.29E-19)	2.79E-17 (1.23E-19)	2.62E-17 (9.99E-20)
			without	4.50E-18 (3.67E-20)	6.80E-18 (7.37E-20)	1.32E-17 (8.40E-20)	2.01E-17 (8.25E-20)
5	2	2	with	5.89E-19 (1.89E-20)	3.28E-19 (1.82E-20)	4.54E-19 (1.59E-20)	6.72E-19 (1.58E-20)
			without	3.47E-19 (1.02E-20)	3.22E-19 (1.46E-20)	8.40E-19 (2.14E-20)	1.36E-18 (2.20E-20)
5	3		with	1.04E-16 (2.67E-19)	1.62E-16 (4.06E-19)	1.99E-16 (4.20E-19)	1.94E-16 (3.50E-19)
			without	2.18E-17 (8.83E-20)	3.45E-17 (1.58E-19)	9.02E-17 (2.51E-19)	1.30E-16 (2.69E-19)
5	3	0	with	4.56E-17 (1.69E-19)	6.09E-17 (2.44E-19)	7.48E-17 (2.55E-19)	7.08E-17 (2.09E-19)
			without	9.93E-18 (6.08E-20)	1.39E-17 (9.66E-20)	3.42E-17 (1.54E-19)	4.70E-17 (1.63E-19)
5	3	1	with	2.63E-17 (1.39E-19)	4.34E-17 (2.13E-19)	5.19E-17 (2.19E-19)	5.22E-17 (1.85E-19)
			without	5.05E-18 (4.16E-20)	9.02E-18 (8.34E-20)	2.33E-17 (1.30E-19)	3.32E-17 (1.38E-19)
5	3	2	with	2.94E-18 (5.66E-20)	7.01E-18 (8.79E-20)	9.96E-18 (9.55E-20)	9.19E-18 (7.82E-20)
			without	7.26E-19 (1.69E-20)	1.34E-18 (3.25E-20)	4.72E-18 (5.68E-20)	8.02E-18 (6.59E-20)
5	3	3	with	1.11E-19 (7.90E-21)	2.36E-20 (3.51E-21)	2.28E-20 (3.26E-21)	2.74E-20 (3.40E-21)
			without	1.74E-19 (7.80E-21)	2.25E-20 (2.52E-21)	6.42E-21 (1.24E-21)	2.28E-20 (2.42E-21)
5	4		with	1.08E-16 (2.89E-19)	1.64E-16 (4.59E-19)	2.17E-16 (5.19E-19)	1.98E-16 (4.31E-19)
			without	1.14E-17 (6.05E-20)	1.82E-17 (8.19E-20)	4.88E-17 (2.01E-19)	8.19E-17 (2.45E-19)
5	4	0	with	3.47E-17 (1.61E-19)	4.73E-17 (2.48E-19)	6.30E-17 (2.79E-19)	5.76E-17 (2.34E-19)
			without	3.54E-18 (3.41E-20)	6.69E-18 (4.66E-20)	1.88E-17 (1.25E-19)	2.98E-17 (1.49E-19)
5	4	1	with	2.95E-17 (1.55E-19)	4.22E-17 (2.36E-19)	5.48E-17 (2.65E-19)	5.09E-17 (2.22E-19)
			without	2.92E-18 (3.08E-20)	4.51E-18 (4.29E-20)	1.24E-17 (1.03E-19)	2.07E-17 (1.24E-19)
5	4	2	with	6.96E-18 (7.18E-20)	1.56E-17 (1.41E-19)	2.19E-17 (1.64E-19)	1.86E-17 (1.31E-19)
			without	8.65E-19 (1.60E-20)	1.12E-18 (2.07E-20)	2.50E-18 (4.37E-20)	5.21E-18 (5.21E-18)
5	4	3	with	3.71E-19 (1.71E-20)	2.63E-19 (1.38E-20)	4.77E-19 (2.14E-20)	6.26E-19 (2.25E-20)
			without	1.80E-19 (8.10E-21)	8.89E-20 (5.27E-21)	5.49E-20 (3.96E-21)	5.91E-20 (5.29E-21)
5	4	4	with	6.82E-20 (7.53E-21)	1.05E-20 (2.72E-21)	-	-
			without	6.38E-21 (1.43E-21)	5.42E-21 (1.36E-21)	-	-

TABLE V. Cross Sections for Electron Capture and statistical error values (in parenthesis) from H(1s) by B^{5+}

See page 93 for Explanation of Tables

$B^{5+} + H(1s) \rightarrow B^{4+}(nlm) + H^{+}$

Final state			correction	Energy (keV/amu)			
n	*l*	*m*		50	60	70	80
1	0	0	with	2.27E-19 (2.67E-21)	2.39E-19 (2.57E-21)	2.37E-19 (2.46E-21)	2.38E-19 (2.04E-21)
			without	2.36E-20 (9.17E-22)	3.24E-20 (1.08E-21)	4.13E-20 (1.13E-21)	5.56E-20 (1.34E-21)
2			with	2.14E-17 (5.95E-20)	2.09E-17 (5.52E-20)	1.91E-17 (5.08E-20)	1.68E-17 (3.97E-20)
			without	3.77E-17 (7.25E-20)	3.67E-17 (6.87E-20)	3.38E-17 (6.29E-20)	3.08E-17 (5.90E-20)
2	0	0	with	5.56E-18 (3.41E-20)	4.84E-18 (2.87E-20)	4.06E-18 (2.40E-20)	3.32E-18 (1.72E-20)
			without	8.31E-18 (3.92E-20)	7.51E-18 (3.58E-20)	6.40E-18 (3.12E-20)	5.32E-18 (2.72E-20)
2	1		with	1.58E-17 (4.95E-20)	1.60E-17 (4.75E-20)	1.50E-17 (4.49E-20)	1.35E-17 (3.59E-20)
			without	2.94E-17 (6.21E-20)	2.92E-17 (5.97E-20)	2.74E-17 (5.53E-20)	2.54E-17 (5.28E-20)
2	1	0	with	3.59E-18 (1.91E-20)	3.66E-18 (1.86E-20)	3.54E-18 (1.82E-20)	3.36E-18 (1.53E-20)
			without	9.47E-18 (3.11E-20)	9.68E-18 (3.02E-20)	9.47E-18 (2.87E-20)	9.04E-18 (2.78E-20)
2	1	1	with	6.15E-18 (3.37E-20)	6.22E-18 (3.22E-20)	5.76E-18 (3.00E-20)	5.09E-18 (2.36E-20)
			without	1.03E-17 (4.02E-20)	1.00E-17 (3.84E-20)	9.10E-18 (3.51E-20)	8.27E-18 (3.32E-20)
3			with	4.07E-16 (3.41E-19)	2.93E-16 (2.68E-19)	2.12E-16 (2.17E-19)	1.54E-16 (1.52E-19)
			without	4.42E-16 (3.20E-19)	3.18E-16 (2.60E-19)	2.33E-16 (2.12E-19)	1.74E-16 (1.79E-19)
3	0	0	with	1.56E-17 (6.21E-20)	1.09E-17 (4.62E-20)	7.80E-18 (3.59E-20)	5.77E-18 (2.47E-20)
			without	1.20E-17 (4.92E-20)	8.64E-18 (3.89E-20)	6.56E-18 (3.21E-20)	5.08E-18 (2.71E-20)
3	1		with	7.92E-17 (1.37E-19)	5.79E-17 (1.05E-19)	4.27E-17 (8.32E-20)	3.20E-17 (5.81E-20)
			without	9.76E-17 (1.45E-19)	6.82E-17 (1.13E-19)	4.91E-17 (8.85E-20)	3.62E-17 (7.27E-20)
3	1	0	with	3.91E-17 (9.68E-20)	2.84E-17 (7.37E-20)	2.09E-17 (5.84E-20)	1.55E-17 (4.04E-20)
			without	4.75E-17 (1.01E-19)	3.39E-17 (7.95E-20)	2.49E-17 (6.30E-20)	1.86E-17 (5.21E-20)
3	1	1	with	2.00E-17 (7.00E-20)	1.47E-17 (5.35E-20)	1.09E-17 (4.25E-20)	8.28E-18 (2.99E-20)
			without	2.51E-17 (7.52E-20)	1.72E-17 (5.74E-20)	1.22E-17 (4.47E-20)	8.82E-18 (3.64E-20)
3	2		with	3.13E-16 (3.18E-19)	2.24E-16 (2.53E-19)	1.61E-16 (2.07E-19)	1.16E-16 (1.46E-19)
			without	3.32E-16 (2.95E-19)	2.41E-16 (2.41E-19)	1.78E-16 (1.97E-19)	1.33E-16 (1.68E-19)
3	2	0	with	8.95E-17 (1.69E-19)	6.55E-17 (1.37E-19)	4.78E-17 (1.13E-19)	3.49E-17 (8.14E-20)
			without	1.00E-16 (1.59E-19)	7.61E-17 (1.32E-19)	5.85E-17 (1.10E-19)	4.52E-17 (9.54E-20)
3	2	1	with	9.70E-17 (1.85E-19)	7.03E-17 (1.46E-19)	5.06E-17 (1.18E-19)	3.66E-17 (8.33E-20)
			without	8.71E-17 (1.59E-19)	6.42E-17 (1.30E-19)	4.75E-17 (1.06E-19)	3.57E-17 (9.04E-20)
3	2	2	with	1.43E-17 (7.31E-20)	8.92E-18 (5.28E-20)	6.00E-18 (4.10E-20)	4.08E-18 (2.78E-20)
			without	2.92E-17 (9.71E-20)	1.86E-17 (7.32E-20)	1.20E-17 (5.54E-20)	7.99E-18 (4.41E-20)

TABLE V. Cross Sections for Electron Capture and statistical error values (in parenthesis) from H(1s) by B^{5+}

See page 93 for Explanation of Tables

Final State			correction	Energy (keV/amu)			
n	*l*	*m*		50	60	70	80
4			with	6.32E-16 (4.93E-19)	4.45E-16 (3.80E-19)	3.14E-16 (3.00E-19)	2.22E-16 (2.06E-19)
			without	5.94E-16 (4.19E-19)	4.26E-16 (3.40E-19)	3.04E-16 (2.74E-19)	2.19E-16 (2.27E-19)
4	0	0	with	1.26E-17 (5.69E-20)	9.42E-18 (4.46E-20)	6.98E-18 (3.56E-20)	5.29E-18 (2.49E-20)
			without	8.06E-18 (3.93E-20)	6.26E-18 (3.33E-20)	4.81E-18 (2.76E-20)	3.77E-18 (2.37E-20)
4	1		with	5.69E-17 (1.21E-19)	4.48E-17 (9.67E-20)	3.48E-17 (7.88E-20)	2.69E-17 (5.58E-20)
			without	6.13E-17 (1.09E-19)	4.43E-17 (8.73E-20)	3.24E-17 (7.05E-20)	2.44E-17 (5.93E-20)
4	1	0	with	3.48E-17 (9.60E-20)	2.69E-17 (7.59E-20)	2.06E-17 (6.15E-20)	1.57E-17 (4.30E-20)
			without	3.63E-17 (8.42E-20)	2.58E-17 (6.71E-20)	1.87E-17 (5.39E-20)	1.40E-17 (4.54E-20)
4	1	1	with	1.10E-17 (5.29E-20)	8.93E-18 (4.29E-20)	7.06E-18 (3.51E-20)	5.65E-18 (2.54E-20)
			without	1.25E-17 (4.95E-20)	9.26E-18 (4.01E-20)	6.84E-18 (3.24E-20)	5.20E-18 (2.73E-20)
4	2		with	1.69E-16 (1.69E-16)	1.26E-16 (1.80E-19)	9.40E-17 (1.46E-19)	6.90E-17 (1.03E-19)
			without	1.64E-16 (2.00E-19)	1.18E-16 (1.62E-19)	8.67E-17 (1.31E-19)	6.46E-17 (1.10E-19)
4	2	0	with	6.93E-17 (1.44E-19)	5.06E-17 (1.13E-19)	3.64E-17 (8.95E-20)	2.51E-17 (6.07E-20)
			without	6.61E-17 (1.25E-19)	4.74E-17 (1.01E-19)	3.47E-17 (8.14E-20)	2.58E-17 (6.82E-20)
4	2	1	with	4.73E-17 (1.23E-19)	3.59E-17 (9.87E-20)	2.74E-17 (8.12E-20)	2.10E-17 (5.82E-20)
			without	4.37E-17 (1.08E-19)	3.15E-17 (8.64E-20)	2.31E-17 (6.98E-20)	1.72E-17 (5.86E-20)
4	2	2	with	2.46E-18 (2.87E-20)	1.72E-18 (2.22E-20)	1.35E-18 (1.86E-20)	1.03E-18 (1.34E-20)
			without	5.19E-18 (3.80E-20)	4.01E-18 (3.15E-20)	2.94E-18 (2.56E-20)	2.17E-18 (2.15E-20)
4	3		with	3.94E-16 (4.77E-19)	2.64E-16 (3.65E-19)	1.78E-16 (2.88E-19)	1.21E-16 (1.98E-19)
			without	3.60E-16 (4.08E-19)	2.57E-16 (3.28E-19)	1.80E-16 (2.61E-19)	1.26E-16 (2.14E-19)
4	3	0	with	1.21E-16 (2.69E-19)	8.00E-17 (2.08E-19)	5.45E-17 (1.67E-19)	3.87E-17 (1.17E-19)
			without	1.19E-16 (2.40E-19)	8.51E-17 (1.92E-19)	6.01E-17 (1.53E-19)	4.21E-17 (1.25E-19)
4	3	1	with	1.11E-16 (2.58E-19)	7.61E-17 (1.98E-19)	5.19E-17 (1.55E-19)	3.49E-17 (1.06E-19)
			without	9.10E-17 (2.12E-19)	6.49E-17 (1.69E-19)	4.58E-17 (1.34E-19)	3.20E-17 (1.10E-19)
4	3	2	with	2.53E-17 (1.25E-19)	1.55E-17 (8.92E-20)	1.00E-17 (6.79E-20)	6.25E-18 (4.38E-20)
			without	2.92E-17 (1.17E-19)	2.06E-17 (9.32E-20)	1.42E-17 (7.30E-20)	9.68E-18 (5.87E-20)
4	3	3	with	1.64E-19 (9.14E-21)	9.71E-20 (6.57E-21)	5.98E-20 (4.90E-21)	2.79E-20 (2.76E-21)
			without	4.99E-19 (1.37E-20)	3.90E-19 (1.15E-20)	2.74E-19 (9.16E-21)	1.69E-19 (7.04E-21)

TABLE V. Cross Sections for Electron Capture and statistical error values (in parenthesis) from H(1s) by B^{5+}

See page 93 for Explanation of Tables

Final state			correction	Energy (keV/amu)			
n	*l*	*m*		50	60	70	80
5			with	4.38E-16 (4.56E-19)	3.26E-16 (3.58E-19)	2.40E-16 (2.86E-19)	1.75E-16 (1.98E-19)
			without	3.48E-16 (3.45E-19)	2.90E-16 (3.00E-19)	2.24E-16 (2.50E-19)	1.67E-16 (2.11E-19)
5	0	0	with	7.36E-18 (4.70E-20)	6.00E-18 (3.77E-20)	4.86E-18 (3.13E-20)	3.76E-18 (2.22E-20)
			without	5.11E-18 (3.11E-20)	4.19E-18 (2.73E-20)	3.26E-18 (2.30E-20)	2.59E-18 (1.98E-20)
5	1		with	3.41E-17 (9.83E-20)	2.81E-17 (7.98E-20)	2.30E-17 (6.66E-20)	1.86E-17 (4.82E-20)
			without	3.77E-17 (8.35E-20)	2.90E-17 (7.03E-20)	2.18E-17 (5.79E-20)	1.64E-17 (4.89E-20)
5	1	0	with	2.34E-17 (8.30E-20)	1.88E-17 (6.66E-20)	1.51E-17 (5.50E-20)	1.19E-17 (3.92E-20)
			without	2.52E-17 (6.83E-20)	1.85E-17 (5.65E-20)	1.35E-17 (4.61E-20)	1.01E-17 (3.88E-20)
5	1	1	with	5.35E-18 (3.77E-20)	4.63E-18 (3.14E-20)	3.94E-18 (2.69E-20)	3.31E-18 (1.99E-20)
			without	6.23E-18 (3.42E-20)	5.28E-18 (2.99E-20)	4.09E-18 (2.48E-20)	3.21E-18 (2.14E-20)
5	2		with	8.70E-17 (1.68E-19)	6.97E-17 (1.38E-19)	5.58E-17 (1.16E-19)	4.37E-17 (8.39E-20)
			without	8.30E-17 (1.47E-19)	6.78E-17 (1.25E-19)	5.20E-17 (1.03E-19)	3.99E-17 (8.83E-20)
5	2	0	with	4.10E-17 (1.15E-19)	3.16E-17 (9.27E-20)	2.40E-17 (7.53E-20)	1.77E-17 (5.26E-20)
			without	3.85E-17 (9.82E-20)	3.02E-17 (8.17E-20)	2.26E-17 (6.67E-20)	1.71E-17 (5.67E-20)
5	2	1	with	2.23E-17 (8.64E-20)	1.84E-17 (7.22E-20)	1.54E-17 (6.23E-20)	1.25E-17 (4.58E-20)
			without	2.07E-17 (7.64E-20)	1.73E-17 (6.54E-20)	1.35E-17 (5.42E-20)	1.04E-17 (4.63E-20)
5	2	2	with	6.89E-19 (1.51E-20)	6.29E-19 (1.34E-20)	5.50E-19 (1.20E-20)	4.57E-19 (8.98E-21)
			without	1.57E-18 (2.13E-20)	1.45E-18 (1.91E-20)	1.24E-18 (1.67E-20)	9.97E-19 (1.45E-20)
5	3		with	1.58E-16 (2.98E-19)	2.01E-20 (2.73E-21)	8.83E-17 (1.99E-19)	6.62E-17 (1.44E-19)
			without	1.34E-16 (2.55E-19)	1.15E-16 (2.20E-19)	9.04E-17 (1.84E-19)	6.85E-17 (1.56E-19)
5	3	0	with	5.35E-17 (1.72E-19)	3.65E-17 (1.33E-19)	2.57E-17 (1.09E-19)	1.92E-17 (7.96E-20)
			without	4.78E-17 (1.53E-19)	4.04E-17 (1.31E-19)	3.13E-17 (1.08E-19)	2.34E-17 (9.15E-20)
5	3	1	with	4.45E-17 (1.60E-19)	3.50E-17 (1.31E-19)	2.67E-17 (1.09E-19)	2.01E-17 (7.89E-20)
			without	3.42E-17 (1.30E-19)	2.90E-17 (1.12E-19)	2.29E-17 (9.38E-20)	1.74E-17 (7.99E-20)
5	3	2	with	7.74E-18 (6.76E-20)	5.99E-18 (5.49E-20)	4.58E-18 (4.55E-20)	3.37E-18 (3.23E-20)
			without	9.13E-18 (6.61E-20)	8.17E-18 (5.88E-20)	6.66E-18 (5.00E-20)	5.12E-18 (4.28E-20)
5	3	3	with	2.50E-20 (3.21E-21)	2.01E-20 (2.73E-21)	1.84E-20 (2.56E-21)	1.03E-20 (1.61E-21)
			without	6.81E-20 (4.78E-21)	7.30E-20 (4.91E-21)	7.17E-20 (4.57E-21)	5.90E-20 (4.11E-21)
5	4		with	1.51E-16 (3.60E-19)	1.03E-16 (2.76E-19)	6.77E-17 (2.13E-19)	4.33E-17 (1.41E-19)
			without	8.77E-17 (2.43E-19)	7.40E-17 (2.12E-19)	5.60E-17 (1.75E-19)	3.92E-17 (1.43E-19)
5	4	0	with	4.54E-17 (2.00E-19)	3.26E-17 (1.58E-19)	2.25E-17 (1.24E-19)	1.48E-17 (8.31E-20)
			without	3.07E-17 (1.45E-19)	2.56E-17 (1.26E-19)	1.92E-17 (1.03E-19)	1.35E-17 (8.48E-20)
5	4	1	with	3.91E-17 (1.84E-19)	2.66E-17 (1.41E-19)	1.73E-17 (1.08E-19)	1.12E-17 (7.20E-20)
			without	2.23E-17 (1.23E-19)	1.85E-17 (1.07E-19)	1.42E-17 (8.84E-20)	1.00E-17 (7.28E-20)
5	4	2	with	1.34E-17 (1.06E-19)	8.49E-18 (7.80E-20)	5.08E-18 (5.72E-20)	2.97E-18 (3.62E-20)
			without	6.15E-18 (6.30E-20)	5.56E-18 (5.69E-20)	4.20E-18 (4.68E-20)	2.85E-18 (3.76E-20)
5	4	3	with	4.93E-19 (1.92E-20)	2.57E-19 (1.28E-20)	1.24E-19 (8.45E-21)	4.58E-20 (4.24E-21)
			without	1.12E-19 (7.72E-21)	1.06E-19 (7.25E-21)	9.10E-20 (6.43E-21)	5.50E-20 (4.86E-21)
5	4	4	with	-	-	-	-
			without	-	-	-	-

TABLE V. Cross Sections for Electron Capture and statistical error values (in parenthesis) from H(1s) by B^{5+}

See page 93 for Explanation of Tables

$B^{5+} + H(1s) \rightarrow B^{4+}(nlm) + H^{+}$

Final state			correction	Energy (keV/amu)			
n	*l*	*m*		90	100	150	200
1	0	0	with	2.51E-19 (2.02E-21)	2.67E-19 (2.01E-21)	3.58E-19 (1.62E-21)	4.24E-19 (1.59E-21)
			without	6.96E-20 (1.26E-21)	8.18E-20 (1.32E-21)	1.46E-19 (1.29E-21)	1.63E-19 (1.27E-21)
2			with	1.47E-17 (3.56E-20)	1.29E-17 (3.19E-20)	6.29E-18 (1.44E-20)	3.49E-18 (8.75E-21)
			without	2.70E-17 (4.69E-20)	2.34E-17 (4.13E-20)	1.16E-17 (1.89E-20)	6.06E-18 (1.18E-20)
2	0	0	with	2.76E-18 (1.45E-20)	2.29E-18 (1.22E-20)	9.63E-19 (4.61E-21)	5.40E-19 (2.89E-21)
			without	4.37E-18 (2.06E-20)	3.58E-18 (1.72E-20)	1.59E-18 (6.71E-21)	8.10E-19 (3.86E-21)
2	1		with	1.20E-17 (3.27E-20)	1.06E-17 (2.96E-20)	5.32E-18 (1.39E-20)	2.95E-18 (8.38E-21)
			without	2.26E-17 (4.25E-20)	1.99E-17 (3.77E-20)	1.00E-17 (1.77E-20)	5.25E-18 (1.12E-20)
2	1	0	with	3.15E-18 (1.48E-20)	2.95E-18 (1.42E-20)	1.99E-18 (8.44E-21)	1.30E-18 (5.70E-21)
			without	8.40E-18 (2.29E-20)	7.67E-18 (2.09E-20)	4.50E-18 (1.09E-20)	2.58E-18 (7.37E-21)
2	1	1	with	4.39E-18 (2.10E-20)	3.82E-18 (1.87E-20)	1.66E-18 (7.79E-21)	8.32E-19 (4.38E-21)
			without	7.15E-18 (2.64E-20)	6.13E-18 (2.31E-20)	2.77E-18 (1.02E-20)	1.34E-18 (6.07E-21)
3			with	1.17E-16 (1.26E-19)	8.66E-17 (1.02E-19)	2.39E-17 (3.45E-20)	8.06E-18 (1.69E-20)
			without	1.31E-16 (1.31E-19)	9.94E-17 (1.08E-19)	3.02E-17 (3.76E-20)	1.14E-17 (1.91E-20)
3	0	0	with	4.44E-18 (1.99E-20)	3.33E-18 (1.59E-20)	9.53E-19 (4.90E-21)	3.20E-19 (2.23E-21)
			without	3.99E-18 (2.01E-20)	3.28E-18 (1.71E-20)	1.36E-18 (6.60E-21)	6.66E-19 (3.59E-21)
3	1		with	2.48E-17 (4.76E-20)	1.89E-17 (3.86E-20)	5.39E-18 (1.24E-20)	1.71E-18 (6.21E-21)
			without	2.74E-17 (5.26E-20)	2.12E-17 (4.30E-20)	7.63E-18 (1.56E-20)	3.37E-18 (8.44E-21)
3	1	0	with	1.20E-17 (3.28E-20)	9.11E-18 (2.64E-20)	2.44E-18 (8.04E-21)	7.62E-19 (4.25E-21)
			without	1.43E-17 (3.79E-20)	1.13E-17 (3.12E-20)	4.41E-18 (1.16E-20)	2.03E-18 (6.39E-21)
3	1	1	with	6.38E-18 (2.46E-20)	4.87E-18 (2.01E-20)	1.47E-18 (6.74E-21)	4.73E-19 (3.20E-21)
			without	6.56E-18 (2.61E-20)	4.95E-18 (2.11E-20)	1.61E-18 (7.42E-21)	6.73E-19 (3.93E-21)
3	2		with	8.73E-17 (1.22E-19)	6.44E-17 (1.00E-19)	1.76E-17 (3.51E-20)	6.02E-18 (1.68E-20)
			without	9.95E-17 (1.23E-19)	7.49E-17 (1.01E-19)	2.12E-17 (3.56E-20)	7.40E-18 (1.84E-20)
3	2	0	with	2.65E-17 (6.91E-20)	1.98E-17 (5.80E-20)	6.01E-18 (2.19E-20)	2.31E-18 (1.08E-20)
			without	3.49E-17 (7.11E-20)	2.70E-17 (5.91E-20)	8.38E-18 (2.21E-20)	3.12E-18 (1.19E-20)
3	2	1	with	2.74E-17 (6.86E-20)	2.01E-17 (5.58E-20)	5.33E-18 (1.89E-20)	1.75E-18 (8.88E-21)
			without	2.69E-17 (6.64E-20)	2.03E-17 (5.44E-20)	5.70E-18 (1.88E-20)	1.95E-18 (9.56E-21)
3	2	2	with	2.92E-18 (2.23E-20)	2.14E-18 (1.81E-20)	4.68E-19 (5.36E-21)	1.07E-19 (2.11E-21)
			without	5.41E-18 (3.06E-20)	3.66E-18 (2.37E-20)	7.13E-19 (6.75E-21)	1.88E-19 (2.96E-21)

TABLE V. Cross Sections for Electron Capture and statistical error values (in parenthesis) from H(1s) by B^{5+}

See page 93 for Explanation of Tables

Final State			correction	Energy (keV/amu)			
n	*l*	*m*		90	100	150	200
4			with	1.62E-16 (1.66E-19)	1.17E-16 (1.32E-19)	2.76E-17 (3.92E-20)	8.20E-18 (1.75E-20)
			without	1.58E-16 (1.63E-19)	1.15E-16 (1.31E-19)	2.93E-17 (4.09E-20)	9.69E-18 (1.90E-20)
4	0	0	with	4.00E-18 (2.00E-20)	3.08E-18 (1.62E-20)	8.63E-19 (4.82E-21)	2.74E-19 (2.01E-21)
			without	2.96E-18 (1.76E-20)	2.38E-18 (1.50E-20)	9.68E-19 (5.79E-21)	4.60E-19 (3.08E-21)
4	1		with	2.13E-17 (4.60E-20)	1.68E-17 (3.77E-20)	4.92E-18 (1.18E-20)	1.46E-18 (5.33E-21)
			without	1.86E-17 (4.35E-20)	1.44E-17 (3.59E-20)	5.12E-18 (1.31E-20)	2.19E-18 (6.94E-21)
4	1	0	with	1.22E-17 (3.51E-20)	9.49E-18 (2.87E-20)	2.52E-18 (8.26E-21)	6.64E-19 (3.65E-21)
			without	1.07E-17 (3.33E-20)	8.38E-18 (2.76E-20)	3.12E-18 (1.02E-20)	1.38E-18 (5.47E-21)
4	1	1	with	4.57E-18 (2.12E-20)	3.63E-18 (1.75E-20)	1.21E-18 (6.02E-21)	4.00E-19 (2.75E-21)
			without	3.97E-18 (2.01E-20)	3.03E-18 (1.64E-20)	1.01E-18 (5.89E-21)	4.09E-19 (3.03E-21)
4	2		with	5.13E-17 (8.41E-20)	3.81E-17 (6.91E-20)	1.01E-17 (2.42E-20)	3.60E-18 (1.24E-20)
			without	4.87E-17 (8.11E-20)	3.70E-17 (6.66E-20)	1.11E-17 (2.42E-20)	4.08E-18 (1.30E-20)
4	2	0	with	1.73E-17 (4.81E-20)	1.20E-17 (3.85E-20)	2.85E-18 (1.37E-20)	1.15E-18 (7.27E-21)
			without	1.95E-17 (5.01E-20)	1.50E-17 (4.14E-20)	4.57E-18 (1.53E-20)	1.73E-18 (8.44E-21)
4	2	1	with	1.62E-17 (4.83E-20)	1.24E-17 (3.99E-20)	3.41E-18 (1.38E-20)	1.16E-18 (6.97E-21)
			without	1.29E-17 (4.29E-20)	9.81E-18 (3.52E-20)	2.93E-18 (1.25E-20)	1.07E-18 (6.73E-21)
4	2	2	with	8.19E-19 (1.14E-20)	6.62E-19 (9.72E-21)	2.17E-19 (3.61E-21)	6.57E-20 (1.67E-21)
			without	1.65E-18 (1.59E-20)	1.18E-18 (1.27E-20)	3.19E-19 (4.40E-21)	1.00E-19 (2.15E-21)
4	3		with	8.53E-17 (1.59E-19)	5.92E-17 (1.25E-19)	1.17E-17 (3.54E-20)	2.86E-18 (1.44E-20)
			without	8.79E-17 (1.52E-19)	6.15E-17 (1.21E-19)	1.21E-17 (3.59E-20)	2.96E-18 (1.54E-20)
4	3	0	with	2.82E-17 (9.51E-20)	2.05E-17 (7.65E-20)	4.46E-18 (2.24E-20)	1.19E-18 (9.39E-21)
			without	2.99E-17 (9.00E-20)	2.10E-17 (7.17E-20)	4.41E-18 (2.20E-20)	1.15E-18 (9.74E-21)
4	3	1	with	2.44E-17 (8.43E-20)	1.66E-17 (6.59E-20)	3.17E-18 (1.82E-20)	7.69E-19 (7.41E-21)
			without	2.23E-17 (7.77E-20)	1.57E-17 (6.20E-20)	3.10E-18 (1.82E-20)	7.73E-19 (7.89E-21)
4	3	2	with	4.22E-18 (3.41E-20)	2.79E-18 (2.62E-20)	4.55E-19 (6.73E-21)	7.10E-20 (2.20E-21)
			without	6.55E-18 (4.09E-20)	4.50E-18 (3.21E-20)	7.05E-19 (8.30E-21)	1.35E-19 (3.14E-21)
4	3	3	with	1.84E-20 (2.14E-21)	1.13E-20 (1.58E-21)	-	-
			without	1.06E-19 (4.73E-21)	5.96E-20 (3.37E-21)	-	-

TABLE V. Cross Sections for Electron Capture and statistical error values (in parenthesis) from H(1s) by B^{5+}

See page 93 for Explanation of Tables

Final state			correction	Energy (keV/amu)			
n	*l*	*m*		90	100	150	200
5			with	1.29E-16 (1.59E-19)	9.56E-17 (1.27E-19)	2.19E-17 (3.62E-20)	6.23E-18 (1.56E-20)
			without	1.23E-16 (1.52E-19)	8.99E-17 (1.22E-19)	2.19E-17 (3.73E-20)	6.82E-18 (1.67E-20)
5	0	0	with	2.93E-18 (1.80E-20)	2.32E-18 (1.48E-20)	6.61E-19 (4.36E-21)	2.06E-19 (1.75E-21)
			without	2.05E-18 (1.49E-20)	1.64E-18 (1.26E-20)	6.51E-19 (4.82E-21)	3.06E-19 (2.54E-21)
5	1		with	1.50E-17 (3.99E-20)	1.21E-17 (3.31E-20)	3.74E-18 (1.05E-20)	1.07E-18 (4.54E-21)
			without	1.26E-17 (3.62E-20)	9.73E-18 (2.99E-20)	3.38E-18 (1.08E-20)	1.40E-18 (5.63E-21)
5	1	0	with	9.35E-18 (3.19E-20)	7.41E-18 (2.61E-20)	2.01E-18 (7.65E-21)	4.82E-19 (3.13E-21)
			without	7.69E-18 (2.87E-20)	5.93E-18 (2.37E-20)	2.12E-18 (8.67E-21)	8.90E-19 (4.52E-21)
5	1	1	with	2.82E-18 (1.71E-20)	2.36E-18 (1.45E-20)	8.67E-19 (5.13E-21)	2.88E-19 (2.32E-21)
			without	2.46E-18 (1.58E-20)	1.90E-18 (1.30E-20)	6.29E-19 (4.62E-21)	2.56E-19 (2.39E-21)
5	2		with	3.36E-17 (6.95E-20)	2.54E-17 (5.72E-20)	6.74E-18 (1.97E-20)	2.31E-18 (9.87E-21)
			without	3.06E-17 (6.52E-20)	2.34E-17 (5.38E-20)	7.00E-18 (1.94E-20)	2.50E-18 (1.03E-20)
5	2	0	with	1.26E-17 (4.16E-20)	8.68E-18 (3.29E-20)	1.92E-18 (1.11E-20)	7.15E-19 (5.65E-21)
			without	1.30E-17 (4.18E-20)	9.98E-18 (3.45E-20)	2.99E-18 (1.26E-20)	1.08E-18 (6.79E-21)
5	2	1	with	1.02E-17 (3.90E-20)	8.00E-18 (3.25E-20)	2.29E-18 (1.12E-20)	7.61E-19 (5.60E-21)
			without	7.97E-18 (3.39E-20)	6.07E-18 (2.78E-20)	1.84E-18 (9.96E-21)	6.52E-19 (5.22E-21)
5	2	2	with	3.82E-19 (7.76E-21)	3.19E-19 (6.78E-21)	1.16E-19 (2.63E-21)	3.73E-20 (1.25E-21)
			without	7.97E-19 (1.10E-20)	6.22E-19 (9.18E-21)	1.71E-19 (3.20E-21)	5.63E-20 (1.60E-21)
5	3		with	5.04E-17 (1.20E-19)	3.90E-17 (1.01E-19)	9.68E-18 (3.26E-20)	2.60E-18 (1.41E-20)
			without	5.09E-17 (1.15E-19)	3.78E-17 (9.40E-20)	8.99E-18 (3.11E-20)	2.44E-18 (1.42E-20)
5	3	0	with	1.52E-17 (6.79E-20)	1.23E-17 (5.81E-20)	3.62E-18 (2.04E-20)	1.09E-18 (9.22E-21)
			without	1.73E-17 (6.70E-20)	1.29E-17 (5.51E-20)	3.21E-18 (1.88E-20)	9.42E-19 (8.95E-21)
5	3	1	with	1.51E-17 (6.57E-20)	1.16E-17 (5.48E-20)	2.64E-18 (1.69E-20)	6.99E-19 (7.24E-21)
			without	1.30E-17 (5.86E-20)	9.66E-18 (4.79E-20)	2.34E-18 (1.59E-20)	6.26E-19 (7.21E-21)
5	3	2	with	2.47E-18 (2.64E-20)	1.81E-18 (2.14E-20)	3.59E-19 (6.08E-21)	6.93E-20 (2.23E-21)
			without	3.79E-18 (3.12E-20)	2.76E-18 (2.52E-20)	5.58E-19 (7.50E-21)	1.12E-19 (2.90E-21)
5	3	3	with	8.54E-21 (1.40E-21)	5.65E-21 (1.13E-21)	-	-
			without	4.09E-20 (2.90E-21)	2.38E-20 (2.09E-21)	-	-
5	4		with	2.75E-17 (1.07E-19)	1.67E-17 (7.87E-20)	1.07E-18 (1.26E-20)	4.39E-20 (2.14E-21)
			without	2.64E-17 (9.97E-20)	1.73E-17 (7.64E-20)	1.90E-18 (1.67E-20)	6.82E-18 (1.67E-20)
5	4	0	with	9.83E-18 (6.43E-20)	6.39E-18 (4.91E-20)	4.94E-19 (8.64E-21)	2.51E-20 (1.62E-21)
			without	9.08E-18 (5.91E-20)	6.11E-18 (4.60E-20)	7.54E-19 (1.06E-20)	8.45E-20 (3.03E-21)
5	4	1	with	7.11E-18 (5.43E-20)	4.38E-18 (4.04E-20)	2.62E-19 (6.24E-21)	9.15E-21 (9.70E-22)
			without	6.80E-18 (5.08E-20)	4.39E-18 (3.87E-20)	4.93E-19 (8.50E-21)	4.26E-20 (2.14E-21)
5	4	2	with	1.61E-18 (2.52E-20)	8.07E-19 (1.69E-20)	2.36E-20 (1.82E-21)	-
			without	1.92E-18 (2.62E-20)	1.19E-18 (1.95E-20)	7.69E-20 (3.24E-21)	-
5	4	3	with	1.35E-20 (2.16E-21)	4.95E-21 (1.24E-21)	-	-
			without	2.89E-20 (2.97E-21)	1.30E-20 (1.87E-21)	-	-
5	4	4	with	-	-	-	-
			without	-	-	-	-

TABLE VI. Cross Sections for Electron Capture and statistical error values (in parenthesis) from H(1s) by C^{6+}

See page 93 for Explanation of Tables

$C^{6+} + H(1s) \rightarrow C^{5+}(nlm) + H^{+}$

Final state			correction	Energy (keV/amu)			
n	*l*	*m*		10	20	30	40
1	0	0	with	4.23E-20 (1.06E-21)	7.14E-20 (1.51E-21)	9.67E-20 (1.79E-21)	1.13E-19 (1.77E-21)
			without	2.57E-20 (2.74E-21)	1.82E-20 (2.68E-21)	1.12E-20 (1.65E-21)	9.99E-21 (1.13E-21)
2			with	1.99E-18 (1.71E-20)	2.70E-18 (2.08E-20)	3.29E-18 (2.25E-20)	3.74E-18 (2.11E-20)
			without	9.34E-19 (1.07E-20)	2.36E-18 (1.89E-20)	4.33E-18 (2.58E-20)	6.46E-18 (2.83E-20)
2	0	0	with	5.65E-19 (9.00E-21)	9.96E-19 (1.34E-20)	1.33E-18 (1.53E-20)	1.43E-18 (1.38E-20)
			without	4.24E-19 (7.40E-21)	7.55E-19 (1.12E-20)	1.18E-18 (1.45E-20)	1.65E-18 (1.58E-20)
2	1		with	1.42E-18 (1.46E-20)	1.71E-18 (1.60E-20)	1.97E-18 (1.67E-20)	2.31E-18 (1.60E-20)
			without	5.10E-19 (7.74E-21)	1.61E-18 (1.52E-20)	3.15E-18 (2.15E-20)	4.81E-18 (2.37E-20)
2	1	0	with	3.57E-19 (6.68E-21)	3.98E-19 (6.64E-21)	3.89E-19 (6.00E-21)	4.52E-19 (5.60E-21)
			without	1.91E-19 (4.51E-21)	4.94E-19 (7.55E-21)	9.43E-19 (1.03E-20)	1.45E-18 (1.12E-20)
2	1	1	with	5.45E-19 (9.40E-21)	6.32E-19 (1.03E-20)	7.82E-19 (1.14E-20)	9.24E-19 (1.10E-20)
			without	1.68E-19 (4.57E-21)	5.96E-19 (9.88E-21)	1.20E-18 (1.43E-20)	1.78E-18 (1.59E-20)
3			with	2.13E-16 (3.57E-19)	2.99E-16 (4.20E-19)	3.16E-16 (3.75E-19)	2.68E-16 (2.92E-19)
			without	4.02E-16 (3.71E-19)	4.41E-16 (3.84E-19)	4.17E-16 (3.62E-19)	3.45E-16 (2.97E-19)
3	0	0	with	4.50E-17 (1.98E-19)	4.01E-17 (1.78E-19)	2.56E-17 (1.24E-19)	1.70E-17 (8.06E-20)
			without	3.72E-17 (1.10E-19)	3.19E-17 (1.04E-19)	2.43E-17 (9.31E-20)	1.70E-17 (6.91E-20)
3	1		with	6.63E-17 (2.09E-19)	8.57E-17 (2.28E-19)	8.23E-17 (2.05E-19)	6.63E-17 (1.51E-19)
			without	1.42E-16 (2.32E-19)	1.52E-16 (2.36E-19)	1.34E-16 (2.22E-19)	1.05E-16 (1.76E-19)
3	1	0	with	1.99E-17 (1.04E-19)	3.05E-17 (1.29E-19)	3.27E-17 (1.24E-19)	2.79E-17 (9.59E-20)
			without	5.57E-17 (1.44E-19)	5.37E-17 (1.35E-19)	4.95E-17 (1.28E-19)	4.15E-17 (1.06E-19)
3	1	1	with	2.38E-17 (1.32E-19)	2.82E-17 (1.36E-19)	2.50E-17 (1.17E-19)	1.93E-17 (8.38E-20)
			without	4.38E-17 (1.32E-19)	4.92E-17 (1.41E-19)	4.22E-17 (1.31E-19)	3.19E-17 (1.01E-19)
3	2		with	1.02E-16 (2.30E-19)	1.73E-16 (3.16E-19)	2.08E-16 (2.99E-19)	1.85E-16 (2.42E-19)
			without	2.22E-16 (2.85E-19)	2.57E-16 (3.02E-19)	2.59E-16 (2.87E-19)	2.22E-16 (2.40E-19)
3	2	0	with	3.11E-17 (1.14E-19)	4.05E-17 (1.45E-19)	4.50E-17 (1.24E-19)	4.01E-17 (1.01E-19)
			without	4.11E-17 (1.13E-19)	4.64E-17 (1.19E-19)	5.45E-17 (1.19E-19)	5.10E-17 (1.04E-19)
3	2	1	with	2.54E-17 (1.19E-19)	4.93E-17 (1.72E-19)	6.08E-17 (1.67E-19)	5.48E-17 (1.37E-19)
			without	4.20E-17 (1.25E-19)	4.86E-17 (1.32E-19)	5.32E-17 (1.31E-19)	4.84E-17 (1.14E-19)
3	2	2	with	1.04E-17 (8.56E-20)	1.73E-17 (1.08E-19)	2.04E-17 (1.09E-19)	1.85E-16 (2.42E-19)
			without	4.87E-17 (1.46E-19)	5.68E-17 (1.58E-19)	4.92E-17 (1.46E-19)	3.74E-17 (1.15E-19)

TABLE VI. Cross Sections for Electron Capture and statistical error values (in parenthesis) from H(1s) by C^{6+}

See page 93 for Explanation of Tables

Final state			correction	Energy (keV/amu)			
n	*l*	*m*		10	20	30	40
4			with	3.03E-15 (1.49E-18)	2.35E-15 (1.18E-18)	1.57E-15 (9.39E-19)	1.07E-15 (6.69E-19)
			without	2.27E-15 (9.49E-19)	2.07E-15 (8.38E-19)	1.53E-15 (7.44E-19)	1.07E-15 (5.85E-19)
4	0	0	with	1.15E-16 (3.37E-19)	4.63E-17 (1.79E-19)	2.74E-17 (1.17E-19)	1.87E-17 (7.78E-20)
			without	3.33E-17 (1.12E-19)	1.33E-17 (7.13E-20)	1.39E-17 (6.17E-20)	1.11E-17 (5.00E-20)
4	1		with	2.46E-16 (4.44E-19)	1.41E-16 (3.10E-19)	9.58E-17 (2.23E-19)	7.00E-17 (1.54E-19)
			without	1.54E-16 (2.36E-19)	1.32E-16 (2.11E-19)	1.18E-16 (1.90E-19)	8.66E-17 (1.46E-19)
4	1	0	with	1.01E-16 (2.68E-19)	7.14E-17 (2.13E-19)	5.27E-17 (1.64E-19)	3.90E-17 (1.14E-19)
			without	8.60E-17 (1.79E-19)	8.80E-17 (1.66E-19)	7.21E-17 (1.47E-19)	5.01E-17 (1.11E-19)
4	1	1	with	7.26E-17 (2.57E-19)	3.47E-17 (1.62E-19)	2.17E-17 (1.10E-19)	1.56E-17 (7.38E-20)
			without	3.39E-17 (1.12E-19)	2.21E-17 (9.56E-20)	2.28E-17 (8.72E-20)	1.83E-17 (6.87E-20)
4	2		with	8.48E-16 (8.69E-19)	6.65E-16 (6.55E-19)	4.28E-16 (4.73E-19)	2.72E-16 (3.09E-19)
			without	5.68E-16 (5.29E-19)	5.54E-16 (4.69E-19)	4.25E-16 (3.94E-19)	2.81E-16 (2.83E-19)
4	2	0	with	2.86E-16 (5.08E-19)	2.43E-16 (3.81E-19)	1.56E-16 (2.80E-19)	1.00E-16 (1.86E-19)
			without	2.13E-16 (3.42E-19)	2.14E-16 (2.90E-19)	1.59E-16 (2.40E-19)	1.05E-16 (1.71E-19)
4	2	1	with	2.21E-16 (4.60E-19)	1.84E-16 (3.69E-19)	1.24E-16 (2.68E-19)	7.97E-17 (1.75E-19)
			without	1.50E-16 (2.79E-19)	1.51E-16 (2.62E-19)	1.16E-16 (2.19E-19)	7.61E-17 (1.55E-19)
4	2	2	with	6.05E-17 (2.54E-19)	2.68E-17 (1.56E-19)	1.19E-17 (8.85E-20)	6.19E-18 (5.07E-20)
			without	2.75E-17 (1.23E-19)	1.92E-17 (1.04E-19)	1.68E-17 (8.72E-20)	1.21E-17 (6.38E-20)
4	3		with	1.82E-15 (1.30E-18)	1.50E-15 (1.07E-18)	1.02E-15 (8.76E-19)	7.07E-16 (6.38E-19)
			without	1.52E-15 (9.27E-19)	1.37E-15 (8.29E-19)	9.71E-16 (7.31E-19)	6.92E-16 (5.69E-19)
4	3	0	with	4.91E-16 (6.97E-19)	3.85E-16 (5.56E-19)	2.71E-16 (4.54E-19)	1.92E-16 (3.34E-19)
			without	3.93E-16 (5.26E-19)	3.72E-16 (4.59E-19)	2.64E-16 (3.93E-19)	1.90E-16 (3.04E-19)
4	3	1	with	4.06E-16 (6.60E-19)	3.68E-16 (5.65E-19)	2.60E-16 (4.65E-19)	1.89E-16 (3.43E-19)
			without	3.49E-16 (4.94E-19)	3.22E-16 (4.43E-19)	2.28E-16 (3.79E-19)	1.64E-16 (2.91E-19)
4	3	2	with	2.31E-16 (5.14E-19)	1.80E-16 (4.30E-19)	1.10E-16 (3.21E-19)	6.71E-17 (2.14E-19)
			without	1.98E-16 (3.60E-19)	1.70E-16 (3.34E-19)	1.20E-16 (2.84E-19)	8.37E-17 (2.13E-19)
4	3	3	with	2.57E-17 (1.70E-19)	9.24E-18 (9.97E-20)	2.88E-18 (5.14E-20)	1.06E-18 (2.57E-20)
			without	1.49E-17 (9.69E-20)	8.48E-18 (7.45E-20)	5.36E-18 (5.71E-20)	3.88E-18 (4.24E-20)

TABLE VI. Cross Sections for Electron Capture and statistical error values (in parenthesis) from H(1s) by C^{6+}

See page 93 for Explanation of Tables

Final state			correction	Energy (keV/amu)			
n	*l*	*m*		10	20	30	40
5			with	1.78E-15 (1.23E-18)	1.42E-15 (1.15E-18)	1.24E-15 (9.85E-19)	9.67E-16 (7.36E-19)
			without	2.61E-16 (3.20E-19)	3.27E-16 (4.74E-19)	6.03E-16 (5.87E-19)	7.07E-16 (5.33E-19)
5	0	0	with	2.17E-17 (1.25E-19)	1.58E-17 (9.45E-20)	1.44E-17 (8.43E-20)	1.13E-17 (6.41E-20)
			without	1.25E-17 (6.32E-20)	4.56E-18 (6.13E-20)	3.99E-18 (4.18E-20)	6.15E-18 (3.54E-20)
5	1		with	8.38E-17 (2.59E-19)	5.21E-17 (1.96E-19)	4.92E-17 (1.66E-19)	4.21E-17 (1.26E-19)
			without	3.17E-17 (1.03E-19)	1.71E-17 (1.21E-19)	3.25E-17 (1.02E-19)	5.00E-17 (1.04E-19)
5	1	0	with	5.28E-17 (2.07E-19)	3.53E-17 (1.56E-19)	3.37E-17 (1.37E-19)	2.85E-17 (1.04E-19)
			without	2.17E-17 (9.02E-20)	1.15E-17 (9.93E-20)	2.62E-17 (8.90E-20)	3.62E-17 (8.81E-20)
5	1	1	with	1.54E-17 (1.11E-19)	8.30E-18 (8.57E-20)	7.75E-18 (6.74E-20)	6.79E-18 (5.04E-20)
			without	5.05E-18 (3.76E-20)	2.77E-18 (4.91E-20)	3.09E-18 (3.68E-20)	6.92E-18 (4.01E-20)
5	2		with	1.90E-16 (3.69E-19)	1.79E-16 (3.47E-19)	1.69E-16 (2.91E-19)	1.31E-16 (2.14E-19)
			without	5.13E-17 (1.36E-19)	4.37E-17 (1.76E-19)	9.69E-17 (1.89E-19)	1.22E-16 (1.80E-19)
5	2	0	with	9.13E-17 (2.45E-19)	8.51E-17 (2.27E-19)	7.78E-17 (1.91E-19)	5.95E-17 (1.42E-19)
			without	2.63E-17 (9.82E-20)	2.06E-17 (1.12E-19)	5.10E-17 (1.30E-19)	5.90E-17 (1.21E-19)
5	2	1	with	4.55E-17 (1.90E-19)	4.56E-17 (1.87E-19)	4.43E-17 (1.57E-19)	3.47E-17 (1.14E-19)
			without	1.15E-17 (6.37E-20)	1.06E-17 (9.43E-20)	2.22E-17 (9.79E-20)	3.04E-17 (9.47E-20)
5	2	2	with	3.73E-18 (6.18E-20)	1.23E-18 (3.61E-20)	1.19E-18 (2.70E-20)	1.09E-18 (2.08E-20)
			without	1.02E-18 (2.13E-20)	8.81E-19 (2.64E-20)	9.56E-19 (2.46E-20)	1.23E-18 (2.08E-20)
5	3		with	4.86E-16 (6.37E-19)	3.87E-16 (5.78E-19)	3.10E-16 (4.94E-19)	2.48E-16 (3.73E-19)
			without	8.21E-17 (1.89E-19)	9.87E-17 (2.50E-19)	1.70E-16 (3.23E-19)	1.97E-16 (3.09E-19)
5	3	0	with	1.81E-16 (3.84E-19)	1.40E-16 (3.36E-19)	1.15E-16 (2.97E-19)	9.13E-17 (2.23E-19)
			without	3.50E-17 (1.26E-19)	3.76E-17 (1.41E-19)	6.31E-17 (1.91E-19)	6.98E-17 (1.83E-19)
5	3	1	with	1.26E-16 (3.30E-19)	1.01E-16 (3.05E-19)	8.10E-17 (2.59E-19)	6.58E-17 (1.97E-19)
			without	2.07E-17 (9.38E-20)	2.45E-17 (1.32E-19)	4.31E-17 (1.67E-19)	4.98E-17 (1.58E-19)
5	3	2	with	2.66E-17 (1.75E-19)	2.27E-17 (1.58E-19)	1.64E-17 (1.21E-19)	1.20E-17 (8.67E-20)
			without	2.66E-18 (4.01E-20)	6.04E-18 (7.27E-20)	1.05E-17 (8.52E-20)	1.35E-17 (8.29E-20)
5	3	3	with	7.16E-19 (2.51E-20)	5.73E-20 (6.90E-21)	5.21E-20 (5.72E-21)	4.41E-20 (4.32E-21)
			without	2.45E-19 (9.27E-21)	3.43E-20 (3.54E-21)	2.91E-20 (3.67E-21)	1.29E-19 (7.04E-21)
5	4		with	9.99E-16 (1.08E-18)	7.92E-16 (1.04E-18)	6.92E-16 (9.19E-19)	5.35E-16 (6.86E-19)
			without	8.37E-17 (2.03E-19)	1.63E-16 (3.48E-19)	8.28E-21 (1.62E-21)	3.32E-16 (4.91E-19)
5	4	0	with	2.92E-16 (6.01E-19)	2.20E-16 (5.52E-19)	1.94E-16 (4.89E-19)	1.49E-16 (3.65E-19)
			without	2.95E-17 (1.27E-19)	5.73E-17 (2.03E-19)	9.79E-17 (3.03E-19)	1.03E-16 (2.79E-19)
5	4	1	with	2.49E-16 (5.60E-19)	1.91E-16 (5.23E-19)	1.69E-16 (4.65E-19)	1.33E-16 (3.50E-19)
			without	2.12E-17 (1.02E-19)	4.04E-17 (1.79E-19)	7.40E-17 (2.64E-19)	8.09E-17 (2.47E-19)
5	4	2	with	9.99E-17 (3.58E-19)	9.09E-17 (3.67E-19)	7.54E-17 (3.15E-19)	5.60E-17 (2.29E-19)
			without	4.99E-18 (4.50E-20)	1.17E-17 (9.41E-20)	2.57E-17 (1.51E-19)	3.20E-17 (1.52E-19)
5	4	3	with	4.73E-18 (7.30E-20)	3.79E-18 (7.03E-20)	4.26E-18 (7.10E-20)	3.44E-18 (5.41E-20)
			without	7.64E-19 (1.76E-20)	5.86E-19 (1.77E-20)	1.23E-18 (2.96E-20)	2.17E-18 (3.69E-20)
5	4	4	with	4.40E-19 (2.05E-20)	5.28E-20 (6.71E-21)	2.04E-20 (3.85E-21)	-
			without	8.94E-20 (6.14E-21)	2.11E-20 (2.74E-21)	8.28E-21 (1.62E-21)	-

TABLE VI. Cross Sections for Electron Capture and statistical error values (in parenthesis) from H(1s) by C^{6+}

See page 93 for Explanation of Tables

$C^{6+} + H(1s) \rightarrow C^{5+}(nlm) + H^{+}$

Final state			correction	Energy (keV/amu)			
n	*l*	*m*		50	60	70	80
1	0	0	with	1.25E-19 (1.83E-21)	1.34E-19 (1.84E-21)	1.41E-19 (1.85E-21)	1.44E-19 (1.57E-21)
			without	7.27E-21 (7.09E-22)	8.41E-21 (6.53E-22)	9.31E-21 (6.11E-22)	9.78E-21 (4.95E-22)
2			with	3.97E-18 (2.06E-20)	4.24E-18 (2.08E-20)	4.43E-18 (2.07E-20)	4.50E-18 (1.78E-20)
			without	8.30E-18 (3.07E-20)	9.67E-18 (3.31E-20)	1.03E-17 (3.27E-20)	1.03E-17 (2.83E-20)
2	0	0	with	1.44E-18 (1.29E-20)	1.48E-18 (1.27E-20)	1.50E-18 (1.23E-20)	1.46E-18 (1.03E-20)
			without	2.02E-18 (1.73E-20)	2.28E-18 (1.88E-20)	2.38E-18 (1.86E-20)	2.37E-18 (1.61E-20)
2	1		with	2.53E-18 (1.62E-20)	2.76E-18 (1.65E-20)	2.93E-18 (1.66E-20)	3.04E-18 (1.45E-20)
			without	6.29E-18 (2.58E-20)	7.39E-18 (2.78E-20)	7.87E-18 (2.75E-20)	7.94E-18 (2.39E-20)
2	1	0	with	5.04E-19 (5.73E-21)	6.02E-19 (6.29E-21)	6.88E-19 (6.71E-21)	7.28E-19 (6.00E-21)
			without	1.99E-18 (1.24E-20)	2.47E-18 (1.38E-20)	2.64E-18 (1.37E-20)	2.70E-18 (1.19E-20)
2	1	1	with	1.03E-18 (1.12E-20)	1.09E-18 (1.12E-20)	1.13E-18 (1.11E-20)	1.15E-18 (9.60E-21)
			without	2.28E-18 (1.72E-20)	2.57E-18 (1.83E-20)	2.71E-18 (1.81E-20)	2.71E-18 (1.57E-20)
3			with	2.15E-16 (2.44E-19)	1.70E-16 (2.07E-19)	1.34E-16 (1.75E-19)	1.05E-16 (1.31E-19)
			without	2.75E-16 (2.51E-19)	2.19E-16 (2.20E-19)	1.72E-16 (1.84E-19)	1.36E-16 (1.40E-19)
3	0	0	with	1.18E-17 (5.97E-20)	8.49E-18 (4.63E-20)	6.39E-18 (3.70E-20)	4.76E-18 (2.60E-20)
			without	1.21E-17 (5.41E-20)	8.68E-18 (4.38E-20)	6.37E-18 (3.46E-20)	4.68E-18 (2.46E-20)
3	1		with	5.06E-17 (1.18E-19)	3.83E-17 (9.34E-20)	2.94E-17 (7.52E-20)	2.27E-17 (5.42E-20)
			without	7.96E-17 (1.41E-19)	5.98E-17 (1.17E-19)	4.42E-17 (9.27E-20	3.29E-17 (6.67E-20)
3	1	0	with	2.16E-17 (7.51E-20)	1.64E-17 (5.95E-20)	1.24E-17 (4.74E-20)	9.67E-18 (3.43E-20)
			without	3.32E-17 (8.86E-20)	2.60E-17 (7.54E-20)	1.98E-17 (6.08E-20)	1.53E-17 (4.47E-20)
3	1	1	with	1.45E-17 (6.46E-20)	1.10E-17 (5.15E-20)	8.46E-18 (4.17E-20)	6.48E-18 (3.00E-20)
			without	2.31E-17 (7.88E-20)	1.69E-17 (6.43E-20)	1.22E-17 (5.02E-20)	8.71E-18 (3.52E-20)
3	2		with	1.53E-16 (2.09E-19)	1.23E-16 (1.82E-19)	9.81E-17 (1.58E-19)	7.76E-17 (1.19E-19)
			without	1.83E-16 (2.07E-19)	1.51E-16 (1.86E-19)	1.22E-16 (1.59E-19)	9.82E-17 (1.23E-19)
3	2	0	with	3.41E-17 (8.96E-20)	2.82E-17 (7.99E-20)	2.26E-17 (7.03E-20)	1.85E-17 (5.48E-20)
			without	4.48E-17 (9.32E-20)	3.92E-17 (8.69E-20)	3.35E-17 (7.70E-20)	2.82E-17 (6.09E-20)
3	2	1	with	4.60E-17 (1.19E-19)	3.74E-17 (1.04E-19)	2.99E-17 (8.97E-20)	2.39E-17 (6.82E-20)
			without	4.22E-17 (1.02E-19)	3.62E-17 (9.42E-20)	3.01E-17 (8.20E-20)	2.48E-17 (6.39E-20)
3	2	2	with	1.33E-17 (6.99E-20)	9.92E-18 (5.75E-20)	7.57E-18 (4.78E-20)	5.49E-18 (3.41E-20)
			without	2.71E-17 (9.25E-20)	1.96E-17 (7.71E-20)	1.39E-17 (6.14E-20)	1.02E-17 (4.45E-20)

TABLE VI. Cross Sections for Electron Capture and statistical error values (in parenthesis) from H(1s) by C^{6+}

See page 93 for Explanation of Tables

Final State			correction	Energy (keV/amu)			
n	*l*	*m*		50	60	70	80
4			with	7.39E-16 (5.21E-19)	5.18E-16 (4.17E-19)	3.72E-16 (3.35E-19)	2.69E-16 (2.38E-19)
			without	7.55E-16 (4.71E-19)	5.36E-16 (3.96E-19)	3.87E-16 (3.18E-19)	2.80E-16 (2.31E-19)
4	0	0	with	1.34E-17 (5.92E-20)	9.49E-18 (4.62E-20)	7.03E-18 (3.71E-20)	5.22E-18 (2.63E-20)
			without	8.45E-18 (4.19E-20)	6.38E-18 (3.57E-20)	4.95E-18 (2.97E-20)	3.76E-18 (2.19E-20)
4	1		with	5.30E-17 (1.20E-19)	3.97E-17 (9.56E-20)	3.08E-17 (7.77E-20)	2.38E-17 (5.59E-20)
			without	6.25E-17 (1.16E-19)	4.49E-17 (9.51E-20)	3.27E-17 (7.57E-20)	2.40E-17 (5.46E-20)
4	1	0	with	2.94E-17 (8.91E-20)	2.19E-17 (7.11E-20)	1.69E-17 (5.80E-20)	1.29E-17 (4.14E-20)
			without	3.52E-17 (8.65E-20)	2.50E-17 (7.07E-20)	1.81E-17 (5.61E-20)	1.33E-17 (4.06E-20)
4	1	1	with	1.18E-17 (5.75E-20)	8.93E-18 (4.56E-20)	6.92E-18 (3.70E-20)	5.44E-18 (2.68E-20)
			without	1.37E-17 (5.54E-20)	1.00E-17 (4.57E-20)	7.35E-18 (3.64E-20)	5.39E-18 (2.62E-20)
4	2		with	1.80E-16 (2.29E-19)	1.26E-16 (1.80E-19)	9.28E-17 (1.45E-19)	6.95E-17 (1.05E-19)
			without	1.87E-16 (2.15E-19)	1.28E-16 (1.73E-19)	9.10E-17 (1.36E-19)	6.63E-17 (9.82E-20)
4	2	0	with	6.68E-17 (1.38E-19)	4.67E-17 (1.08E-19)	3.44E-17 (8.67E-20)	2.56E-17 (6.20E-20)
			without	7.00E-17 (1.29E-19)	4.77E-17 (1.03E-19)	3.44E-17 (8.16E-20)	2.52E-17 (5.86E-20)
4	2	1	with	5.30E-17 (1.29E-19)	3.71E-17 (1.01E-19)	2.75E-17 (8.14E-20)	2.07E-17 (5.88E-20)
			without	5.02E-17 (1.16E-19)	3.44E-17 (9.30E-20)	2.45E-17 (7.33E-20)	1.78E-17 (5.26E-20)
4	2	2	with	3.64E-18 (3.49E-20)	2.40E-18 (2.65E-20)	1.68E-18 (2.08E-20)	1.21E-18 (1.46E-20)
			without	8.12E-18 (4.82E-20)	5.51E-18 (3.84E-20)	3.80E-18 (2.98E-20)	2.73E-18 (2.14E-20)
4	3		with	4.93E-16 (5.01E-19)	3.44E-16 (4.02E-19)	2.42E-16 (3.24E-19)	1.71E-16 (2.30E-19)
			without	4.97E-16 (4.56E-19)	3.57E-16 (3.81E-19)	2.58E-16 (3.05E-19)	1.86E-16 (2.21E-19)
4	3	0	with	1.35E-16 (2.64E-19)	9.47E-17 (2.13E-19)	6.69E-17 (1.74E-19)	4.77E-17 (1.26E-19)
			without	1.40E-16 (2.45E-19)	1.03E-16 (2.05E-19)	7.58E-17 (1.65E-19)	5.56E-17 (1.20E-19)
4	3	1	with	1.36E-16 (2.72E-19)	9.78E-17 (2.19E-19)	6.95E-17 (1.76E-19)	4.93E-17 (1.24E-19)
			without	1.19E-16 (2.33E-19)	8.58E-17 (1.94E-19)	6.27E-17 (1.55E-19)	4.53E-17 (1.12E-19)
4	3	2	with	4.17E-17 (1.56E-19)	2.63E-17 (1.16E-19)	1.75E-17 (8.94E-20)	1.18E-17 (6.07E-20)
			without	5.71E-17 (1.64E-19)	3.96E-17 (1.33E-19)	2.73E-17 (1.03E-19)	1.90E-17 (7.29E-20)
4	3	3	with	4.76E-19 (1.56E-20)	2.79E-19 (1.13E-20)	1.44E-19 (7.65E-21)	1.03E-19 (5.41E-21)
			without	2.61E-18 (3.21E-20)	1.76E-18 (2.55E-20)	1.14E-18 (1.92E-20)	7.48E-19 (1.31E-20)

TABLE VI. Cross Sections for Electron Capture and statistical error values (in parenthesis) from H(1s) by C^{6+}

See page 93 for Explanation of Tables

Final state			correction	Energy (keV/amu)			
n	*l*	*m*		50	60	70	80
5			with	7.18E-16 (5.83E-19)	5.26E-16 (4.70E-19)	3.81E-16 (3.75E-19)	2.80E-16 (2.67E-19)
			without	6.19E-16 (4.68E-19)	4.85E-16 (4.10E-19)	3.67E-16 (3.36E-19)	2.72E-16 (2.46E-19)
5	0	0	with	8.63E-18 (5.01E-20)	6.86E-18 (4.10E-20)	5.40E-18 (3.38E-20)	4.05E-18 (2.41E-20)
			without	5.58E-18 (3.31E-20)	4.51E-18 (2.97E-20)	3.55E-18 (2.52E-20)	2.74E-18 (1.89E-20)
5	1		with	3.53E-17 (1.02E-19)	2.87E-17 (8.47E-20)	2.31E-17 (7.03E-20)	1.81E-17 (5.07E-20)
			without	4.19E-17 (9.08E-20)	3.16E-17 (7.79E-20)	2.35E-17 (6.33E-20)	1.75E-17 (4.63E-20)
5	1	0	with	2.34E-17 (8.39E-20)	1.88E-17 (6.91E-20)	1.49E-17 (5.68E-20)	1.13E-17 (4.04E-20)
			without	2.78E-17 (7.39E-20)	2.02E-17 (6.24E-20)	1.46E-17 (5.02E-20)	1.07E-17 (3.64E-20)
5	1	1	with	5.93E-18 (4.18E-20)	4.90E-18 (3.46E-20)	4.11E-18 (2.94E-20)	3.42E-18 (2.19E-20)
			without	7.05E-18 (3.77E-20)	5.72E-18 (3.32E-20)	4.45E-18 (2.75E-20)	3.40E-18 (2.05E-20)
5	2		with	9.96E-17 (1.71E-19)	7.71E-17 (1.42E-19)	6.03E-17 (1.18E-19)	4.76E-17 (8.75E-20)
			without	1.02E-16 (1.54E-19)	7.72E-17 (1.31E-19)	5.80E-17 (1.07E-19)	4.34E-17 (7.84E-20)
5	2	0	with	4.44E-17 (1.13E-19)	3.37E-17 (9.30E-20)	2.60E-17 (7.67E-20)	2.02E-17 (5.59E-20)
			without	4.67E-17 (1.01E-19)	3.38E-17 (8.44E-20)	2.48E-17 (6.81E-20)	1.84E-17 (4.99E-20)
5	2	1	with	2.67E-17 (9.10E-20)	2.10E-17 (7.59E-20)	1.66E-17 (6.37E-20)	1.33E-17 (4.72E-20)
			without	2.63E-17 (8.13E-20)	2.01E-17 (6.92E-20)	1.53E-17 (5.67E-20)	1.14E-17 (4.14E-20)
5	2	2	with	9.27E-19 (1.76E-20)	6.97E-19 (1.42E-20)	5.24E-19 (1.16E-20)	4.38E-19 (8.88E-21)
			without	1.59E-18 (2.06E-20)	1.50E-18 (1.93E-20)	1.31E-18 (1.69E-20)	1.05E-18 (1.29E-20)
5	3		with	1.94E-16 (3.05E-19)	1.50E-16 (2.53E-19)	1.16E-16 (2.10E-19)	8.74E-17 (1.53E-19)
			without	1.77E-16 (2.70E-19)	1.43E-16 (2.34E-19)	1.12E-16 (1.93E-19)	8.65E-17 (1.43E-19)
5	3	0	with	6.86E-17 (1.79E-19)	5.09E-17 (1.45E-19)	3.68E-17 (1.16E-19)	2.56E-17 (8.17E-20)
			without	6.06E-17 (1.57E-19)	4.79E-17 (1.34E-19)	3.71E-17 (1.10E-19)	2.83E-17 (8.05E-20)
5	3	1	with	5.36E-17 (1.64E-19)	4.23E-17 (1.37E-19)	3.40E-17 (1.16E-19)	2.64E-17 (8.54E-20)
			without	4.46E-17 (1.38E-19)	3.58E-17 (1.20E-19)	2.80E-17 (9.84E-20)	2.15E-17 (7.29E-20)
5	3	2	with	9.16E-18 (6.92E-20)	7.19E-18 (5.79E-20)	5.67E-18 (4.89E-20)	4.53E-18 (3.65E-20)
			without	1.36E-17 (7.66E-20)	1.17E-17 (6.89E-20)	9.45E-18 (5.81E-20)	7.37E-18 (4.35E-20)
5	3	3	with	4.22E-20 (4.20E-21)	3.32E-20 (3.62E-21)	3.11E-20 (3.45E-21)	2.11E-20 (2.30E-21)
			without	2.11E-19 (8.61E-21)	2.40E-19 (9.07E-21)	2.43E-19 (8.56E-21)	1.94E-19 (6.48E-21)
5	4		with	3.80E-16 (5.40E-19)	2.63E-16 (4.30E-19)	1.77E-16 (3.38E-19)	1.23E-16 (2.38E-19)
			without	2.92E-16 (4.30E-19)	2.28E-16 (3.71E-19)	1.70E-16 (3.00E-19)	1.22E-16 (2.16E-19)
5	4	0	with	1.06E-16 (2.89E-19)	7.29E-17 (2.31E-19)	4.92E-17 (1.84E-19)	3.56E-17 (1.32E-19)
			without	8.86E-17 (2.41E-19)	6.85E-17 (2.07E-19)	5.09E-17 (1.67E-19)	3.64E-17 (1.20E-19)
5	4	1	with	9.64E-17 (2.76E-19)	6.78E-17 (2.21E-19)	4.64E-17 (1.74E-19)	3.25E-17 (1.23E-19)
			without	7.01E-17 (2.15E-19)	5.44E-17 (1.84E-19)	4.06E-17 (1.49E-19)	2.92E-17 (1.07E-19)
5	4	2	with	3.87E-17 (1.76E-19)	2.59E-17 (1.36E-19)	1.67E-17 (1.04E-19)	1.08E-17 (6.97E-20)
			without	2.97E-17 (1.37E-19)	2.34E-17 (1.19E-19)	1.75E-17 (9.62E-20)	1.24E-17 (6.88E-20)
5	4	3	with	2.34E-18 (4.14E-20)	1.28E-18 (2.90E-20)	7.21E-19 (2.05E-20)	4.24E-19 (1.32E-20)
			without	2.50E-18 (3.72E-20)	2.21E-18 (3.43E-20)	1.66E-18 (2.79E-20)	1.17E-18 (1.99E-20)
5	4	4	with	-	-	-	-
			without	-	-	-	-

TABLE VI. Cross Sections for Electron Capture and statistical error values (in parenthesis) from H(1s) by C^{6+}

See page 93 for Explanation of Tables

$C^{6+} + H(1s) \rightarrow C^{5+}(nlm) + H^{+}$

Final state			correction	Energy (keV/amu)			
n	*l*	*m*		90	100	150	200
1	0	0	with	1.47E-19 (1.53E-21)	1.44E-19 (1.39E-21)	1.66E-19 (1.03E-21)	2.08E-19 (1.06E-21)
			without	1.20E-20 (5.16E-22)	1.42E-20 (5.33E-22)	2.79E-20 (5.10E-22)	4.15E-20 (5.73E-22)
2			with	4.50E-18 (1.71E-20)	4.37E-18 (1.57E-20)	3.46E-18 (9.77E-21)	2.61E-18 (7.36E-21)
			without	1.03E-17 (2.73E-20)	9.89E-18 (2.58E-20)	6.94E-18 (1.46E-20)	4.34E-18 (9.80E-21)
2	0	0	with	1.42E-18 (9.63E-21)	1.32E-18 (8.54E-21)	8.41E-19 (4.37E-21)	5.58E-19 (3.03E-21)
			without	2.29E-18 (1.51E-20)	2.11E-18 (1.40E-20)	1.16E-18 (6.41E-21)	6.29E-19 (3.67E-21)
2	1		with	3.08E-18 (1.41E-20)	3.04E-18 (1.32E-20)	2.62E-18 (8.82E-21)	2.05E-18 (6.78E-21)
			without	8.04E-18 (2.32E-20)	7.78E-18 (2.22E-20)	5.78E-18 (1.31E-20)	3.72E-18 (9.10E-21)
2	1	0	with	7.77E-19 (6.14E-21)	8.03E-19 (6.01E-21)	8.54E-19 (4.87E-21)	7.65E-19 (4.17E-21)
			without	2.76E-18 (1.16E-20)	2.72E-18 (1.12E-20)	2.26E-18 (7.10E-21)	1.63E-18 (5.33E-21)
2	1	1	with	1.16E-18 (9.22E-21)	1.12E-18 (8.48E-21)	8.82E-19 (5.21E-21)	6.36E-19 (3.76E-21)
			without	2.69E-18 (1.51E-20)	2.57E-18 (1.44E-20)	1.77E-18 (8.26E-21)	1.05E-18 (5.47E-21)
3			with	8.24E-17 (1.10E-19)	6.51E-17 (9.01E-20)	2.17E-17 (3.53E-20)	8.31E-18 (1.87E-20)
			without	1.08E-16 (1.18E-19)	8.72E-17 (1.02E-19)	3.27E-17 (4.06E-20)	1.41E-17 (2.18E-20)
3	0	0	with	3.61E-18 (2.07E-20)	2.76E-18 (1.61E-20)	8.66E-19 (5.49E-21)	3.16E-19 (2.70E-21)
			without	3.65E-18 (2.04E-20)	2.89E-18 (1.72E-20)	1.19E-18 (6.88E-21)	6.08E-19 (3.83E-21)
3	1		with	1.75E-17 (4.40E-20)	1.36E-17 (3.52E-20)	4.22E-18 (1.24E-20)	1.50E-18 (6.20E-21)
			without	2.51E-17 (5.43E-20)	1.96E-17 (4.52E-20)	6.95E-18 (1.63E-20)	3.28E-18 (8.81E-21)
3	1	0	with	7.47E-18 (2.79E-20)	5.85E-18 (2.25E-20)	1.93E-18 (8.06E-21)	7.28E-19 (4.14E-21)
			without	1.21E-17 (3.71E-20)	9.62E-18 (3.12E-20)	3.73E-18 (1.17E-20)	1.90E-18 (6.44E-21)
3	1	1	with	5.00E-18 (2.43E-20)	3.87E-18 (1.94E-20)	1.15E-18 (6.73E-21)	3.83E-19 (3.27E-21)
			without	6.48E-18 (2.82E-20)	5.00E-18 (2.34E-20)	1.62E-18 (8.16E-21)	6.93E-19 (4.34E-21)
3	2		with	6.13E-17 (1.01E-19)	4.88E-17 (8.42E-20)	1.66E-17 (3.43E-20)	6.50E-18 (1.85E-20)
			without	7.95E-17 (1.05E-19)	6.47E-17 (9.14E-20)	2.46E-17 (3.74E-20)	1.02E-17 (2.04E-20)
3	2	0	with	1.49E-17 (4.74E-20)	1.22E-17 (4.03E-20)	4.80E-18 (1.86E-20)	2.22E-18 (1.11E-20)
			without	2.39E-17 (5.34E-20)	2.00E-17 (4.71E-20)	8.74E-18 (2.09E-20)	3.95E-18 (1.21E-20)
3	2	1	with	1.91E-17 (5.81E-20)	1.52E-17 (4.81E-20)	5.13E-18 (1.92E-20)	1.95E-18 (1.00E-20)
			without	2.04E-17 (5.54E-20)	1.70E-17 (4.89E-20)	6.62E-18 (2.02E-20)	2.72E-18 (1.09E-20)
3	2	2	with	4.14E-18 (2.78E-20)	3.16E-18 (2.24E-20)	7.83E-19 (7.34E-21)	1.96E-19 (3.09E-21)
			without	7.38E-18 (3.59E-20)	5.37E-18 (2.94E-20)	1.31E-18 (9.43E-21)	3.81E-19 (4.26E-21)

TABLE VI. Cross Sections for Electron Capture and statistical error values (in parenthesis) from H(1s) by C^{6+}

See page 93 for Explanation of Tables

Final State			correction	Energy (keV/amu)			
n	*l*	*m*		90	100	150	200
4			with	1.96E-16 (1.90E-19)	1.45E-16 (1.49E-19)	3.84E-17 (5.04E-20)	1.23E-17 (2.42E-20)
			without	2.07E-16 (1.88E-19)	1.56E-16 (1.56E-19)	4.45E-17 (5.36E-20)	1.59E-17 (2.58E-20)
4	0	0	with	3.95E-18 (2.10E-20)	3.00E-18 (1.64E-20)	8.71E-19 (5.34E-21)	2.79E-19 (2.43E-21)
			without	2.96E-18 (1.84E-20)	2.34E-18 (1.56E-20)	9.11E-19 (6.19E-21)	4.52E-19 (3.46E-21)
4	1		with	1.82E-17 (4.51E-20)	1.44E-17 (3.62E-20)	4.45E-18 (1.26E-20)	1.50E-18 (5.85E-21)
			without	1.82E-17 (4.47E-20)	1.42E-17 (3.76E-20)	5.07E-18 (1.42E-20)	2.32E-18 (7.65E-21)
4	1	0	with	9.88E-18 (3.35E-20)	7.69E-18 (2.67E-20)	2.32E-18 (9.05E-21)	7.90E-19 (4.05E-21)
			without	1.01E-17 (3.33E-20)	8.01E-18 (2.82E-20)	3.00E-18 (1.09E-20)	1.45E-18 (5.96E-21)
4	1	1	with	4.19E-18 (2.16E-20)	3.35E-18 (1.75E-20)	1.07E-18 (6.26E-21)	3.59E-19 (3.02E-21)
			without	4.00E-18 (2.12E-20)	3.09E-18 (1.77E-20)	1.04E-18 (6.48E-21)	4.32E-19 (3.39E-21)
4	2		with	5.24E-17 (8.47E-20)	4.00E-17 (6.75E-20)	1.11E-17 (2.36E-20)	3.72E-18 (1.24E-20)
			without	5.04E-17 (8.07E-20)	3.91E-17 (6.78E-20)	1.32E-17 (2.52E-20)	5.45E-18 (1.36E-20)
4	2	0	with	1.90E-17 (4.96E-20)	1.42E-17 (3.88E-20)	3.15E-18 (1.20E-20)	9.97E-19 (6.61E-21)
			without	1.94E-17 (4.84E-20)	1.52E-17 (4.07E-20)	5.39E-18 (1.53E-20)	2.28E-18 (8.38E-21)
4	2	1	with	1.57E-17 (4.78E-20)	1.22E-17 (3.84E-20)	3.66E-18 (1.38E-20)	1.24E-18 (7.10E-21)
			without	1.35E-17 (4.30E-20)	1.05E-17 (3.62E-20)	3.52E-18 (1.35E-20)	1.43E-18 (7.20E-21)
4	2	2	with	9.60E-19 (1.22E-20)	7.78E-19 (1.01E-20)	3.03E-19 (4.23E-21)	1.09E-19 (2.21E-21)
			without	2.02E-18 (1.74E-20)	1.50E-18 (1.44E-20)	4.23E-19 (5.02E-21)	1.54E-19 (2.60E-21)
4	3		with	1.21E-16 (1.84E-19)	8.75E-17 (1.45E-19)	2.19E-17 (4.93E-20)	6.79E-18 (2.30E-20)
			without	1.36E-16 (1.79E-19)	1.00E-16 (1.49E-19)	2.53E-17 (5.04E-20)	7.63E-18 (2.39E-20)
4	3	0	with	3.41E-17 (1.03E-19)	2.47E-17 (8.20E-20)	6.75E-18 (2.87E-20)	2.27E-18 (1.37E-20)
			without	4.11E-17 (9.80E-20)	3.10E-17 (8.21E-20)	8.39E-18 (2.90E-20)	2.68E-18 (1.43E-20)
4	3	1	with	3.52E-17 (9.93E-20)	2.52E-17 (7.77E-20)	6.07E-18 (2.57E-20)	1.86E-18 (1.20E-20)
			without	3.34E-17 (9.11E-20)	2.47E-17 (7.54E-20)	6.37E-18 (2.56E-20)	1.94E-18 (1.21E-20)
4	3	2	with	8.35E-18 (4.79E-20)	6.12E-18 (3.76E-20)	1.51E-18 (1.23E-20)	3.92E-19 (5.32E-21)
			without	1.34E-17 (5.79E-20)	9.48E-18 (4.67E-20)	2.01E-18 (1.41E-20)	5.24E-19 (6.10E-21)
4	3	3	with	6.54E-20 (4.13E-21)	5.30E-20 (3.39E-21)	7.76E-21 (8.57E-22)	-
			without	4.92E-19 (1.01E-20)	3.18E-19 (7.76E-21)	4.77E-20 (2.00E-21)	-

TABLE VI. Cross Sections for Electron Capture and statistical error values (in parenthesis) from H(1s) by C^{6+}

See page 93 for Explanation of Tables

Final state			correction	Energy (keV/amu)			
n	*l*	*m*		90	100	150	200
5			with	2.07E-16 (2.13E-19)	1.52E-16 (1.66E-19)	3.71E-17 (5.18E-20)	1.11E-17 (2.36E-20)
			without	2.02E-16 (2.01E-19)	1.50E-16 (1.66E-19)	3.92E-17 (5.37E-20)	1.29E-17 (2.47E-20)
5	0	0	with	3.18E-18 (1.96E-20)	2.47E-18 (1.56E-20)	7.29E-19 (5.03E-21)	2.29E-19 (2.23E-21)
			without	2.17E-18 (1.59E-20)	1.73E-18 (1.37E-20)	6.53E-19 (5.31E-21)	3.09E-19 (2.90E-21)
5	1		with	1.47E-17 (4.21E-20)	1.16E-17 (3.38E-20)	3.75E-18 (1.18E-20)	1.25E-18 (5.33E-21)
			without	1.33E-17 (3.83E-20)	1.03E-17 (3.22E-20)	3.53E-18 (1.20E-20)	1.59E-18 (6.44E-21)
5	1	0	with	8.99E-18 (3.34E-20)	7.05E-18 (2.67E-20)	2.15E-18 (9.03E-21)	6.86E-19 (3.82E-21)
			without	8.10E-18 (3.01E-20)	6.22E-18 (2.52E-20)	2.18E-18 (9.48E-21)	1.03E-18 (5.15E-21)
5	1	1	with	2.85E-18 (1.83E-20)	2.29E-18 (1.47E-20)	7.99E-19 (5.39E-21)	2.81E-19 (2.63E-21)
			without	2.59E-18 (1.68E-20)	2.03E-18 (1.42E-20)	6.69E-19 (5.19E-21)	2.80E-19 (2.75E-21)
5	2		with	3.79E-17 (7.27E-20)	3.01E-17 (5.91E-20)	8.77E-18 (2.05E-20)	2.72E-18 (1.02E-20)
			without	3.34E-17 (6.53E-20)	2.59E-17 (5.51E-20)	8.79E-18 (2.06E-20)	3.57E-18 (1.10E-20)
5	2	0	with	1.56E-17 (4.57E-20)	1.21E-17 (3.65E-20)	2.76E-18 (1.10E-20)	7.17E-19 (5.40E-21)
			without	1.41E-17 (4.14E-20)	1.09E-17 (3.49E-20)	3.76E-18 (1.30E-20)	1.56E-18 (7.03E-21)
5	2	1	with	1.07E-17 (3.97E-20)	8.74E-18 (3.28E-20)	2.86E-18 (1.20E-20)	9.37E-19 (5.94E-21)
			without	8.86E-18 (3.46E-20)	6.79E-18 (2.89E-20)	2.30E-18 (1.08E-20)	9.21E-19 (5.71E-21)
5	2	2	with	3.66E-19 (7.51E-21)	3.20E-19 (6.50E-21)	1.45E-19 (2.89E-21)	5.96E-20 (1.60E-21)
			without	8.62E-19 (1.11E-20)	6.72E-19 (9.43E-21)	2.12E-19 (3.51E-21)	8.32E-20 (1.89E-21)
5	3		with	6.57E-17 (1.26E-19)	4.92E-17 (1.01E-19)	1.42E-17 (3.82E-20)	5.13E-18 (1.99E-20)
			without	6.63E-17 (1.19E-19)	5.08E-17 (1.00E-19)	1.51E-17 (3.74E-20)	5.22E-18 (1.94E-20)
5	3	0	with	1.79E-17 (6.51E-20)	1.27E-17 (5.20E-20)	3.79E-18 (2.05E-20)	1.55E-18 (1.12E-20)
			without	2.19E-17 (6.69E-20)	1.65E-17 (5.57E-20)	5.05E-18 (2.13E-20)	1.80E-18 (1.14E-20)
5	3	1	with	2.04E-17 (7.07E-20)	1.54E-17 (5.68E-20)	4.23E-18 (2.06E-20)	1.49E-18 (1.07E-20)
			without	1.64E-17 (6.02E-20)	1.27E-17 (5.08E-20)	3.81E-18 (1.89E-20)	1.33E-18 (9.87E-21)
5	3	2	with	3.58E-18 (3.05E-20)	2.76E-18 (2.46E-20)	9.53E-19 (9.77E-21)	3.17E-19 (4.84E-21)
			without	5.64E-18 (3.60E-20)	4.39E-18 (3.07E-20)	1.22E-18 (1.08E-20)	3.74E-19 (5.15E-21)
5	3	3	with	1.92E-20 (2.15E-21)	1.17E-20 (1.52E-21)	3.11E-21 (5.42E-22)	-
			without	1.48E-19 (5.37E-21)	1.05E-19 (4.33E-21)	2.26E-20 (1.34E-21)	-
5	4		with	8.55E-17 (1.87E-19)	5.88E-17 (1.43E-19)	9.65E-18 (3.84E-20)	1.75E-18 (1.39E-20)
			without	8.64E-17 (1.73E-19)	6.11E-17 (1.41E-19)	1.11E-17 (4.00E-20)	2.23E-18 (1.53E-20)
5	4	0	with	2.58E-17 (1.05E-19)	1.88E-17 (8.24E-20)	3.55E-18 (2.35E-20)	7.09E-19 (8.93E-21)
			without	2.60E-17 (9.64E-20)	1.85E-17 (7.84E-20)	3.59E-18 (2.30E-20)	7.97E-19 (9.25E-21)
5	4	1	with	2.26E-17 (9.63E-20)	1.54E-17 (7.33E-20)	2.51E-18 (1.96E-20)	4.58E-19 (7.15E-21)
			without	2.08E-17 (8.62E-20)	1.47E-17 (6.97E-20)	2.74E-18 (2.00E-20)	5.60E-19 (7.69E-21)
5	4	2	with	6.85E-18 (5.20E-20)	4.34E-18 (3.81E-20)	5.44E-19 (8.96E-21)	6.20E-20 (2.56E-21)
			without	8.72E-18 (5.46E-20)	6.06E-18 (4.37E-20)	9.82E-19 (1.16E-20)	1.50E-19 (3.85E-21)
5	4	3	with	2.59E-19 (9.66E-21)	1.55E-19 (6.88E-21)	7.12E-21 (9.68E-22)	-
			without	7.94E-19 (1.55E-20)	5.12E-19 (1.20E-20)	4.04E-20 (2.21E-21)	-
5	4	4	with	-	-	-	-
			without	-	-	-	-

TABLE VII. Cross Sections for Electron Capture and statistical error values (in parenthesis) from H(1s) by N^{7+}

See page 93 for Explanation of Tables

$N^{7+} + H(1s) \rightarrow N^{6+}(nlm) + H^{+}$

Final state			correction	Energy (keV/amu)			
n	*l*	*m*		10	20	30	40
1	0	0	with	1.98E-20 (6.23E-22)	3.90E-20 (1.03E-21)	5.36E-20 (1.25E-21)	5.98E-20 (1.22E-21)
			without	1.75E-20 (2.58E-21)	1.13E-20 (2.35E-21)	1.04E-20 (2.17E-21)	-
2			with	8.90E-19 (1.02E-20)	1.28E-18 (1.30E-20)	1.61E-18 (1.48E-20)	1.91E-18 (1.47E-20)
			without	1.24E-19 (4.34E-21)	3.39E-19 (6.76E-21)	7.11E-19 (9.74E-21)	1.20E-18 (1.14E-20)
2	0	0	with	2.51E-19 (5.29E-21)	4.36E-19 (7.77E-21)	6.64E-19 (1.01E-20)	8.38E-19 (1.03E-20)
			without	8.89E-20 (4.11E-21)	1.37E-19 (5.02E-21)	2.26E-19 (5.97E-21)	3.46E-19 (6.72E-21)
2	1		with	6.39E-19 (8.74E-21)	8.49E-19 (1.05E-20)	9.43E-19 (1.09E-20)	1.07E-18 (1.05E-20)
			without	3.55E-20 (1.89E-21)	2.02E-19 (4.80E-21)	4.85E-19 (7.77E-21)	8.54E-19 (9.34E-21)
2	1	0	with	1.63E-19 (4.04E-21)	2.16E-19 (4.66E-21)	2.16E-19 (4.42E-21)	2.13E-19 (3.80E-21)
			without	1.58E-20 (1.24E-21)	6.01E-20 (2.22E-21)	1.44E-19 (3.65E-21)	2.54E-19 (4.32E-21)
2	1	1	with	2.42E-19 (5.60E-21)	3.27E-19 (6.85E-21)	3.66E-19 (7.23E-21)	4.26E-19 (7.11E-21)
			without	9.94E-21 (9.85E-22)	7.64E-20 (3.25E-21)	1.85E-19 (5.30E-21)	3.17E-19 (6.29E-21)
3			with	2.75E-17 (1.02E-19)	4.28E-17 (1.48E-19)	7.16E-17 (1.78E-19)	8.13E-17 (1.62E-19)
			without	7.27E-17 (1.42E-19)	1.08E-16 (1.88E-19)	1.33E-16 (1.98E-19)	1.37E-16 (1.83E-19)
3	0	0	with	6.86E-18 (6.29E-20)	1.05E-17 (8.33E-20)	1.05E-17 (8.07E-20)	8.61E-18 (6.24E-20)
			without	1.07E-17 (5.84E-20)	1.34E-17 (6.86E-20)	1.44E-17 (7.40E-20)	1.27E-17 (6.35E-20)
3	1		with	9.89E-18 (6.27E-20)	1.68E-17 (9.22E-20)	2.32E-17 (1.08E-19)	2.49E-17 (9.83E-20)
			without	2.54E-17 (8.84E-20)	3.71E-17 (1.12E-19)	4.46E-17 (1.21E-19)	4.67E-17 (1.15E-19)
3	1	0	with	3.01E-18 (3.00E-20)	5.87E-18 (5.10E-20)	7.93E-18 (5.92E-20)	8.42E-18 (5.38E-20)
			without	9.28E-18 (5.07E-20)	1.14E-17 (5.87E-20)	1.38E-17 (6.05E-20)	1.46E-17 (5.76E-20)
3	1	1	with	3.53E-18 (4.06E-20)	5.58E-18 (5.55E-20)	7.77E-18 (6.48E-20)	8.29E-18 (5.89E-20)
			without	8.28E-18 (5.25E-20)	1.31E-17 (6.95E-20)	1.56E-17 (7.63E-20)	1.62E-17 (7.23E-20)
3	2		with	1.08E-17 (5.73E-20)	1.55E-17 (8.47E-20)	3.79E-17 (1.21E-19)	4.78E-17 (1.17E-19)
			without	3.66E-17 (9.75E-20)	5.78E-17 (1.38E-19)	7.45E-17 (1.44E-19)	7.80E-17 (1.32E-19)
3	2	0	with	2.67E-18 (2.51E-20)	3.15E-18 (3.29E-20)	6.83E-18 (4.17E-20)	8.64E-18 (3.95E-20)
			without	7.20E-18 (3.60E-20)	1.01E-17 (5.09E-20)	1.50E-17 (5.54E-20)	1.67E-17 (5.22E-20)
3	2	1	with	3.05E-18 (3.13E-20)	5.21E-18 (5.12E-20)	1.20E-17 (7.13E-20)	1.44E-17 (6.70E-20)
			without	6.91E-18 (4.13E-20)	1.04E-17 (5.77E-20)	1.43E-17 (6.22E-20)	1.54E-17 (5.83E-20)
3	2	2	with	1.07E-18 (2.11E-20)	9.68E-19 (2.28E-20)	3.49E-18 (4.35E-20)	5.26E-18 (4.76E-20)
			without	8.02E-18 (5.38E-20)	1.37E-17 (7.32E-20)	1.57E-17 (7.67E-20)	1.53E-17 (6.92E-20)

TABLE VII. Cross Sections for Electron Capture and statistical error values (in parenthesis) from H(1s) by N^{7+}

See page 93 for Explanation of Tables

Final state			correction	Energy (keV/amu)			
n	*l*	*m*		10	20	30	40
4			with	1.53E-15 (1.10E-18)	1.54E-15 (9.98E-19)	1.16E-15 (8.26E-19)	8.34E-16 (6.19E-19)
			without	2.10E-15 (9.75E-19)	1.84E-15 (8.45E-19)	1.33E-15 (7.14E-19)	9.43E-16 (5.59E-19)
4	0	0	with	1.10E-16 (3.52E-19)	5.25E-17 (2.14E-19)	2.77E-17 (1.31E-19)	1.76E-17 (8.38E-20)
			without	3.68E-17 (1.31E-19)	2.19E-17 (9.65E-20)	1.65E-17 (7.46E-20)	1.18E-17 (5.58E-20)
4	1		with	1.77E-16 (4.04E-19)	1.25E-16 (3.11E-19)	8.42E-17 (2.26E-19)	5.86E-17 (1.54E-19)
			without	2.00E-16 (3.04E-19)	1.84E-16 (2.79E-19)	1.31E-16 (2.26E-19)	8.82E-17 (1.63E-19)
4	1	0	with	5.85E-17 (2.14E-19)	5.29E-17 (1.94E-19)	3.95E-17 (1.52E-19)	2.85E-17 (1.06E-19)
			without	1.01E-16 (2.13E-19)	1.00E-16 (1.96E-19)	6.95E-17 (1.61E-19)	4.65E-17 (1.16E-19)
4	1	1	with	5.98E-17 (2.48E-19)	3.64E-17 (1.76E-19)	2.22E-17 (1.19E-19)	1.50E-17 (7.99E-20)
			without	4.98E-17 (1.58E-19)	4.21E-17 (1.46E-19)	3.06E-17 (1.15E-19)	2.08E-17 (8.18E-20)
4	2		with	5.10E-16 (6.83E-19)	5.27E-16 (6.14E-19)	3.89E-16 (4.83E-19)	2.58E-16 (3.29E-19)
			without	6.36E-16 (6.06E-19)	5.93E-16 (5.35E-19)	4.39E-16 (4.34E-19)	2.96E-16 (3.15E-19)
4	2	0	with	1.48E-16 (3.58E-19)	1.65E-16 (3.23E-19)	1.24E-16 (2.59E-19)	8.49E-17 (1.82E-19)
			without	1.96E-16 (3.50E-19)	1.79E-16 (2.90E-19)	1.35E-16 (2.36E-19)	9.53E-17 (1.75E-19)
4	2	1	with	1.25E-16 (3.46E-19)	1.44E-16 (3.38E-19)	1.14E-16 (2.74E-19)	7.68E-17 (1.87E-19)
			without	1.63E-16 (3.16E-19)	1.54E-16 (2.85E-19)	1.15E-16 (2.33E-19)	7.87E-17 (1.69E-19)
4	2	2	with	5.57E-17 (2.46E-19)	3.69E-17 (1.93E-19)	1.93E-17 (1.22E-19)	9.69E-18 (6.97E-20)
			without	5.72E-17 (1.94E-19)	5.26E-17 (1.85E-19)	3.73E-17 (1.42E-19)	2.19E-17 (9.42E-20)
4	3		with	7.27E-16 (7.78E-19)	8.34E-16 (7.85E-19)	6.58E-16 (6.82E-19)	5.00E-16 (5.38E-19)
			without	1.23E-15 (8.63E-19)	1.04E-15 (7.40E-19)	7.46E-16 (6.15E-19)	5.47E-16 (4.85E-19)
4	3	0	with	2.05E-16 (3.99E-19)	1.91E-16 (3.69E-19)	1.48E-16 (3.11E-19)	1.13E-16 (2.47E-19)
			without	2.26E-16 (3.87E-19)	2.11E-16 (3.34E-19)	1.61E-16 (2.79E-19)	1.23E-16 (2.23E-19)
4	3	1	with	1.57E-16 (3.76E-19)	2.00E-16 (3.95E-19)	1.62E-16 (3.48E-19)	1.29E-16 (2.80E-19)
			without	2.30E-16 (4.03E-19)	2.03E-16 (3.46E-19)	1.50E-16 (2.87E-19)	1.14E-16 (2.29E-19)
4	3	2	with	8.18E-17 (2.87E-19)	1.04E-16 (3.13E-19)	8.52E-17 (2.76E-19)	6.13E-17 (2.07E-19)
			without	2.14E-16 (3.95E-19)	1.70E-16 (3.41E-19)	1.18E-16 (2.77E-19)	8.42E-17 (2.11E-19)
4	3	3	with	2.22E-17 (1.54E-19)	1.65E-17 (1.32E-19)	7.45E-18 (8.51E-20)	3.15E-18 (4.73E-20)
			without	5.86E-17 (2.07E-19)	4.23E-17 (1.75E-19)	2.47E-17 (1.28E-19)	1.43E-17 (8.65E-20)

TABLE VII. Cross Sections for Electron Capture and statistical error values (in parenthesis) from H(1s) by N^{7+}

See page 93 for Explanation of Tables

Final state			correction	Energy (keV/amu)			
n	*l*	*m*		10	20	30	40
5			with	3.85E-15 (1.74E-18)	2.64E-15 (1.46E-18)	1.84E-15 (1.20E-18)	1.30E-15 (8.85E-19)
			without	1.22E-15 (8.41E-19)	1.30E-15 (8.94E-19)	1.35E-15 (8.31E-19)	1.15E-15 (6.81E-19)
5	0	0	with	4.32E-17 (1.89E-19)	2.56E-17 (1.25E-19)	1.83E-17 (9.95E-20)	1.33E-17 (7.20E-20)
			without	1.44E-17 (8.05E-20)	4.99E-18 (6.85E-20)	5.45E-18 (4.52E-20)	7.04E-18 (3.98E-20)
5	1		with	1.22E-16 (3.25E-19)	7.33E-17 (2.35E-19)	5.63E-17 (1.87E-19)	4.48E-17 (1.38E-19)
			without	4.78E-17 (1.41E-19)	2.98E-17 (1.28E-19)	5.71E-17 (1.34E-19)	5.76E-17 (1.19E-19)
5	1	0	with	5.89E-17 (2.14E-19)	4.21E-17 (1.70E-19)	3.45E-17 (1.44E-19)	2.79E-17 (1.08E-19)
			without	2.88E-17 (1.09E-19)	2.15E-17 (1.01E-19)	4.39E-17 (1.14E-19)	3.92E-17 (9.68E-20)
5	1	1	with	3.19E-17 (1.77E-19)	1.56E-17 (1.17E-19)	1.08E-17 (8.54E-20)	8.53E-18 (6.21E-20)
			without	9.46E-18 (6.40E-20)	4.18E-18 (6.33E-20)	6.64E-18 (5.16E-20)	9.26E-18 (4.96E-20)
5	2		with	3.77E-16 (5.50E-19)	2.92E-16 (4.57E-19)	2.18E-16 (3.49E-19)	1.55E-16 (2.46E-19)
			without	1.15E-16 (2.24E-19)	1.29E-16 (2.46E-19)	1.87E-16 (2.59E-19)	1.63E-16 (2.10E-19)
5	2	0	with	1.48E-16 (3.25E-19)	1.22E-16 (2.79E-19)	8.93E-17 (2.14E-19)	6.31E-17 (1.52E-19)
			without	5.30E-17 (1.52E-19)	6.44E-17 (1.62E-19)	8.89E-17 (1.73E-19)	7.10E-17 (1.35E-19)
5	2	1	with	9.77E-17 (2.93E-19)	7.97E-17 (2.55E-19)	6.10E-17 (1.94E-19)	4.38E-17 (1.36E-19)
			without	2.70E-17 (1.08E-19)	3.01E-17 (1.30E-19)	4.72E-17 (1.38E-19)	4.37E-17 (1.14E-19)
5	2	2	with	1.67E-17 (1.44E-19)	5.43E-18 (7.40E-20)	3.29E-18 (4.86E-20)	2.04E-18 (3.13E-20)
			without	3.94E-18 (5.30E-20)	2.06E-18 (4.57E-20)	1.75E-18 (3.41E-20)	2.25E-18 (2.84E-20)
5	3		with	1.15E-15 (1.07E-18)	7.87E-16 (8.10E-19)	4.67E-16 (6.02E-19)	3.02E-16 (4.18E-19)
			without	2.88E-16 (4.11E-19)	3.39E-16 (4.30E-19)	3.31E-16 (4.18E-19)	2.73E-16 (3.45E-19)
5	3	0	with	3.47E-16 (5.92E-19)	2.48E-16 (4.38E-19)	1.55E-16 (3.38E-19)	1.01E-16 (2.36E-19)
			without	1.06E-16 (2.56E-19)	1.24E-16 (2.46E-19)	1.16E-16 (2.41E-19)	9.14E-17 (1.95E-19)
5	3	1	with	2.83E-16 (5.46E-19)	2.04E-16 (4.34E-19)	1.25E-16 (3.21E-19)	8.20E-17 (2.24E-19)
			without	7.29E-17 (2.05E-19)	8.72E-17 (2.28E-19)	8.55E-17 (2.21E-19)	6.97E-17 (1.80E-19)
5	3	2	with	1.15E-16 (3.85E-19)	6.51E-17 (2.70E-19)	3.16E-17 (1.72E-19)	1.80E-17 (1.10E-19)
			without	1.70E-17 (1.11E-19)	2.01E-17 (1.26E-19)	2.17E-17 (1.18E-19)	2.11E-17 (1.02E-19)
5	3	3	with	5.00E-18 (7.89E-20)	6.48E-19 (2.68E-20)	1.60E-19 (1.08E-20)	7.03E-20 (6.07E-21)
			without	9.21E-19 (2.42E-20)	4.57E-19 (2.02E-20)	3.60E-19 (1.62E-20)	3.60E-19 (1.30E-20)
5	4		with	2.16E-15 (1.56E-18)	1.46E-15 (1.34E-18)	1.08E-15 (1.13E-18)	7.84E-16 (8.43E-19)
			without	7.55E-16 (7.75E-19)	8.00E-16 (8.35E-19)	7.73E-16 (8.19E-19)	6.46E-16 (6.70E-19)
5	4	0	with	5.36E-16 (8.19E-19)	3.55E-16 (6.70E-19)	2.76E-16 (5.75E-19)	2.05E-16 (4.33E-19)
			without	2.34E-16 (4.56E-19)	2.36E-16 (4.62E-19)	2.13E-16 (4.45E-19)	1.74E-16 (3.58E-19)
5	4	1	with	4.74E-16 (7.80E-19)	3.26E-16 (6.58E-19)	2.51E-16 (5.64E-19)	1.88E-16 (4.24E-19)
			without	1.89E-16 (4.03E-19)	1.91E-16 (4.25E-19)	1.79E-16 (4.10E-19)	1.47E-16 (3.31E-19)
5	4	2	with	2.81E-16 (6.16E-19)	1.96E-16 (5.32E-19)	1.36E-16 (4.28E-19)	9.23E-17 (3.06E-19)
			without	6.58E-17 (2.29E-19)	8.31E-17 (2.83E-19)	9.05E-17 (2.89E-19)	7.81E-17 (2.39E-19)
5	4	3	with	5.36E-17 (2.75E-19)	2.93E-17 (2.09E-19)	1.66E-17 (1.49E-19)	8.96E-18 (9.31E-20)
			without	5.12E-18 (5.89E-20)	7.56E-18 (8.25E-20)	1.04E-17 (9.40E-20)	1.11E-17 (8.57E-20)
5	4	4	with	1.20E-18 (3.50E-20)	2.00E-19 (1.40E-20)	3.32E-20 (5.24E-21)	-
			without	3.25E-19 (1.26E-20)	4.85E-20 (4.54E-21)	2.15E-20 (2.77E-21)	-

TABLE VII. Cross Sections for Electron Capture and statistical error values (in parenthesis) from H(1s) by N^{7+}

See page 93 for Explanation of Tables

$N^{7+} + H(1s) \rightarrow N^{6+}(nlm) + H^{+}$

Final state			correction	Energy (keV/amu)			
n	*l*	*m*		50	60	70	80
1	0	0	with	7.08E-20 (1.37E-21)	7.55E-20 (1.42E-21)	8.28E-20 (1.44E-21)	8.99E-20 (1.61E-21)
			without	-	-	-	-
2			with	2.16E-18 (1.56E-20)	2.33E-18 (1.59E-20)	2.42E-18 (1.55E-20)	2.46E-18 (1.66E-20)
			without	1.76E-18 (1.33E-20)	2.32E-18 (1.54E-20)	2.74E-18 (1.46E-20)	3.05E-18 (1.51E-20)
2	0	0	with	9.35E-19 (1.09E-20)	9.67E-19 (1.06E-20)	9.69E-19 (1.00E-20)	9.32E-19 (1.02E-20)
			without	4.72E-19 (7.80E-21)	5.91E-19 (8.97E-21)	6.79E-19 (8.57E-21)	7.47E-19 (8.88E-21)
2	1		with	1.23E-18 (1.13E-20)	1.37E-18 (1.19E-20)	1.45E-18 (1.18E-20)	1.52E-18 (1.31E-20)
			without	1.29E-18 (1.10E-20)	1.73E-18 (1.28E-20)	2.07E-18 (1.21E-20)	2.31E-18 (1.26E-20)
2	1	0	with	2.30E-19 (3.84E-21)	2.50E-19 (3.98E-21)	2.69E-19 (4.03E-21)	3.06E-19 (4.82E-21)
			without	4.03E-19 (5.18E-21)	5.64E-19 (6.12E-21)	6.87E-19 (5.85E-21)	7.71E-19 (6.07E-21)
2	1	1	with	4.85E-19 (7.68E-21)	5.50E-19 (8.10E-21)	5.86E-19 (8.12E-21)	6.15E-19 (8.87E-21)
			without	4.62E-19 (7.35E-21)	6.26E-19 (8.69E-21)	7.34E-19 (8.20E-21)	8.12E-19 (8.52E-21)
3			with	7.73E-17 (1.55E-19)	6.81E-17 (1.41E-19)	5.87E-17 (1.24E-19)	4.96E-17 (1.20E-19)
			without	1.28E-16 (1.70E-19)	1.12E-16 (1.58E-19)	9.59E-17 (1.26E-19)	8.23E-17 (1.13E-19)
3	0	0	with	6.72E-18 (5.23E-20)	5.24E-18 (4.30E-20)	4.13E-18 (3.48E-20)	3.26E-18 (3.18E-20)
			without	9.83E-18 (5.29E-20)	7.29E-18 (4.38E-20)	5.49E-18 (3.17E-20)	4.19E-18 (2.62E-20)
3	1		with	2.35E-17 (9.23E-20)	2.01E-17 (7.99E-20)	1.68E-17 (6.67E-20)	1.35E-17 (6.11E-20)
			without	4.42E-17 (1.09E-19)	3.80E-17 (9.87E-20)	3.14E-17 (7.62E-20)	2.55E-17 (6.55E-20)
3	1	0	with	8.28E-18 (5.18E-20)	7.27E-18 (4.55E-20)	6.34E-18 (3.89E-20)	5.15E-18 (3.59E-20)
			without	1.46E-17 (5.72E-20)	1.36E-17 (5.51E-20)	1.19E-17 (4.44E-20)	1.03E-17 (3.98E-20)
3	1	1	with	7.69E-18 (5.47E-20)	6.43E-18 (4.69E-20)	5.20E-18 (3.85E-20)	4.13E-18 (3.51E-20)
			without	1.49E-17 (6.69E-20)	1.23E-17 (5.91E-20)	9.78E-18 (4.44E-20)	7.62E-18 (3.73E-20)
3	2		with	4.70E-17 (1.16E-19)	4.28E-17 (1.09E-19)	3.77E-17 (9.88E-20)	3.28E-17 (9.94E-20)
			without	7.35E-17 (1.25E-19)	6.66E-17 (1.19E-19)	5.90E-17 (9.70E-20)	5.26E-17 (8.98E-20)
3	2	0	with	8.36E-18 (3.89E-20)	7.62E-18 (3.70E-20)	6.91E-18 (3.46E-20)	6.16E-18 (3.57E-20)
			without	1.63E-17 (5.01E-20)	1.53E-17 (4.88E-20)	1.41E-17 (4.08E-20)	1.32E-17 (3.91E-20)
3	2	1	with	1.38E-17 (6.51E-20)	1.25E-17 (6.05E-20)	1.09E-17 (5.45E-20)	9.48E-18 (5.48E-20)
			without	1.50E-17 (5.61E-20)	1.42E-17 (5.51E-20)	1.28E-17 (4.56E-20)	1.20E-17 (4.37E-20)
3	2	2	with	5.56E-18 (4.88E-20)	4.98E-18 (4.48E-20)	4.38E-18 (4.00E-20)	3.75E-18 (3.93E-20)
			without	1.36E-17 (6.38E-20)	1.14E-17 (5.85E-20)	9.65E-18 (4.65E-20)	7.77E-18 (4.05E-20)

TABLE VII. Cross Sections for Electron Capture and statistical error values (in parenthesis) from H(1s) by N^{7+}

See page 93 for Explanation of Tables

Final State			correction	Energy (keV/amu)			
n	*l*	*m*		50	60	70	80
4			with	6.00E-16 (5.16E-19)	4.37E-16 (4.23E-19)	3.22E-16 (3.41E-19)	2.39E-16 (3.08E-19)
			without	6.77E-16 (4.62E-19)	4.95E-16 (3.94E-19)	3.64E-16 (2.91E-19)	2.75E-16 (2.45E-19)
4	0	0	with	1.21E-17 (6.53E-20)	8.59E-18 (5.09E-20)	6.32E-18 (4.01E-20)	4.71E-18 (3.56E-20)
			without	8.63E-18 (4.58E-20)	6.39E-18 (3.86E-20)	4.78E-18 (2.83E-20)	3.68E-18 (2.39E-20)
4	1		with	4.26E-17 (1.23E-19)	3.19E-17 (9.80E-20)	2.45E-17 (7.82E-20)	1.87E-17 (6.95E-20)
			without	6.05E-17 (1.26E-19)	4.27E-17 (1.02E-19)	3.06E-17 (7.20E-20)	2.29E-17 (5.92E-20)
4	1	0	with	2.09E-17 (8.47E-20)	1.56E-17 (6.74E-20)	1.19E-17 (5.36E-20)	9.08E-18 (4.74E-20)
			without	3.17E-17 (8.97E-20)	2.23E-17 (7.22E-20)	1.59E-17 (5.12E-20)	1.20E-17 (4.23E-20)
4	1	1	with	1.09E-17 (6.34E-20)	8.07E-18 (5.05E-20)	6.28E-18 (4.05E-20)	4.79E-18 (3.61E-20)
			without	1.44E-17 (6.34E-20)	1.03E-17 (5.13E-20)	7.32E-18 (3.62E-20)	5.46E-18 (2.96E-20)
4	2		with	1.69E-16 (2.51E-19)	1.13E-16 (1.91E-19)	7.96E-17 (1.48E-19)	5.78E-17 (1.30E-19)
			without	1.97E-16 (2.43E-19)	1.34E-16 (1.93E-19)	9.19E-17 (1.35E-19)	6.59E-17 (1.08E-19)
4	2	0	with	5.67E-17 (1.41E-19)	3.85E-17 (1.08E-19)	2.72E-17 (8.34E-20)	1.95E-17 (7.26E-20)
			without	6.59E-17 (1.37E-19)	4.62E-17 (1.10E-19)	3.25E-17 (7.76E-20)	2.39E-17 (6.29E-20)
4	2	1	with	5.05E-17 (1.42E-19)	3.42E-17 (1.09E-19)	2.41E-17 (8.36E-20)	1.75E-17 (7.37E-20)
			without	5.30E-17 (1.31E-19)	3.59E-17 (1.04E-19)	2.47E-17 (7.19E-20)	1.77E-17 (5.79E-20)
4	2	2	with	5.46E-18 (4.84E-20)	3.33E-18 (3.49E-20)	2.25E-18 (2.64E-20)	1.59E-18 (2.30E-20)
			without	1.28E-17 (6.68E-20)	7.74E-18 (4.97E-20)	4.99E-18 (3.34E-20)	3.42E-18 (2.64E-20)
4	3		with	3.77E-16 (4.64E-19)	2.83E-16 (3.90E-19)	2.12E-16 (3.19E-19)	1.57E-16 (2.91E-19)
			without	4.11E-16 (4.08E-19)	3.13E-16 (3.53E-19)	2.36E-16 (2.64E-19)	1.82E-16 (2.25E-19)
4	3	0	with	8.69E-17 (2.17E-19)	6.68E-17 (1.86E-19)	5.03E-17 (1.54E-19)	3.80E-17 (1.43E-19)
			without	9.67E-17 (1.92E-19)	7.68E-17 (1.69E-19)	5.99E-17 (1.28E-19)	4.80E-17 (1.11E-19)
4	3	1	with	1.01E-16 (2.45E-19)	7.74E-17 (2.07E-19)	5.87E-17 (1.70E-19)	4.40E-17 (1.55E-19)
			without	8.76E-17 (1.94E-19)	6.86E-17 (1.70E-19)	5.31E-17 (1.28E-19)	4.17E-17 (1.10E-19)
4	3	2	with	4.26E-17 (1.68E-19)	2.98E-17 (1.33E-19)	2.12E-17 (1.05E-19)	1.55E-17 (9.36E-20)
			without	6.12E-17 (1.73E-19)	4.43E-17 (1.44E-19)	3.22E-17 (1.05E-19)	2.34E-17 (8.61E-20)
4	3	3	with	1.42E-18 (3.04E-20)	7.04E-19 (2.00E-20)	3.83E-19 (1.37E-20)	2.46E-19 (1.14E-20)
			without	8.36E-18 (6.20E-20)	4.97E-18 (4.60E-20)	3.02E-18 (3.01E-20)	1.87E-18 (2.26E-20)

TABLE VII. Cross Sections for Electron Capture and statistical error values (in parenthesis) from H(1s) by N^{7+}

See page 93 for Explanation of Tables

Final state			correction	Energy (keV/amu)			
n	*l*	*m*		50	60	70	80
5			with	9.24E-16 (7.27E-19)	6.62E-16 (5.86E-19)	4.78E-16 (4.63E-19)	3.49E-16 (4.12E-19)
			without	8.80E-16 (5.79E-19)	6.55E-16 (4.97E-19)	4.80E-16 (3.66E-19)	3.55E-16 (3.05E-19)
5	0	0	with	1.01E-17 (5.85E-20)	7.62E-18 (4.77E-20)	5.63E-18 (3.75E-20)	4.38E-18 (3.43E-20)
			without	6.25E-18 (3.73E-20)	4.92E-18 (3.31E-20)	3.83E-18 (2.51E-20)	2.93E-18 (2.13E-20)
5	1		with	3.55E-17 (1.14E-19)	2.82E-17 (9.47E-20)	2.18E-17 (7.60E-20)	1.74E-17 (6.95E-20)
			without	4.47E-17 (1.01E-19)	3.32E-17 (8.58E-20)	2.43E-17 (6.25E-20)	1.79E-17 (5.16E-20)
5	1	0	with	2.20E-17 (8.92E-20)	1.73E-17 (7.37E-20)	1.31E-17 (5.88E-20)	1.04E-17 (5.36E-20)
			without	2.86E-17 (8.03E-20)	2.05E-17 (6.70E-20)	1.46E-17 (4.83E-20)	1.07E-17 (3.96E-20)
5	1	1	with	6.72E-18 (5.09E-20)	5.43E-18 (4.22E-20)	4.32E-18 (3.42E-20)	3.52E-18 (3.13E-20)
			without	8.10E-18 (4.41E-20)	6.42E-18 (3.84E-20)	4.84E-18 (2.83E-20)	3.65E-18 (2.35E-20)
5	2		with	1.12E-16 (1.99E-19)	8.23E-17 (1.61E-19)	6.14E-17 (1.29E-19)	4.73E-17 (1.18E-19)
			without	1.19E-16 (1.71E-19)	8.48E-17 (1.42E-19)	6.08E-17 (1.03E-19)	4.50E-17 (8.53E-20)
5	2	0	with	4.48E-17 (1.23E-19)	3.30E-17 (9.98E-20)	2.41E-17 (7.90E-20)	1.85E-17 (7.21E-20)
			without	4.99E-17 (1.08E-19)	3.52E-17 (8.93E-20)	2.50E-17 (6.42E-20)	1.85E-17 (5.32E-20)
5	2	1	with	3.22E-17 (1.10E-19)	2.38E-17 (8.91E-20)	1.81E-17 (7.21E-20)	1.40E-17 (6.57E-20)
			without	3.19E-17 (9.22E-20)	2.27E-17 (7.60E-20)	1.63E-17 (5.49E-20)	1.20E-17 (4.52E-20)
5	2	2	with	1.37E-18 (2.42E-20)	8.82E-19 (1.81E-20)	6.22E-19 (1.38E-20)	4.67E-19 (1.23E-20)
			without	2.44E-18 (2.67E-20)	2.05E-18 (2.36E-20)	1.53E-18 (1.74E-20)	1.20E-18 (1.47E-20)
5	3		with	2.12E-16 (3.38E-19)	1.57E-16 (2.75E-19)	1.21E-16 (2.25E-19)	9.34E-17 (2.06E-19)
			without	2.10E-16 (2.87E-19)	1.58E-16 (2.42E-19)	1.18E-16 (1.78E-19)	8.98E-17 (1.48E-19)
5	3	0	with	7.00E-17 (1.89E-19)	5.16E-17 (1.54E-19)	3.92E-17 (1.25E-19)	2.96E-17 (1.12E-19)
			without	6.83E-17 (1.60E-19)	5.09E-17 (1.34E-19)	3.77E-17 (9.71E-20)	2.85E-17 (8.05E-20)
5	3	1	with	5.86E-17 (1.82E-19)	4.44E-17 (1.49E-19)	3.44E-17 (1.22E-19)	2.69E-17 (1.13E-19)
			without	5.27E-17 (1.48E-19)	3.93E-17 (1.24E-19)	2.91E-17 (9.01E-20)	2.21E-17 (7.53E-20)
5	3	2	with	1.23E-17 (8.69E-20)	8.58E-18 (6.82E-20)	6.51E-18 (5.50E-20)	4.93E-18 (4.98E-20)
			without	1.77E-17 (8.83E-20)	1.41E-17 (7.64E-20)	1.08E-17 (5.70E-20)	8.28E-18 (4.79E-20)
5	3	3	with	5.37E-20 (5.03E-21)	3.67E-20 (4.16E-21)	2.70E-20 (3.38E-21)	1.94E-20 (2.95E-21)
			without	3.71E-19 (1.20E-20)	3.76E-19 (1.15E-20)	3.43E-19 (9.25E-21)	2.92E-19 (8.23E-21)
5	4		with	5.55E-16 (6.92E-19)	3.87E-16 (5.54E-19)	2.68E-16 (4.35E-19)	1.87E-16 (3.84E-19)
			without	5.00E-16 (5.62E-19)	3.74E-16 (4.75E-19)	2.73E-16 (3.46E-19)	1.99E-16 (2.86E-19)
5	4	0	with	1.45E-16 (3.56E-19)	1.00E-16 (2.85E-19)	6.85E-17 (2.25E-19)	4.81E-17 (2.01E-19)
			without	1.34E-16 (2.98E-19)	9.99E-17 (2.50E-19)	7.35E-17 (1.82E-19)	5.39E-17 (1.50E-19)
5	4	1	with	1.37E-16 (3.51E-19)	9.80E-17 (2.83E-19)	6.98E-17 (2.24E-19)	4.93E-17 (1.98E-19)
			without	1.13E-16 (2.76E-19)	8.43E-17 (2.32E-19)	6.17E-17 (1.69E-19)	4.52E-17 (1.39E-19)
5	4	2	with	6.24E-17 (2.42E-19)	4.22E-17 (1.89E-19)	2.80E-17 (1.43E-19)	1.90E-17 (1.23E-19)
			without	6.10E-17 (2.01E-19)	4.54E-17 (1.69E-19)	3.26E-17 (1.22E-19)	2.35E-17 (9.95E-20)
5	4	3	with	5.31E-18 (6.87E-20)	2.94E-18 (4.80E-20)	1.88E-18 (3.57E-20)	1.14E-18 (2.88E-20)
			without	9.62E-18 (7.56E-20)	7.43E-18 (6.48E-20)	5.39E-18 (4.68E-20)	3.78E-18 (3.76E-20)
5	4	4	with	-	-	-	-
			without	-	-	-	-

TABLE VII. Cross Sections for Electron Capture and statistical error values (in parenthesis) from H(1s) by N^{7+}

See page 93 for Explanation of Tables

$N^{7+} + H(1s) \rightarrow N^{6+}(nlm) + H^{+}$

Final state			correction	Energy (keV/amu)			
n	*l*	*m*		90	100	150	200
1	0	0	with	9.29E-20 (1.25E-21)	9.37E-20 (1.12E-21)	9.76E-20 (8.10E-22)	1.08E-19 (7.20E-22)
			without	4.20E-21 (4.06E-22)	3.79E-21 (2.96E-22)	5.86E-21 (2.36E-22)	9.67E-21 (2.69E-22)
2			with	2.50E-18 (1.27E-20)	2.50E-18 (1.14E-20)	2.36E-18 (8.02E-21)	2.06E-18 (6.37E-21)
			without	3.29E-18 (1.51E-20)	3.44E-18 (1.41E-20)	3.33E-18 (1.07E-20)	2.54E-18 (7.84E-21)
2	0	0	with	9.13E-19 (7.56E-21)	8.79E-19 (6.59E-21)	7.19E-19 (4.13E-21)	5.49E-19 (3.01E-21)
			without	8.22E-19 (9.04E-21)	8.34E-19 (8.24E-21)	7.27E-19 (5.83E-21)	4.63E-19 (3.64E-21)
2	1		with	1.59E-18 (1.02E-20)	1.62E-18 (9.26E-21)	1.64E-18 (6.93E-21)	1.51E-18 (5.68E-21)
			without	2.47E-18 (1.25E-20)	2.61E-18 (1.17E-20)	2.60E-18 (9.09E-21)	2.08E-18 (6.98E-21)
2	1	0	with	3.40E-19 (3.99E-21)	3.63E-19 (3.80E-21)	4.55E-19 (3.45E-21)	4.75E-19 (3.14E-21)
			without	8.41E-19 (6.13E-21)	8.99E-19 (5.76E-21)	9.58E-19 (4.62E-21)	8.26E-19 (3.72E-21)
2	1	1	with	6.29E-19 (6.79E-21)	6.22E-19 (6.04E-21)	5.98E-19 (4.28E-21)	5.13E-19 (3.34E-21)
			without	8.54E-19 (8.38E-21)	8.91E-19 (7.83E-21)	8.32E-19 (5.96E-21)	6.28E-19 (4.47E-21)
3			with	4.14E-17 (8.27E-20)	3.44E-17 (6.70E-20)	1.41E-17 (3.02E-20)	6.43E-18 (1.67E-20)
			without	6.91E-17 (9.82E-20)	5.91E-17 (8.13E-20)	2.73E-17 (4.07E-20)	1.34E-17 (2.32E-20)
3	0	0	with	2.55E-18 (2.05E-20)	2.02E-18 (1.57E-20)	6.79E-19 (5.66E-21)	2.79E-19 (2.80E-21)
			without	3.28E-18 (2.16E-20)	2.57E-18 (1.68E-20)	1.01E-18 (7.26E-21)	5.23E-19 (4.14E-21)
3	1		with	1.09E-17 (4.02E-20)	8.77E-18 (3.14E-20)	3.01E-18 (1.23E-20)	1.20E-18 (6.16E-21)
			without	2.01E-17 (5.40E-20)	1.63E-17 (4.28E-20)	6.15E-18 (1.80E-20)	2.86E-18 (9.52E-21)
3	1	0	with	4.20E-18 (2.36E-20)	3.43E-18 (1.86E-20)	1.30E-18 (7.84E-21)	5.75E-19 (4.19E-21)
			without	8.52E-18 (3.38E-20)	7.15E-18 (2.74E-20)	3.06E-18 (1.23E-20)	1.56E-18 (6.74E-21)
3	1	1	with	3.36E-18 (2.32E-20)	2.67E-18 (1.80E-20)	8.50E-19 (6.66E-21)	3.16E-19 (3.23E-21)
			without	5.83E-18 (3.01E-20)	4.61E-18 (2.36E-20)	1.55E-18 (9.38E-21)	6.60E-19 (4.84E-21)
3	2		with	2.80E-17 (7.00E-20)	2.36E-17 (5.78E-20)	1.04E-17 (2.76E-20)	4.95E-18 (1.56E-20)
			without	4.57E-17 (8.00E-20)	4.02E-17 (6.77E-20)	2.01E-17 (3.61E-20)	9.99E-18 (2.11E-20)
3	2	0	with	5.55E-18 (2.65E-20)	4.88E-18 (2.27E-20)	2.75E-18 (1.30E-20)	1.58E-18 (8.61E-21)
			without	1.19E-17 (3.57E-20)	1.10E-17 (3.11E-20)	6.41E-18 (1.83E-20)	3.55E-18 (1.14E-20)
3	2	1	with	8.15E-18 (3.88E-20)	6.85E-18 (3.21E-20)	3.07E-18 (1.54E-20)	1.49E-18 (8.64E-21)
			without	1.08E-17 (4.01E-20)	9.72E-18 (3.45E-20)	5.25E-18 (1.94E-20)	2.68E-18 (1.16E-20)
3	2	2	with	3.06E-18 (2.66E-20)	2.47E-18 (2.12E-20)	7.55E-19 (8.06E-21)	2.04E-19 (3.38E-21)
			without	6.19E-18 (3.43E-20)	4.86E-18 (2.73E-20)	1.62E-18 (1.16E-20)	5.42E-19 (5.51E-21)

TABLE VII. Cross Sections for Electron Capture and statistical error values (in parenthesis) from H(1s) by N^{7+}

See page 93 for Explanation of Tables

Final State			correction	Energy (keV/amu)			
n	*l*	*m*		90	100	150	200
4			with	1.79E-16 (1.98E-19)	1.37E-16 (1.53E-19)	4.00E-17 (5.71E-20)	1.38E-17 (2.76E-20)
			without	2.07E-16 (2.00E-19)	1.60E-16 (1.57E-19)	5.16E-17 (6.47E-20)	1.99E-17 (3.22E-20)
4	0	0	with	3.59E-18 (2.28E-20)	2.76E-18 (1.74E-20)	8.49E-19 (6.11E-21)	2.99E-19 (2.85E-21)
			without	2.86E-18 (1.98E-20)	2.27E-18 (1.56E-20)	8.74E-19 (6.88E-21)	4.25E-19 (3.87E-21)
4	1		with	1.46E-17 (4.48E-20)	1.15E-17 (3.45E-20)	3.69E-18 (1.29E-20)	1.29E-18 (6.12E-21)
			without	1.71E-17 (4.78E-20)	1.34E-17 (3.74E-20)	4.68E-18 (1.56E-20)	2.14E-18 (8.40E-21)
4	1	0	with	7.15E-18 (3.06E-20)	5.58E-18 (2.34E-20)	1.78E-18 (8.70E-21)	6.34E-19 (4.19E-21)
			without	9.07E-18 (3.43E-20)	7.13E-18 (2.69E-20)	2.65E-18 (1.16E-20)	1.28E-18 (6.39E-21)
4	1	1	with	3.75E-18 (2.33E-20)	2.99E-18 (1.81E-20)	9.60E-19 (6.72E-21)	3.29E-19 (3.21E-21)
			without	4.03E-18 (2.37E-20)	3.08E-18 (1.84E-20)	1.02E-18 (7.36E-21)	4.35E-19 (3.89E-21)
4	2		with	4.30E-17 (8.30E-20)	3.29E-17 (6.39E-20)	9.99E-18 (2.39E-20)	3.36E-18 (1.15E-20)
			without	4.80E-17 (8.58E-20)	3.68E-17 (6.63E-20)	1.28E-17 (2.74E-20)	5.66E-18 (1.45E-20)
4	2	0	with	1.44E-17 (4.59E-20)	1.09E-17 (3.50E-20)	3.11E-18 (1.23E-20)	1.03E-18 (5.85E-21)
			without	1.75E-17 (4.98E-20)	1.36E-17 (3.86E-20)	5.03E-18 (1.62E-20)	2.35E-18 (8.66E-21)
4	2	1	with	1.31E-17 (4.72E-20)	1.01E-17 (3.65E-20)	3.14E-18 (1.40E-20)	1.06E-18 (6.72E-21)
			without	1.29E-17 (4.58E-20)	9.87E-18 (3.54E-20)	3.40E-18 (1.47E-20)	1.46E-18 (7.81E-21)
4	2	2	with	1.18E-18 (1.47E-20)	9.06E-19 (1.13E-20)	3.05E-19 (4.45E-21)	1.06E-19 (2.18E-21)
			without	2.39E-18 (2.06E-20)	1.72E-18 (1.55E-20)	4.71E-19 (5.79E-21)	1.84E-19 (3.01E-21)
4	3		with	1.18E-16 (1.89E-19)	8.97E-17 (1.47E-19)	2.54E-17 (5.59E-20)	8.90E-18 (2.69E-20)
			without	1.39E-16 (1.85E-19)	1.07E-16 (1.46E-19)	3.32E-17 (6.06E-20)	1.17E-17 (3.04E-20)
4	3	0	with	2.88E-17 (9.45E-20)	2.19E-17 (7.40E-20)	6.64E-18 (3.02E-20)	2.58E-18 (1.50E-20)
			without	3.76E-17 (9.31E-20)	2.98E-17 (7.42E-20)	1.02E-17 (3.25E-20)	3.83E-18 (1.70E-20)
4	3	1	with	3.29E-17 (1.01E-19)	2.50E-17 (7.79E-20)	6.87E-18 (2.90E-20)	2.38E-18 (1.39E-20)
			without	3.21E-17 (9.13E-20)	2.53E-17 (7.26E-20)	8.16E-18 (3.06E-20)	2.94E-18 (1.55E-20)
4	3	2	with	1.13E-17 (5.92E-20)	8.65E-18 (4.58E-20)	2.46E-18 (1.67E-20)	7.84E-19 (7.66E-21)
			without	1.71E-17 (6.91E-20)	1.27E-17 (5.31E-20)	3.24E-18 (1.95E-20)	9.74E-19 (8.83E-21)
4	3	3	with	1.55E-19 (6.66E-21)	1.02E-19 (4.78E-21)	2.00E-20 (1.44E-21)	3.77E-21 (5.00E-22)
			without	1.21E-18 (1.69E-20)	7.72E-19 (1.20E-20)	1.29E-19 (3.54E-21)	2.45E-20 (1.26E-21)

TABLE VII. Cross Sections for Electron Capture and statistical error values (in parenthesis) from H(1s) by N^{7+}

See page 93 for Explanation of Tables

Final state			correction	Energy (keV/amu)			
n	*l*	*m*		90	100	150	200
5			with	2.55E-16 (2.60E-19)	1.89E-16 (1.96E-19)	4.88E-17 (6.63E-20)	1.53E-17 (3.01E-20)
			without	2.62E-16 (2.47E-19)	1.97E-16 (1.91E-19)	5.49E-17 (7.23E-20)	1.89E-17 (3.37E-20)
5	0	0	with	3.31E-18 (2.19E-20)	2.55E-18 (1.68E-20)	7.62E-19 (5.70E-21)	2.48E-19 (2.54E-21)
			without	2.29E-18 (1.78E-20)	1.79E-18 (1.40E-20)	6.55E-19 (6.05E-21)	3.08E-19 (3.35E-21)
5	1		with	1.35E-17 (4.45E-20)	1.07E-17 (3.44E-20)	3.42E-18 (1.25E-20)	1.16E-18 (5.77E-21)
			without	1.35E-17 (4.19E-20)	1.04E-17 (3.29E-20)	3.50E-18 (1.35E-20)	1.53E-18 (7.19E-21)
5	1	0	with	7.90E-18 (3.42E-20)	6.25E-18 (2.64E-20)	1.90E-18 (9.39E-21)	6.31E-19 (4.22E-21)
			without	7.99E-18 (3.22E-20)	6.16E-18 (2.51E-20)	2.13E-18 (1.06E-20)	9.67E-19 (5.68E-21)
5	1	1	with	2.80E-18 (2.02E-20)	2.25E-18 (1.57E-20)	7.57E-19 (5.83E-21)	2.65E-19 (2.78E-21)
			without	2.74E-18 (1.92E-20)	2.16E-18 (1.52E-20)	6.97E-19 (6.07E-21)	2.86E-19 (3.15E-21)
5	2		with	3.60E-17 (7.61E-20)	2.80E-17 (5.88E-20)	8.94E-18 (2.19E-20)	2.91E-18 (1.02E-20)
			without	3.36E-17 (6.93E-20)	2.59E-17 (5.43E-20)	8.88E-18 (2.28E-20)	3.89E-18 (1.20E-20)
5	2	0	with	1.39E-17 (4.64E-20)	1.07E-17 (3.54E-20)	3.21E-18 (1.23E-20)	9.13E-19 (5.27E-21)
			without	1.38E-17 (4.32E-20)	1.06E-17 (3.38E-20)	3.73E-18 (1.42E-20)	1.71E-18 (7.57E-21)
5	2	1	with	1.07E-17 (4.23E-20)	8.38E-18 (3.29E-20)	2.74E-18 (1.27E-20)	9.42E-19 (6.00E-21)
			without	8.96E-18 (3.68E-20)	6.89E-18 (2.88E-20)	2.34E-18 (1.20E-20)	9.95E-19 (6.37E-21)
5	2	2	with	3.47E-19 (7.82E-21)	2.93E-19 (6.31E-21)	1.32E-19 (2.85E-21)	5.62E-20 (1.55E-21)
			without	9.36E-19 (1.23E-20)	7.27E-19 (9.65E-21)	2.39E-19 (4.04E-21)	9.66E-20 (2.15E-21)
5	3		with	7.13E-17 (1.33E-19)	5.42E-17 (1.02E-19)	1.49E-17 (3.85E-20)	5.42E-18 (1.99E-20)
			without	6.87E-17 (1.21E-19)	5.36E-17 (9.57E-20)	1.78E-17 (4.09E-20)	6.87E-18 (2.17E-20)
5	3	0	with	2.16E-17 (7.08E-20)	1.54E-17 (5.27E-20)	3.20E-18 (1.82E-20)	1.23E-18 (9.80E-21)
			without	2.19E-17 (6.57E-20)	1.71E-17 (5.16E-20)	5.75E-18 (2.21E-20)	2.27E-18 (1.20E-20)
5	3	1	with	2.09E-17 (7.36E-20)	1.62E-17 (5.69E-20)	4.56E-18 (2.12E-20)	1.55E-18 (1.06E-20)
			without	1.68E-17 (6.13E-20)	1.32E-17 (4.86E-20)	4.41E-18 (2.07E-20)	1.71E-18 (1.10E-20)
5	3	2	with	3.88E-18 (3.28E-20)	3.21E-18 (2.63E-20)	1.27E-18 (1.15E-20)	5.37E-19 (6.19E-21)
			without	6.38E-18 (3.96E-20)	4.91E-18 (3.10E-20)	1.58E-18 (1.31E-20)	5.69E-19 (6.59E-21)
5	3	3	with	2.02E-20 (2.22E-21)	1.79E-20 (1.88E-21)	-	-
			without	2.46E-19 (7.12E-21)	1.96E-19 (5.70E-21)	5.04E-20 (2.14E-21)	1.27E-20 (8.98E-22)
5	4		with	1.31E-16 (2.42E-19)	9.32E-17 (1.81E-19)	2.08E-17 (5.90E-20)	5.55E-18 (2.48E-20)
			without	1.44E-16 (2.29E-19)	1.05E-16 (1.75E-19)	2.40E-17 (6.27E-20)	6.33E-18 (2.70E-20)
5	4	0	with	3.43E-17 (1.29E-19)	2.51E-17 (9.85E-20)	6.25E-18 (3.33E-20)	1.82E-18 (1.44E-20)
			without	3.92E-17 (1.21E-19)	2.88E-17 (9.27E-20)	7.01E-18 (3.42E-20)	1.98E-18 (1.53E-20)
5	4	1	with	3.48E-17 (1.25E-19)	2.47E-17 (9.31E-20)	5.40E-18 (3.00E-20)	1.44E-18 (1.27E-20)
			without	3.28E-17 (1.11E-19)	2.40E-17 (8.53E-20)	5.67E-18 (3.08E-20)	1.53E-18 (1.34E-20)
5	4	2	with	1.28E-17 (7.47E-20)	8.90E-18 (5.47E-20)	1.77E-18 (1.67E-20)	4.22E-19 (6.70E-21)
			without	1.68E-17 (7.90E-20)	1.21E-17 (5.99E-20)	2.52E-18 (2.00E-20)	5.97E-19 (8.12E-21)
5	4	3	with	7.08E-19 (1.69E-20)	5.00E-19 (1.25E-20)	7.57E-20 (3.34E-21)	8.47E-21 (9.13E-22)
			without	2.61E-18 (2.94E-20)	1.76E-18 (2.16E-20)	2.86E-19 (6.35E-21)	3.73E-20 (1.90E-21)
5	4	4	with	-	-	-	-
			without	-	-	-	-

TABLE VIII. Cross Sections for Electron Capture and statistical error values (in parenthesis) from H(1s) by O^{8+}

See page 93 for Explanation of Tables

$O^{8+} + H(1s) \rightarrow O^{7+}(nlm) + H^{+}$

Final state			correction	Energy (keV/amu)			
n	*l*	*m*		10	20	30	40
1	0	0	with	9.60E-21 (3.62E-22)	2.18E-20 (6.31E-22)	2.80E-20 (7.53E-22)	3.47E-20 (7.87E-22)
			without	-	-	-	-
2			with	4.58E-19 (6.16E-21)	6.87E-19 (8.04E-21)	8.91E-19 (9.49E-21)	1.05E-18 (9.38E-21)
			without	5.40E-20 (3.77E-21)	6.86E-20 (2.80E-21)	1.33E-19 (3.76E-21)	2.31E-19 (4.02E-21)
2	0	0	with	1.31E-19 (3.25E-21)	2.44E-19 (4.91E-21)	3.58E-19 (6.31E-21)	4.57E-19 (6.62E-21)
			without	-	4.25E-20 (2.88E-21)	5.82E-20 (2.92E-21)	7.09E-20 (2.46E-21)
2	1		with	3.27E-19 (5.24E-21)	4.43E-19 (6.37E-21)	5.33E-19 (7.13E-21)	5.89E-19 (6.73E-21)
			without	-	2.61E-20 (1.34E-21)	7.44E-20 (2.56E-21)	1.60E-19 (3.21E-21)
2	1	0	with	9.22E-20 (2.56E-21)	1.20E-19 (2.99E-21)	1.37E-19 (3.20E-21)	1.38E-19 (2.81E-21)
			without	-	9.05E-21 (6.62E-22)	2.33E-20 (1.22E-21)	4.46E-20 (1.42E-21)
2	1	1	with	1.23E-19 (3.35E-21)	1.65E-19 (4.09E-21)	1.97E-19 (4.57E-21)	2.30E-19 (4.46E-21)
			without	-	9.51E-21 (9.28E-22)	2.74E-20 (1.72E-21)	6.24E-20 (2.21E-21)
3			with	7.90E-18 (4.38E-20)	9.07E-18 (4.90E-20)	1.11E-17 (5.59E-20)	1.51E-17 (5.89E-20)
			without	1.23E-17 (4.59E-20)	2.35E-17 (7.35E-20)	3.69E-17 (9.02E-20)	4.48E-17 (8.33E-20)
3	0	0	with	1.60E-18 (2.21E-20)	2.29E-18 (2.79E-20)	2.54E-18 (3.01E-20)	2.77E-18 (2.90E-20)
			without	2.11E-18 (2.17E-20)	3.55E-18 (2.92E-20)	4.80E-18 (3.66E-20)	5.28E-18 (3.33E-20)
3	1		with	3.02E-18 (2.61E-20)	3.82E-18 (3.04E-20)	4.78E-18 (3.60E-20)	5.78E-18 (3.72E-20)
			without	4.05E-18 (2.77E-20)	7.76E-18 (4.26E-20)	1.22E-17 (5.32E-20)	1.49E-17 (5.08E-20)
3	1	0	with	9.05E-19 (1.28E-20)	1.07E-18 (1.40E-20)	1.48E-18 (1.81E-20)	1.77E-18 (1.86E-20)
			without	1.51E-18 (1.57E-20)	2.36E-18 (2.20E-20)	3.64E-18 (2.55E-20)	4.42E-18 (2.42E-20)
3	1	1	with	1.05E-18 (1.62E-20)	1.39E-18 (1.96E-20)	1.69E-18 (2.26E-20)	2.04E-18 (2.33E-20)
			without	1.31E-18 (1.68E-20)	2.81E-18 (2.67E-20)	4.47E-18 (3.46E-20)	5.35E-18 (3.28E-20)
3	2		with	3.29E-18 (2.79E-20)	2.96E-18 (2.74E-20)	3.78E-18 (3.14E-20)	6.59E-18 (3.64E-20)
			without	6.15E-18 (3.04E-20)	1.22E-17 (5.25E-20)	1.99E-17 (6.42E-20)	2.46E-17 (5.87E-20)
3	2	0	with	6.45E-19 (1.11E-20)	5.41E-19 (9.57E-21)	6.29E-19 (1.00E-20)	1.10E-18 (1.10E-20)
			without	1.33E-18 (1.16E-20)	2.16E-18 (1.89E-20)	3.92E-18 (2.37E-20)	5.33E-18 (2.27E-20)
3	2	1	with	9.91E-19 (1.57E-20)	1.00E-18 (1.68E-20)	1.33E-18 (1.98E-20)	2.21E-18 (2.25E-20)
			without	1.20E-18 (1.29E-20)	2.22E-18 (2.23E-20)	3.77E-18 (2.76E-20)	4.76E-18 (2.56E-20)
3	2	2	with	3.32E-19 (9.35E-21)	1.99E-19 (7.82E-21)	2.47E-19 (8.96E-21)	5.08E-19 (1.25E-20)
			without	1.26E-18 (1.73E-20)	2.92E-18 (2.81E-20)	4.39E-18 (3.48E-20)	4.95E-18 (3.12E-20)

TABLE VIII. Cross Sections for Electron Capture and statistical error values (in parenthesis) from H(1s) by O^{8+}

See page 93 for Explanation of Tables

Final state			correction	Energy (keV/amu)			
n	*l*	*m*		10	20	30	40
4			with	4.37E-16 (5.31E-19)	6.25E-16 (6.05E-19)	5.89E-16 (5.51E-19)	4.79E-16 (4.32E-19)
			without	9.02E-16 (5.83E-19)	9.34E-16 (5.70E-19)	7.97E-16 (5.21E-19)	6.18E-16 (3.87E-19)
4	0	0	with	4.88E-17 (2.14E-19)	3.77E-17 (1.75E-19)	2.29E-17 (1.20E-19)	1.51E-17 (7.92E-20)
			without	3.10E-17 (1.11E-19)	2.62E-17 (1.01E-19)	1.96E-17 (8.41E-20)	1.29E-17 (5.50E-20)
4	1		with	6.99E-17 (2.35E-19)	7.30E-17 (2.23E-19)	5.97E-17 (1.87E-19)	4.38E-17 (1.33E-19)
			without	1.55E-16 (2.55E-19)	1.55E-16 (2.48E-19)	1.17E-16 (2.14E-19)	8.21E-17 (1.46E-19)
4	1	0	with	2.11E-17 (1.18E-19)	2.61E-17 (1.25E-19)	2.41E-17 (1.16E-19)	1.86E-17 (8.54E-20)
			without	7.02E-17 (1.68E-19)	6.76E-17 (1.53E-19)	5.15E-17 (1.35E-19)	3.72E-17 (9.41E-20)
4	1	1	with	2.47E-17 (1.46E-19)	2.35E-17 (1.32E-19)	1.79E-17 (1.05E-19)	1.27E-17 (7.29E-20)
			without	4.27E-17 (1.40E-19)	4.36E-17 (1.42E-19)	3.25E-17 (1.20E-19)	2.23E-17 (7.95E-20)
4	2		with	1.59E-16 (3.37E-19)	2.34E-16 (3.80E-19)	2.23E-16 (3.46E-19)	1.75E-16 (2.58E-19)
			without	3.14E-16 (3.76E-19)	3.38E-16 (3.70E-19)	2.98E-16 (3.40E-19)	2.31E-16 (2.46E-19)
4	2	0	with	4.47E-17 (1.66E-19)	6.61E-17 (1.86E-19)	6.12E-17 (1.65E-19)	5.01E-17 (1.27E-19)
			without	7.45E-17 (1.79E-19)	7.67E-17 (1.64E-19)	7.26E-17 (1.56E-19)	6.08E-17 (1.18E-19)
4	2	1	with	3.78E-17 (1.66E-19)	6.33E-17 (2.02E-19)	6.42E-17 (1.93E-19)	5.14E-17 (1.46E-19)
			without	7.11E-17 (1.80E-19)	7.48E-17 (1.74E-19)	6.96E-17 (1.68E-19)	5.67E-17 (1.25E-19)
4	2	2	with	2.00E-17 (1.31E-19)	2.09E-17 (1.32E-19)	1.67E-17 (1.10E-19)	1.10E-17 (7.31E-20)
			without	4.89E-17 (1.62E-19)	5.58E-17 (1.76E-19)	4.32E-17 (1.49E-19)	2.80E-17 (9.64E-20)
4	3		with	1.59E-16 (2.96E-19)	2.80E-16 (4.06E-19)	2.84E-16 (3.91E-19)	2.46E-16 (3.27E-19)
			without	4.02E-16 (4.07E-19)	4.15E-16 (4.04E-19)	3.63E-16 (3.70E-19)	2.92E-16 (2.81E-19)
4	3	0	with	4.83E-17 (1.49E-19)	5.82E-17 (1.73E-19)	5.43E-17 (1.53E-19)	4.61E-17 (1.28E-19)
			without	5.54E-17 (1.34E-19)	6.54E-17 (1.45E-19)	6.65E-17 (1.42E-19)	5.63E-17 (1.11E-19)
4	3	1	with	3.60E-17 (1.45E-19)	7.05E-17 (2.06E-19)	7.13E-17 (1.99E-19)	6.21E-17 (1.66E-19)
			without	5.60E-17 (1.48E-19)	6.46E-17 (1.56E-19)	6.19E-17 (1.51E-19)	5.18E-17 (1.17E-19)
4	3	2	with	1.47E-17 (1.01E-19)	3.20E-17 (1.49E-19)	3.66E-17 (1.57E-19)	3.32E-17 (1.34E-19)
			without	6.39E-17 (1.75E-19)	6.55E-17 (1.76E-19)	5.61E-17 (1.63E-19)	4.59E-17 (1.25E-19)
4	3	3	with	5.07E-18 (6.17E-20)	7.99E-18 (7.92E-20)	6.69E-18 (7.21E-20)	4.36E-18 (5.10E-20)
			without	5.30E-17 (1.72E-19)	4.47E-17 (1.58E-19)	3.04E-17 (1.30E-19)	2.02E-17 (8.74E-20)

TABLE VIII. Cross Sections for Electron Capture and statistical error values (in parenthesis) from H(1s) by O^{8+}

See page 93 for Explanation of Tables

Final state			correction	Energy (keV/amu)			
n	*l*	*m*		10	20	30	40
5			with	3.83E-15 (1.67E-18)	2.89E-15 (1.35E-18)	1.96E-15 (1.13E-18)	1.36E-15 (8.29E-19)
			without	2.78E-15 (1.09E-18)	2.50E-15 (9.83E-19)	1.92E-15 (8.69E-19)	1.40E-15 (6.33E-19)
5	0	0	with	8.32E-17 (2.85E-19)	3.31E-17 (1.45E-19)	2.09E-17 (1.03E-19)	1.50E-17 (7.29E-20)
			without	1.69E-17 (9.07E-20)	6.62E-18 (6.20E-20)	8.31E-18 (5.01E-20)	8.43E-18 (3.92E-20)
5	1		with	1.60E-16 (3.77E-19)	8.69E-17 (2.46E-19)	5.98E-17 (1.84E-19)	4.44E-17 (1.31E-19)
			without	7.30E-17 (1.64E-19)	6.53E-17 (1.51E-19)	7.66E-17 (1.49E-19)	6.28E-17 (1.12E-19)
5	1	0	with	6.16E-17 (2.16E-19)	4.31E-17 (1.66E-19)	3.22E-17 (1.31E-19)	2.47E-17 (9.53E-20)
			without	3.90E-17 (1.12E-19)	4.70E-17 (1.21E-19)	5.23E-17 (1.19E-19)	3.94E-17 (8.67E-20)
5	1	1	with	4.92E-17 (2.24E-19)	2.20E-17 (1.30E-19)	1.38E-17 (9.23E-20)	9.85E-18 (6.40E-20)
			without	1.71E-17 (8.88E-20)	9.13E-18 (6.98E-20)	1.21E-17 (6.56E-20)	1.16E-17 (5.04E-20)
5	2		with	4.98E-16 (6.54E-19)	3.90E-16 (5.25E-19)	2.53E-16 (3.72E-19)	1.69E-16 (2.48E-19)
			without	2.76E-16 (3.53E-19)	2.95E-16 (3.39E-19)	2.63E-16 (2.99E-19)	1.91E-16 (2.04E-19)
5	2	0	with	1.61E-16 (3.51E-19)	1.46E-16 (3.04E-19)	9.48E-17 (2.17E-19)	6.17E-17 (1.43E-19)
			without	1.14E-16 (2.29E-19)	1.29E-16 (2.15E-19)	1.06E-16 (1.84E-19)	7.40E-17 (1.23E-19)
5	2	1	with	1.31E-16 (3.47E-19)	1.08E-16 (2.92E-19)	7.33E-17 (2.10E-19)	5.02E-17 (1.41E-19)
			without	6.73E-17 (1.73E-19)	7.72E-17 (1.84E-19)	7.25E-17 (1.65E-19)	5.24E-17 (1.11E-19)
5	2	2	with	3.73E-17 (2.10E-19)	1.36E-17 (1.12E-19)	6.08E-18 (6.46E-20)	3.30E-18 (3.88E-20)
			without	1.33E-17 (9.73E-20)	6.09E-18 (6.65E-20)	6.27E-18 (5.51E-20)	5.88E-18 (4.02E-20)
5	3		with	1.31E-15 (1.12E-18)	1.01E-15 (8.47E-19)	6.06E-16 (6.44E-19)	3.65E-16 (4.31E-19)
			without	7.93E-16 (6.71E-19)	7.81E-16 (6.00E-19)	5.55E-16 (5.01E-19)	3.69E-16 (3.39E-19)
5	3	0	with	3.39E-16 (5.74E-19)	2.73E-16 (4.15E-19)	1.74E-16 (3.33E-19)	1.09E-16 (2.28E-19)
			without	2.31E-16 (3.75E-19)	2.37E-16 (3.23E-19)	1.68E-16 (2.69E-19)	1.12E-16 (1.81E-19)
5	3	1	with	2.95E-16 (5.49E-19)	2.50E-16 (4.41E-19)	1.58E-16 (3.40E-19)	9.94E-17 (2.32E-19)
			without	1.91E-16 (3.38E-19)	1.92E-16 (3.16E-19)	1.39E-16 (2.64E-19)	9.15E-17 (1.75E-19)
5	3	2	with	1.70E-16 (4.46E-19)	1.16E-16 (3.43E-19)	5.68E-17 (2.22E-19)	2.82E-17 (1.31E-19)
			without	8.21E-17 (2.34E-19)	7.71E-17 (2.19E-19)	5.34E-17 (1.74E-19)	3.64E-17 (1.16E-19)
5	3	3	with	1.97E-17 (1.58E-19)	4.57E-18 (6.98E-20)	6.98E-19 (2.41E-20)	1.98E-19 (1.04E-20)
			without	7.47E-18 (7.82E-20)	2.88E-18 (4.94E-20)	1.44E-18 (3.14E-20)	7.89E-19 (1.77E-20)
5	4		with	1.78E-15 (1.30E-18)	1.37E-15 (1.12E-18)	1.02E-15 (9.85E-19)	7.65E-16 (7.51E-19)
			without	1.63E-15 (1.01E-18)	1.35E-15 (9.25E-19)	1.01E-15 (8.26E-19)	7.70E-16 (5.99E-19)
5	4	0	with	4.21E-16 (6.48E-19)	3.02E-16 (5.29E-19)	2.32E-16 (4.68E-19)	1.78E-16 (3.60E-19)
			without	3.70E-16 (5.19E-19)	3.16E-16 (4.63E-19)	2.28E-16 (4.03E-19)	1.75E-16 (2.91E-19)
5	4	1	with	3.66E-16 (6.21E-19)	2.88E-16 (5.32E-19)	2.23E-16 (4.73E-19)	1.76E-16 (3.68E-19)
			without	3.37E-16 (4.98E-19)	2.82E-16 (4.50E-19)	2.07E-16 (3.91E-19)	1.57E-16 (2.81E-19)
5	4	2	with	2.29E-16 (5.09E-19)	1.89E-16 (4.55E-19)	1.39E-16 (3.91E-19)	1.01E-16 (2.93E-19)
			without	2.26E-16 (4.06E-19)	1.85E-16 (3.76E-19)	1.44E-16 (3.33E-19)	1.10E-16 (2.39E-19)
5	4	3	with	8.46E-17 (3.23E-19)	5.54E-17 (2.60E-19)	3.10E-17 (1.89E-19)	1.65E-17 (1.18E-19)
			without	6.33E-17 (2.19E-19)	5.03E-17 (1.99E-19)	4.12E-17 (1.76E-19)	3.16E-17 (1.26E-19)
5	4	4	with	3.28E-18 (6.08E-20)	5.90E-19 (2.47E-20)	7.63E-20 (7.87E-21)	-
			without	1.26E-18 (2.68E-20)	2.65E-19 (1.21E-20)	1.10E-19 (7.27E-21)	-

TABLE VIII. Cross Sections for Electron Capture and statistical error values (in parenthesis) from H(1s) by O^{8+}

See page 93 for Explanation of Tables

$O^{8+} + H(1s) \rightarrow O^{7+}(nlm) + H^{+}$

Final state			correction	Energy (keV/amu)			
n	*l*	*m*		50	60	70	80
1	0	0	with	4.31E-20 (9.19E-22)	4.88E-20 (9.76E-22)	5.06E-20 (9.08E-22)	5.38E-20 (8.34E-22)
			without	-	-	-	-
2			with	1.20E-18 (1.01E-20)	1.34E-18 (1.04E-20)	1.48E-18 (9.90E-21)	1.58E-18 (9.10E-21)
			without	3.78E-19 (5.43E-21)	5.38E-19 (6.01E-21)	7.13E-19 (6.95E-21)	8.69E-19 (6.77E-21)
2	0	0	with	5.52E-19 (7.30E-21)	6.25E-19 (7.52E-21)	6.79E-19 (7.02E-21)	7.17E-19 (6.33E-21)
			without	1.11E-19 (3.28E-21)	1.47E-19 (3.59E-21)	1.88E-19 (4.15E-21)	2.28E-19 (4.10E-21)
2	1		with	6.49E-19 (7.11E-21)	7.18E-19 (7.23E-21)	7.97E-19 (7.03E-21)	8.64E-19 (6.57E-21)
			without	2.67E-19 (4.39E-21)	3.91E-19 (4.91E-21)	5.25E-19 (5.70E-21)	6.41E-19 (5.54E-21)
2	1	0	with	1.39E-19 (2.71E-21)	1.39E-19 (2.50E-21)	1.51E-19 (2.41E-21)	1.54E-19 (2.17E-21)
			without	8.23E-20 (2.04E-21)	1.23E-19 (2.28E-21)	1.68E-19 (2.67E-21)	2.12E-19 (2.65E-21)
2	1	1	with	2.58E-19 (4.83E-21)	2.95E-19 (5.04E-21)	3.27E-19 (4.87E-21)	3.60E-19 (4.58E-21)
			without	9.75E-20 (2.95E-21)	1.41E-19 (3.34E-21)	1.95E-19 (3.94E-21)	2.31E-19 (3.80E-21)
3			with	1.84E-17 (6.40E-20)	1.95E-17 (6.33E-20)	1.91E-17 (5.66E-20)	1.78E-17 (4.80E-20)
			without	4.85E-17 (9.26E-20)	4.79E-17 (8.62E-20)	4.55E-17 (8.36E-20)	4.25E-17 (7.04E-20)
3	0	0	with	2.69E-18 (2.86E-20)	2.55E-18 (2.65E-20)	2.21E-18 (2.18E-20)	1.82E-18 (1.68E-20)
			without	5.43E-18 (3.63E-20)	4.94E-18 (3.23E-20)	4.09E-18 (2.85E-20)	3.35E-18 (2.18E-20)
3	1		with	6.53E-18 (4.05E-20)	6.81E-18 (4.00E-20)	6.70E-18 (3.57E-20)	6.24E-18 (3.00E-20)
			without	1.68E-17 (5.82E-20)	1.70E-17 (5.51E-20)	1.64E-17 (5.39E-20)	1.52E-17 (4.50E-20)
3	1	0	with	2.00E-18 (2.03E-20)	2.11E-18 (2.01E-20)	2.17E-18 (1.86E-20)	2.12E-18 (1.61E-20)
			without	5.01E-18 (2.81E-20)	5.17E-18 (2.71E-20)	5.19E-18 (2.73E-20)	5.07E-18 (2.38E-20)
3	1	1	with	2.31E-18 (2.53E-20)	2.34E-18 (2.48E-20)	2.28E-18 (2.19E-20)	2.08E-18 (1.82E-20)
			without	5.99E-18 (3.72E-20)	5.91E-18 (3.46E-20)	5.60E-18 (3.34E-20)	5.09E-18 (2.76E-20)
3	2		with	9.16E-18 (4.21E-20)	1.01E-17 (4.27E-20)	1.02E-17 (3.91E-20)	9.71E-18 (3.40E-20)
			without	2.63E-17 (6.45E-20)	2.60E-17 (6.01E-20)	2.50E-17 (5.89E-20)	2.40E-17 (5.07E-20)
3	2	0	with	1.65E-18 (1.33E-20)	1.80E-18 (1.35E-20)	1.78E-18 (1.23E-20)	1.75E-18 (1.11E-20)
			without	5.92E-18 (2.55E-20)	5.92E-18 (2.38E-20)	5.80E-18 (2.36E-20)	5.66E-18 (2.05E-20)
3	2	1	with	2.89E-18 (2.51E-20)	3.08E-18 (2.48E-20)	3.01E-18 (2.21E-20)	2.82E-18 (1.89E-20)
			without	5.19E-18 (2.85E-20)	5.18E-18 (2.67E-20)	5.05E-18 (2.65E-20)	5.00E-18 (2.33E-20)
3	2	2	with	8.32E-19 (1.65E-20)	1.08E-18 (1.83E-20)	1.14E-18 (1.71E-20)	1.13E-18 (1.51E-20)
			without	5.05E-18 (3.37E-20)	4.85E-18 (3.11E-20)	4.52E-18 (3.01E-20)	4.22E-18 (2.55E-20)

TABLE VIII. Cross Sections for Electron Capture and statistical error values (in parenthesis) from H(1s) by O^{8+}

See page 93 for Explanation of Tables

Final State			correction	Energy (keV/amu)			
n	*l*	*m*		50	60	70	80
4			with	3.75E-16 (3.76E-19)	2.91E-16 (3.13E-19)	2.26E-16 (2.46E-19)	1.76E-16 (1.89E-19)
			without	4.76E-16 (3.60E-19)	3.64E-16 (2.94E-19)	2.82E-16 (2.56E-19)	2.22E-16 (1.96E-19)
4	0	0	with	1.05E-17 (6.18E-20)	7.47E-18 (4.75E-20)	5.48E-18 (3.53E-20)	4.11E-18 (2.59E-20)
			without	8.77E-18 (4.60E-20)	6.21E-18 (3.51E-20)	4.57E-18 (2.90E-20)	3.47E-18 (2.15E-20)
4	1		with	3.24E-17 (1.07E-19)	2.45E-17 (8.46E-20)	1.90E-17 (6.38E-20)	1.49E-17 (4.76E-20)
			without	5.75E-17 (1.24E-19)	4.01E-17 (9.25E-20)	2.89E-17 (7.51E-20)	2.11E-17 (5.38E-20)
4	1	0	with	1.38E-17 (6.84E-20)	1.05E-17 (5.40E-20)	8.10E-18 (4.02E-20)	6.38E-18 (2.99E-20)
			without	2.70E-17 (8.19E-20)	1.93E-17 (6.24E-20)	1.42E-17 (5.13E-20)	1.05E-17 (3.71E-20)
4	1	1	with	9.31E-18 (5.86E-20)	7.00E-18 (4.63E-20)	5.46E-18 (3.53E-20)	4.24E-18 (2.63E-20)
			without	1.53E-17 (6.66E-20)	1.04E-17 (4.87E-20)	7.39E-18 (3.92E-20)	5.29E-18 (2.78E-20)
4	2		with	1.28E-16 (2.10E-19)	9.07E-17 (1.62E-19)	6.56E-17 (1.20E-19)	4.79E-17 (8.77E-20)
			without	1.69E-16 (2.18E-19)	1.21E-16 (1.69E-19)	8.65E-17 (1.38E-19)	6.37E-17 (1.01E-19)
4	2	0	with	3.82E-17 (1.07E-19)	2.78E-17 (8.39E-20)	2.02E-17 (6.23E-20)	1.48E-17 (4.57E-20)
			without	4.80E-17 (1.10E-19)	3.66E-17 (8.82E-20)	2.74E-17 (7.39E-20)	2.09E-17 (5.49E-20)
4	2	1	with	3.80E-17 (1.19E-19)	2.70E-17 (9.20E-20)	1.97E-17 (6.85E-20)	1.44E-17 (4.99E-20)
			without	4.29E-17 (1.13E-19)	3.13E-17 (8.80E-20)	2.29E-17 (7.29E-20)	1.71E-17 (5.38E-20)
4	2	2	with	6.95E-18 (5.39E-20)	4.46E-18 (3.93E-20)	3.04E-18 (2.80E-20)	2.13E-18 (2.01E-20)
			without	1.74E-17 (7.76E-20)	1.06E-17 (5.44E-20)	6.61E-18 (4.13E-20)	4.32E-18 (2.82E-20)
4	3		with	2.05E-16 (3.00E-19)	1.68E-16 (2.62E-19)	1.36E-16 (2.13E-19)	1.09E-16 (1.68E-19)
			without	2.41E-16 (2.73E-19)	1.98E-16 (2.32E-19)	1.62E-16 (2.09E-19)	1.33E-16 (1.65E-19)
4	3	0	with	3.83E-17 (1.19E-19)	3.21E-17 (1.07E-19)	2.65E-17 (8.90E-20)	2.15E-17 (7.13E-20)
			without	4.86E-17 (1.11E-19)	4.17E-17 (9.69E-20)	3.59E-17 (9.02E-20)	3.08E-17 (7.32E-20)
4	3	1	with	5.27E-17 (1.54E-19)	4.38E-17 (1.35E-19)	3.55E-17 (1.10E-19)	2.87E-17 (8.69E-20)
			without	4.49E-17 (1.17E-19)	3.82E-17 (1.02E-19)	3.26E-17 (9.41E-20)	2.76E-17 (7.57E-20)
4	3	2	with	2.80E-17 (1.22E-19)	2.28E-17 (1.04E-19)	1.81E-17 (8.28E-20)	1.45E-17 (6.45E-20)
			without	3.83E-17 (1.21E-19)	3.12E-17 (1.02E-19)	2.50E-17 (9.05E-20)	2.01E-17 (7.03E-20)
4	3	3	with	2.50E-18 (3.73E-20)	1.41E-18 (2.60E-20)	8.33E-19 (1.76E-20)	4.99E-19 (1.17E-20)
			without	1.30E-17 (7.28E-20)	8.49E-18 (5.38E-20)	5.44E-18 (4.18E-20)	3.54E-18 (2.87E-20)

TABLE VIII. Cross Sections for Electron Capture and statistical error values (in parenthesis) from H(1s) by O^{8+}

See page 93 for Explanation of Tables

Final state			correction	Energy (keV/amu)			
n	*l*	*m*		50	60	70	80
5			with	9.58E-16 (6.84E-19)	6.83E-16 (5.43E-19)	4.95E-16 (4.10E-19)	3.64E-16 (3.03E-19)
			without	1.01E-15 (5.77E-19)	7.29E-16 (4.61E-19)	5.32E-16 (3.91E-19)	3.93E-16 (2.90E-19)
5	0	0	with	1.07E-17 (5.78E-20)	7.92E-18 (4.58E-20)	5.84E-18 (3.43E-20)	4.35E-18 (2.51E-20)
			without	6.85E-18 (3.78E-20)	5.26E-18 (3.10E-20)	4.05E-18 (2.68E-20)	3.12E-18 (2.02E-20)
5	1		with	3.39E-17 (1.07E-19)	2.59E-17 (8.54E-20)	2.01E-17 (6.49E-20)	1.58E-17 (4.88E-20)
			without	4.64E-17 (1.01E-19)	3.38E-17 (7.89E-20)	2.46E-17 (6.57E-20)	1.82E-17 (4.84E-20)
5	1	0	with	1.90E-17 (7.85E-20)	1.45E-17 (6.28E-20)	1.12E-17 (4.78E-20)	8.79E-18 (3.60E-20)
			without	2.78E-17 (7.66E-20)	1.97E-17 (5.93E-20)	1.42E-17 (4.91E-20)	1.05E-17 (3.61E-20)
5	1	1	with	7.47E-18 (5.19E-20)	5.63E-18 (4.08E-20)	4.47E-18 (3.14E-20)	3.48E-18 (2.34E-20)
			without	9.24E-18 (4.65E-20)	6.99E-18 (3.70E-20)	5.17E-18 (3.09E-20)	3.87E-18 (2.28E-20)
5	2		with	1.16E-16 (1.93E-19)	8.18E-17 (1.49E-19)	5.99E-17 (1.11E-19)	4.44E-17 (8.19E-20)
			without	1.30E-16 (1.74E-19)	8.93E-17 (1.32E-19)	6.30E-17 (1.08E-19)	4.54E-17 (7.86E-20)
5	2	0	with	4.24E-17 (1.12E-19)	2.98E-17 (8.63E-20)	2.18E-17 (6.45E-20)	1.61E-17 (4.75E-20)
			without	5.00E-17 (1.05E-19)	3.45E-17 (7.94E-20)	2.44E-17 (6.51E-20)	1.76E-17 (4.72E-20)
5	2	1	with	3.51E-17 (1.10E-19)	2.48E-17 (8.48E-20)	1.82E-17 (6.34E-20)	1.36E-17 (4.68E-20)
			without	3.54E-17 (9.39E-20)	2.43E-17 (7.11E-20)	1.71E-17 (5.81E-20)	1.24E-17 (4.22E-20)
5	2	2	with	1.97E-18 (2.79E-20)	1.27E-18 (2.04E-20)	8.37E-19 (1.42E-20)	5.89E-19 (1.01E-20)
			without	4.41E-18 (3.52E-20)	3.14E-18 (2.70E-20)	2.20E-18 (2.19E-20)	1.52E-18 (1.55E-20)
5	3		with	2.32E-16 (3.29E-19)	1.58E-16 (2.51E-19)	1.15E-16 (1.87E-19)	8.60E-17 (1.39E-19)
			without	2.47E-16 (2.88E-19)	1.71E-16 (2.18E-19)	1.22E-16 (1.79E-19)	9.03E-17 (1.32E-19)
5	3	0	with	7.05E-17 (1.75E-19)	4.74E-17 (1.32E-19)	3.43E-17 (9.82E-20)	2.55E-17 (7.27E-20)
			without	7.54E-17 (1.53E-19)	5.22E-17 (1.15E-19)	3.73E-17 (9.41E-20)	2.76E-17 (6.92E-20)
5	3	1	with	6.47E-17 (1.78E-19)	4.50E-17 (1.37E-19)	3.30E-17 (1.02E-19)	2.48E-17 (7.63E-20)
			without	6.07E-17 (1.47E-19)	4.17E-17 (1.10E-19)	2.96E-17 (9.00E-20)	2.18E-17 (6.61E-20)
5	3	2	with	1.62E-17 (9.40E-20)	1.04E-17 (6.89E-20)	7.17E-18 (4.99E-20)	5.40E-18 (3.69E-20)
			without	2.46E-17 (9.81E-20)	1.72E-17 (7.49E-20)	1.23E-17 (6.15E-20)	9.15E-18 (4.54E-20)
5	3	3	with	8.30E-20 (6.24E-21)	4.87E-20 (4.39E-21)	3.88E-20 (3.51E-21)	2.84E-20 (2.56E-21)
			without	6.31E-19 (1.50E-20)	5.08E-19 (1.18E-20)	4.45E-19 (1.06E-20)	3.45E-19 (7.95E-21)
5	4		with	5.64E-16 (6.34E-19)	4.09E-16 (5.10E-19)	2.95E-16 (3.85E-19)	2.13E-16 (2.85E-19)
			without	5.78E-16 (5.44E-19)	4.29E-16 (4.33E-19)	3.18E-16 (3.66E-19)	2.36E-16 (2.72E-19)
5	4	0	with	1.33E-16 (3.06E-19)	9.67E-17 (2.48E-19)	6.95E-17 (1.89E-19)	5.05E-17 (1.41E-19)
			without	1.34E-16 (2.65E-19)	1.01E-16 (2.11E-19)	7.68E-17 (1.80E-19)	5.79E-17 (1.35E-19)
5	4	1	with	1.35E-16 (3.16E-19)	1.01E-16 (2.57E-19)	7.48E-17 (1.96E-19)	5.50E-17 (1.46E-19)
			without	1.19E-16 (2.54E-19)	8.96E-17 (2.03E-19)	6.70E-17 (1.71E-19)	5.05E-17 (1.28E-19)
5	4	2	with	7.16E-17 (2.38E-19)	4.98E-17 (1.86E-19)	3.45E-17 (1.36E-19)	2.40E-17 (9.72E-20)
			without	8.09E-17 (2.14E-19)	5.87E-17 (1.67E-19)	4.26E-17 (1.39E-19)	3.11E-17 (1.02E-19)
5	4	3	with	9.13E-18 (8.36E-20)	5.15E-18 (5.80E-20)	3.22E-18 (3.98E-20)	2.10E-18 (2.77E-20)
			without	2.24E-17 (1.09E-19)	1.56E-17 (8.29E-20)	1.08E-17 (6.69E-20)	7.42E-18 (4.75E-20)
5	4	4	with	-	-	-	-
			without	-	-	-	-

TABLE VIII. Cross Sections for Electron Capture and statistical error values (in parenthesis) from H(1s) by O^{8+}

See page 93 for Explanation of Tables

$O^{8+} + H(1s) \rightarrow O^{7+}(nlm) + H^{+}$

Final state			correction	Energy (keV/amu)			
n	*l*	*m*		90	100	150	200
1	0	0	with	5.52E-20 (8.14E-22)	6.04E-20 (1.19E-21)	6.69E-20 (6.73E-22)	6.73E-20 (5.58E-22)
			without	-	-	-	3.31E-21 (1.76E-22)
2			with	1.62E-18 (8.77E-21)	1.65E-18 (1.22E-20)	1.73E-18 (6.78E-21)	1.63E-18 (5.59E-21)
			without	1.01E-18 (7.26E-21)	1.13E-18 (7.72E-21)	1.38E-18 (6.72E-21)	1.33E-18 (5.99E-21)
2	0	0	with	7.17E-19 (5.93E-21)	6.99E-19 (7.92E-21)	6.24E-19 (3.88E-21)	5.22E-19 (2.94E-21)
			without	2.57E-19 (4.37E-21)	2.91E-19 (4.68E-21)	3.48E-19 (4.06E-21)	2.93E-19 (3.25E-21)
2	1		with	9.08E-19 (6.47E-21)	9.53E-19 (9.25E-21)	1.10E-18 (5.58E-21)	1.11E-18 (4.80E-21)
			without	7.50E-19 (5.98E-21)	8.35E-19 (6.33E-21)	1.03E-18 (5.53E-21)	1.03E-18 (5.11E-21)
2	1	0	with	1.65E-19 (2.20E-21)	1.82E-19 (3.30E-21)	2.58E-19 (2.45E-21)	2.99E-19 (2.40E-21)
			without	2.51E-19 (2.86E-21)	2.84E-19 (3.06E-21)	3.62E-19 (2.69E-21)	3.90E-19 (2.60E-21)
2	1	1	with	3.69E-19 (4.44E-21)	3.89E-19 (6.32E-21)	4.26E-19 (3.60E-21)	4.03E-19 (2.94E-21)
			without	2.63E-19 (4.08E-21)	2.90E-19 (4.30E-21)	3.47E-19 (3.76E-21)	3.26E-19 (3.38E-21)
3			with	1.62E-17 (4.37E-20)	1.45E-17 (5.66E-20)	7.92E-18 (2.21E-20)	4.50E-18 (1.35E-20)
			without	3.87E-17 (6.65E-20)	3.44E-17 (6.19E-20)	1.93E-17 (3.48E-20)	1.11E-17 (2.30E-20)
3	0	0	with	1.52E-18 (1.42E-20)	1.24E-18 (1.72E-20)	5.21E-19 (5.22E-21)	2.44E-19 (2.74E-21)
			without	2.67E-18 (1.88E-20)	2.17E-18 (1.64E-20)	8.71E-19 (7.22E-21)	4.42E-19 (4.28E-21)
3	1		with	5.63E-18 (2.68E-20)	4.82E-18 (3.34E-20)	2.12E-18 (1.11E-20)	9.83E-19 (5.94E-21)
			without	1.35E-17 (4.18E-20)	1.15E-17 (3.77E-20)	5.16E-18 (1.79E-20)	2.52E-18 (1.03E-20)
3	1	0	with	2.01E-18 (1.49E-20)	1.78E-18 (1.89E-20)	9.14E-19 (7.08E-21)	4.72E-19 (4.13E-21)
			without	4.84E-18 (2.31E-20)	4.35E-18 (2.17E-20)	2.31E-18 (1.14E-20)	1.27E-18 (7.05E-21)
3	1	1	with	1.81E-18 (1.59E-20)	1.53E-18 (1.97E-20)	6.03E-19 (6.01E-21)	2.50E-19 (2.97E-21)
			without	4.36E-18 (2.50E-20)	3.61E-18 (2.22E-20)	1.43E-18 (9.78E-21)	6.14E-19 (5.34E-21)
3	2		with	9.10E-18 (3.18E-20)	8.41E-18 (4.26E-20)	5.27E-18 (1.85E-20)	3.27E-18 (1.19E-20)
			without	2.25E-17 (4.91E-20)	2.07E-17 (4.68E-20)	1.33E-17 (2.91E-20)	8.15E-18 (2.03E-20)
3	2	0	with	1.66E-18 (1.05E-20)	1.61E-18 (1.47E-20)	1.36E-18 (8.26E-21)	1.02E-18 (6.20E-21)
			without	5.39E-18 (2.00E-20)	5.12E-18 (1.95E-20)	3.83E-18 (1.34E-20)	2.63E-18 (1.00E-20)
3	2	1	with	2.60E-18 (1.74E-20)	2.41E-18 (2.34E-20)	1.54E-18 (1.02E-20)	9.85E-19 (6.63E-21)
			without	4.80E-18 (2.30E-20)	4.50E-18 (2.23E-20)	3.24E-18 (1.52E-20)	2.12E-18 (1.11E-20)
3	2	2	with	1.10E-18 (1.43E-20)	1.03E-18 (1.91E-20)	4.28E-19 (6.42E-21)	1.39E-19 (2.91E-21)
			without	3.82E-18 (2.42E-20)	3.23E-18 (2.21E-20)	1.48E-18 (1.13E-20)	6.53E-19 (6.60E-21)

TABLE VIII. Cross Sections for Electron Capture and statistical error values (in parenthesis) from H(1s) by O^{8+}

See page 93 for Explanation of Tables

Final State			correction	Energy (keV/amu)			
n	*l*	*m*		90	100	150	200
4			with	1.37E-16 (1.57E-19)	1.08E-16 (1.90E-19)	3.52E-17 (5.62E-20)	1.32E-17 (2.83E-20)
			without	1.75E-16 (1.72E-19)	1.40E-16 (1.51E-19)	5.10E-17 (6.68E-20)	2.20E-17 (3.77E-20)
4	0	0	with	3.16E-18 (2.09E-20)	2.48E-18 (2.48E-20)	8.03E-19 (6.67E-21)	2.91E-19 (3.11E-21)
			without	2.71E-18 (1.85E-20)	2.19E-18 (1.62E-20)	8.25E-19 (7.09E-21)	4.00E-19 (4.21E-21)
4	1		with	1.18E-17 (3.88E-20)	9.34E-18 (4.58E-20)	3.16E-18 (1.29E-20)	1.14E-18 (6.26E-21)
			without	1.59E-17 (4.50E-20)	1.22E-17 (3.82E-20)	4.33E-18 (1.59E-20)	2.00E-18 (9.16E-21)
4	1	0	with	5.11E-18 (2.44E-20)	4.01E-18 (2.85E-20)	1.41E-18 (8.21E-21)	5.51E-19 (4.25E-21)
			without	8.01E-18 (3.11E-20)	6.18E-18 (2.64E-20)	2.35E-18 (1.15E-20)	1.14E-18 (6.79E-21)
4	1	1	with	3.33E-18 (2.15E-20)	2.64E-18 (2.55E-20)	8.68E-19 (7.03E-21)	2.92E-19 (3.25E-21)
			without	3.98E-18 (2.32E-20)	3.02E-18 (1.96E-20)	9.90E-19 (7.85E-21)	4.29E-19 (4.38E-21)
4	2		with	3.54E-17 (7.00E-20)	2.69E-17 (8.22E-20)	8.09E-18 (2.28E-20)	2.95E-18 (1.11E-20)
			without	4.72E-17 (8.37E-20)	3.57E-17 (7.04E-20)	1.16E-17 (2.78E-20)	5.36E-18 (1.58E-20)
4	2	0	with	1.10E-17 (3.65E-20)	8.29E-18 (4.25E-20)	2.47E-18 (1.16E-20)	9.61E-19 (5.69E-21)
			without	1.60E-17 (4.65E-20)	1.24E-17 (3.95E-20)	4.37E-18 (1.60E-20)	2.15E-18 (9.24E-21)
4	2	1	with	1.06E-17 (3.96E-20)	8.17E-18 (4.70E-20)	2.50E-18 (1.33E-20)	8.91E-19 (6.53E-21)
			without	1.27E-17 (4.47E-20)	9.54E-18 (3.75E-20)	3.10E-18 (1.49E-20)	1.40E-18 (8.56E-21)
4	2	2	with	1.52E-18 (1.57E-20)	1.10E-18 (1.80E-20)	3.13E-19 (4.79E-21)	1.01E-19 (2.22E-21)
			without	2.92E-18 (2.23E-20)	2.06E-18 (1.81E-20)	5.22E-19 (6.46E-21)	1.98E-19 (3.42E-21)
4	3		with	8.66E-17 (1.42E-19)	6.89E-17 (1.74E-19)	2.31E-17 (5.34E-20)	8.86E-18 (2.72E-20)
			without	1.10E-16 (1.48E-19)	8.95E-17 (1.32E-19)	3.42E-17 (6.13E-20)	1.43E-17 (3.49E-20)
4	3	0	with	1.75E-17 (6.16E-20)	1.42E-17 (7.69E-20)	5.33E-18 (2.57E-20)	2.33E-18 (1.43E-20)
			without	2.62E-17 (6.72E-20)	2.21E-17 (6.11E-20)	9.66E-18 (3.05E-20)	4.35E-18 (1.82E-20)
4	3	1	with	2.28E-17 (7.35E-20)	1.82E-17 (8.99E-20)	6.00E-18 (2.75E-20)	2.30E-18 (1.39E-20)
			without	2.34E-17 (6.93E-20)	1.95E-17 (6.27E-20)	8.04E-18 (3.05E-20)	3.47E-18 (1.77E-20)
4	3	2	with	1.14E-17 (5.37E-20)	8.94E-18 (6.45E-20)	2.88E-18 (1.87E-20)	9.56E-19 (8.76E-21)
			without	1.60E-17 (6.17E-20)	1.26E-17 (5.38E-20)	3.93E-18 (2.20E-20)	1.41E-18 (1.15E-20)
4	3	3	with	3.00E-19 (8.47E-21)	1.84E-19 (8.78E-21)	3.77E-20 (1.99E-21)	8.95E-21 (7.70E-22)
			without	2.27E-18 (2.23E-20)	1.51E-18 (1.76E-20)	2.54E-19 (5.14E-21)	6.15E-20 (2.18E-21)

TABLE VIII. Cross Sections for Electron Capture and statistical error values (in parenthesis) from H(1s) by O^{8+}

See page 93 for Explanation of Tables

Final state			correction	Energy (keV/amu)			
n	*l*	*m*		90	100	150	200
5			with	2.68E-16 (2.43E-19)	2.02E-16 (2.84E-19)	5.52E-17 (7.49E-20)	1.85E-17 (3.52E-20)
			without	2.94E-16 (2.48E-19)	2.24E-16 (2.12E-19)	6.62E-17 (8.34E-20)	2.48E-17 (4.34E-20)
5	0	0	with	3.31E-18 (2.04E-20)	2.55E-18 (2.39E-20)	7.89E-19 (6.33E-21)	2.80E-19 (2.98E-21)
			without	2.44E-18 (1.76E-20)	1.92E-18 (1.53E-20)	6.82E-19 (6.55E-21)	3.11E-19 (3.75E-21)
5	1		with	1.22E-17 (3.93E-20)	9.50E-18 (4.59E-20)	3.15E-18 (1.26E-20)	1.14E-18 (6.08E-21)
			without	1.37E-17 (4.08E-20)	1.06E-17 (3.50E-20)	3.47E-18 (1.43E-20)	1.52E-18 (8.08E-21)
5	1	0	with	6.76E-18 (2.89E-20)	5.16E-18 (3.33E-20)	1.63E-18 (8.87E-21)	5.83E-19 (4.26E-21)
			without	7.84E-18 (3.04E-20)	6.10E-18 (2.62E-20)	2.04E-18 (1.08E-20)	9.24E-19 (6.23E-21)
5	1	1	with	2.73E-18 (1.90E-20)	2.18E-18 (2.24E-20)	7.55E-19 (6.33E-21)	2.78E-19 (3.08E-21)
			without	2.91E-18 (1.93E-20)	2.25E-18 (1.65E-20)	7.15E-19 (6.62E-21)	2.96E-19 (3.62E-21)
5	2		with	3.35E-17 (6.59E-20)	2.58E-17 (7.81E-20)	7.81E-18 (2.16E-20)	2.80E-18 (1.04E-20)
			without	3.38E-17 (6.63E-20)	2.57E-17 (5.65E-20)	8.50E-18 (2.34E-20)	3.83E-18 (1.34E-20)
5	2	0	with	1.21E-17 (3.82E-20)	9.29E-18 (4.49E-20)	2.69E-18 (1.20E-20)	9.59E-19 (5.58E-21)
			without	1.32E-17 (4.00E-20)	1.02E-17 (3.44E-20)	3.52E-18 (1.45E-20)	1.64E-18 (8.33E-21)
5	2	1	with	1.02E-17 (3.74E-20)	7.85E-18 (4.43E-20)	2.42E-18 (1.24E-20)	8.77E-19 (6.13E-21)
			without	9.17E-18 (3.55E-20)	6.91E-18 (3.01E-20)	2.24E-18 (1.24E-20)	1.00E-18 (7.11E-21)
5	2	2	with	4.46E-19 (8.14E-21)	3.72E-19 (1.00E-20)	1.31E-19 (2.95E-21)	5.18E-20 (1.51E-21)
			without	1.08E-18 (1.26E-20)	8.05E-19 (1.07E-20)	2.40E-19 (4.22E-21)	9.69E-20 (2.33E-21)
5	3		with	6.52E-17 (1.13E-19)	5.10E-17 (1.34E-19)	1.50E-17 (3.75E-20)	5.20E-18 (1.89E-20)
			without	6.78E-17 (1.11E-19)	5.28E-17 (9.55E-20)	1.80E-17 (4.03E-20)	7.77E-18 (2.33E-20)
5	3	0	with	1.90E-17 (5.83E-20)	1.47E-17 (6.89E-20)	3.44E-18 (1.69E-20)	1.08E-18 (8.56E-21)
			without	2.09E-17 (5.84E-20)	1.62E-17 (4.98E-20)	5.72E-18 (2.10E-20)	2.53E-18 (1.22E-20)
5	3	1	with	1.87E-17 (6.16E-20)	1.47E-17 (7.35E-20)	4.35E-18 (2.05E-20)	1.46E-18 (1.00E-20)
			without	1.64E-17 (5.57E-20)	1.28E-17 (4.82E-20)	4.40E-18 (2.05E-20)	1.91E-18 (1.19E-20)
5	3	2	with	4.20E-18 (3.02E-20)	3.47E-18 (3.71E-20)	1.40E-18 (1.20E-20)	5.89E-19 (6.44E-21)
			without	6.76E-18 (3.81E-20)	5.21E-18 (3.27E-20)	1.69E-18 (1.36E-20)	6.77E-19 (7.59E-21)
5	3	3	with	1.96E-20 (2.00E-21)	-	-	-
			without	2.98E-19 (7.23E-21)	2.29E-19 (6.22E-21)	7.30E-20 (2.61E-21)	2.45E-20 (1.33E-21)
5	4		with	1.54E-16 (2.28E-19)	1.13E-16 (2.67E-19)	2.85E-17 (7.00E-20)	9.04E-18 (3.20E-20)
			without	1.77E-16 (2.31E-19)	1.33E-16 (1.97E-19)	3.55E-17 (7.63E-20)	1.14E-17 (3.83E-20)
5	4	0	with	3.64E-17 (1.15E-19)	2.69E-17 (1.36E-19)	7.14E-18 (3.68E-20)	2.44E-18 (1.71E-20)
			without	4.40E-17 (1.15E-19)	3.37E-17 (9.89E-20)	9.59E-18 (3.96E-20)	3.27E-18 (2.07E-20)
5	4	1	with	3.99E-17 (1.17E-19)	2.94E-17 (1.36E-19)	7.14E-18 (3.51E-20)	2.25E-18 (1.60E-20)
			without	3.80E-17 (1.09E-19)	2.89E-17 (9.33E-20)	8.05E-18 (3.67E-20)	2.66E-18 (1.87E-20)
5	4	2	with	1.73E-17 (7.70E-20)	1.26E-17 (8.83E-20)	3.32E-18 (2.31E-20)	9.95E-19 (1.03E-20)
			without	2.29E-17 (8.56E-20)	1.69E-17 (7.21E-20)	4.17E-18 (2.62E-20)	1.23E-18 (1.25E-20)
5	4	3	with	1.46E-18 (2.15E-20)	1.00E-18 (2.40E-20)	2.27E-19 (5.79E-21)	4.56E-20 (2.12E-21)
			without	5.24E-18 (3.89E-20)	3.60E-18 (3.16E-20)	7.08E-19 (1.02E-20)	1.46E-19 (4.05E-21)
5	4	4	with	-	-	-	-
			without	-	-	-	-